# A Double Acting Solar Thermal Water Pump

**by**

**Daniel R. Foster**

Master of Engineering Thesis

June 1998

**Department of Mechanical Engineering**

**University of Canterbury**

**To my MUM and DAD**

# Acknowledgements

The author would like to express his sincere thanks to the staff and fellow students of the University of Canterbury in particular Associate Professor J.K. Raine, Dr A.S. Tucker and Professor A.G. Williamson for their supervision, advice and expertise. Thanks also to E. Cox, R. Tinker, O. Bolt, K. Brown and S. Amies for their practical assistance during the manufacture and testing of the prototype pump.

Lastly my most sincere thanks to friends and family, especially Pauline Foster, Donald Foster and Vicki Borcoskie for their patience, support, encouragement and assistance.

# Table of Contents

# Abstract

Mankind's need for sustainable technology is increasing with the ever growing demand for and depletion of finite energy reserves. Research into the conversion of sustainable energy resources such as wind, hydro and solar into high quality mechanical, chemical or electrical energy is becoming more significant and of greater urgency in modern society.

The research reported in this thesis continues from previous work carried out in the development of a small, low cost solar thermal water pump. The aim of the research was to take a pump previously designed at the University of Canterbury to further develop and refine the system to improve operation, performance, physical and operational design, as well as reliability and maintainability.

The earlier design was a novel single acting, double diaphragm pump operating on a thermal cycle similar to a Rankine cycle, dubbed The 'Modified' Rankine cycle. Although it was adequate to prove the concept it was inefficient and impractical in design. In order to achieve research goals this previous design was dropped and a new double acting unit developed to give greater performance, smoother flow output, be self starting and self priming and therefore be able to operate unattended. The new design is intended to overcome the major failings of the first prototype while being significantly smaller, lighter, more robust and reliable, and be relatively maintenance free.

A complex computer simulation of the collector and pump system was modified and developed for the new design to optimise pump geometry and predict pump operation for any average day at any location and for any water head. Thermodynamic analysis of the pump showed significant exergy loss with the internal energy of the working fluid not being used but was an unavoidable trade off for simplicity, cost and reliability.

The new pump was optimised to pump water through a 6 metre vertical water head, operating on a 2.9 $m^2$ flat plate sheet and tube non tracking solar collector. With n-Pentane as the working fluid operating at 56°C a peak flow rate of 27 litres per minute was predicted with a corresponding efficiency of 0.93%. For a good summer's day 10,000 litres could be lifted through 6 metres.

A suitable initial application of this solar thermal pumping unit would be in solar water heating installations for swimming pools. As a circulation pump a solar thermal unit would have distinct advantages: it would have no running cost, it would add heat to the pumped water reducing the area of water heating panel, and would only pump during daylight hours ie. fully automated and self contained operation.

# CHAPTER 1 - Introduction

This chapter looks briefly at the status and nature of solar energy as a source of power for mankind. Methods of collection and its application / utilisation in the development of a solar thermal water pump will be discussed in the following chapters. Also discussed in this chapter are the objectives of this research and an overview of the work performed.

## 1.1 Solar Energy (an Overview)

With the continued depletion of the worlds finite energy reserves such as coal, oil, natural gas and even nuclear, mankind is under increasing pressure to develop and/or refine technologies that harness the power of sustainable/permanent and non-polluting energy resources such as direct solar, or indirect solar such as hydro, wind, managed biomass, tidal or ocean-thermal.

Strictly speaking, all forms of energy are derived from the sun. Fossil fuels however have taken many years to concentrate this energy into substances with a high energy density, easily utilised by man. Currently approximately 80% of the world energy demand is met by fossil fuels (Serpone et al. 1992). The consumption of these fossil fuels far exceeds the rate at which they can be produced and compounding this problem is escalating population growth and the generation of environmental pollution from the combustion of these fuels ($CO_2$, CO, $SO_2$, $NO_x$, soot and ash). With estimated lifetimes for fuels ranging from 35 years for oil and up to 200 years for coal and natural gas (Hedley, 1986, B.P. 1990, Krieder et al. 1989), it is important, not only for the sustainable development but also the mere continuation of mankind, that we learn to supply a large portion of our energy needs from solar energy as soon as it is delivered to the earth. Initially these appropriate technologies may appear uneconomic using current cost conventions, however with increased acceptance of environmentally friendly energy conversion, technological refinement and the advantages of mass production, and with impending increases in the costs of recovering fossil fuels, the competitive advantage of fossil fuels must dwindle.

The sun is the most abundant renewable source of energy available to man. It arrives in the form of electromagnetic radiation produced by the fusion of hydrogen to form helium within the core of the sun. The amount of solar energy (approx. $1.7 \times 10^{17}$ W) impinging on the upper atmosphere of this planet is 10's of thousands times greater than the present energy consumption of the world. Unfortunately, not all of this radiation reaches the Earth's surface. Approximately 30% of this amount is reflected into space, 47% is converted to low temperature heat and re-radiated into space, 23% powers the evaporation-precipitation cycle of the biosphere and less than 0.5% powers winds and waves and phototsynthetic storage in plants. The radiation reaching the surface of the earth still far exceeds the requirements of man.

Solar energy impinging on the earth's atmosphere is relatively dilute - approximately 1353 W/$m^2$. It is further diluted by attenuation, weather conditions, air pollution and unfortunately is only received intermittently at any particular location. The solar energy that may be used by the solar engineer arrives at the surface of the earth in three forms, direct radiation, diffuse radiation, and reflected radiation. Direct (or beam) radiation is the solar radiation that travels from the sun to a point on the earth's surface with negligible change in direction. It is the type of sunlight that can cast a shadow and on a sunny day may be as much as 80% of the total solar energy striking a surface. Diffuse (or scattered) radiation is dispersed and comes from all directions other than the direction of the sun. It is produced by scattering of sunlight by atmospheric components such as particles, water vapour, and pollution. On very cloudy days the sunlight is 100% diffuse. The third type of radiation relevant to solar design is reflected radiation. This may be either diffuse or direct radiation reflected onto the solar aperture. The amount of reflected radiation varies significantly with the nature of the environment around the collector, a light coloured foreground will give higher values of reflected radiation than a dark coloured foreground. On average the radiation striking the earth's surface is in the range of 100 - 1000 W/$m^2$. Because of this dilute nature of solar radiation, large collection areas are generally required.

The motion of the sun is important in determining the angle of incidence of beam radiation onto the collector aperture not only for calculating the density of solar energy impinging on the surface but also in the calculation of the radiation that is reflected by the surface itself. Determining correct collector angle and position to maximise solar collection during the periods and seasons desired depends on solar altitude and azimuth angles (refer *Figure 1.1*) during the period of collection.

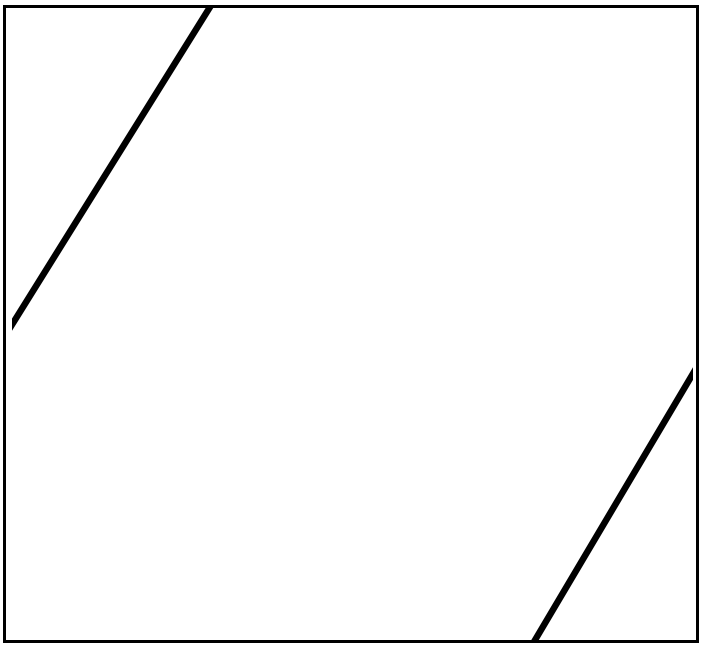

Calculating levels of solar energy impinging on collector surfaces and the conversion of solar energy into heat (collector technologies) are covered briefly in Chapter 2 and documented in greater detail in many texts (for example: Duffie et al. 1974, 1980, Kreider et al. 1989, Kreith et al. 1978, Howell et al 1979). Usually solar collectors have a surface that efficiently absorbs radiation and converts it to heat. Part of this heat energy is removed from the absorber surface by a heat transfer fluid which may be liquid or gaseous or a combination of both liquid and gaseous phases where it can either be stored or used directly in, for example, a heat engine such as that described in this research.

## 1.2 Research Objectives and Overview of Work Carried Out.

The idea of using solar energy to power a thermal heat engine coupled to a water pump is not new, as early as 1615 efforts were made to raise water by the expansion of air in a solar heater by Solomon de Caux (Pytlinski,1978). The design of a compact, practical, simple, but reliable solar thermal water pump of marketable suitability however has eluded designers to date who typically have never progressed further than the prototype stage. Aside from operational and functionality difficulties,

design complexity resulting in high initial capital costs as well as the poor emphasis placed on the worth of solar technologies by society can all contribute to premature project termination.

The current market tends toward DC electric pumps driven by photovoltaic arrays. These devices are convenient, but as a 'high-tech' and expensive option fail to interest many prospective buyers. Solar thermal water pumping promises to be a cheaper option and efforts to develop a low cost, small scale solar thermal water pump at the University of Canterbury began around 1988 with an increasing trend toward the acceptance of solar technologies as an alternative to fossil fuels for appropriate applications.

Research at Canterbury, as has been the case for most other developers of solar thermal water pumping devices, was initially directed at applications in the rural areas of developing (third world) countries, low in natural energy resources. The work of Amor (1992) was the basis for the work described in this thesis. Amor's intention was to build a simple, yet effective, low cost solar water pump, utilising a single working fluid as a replacement for handpumps in the rural third world. He devised a single acting pump designed to operate on a flat plate solar collector using n-Pentane as the working fluid. Flat plate collectors meant the development of a low temperature heat engine (therefore inherently low efficiency) but were chosen to avoid the higher costs associated with concentrating collection devices (discussed later). Various problems with the design prevented successful operation as intended. The initial project brief for this research was to:

(i) improve Amor's unit such that it would operate on a solar collector,
(ii) examine a redesign of Amor's unit to minimise Exergy loss, give versatility of operation (head and flow rate) and
(iii) build a new (and final) prototype suitable for manufacture and test.

It was not the intention of this research to duplicate the work of Amor but to further the development process based on his initial design. On investigation of the prototype unit and study of works by other researchers, however, the author decided to stop development on Amor's single acting design and completely redesign the pump and prime mover to function in a double acting configuration. The double acting design

promised greater versatility of operation with improved flow characteristics and greater efficiency whilst being significantly more compact for a given flow rate. The overall goal of the research remained the same; to develop a novel, low cost, simple, effective, versatile and reliable small scale stand alone solar thermal water pump.

The second prototype would be designed to be ideally suited for water circulation in solar powered heating systems for swimming pools (although not exclusive of other potential applications). Once accepted and proven in a Western application, the advantages of commercial interest and refinement of design, as well as larger volume production would provide a lower cost and more accepted alternative for developing countries. To develop a system aimed directly at a market where commercial interest is low and funding for development difficult to obtain simply increases the complexity of the task and reduces the ability to achieve optimal design.

In the course of this research, relevant works by previous designers would be studied as well as alternative competing conversion technologies. A pump and system would be designed that would best meet a set of defined goals whilst addressing the difficulties highlighted by previous designers. A thermodynamic model of system and flow processes would be refined and system exergy examined. A complex computer simulation initially written by Amor would be extensively rewritten and refined for the new design. The simulation would enable the optimisation of pump geometry to suit any specified installation and predict pump outputs for a chosen system on any given day. The prototype geometry will be optimised such that the system would operate on 2.9 square metres of flat plate solar collector, use n-Pentane as the working fluid and pump a static water head of six metres on a sunny summers day in Christchurch, New Zealand. The pump and its components would be designed, built and the unit tested initially on regulated compressed air to enable some refinement of design a full understanding of pump characteristics to be developed. The second stage of testing proposed was to trial the entire system on a simulated solar boiler whereby heat input to the working fluid could be controlled and closely monitored. In all other aspects all components of the pump would be operating as intended as a closed system, low temperature difference heat engine coupled to a water pump. This stage of testing would also enable the complete experimental analysis and characterisation of the system and give the basis for any further refinement of the theoretical model and

computer simulation. Should the system operate successfully during this stage of testing, the final stage of testing proposed would involve replacing the simulated boiler with an actual solar collector and evaluate the long term performance of the pump under solar conditions and functioning in the intended application.

The development of a small scale low cost water pump does have merit, a functional unit would be of commercial interest as well as generate excitement and intrigue. The following chapters describe the work performed, the problems encountered, the findings and the recommendations for further development of the double acting prototype designed.

# CHAPTER 2 - Building a Solar Water Pump

The building of a solar thermal water pump involves the optimisation and integration of several components. Each component has its own theory and operational characteristics. These characteristics may well conflict between components requiring the optimum point of compromise to be determined.

This chapter outlines the main components of a solar thermal pumping system, the compromises involved in their integration and results of previous research. It discusses configuration options, a potential marketing avenue and working fluid requirements.

## 2.1 Solar Collectors

Although higher operating temperatures resulting in higher efficiencies may be achieved with concentrating collectors, a flat plate collector was chosen for this design because of its simpler construction and reduced cost. Concentrating collectors require some form of one or two dimensional tracking. A significant cost saving with flat plate solar collectors is that their position can be fixed with little loss in performance. The low operating temperatures and inherently low Carnot efficiency by necessity means the engine has to be well designed to minimise unnecessary losses whilst maximising operational reliability. A high speed engine has high frictional losses and significant energy is wasted in fluid turbulence. A low speed, low friction engine with low mechanical and heat losses is required.

The nature of solar energy was discussed briefly in Chapter 1. More detailed analytical and descriptive explanations can be found in a number of texts (Duffie & Beckman 1980, 1974, Kreider et al 1989) and a prolific number of journal publications. Its long term sustainable future promise means it has been the subject of wide research and experimentation.

Solar energy, when it reaches the earth's surface has a relatively low energy density. In order to obtain a practically useful amount of energy, any collection and conversion system must be relatively large.

Solar energy collection technologies are broadly categorised into natural collection systems and technological (man-made) conversion systems. In natural collection systems the total biosphere provides "free" collectors. Conversion devices are required to produce useful energy from the earth, wind and water. In technological conversion systems, the solar energy is itself absorbed/converted into a more useable form and is dependent on the direct level of solar energy impinging on the collector area. The technologies for conversion of solar energy into useful energy are summarised in *Figure 2.1*.

The useful energy comes in many forms including electrical voltage and current, production of hydrogen and other combustible fuels, direct mechanical energy, high and low grade heat. These forms may undergo further transfer or conversion processes before the desired end product is obtained.

Each technology has its own merits. Of specific interest to this research is energy obtained from wind, solar-electric and solar-thermal processes, the most common

forms used for water pumping in isolated locations.

### 2.1.1 Wind Energy Conversion Systems (WECS)

In the traditional form of a rotating windmill coupled to a plunger or displacement pump, the WECS forms the most common type of independent stand-alone water pumps. The simple technology is well proven and will not be discussed in any great detail in this work except as a competitive option to the STWP[1].

### 2.1.2 Photo-Voltaic (PV)

Photo-Voltaic cells produce a DC voltage when exposed to solar radiation. This high grade form of energy is easily converted to mechanical energy for pumping water.

**Photovoltaic Cells**. The photoelectric or photovoltaic effect was first reported in 1941 (Jordan 1988). By 1954, a silicon solar cell, of useful efficiency ≈5% (Sandov 1990) was developed and by 1958 in application in the aerospace industry where the "money is no object" approach resulted in rapid technological advances in this field.

The initial cells were very expensive, restricting use to highly technical applications such as the space and telecommunication industries, but since then significant cost reductions have brought the technology more within general reach and suitable for an increasing range of applications, both "high tech" and "low tech". Examples are the cathodic protection of pipelines, powering of navigational beacons, remote refrigeration units, remote power supplies, electric fencing, village power supplies including water pumping, yacht power supplies, solar cars/bicycles, garden lights, watches and calculators to name only a few.

Photovoltaic cells are made from semiconductors. Energy from the photons and/or electromagnetic radiation, that make up light, causes an electrostatic potential to build across a p-n junction. This potential can be used to drive an external load. Typical output can be seen in *Figure 2.2.*

[1] STWP - Solar Thermal Water Pump.

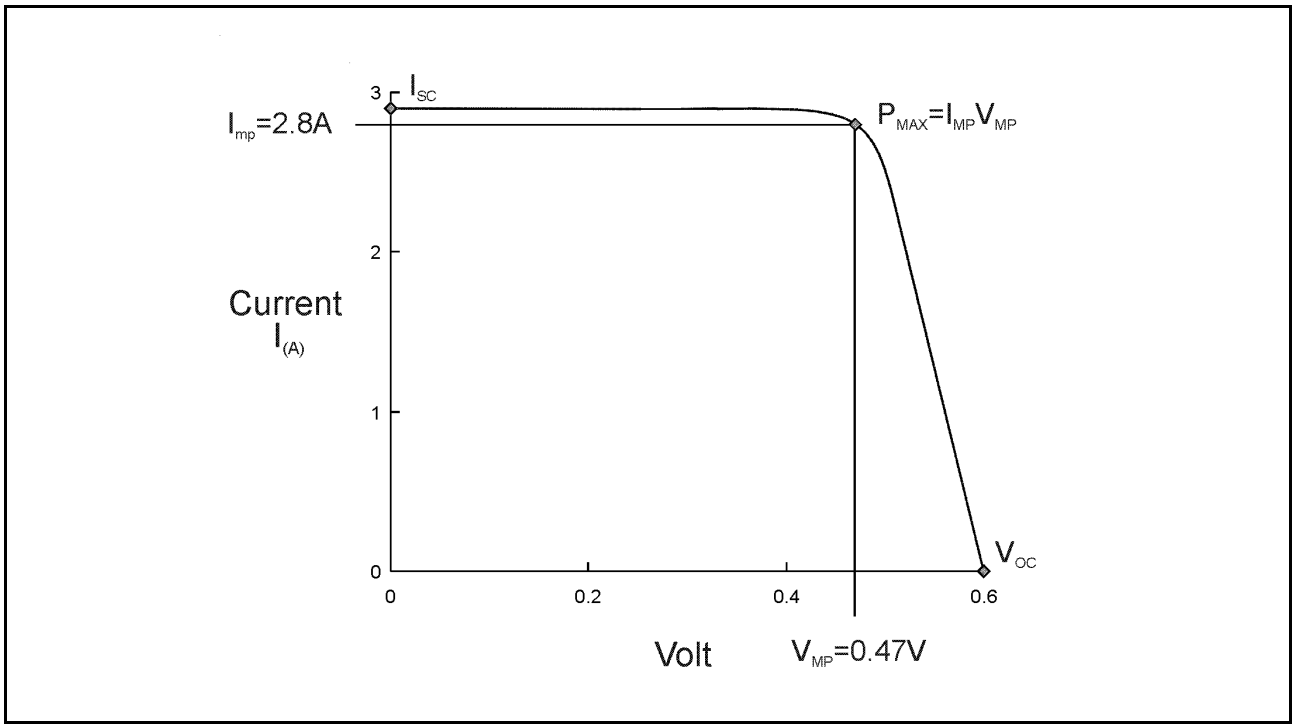


A number of these cells are connected in arrays to provide the voltage and/or current requirements. Typically 30 or more are connected in series to give a nominal 12 V DC once temperature de-rating is allowed for.

Since the initial single crystal silicon cells were developed a number of alternative substances have been shown to exhibit photoelectric properties including hydrogenated amorphous silicon (a-Si:H), polycrystaline silicon (poly-Si), silicon Germanium (a-SiGe), and Fluorinated Silicon Germanium (a-SiGe:F) (Sandov 1990). Conversion efficiencies exceeding 28% (Moore 1992) have been achieved using exotic Gallium Arsenide based cells and HCPV (High Concentration Photo Voltaics). Single Crystal Silicon cells with an efficiency of 11-13%, however have remained the most common because of their lower cost, longer life and extensive development.

### 2.1.3 Solar-Thermal

Technologically the simplest method of utilising incoming solar radiation is to transform the radiant energy into heat in some form of solar collector. Although this

appears to be a simple concept, obtaining the maximum amount of useful energy is an involved analytical and design process. This section covers the basic methods used, simplified methods of analysis and some practical considerations.

A solar collector is a special kind of heat exchanger that uses solar radiant energy to heat a working fluid, usually a liquid or air. Since 1900 at least 50 collector types have been demonstrated as functional. These collectors can be separated into two generic classes: non-concentrating and concentrating.

**Non-concentrating collectors** or flat plate collectors intercept solar radiation on a metallic or glass absorber plate efficiently converting the incident flux to heat. This energy is removed from the absorber plate by means of a heat transfer fluid. Because the temperature of the absorber plate is greater than that of the environment, unrecoverable heat losses occur from the entire absorbing surface of the collector. These collectors have no optical concentration of sunlight, they are generally stationary and typically operate at temperatures below 100°C. For higher temperatures, evacuated tube collectors, where an air space around each absorber tube is evacuated, are used to minimise conductive and convective heat losses, increasing temperature capabilities up to 140°C. Flat plate collectors have the widest application because they are the easiest and least expensive to fabricate, install and maintain.

**Concentrating collectors** attempt to reduce heat loss by reducing the size of the absorber area below that of the aperture. The sun's rays are concentrated on the absorber by shaped reflectors or refractors. Since only direct radiation can be concentrated, most concentrators must track the sun and cannot collect as much diffuse radiation as flat plate collectors. These collectors can achieve high temperatures well in excess of 3000°C depending on the concentration ratio (CR). Concentrating collectors can be full three dimensional imaging (point focus) with $CR \leq 45{,}000$, 2 dimensional imaging (line focus) $CR \leq 212$, or non-imaging concentrators ($CR < 10$ and $T_{max} \leq 175°C$). For systems with $CR \leq 1.7$, no tracking of the sun is necessary. Collectors with $1.7 < CR \leq 5$ generally only require seasonal adjustment. One dimensional or full two dimensional tracking is required for higher CR's.

Two alternative approaches are possible in the preliminary development of a STWP. The first requires the use of a concentrating collector to power a conventional Rankine, Stirling or Brayton cycle engine. The concentrating collectors are necessary to provide the high operating temperatures required by these engines. From an economical approach these systems have to be large (>1kW) to compensate for the high capital cost of engine and collector. A number of studies have covered existing operational systems (Capaldi 1981, Halcrow & Partners 1983).

The second approach is to minimise system costs by using flat plate collectors and designing the engine to operate on small temperature differences by being highly efficient and well matched to collector performance. Although these units may have a lower output per dollar invested (less cost effective) in an appropriate market they may be more practical and affordable. For smaller installations, their size, cost, and simple technology would make them suitable for a very wide range of applications.

This research investigates the design of a compact, low cost engine suitable for operation on a flat plate solar collector. A theoretical discussion of alternative collector forms is omitted.

#### 2.1.3.1 The Flat Plate Solar Collector

Flat plate collectors come in a number of configurations, although typically of the shell and tube type seen in *Figure 2.3.*

Flat Plate collectors basically consist of:

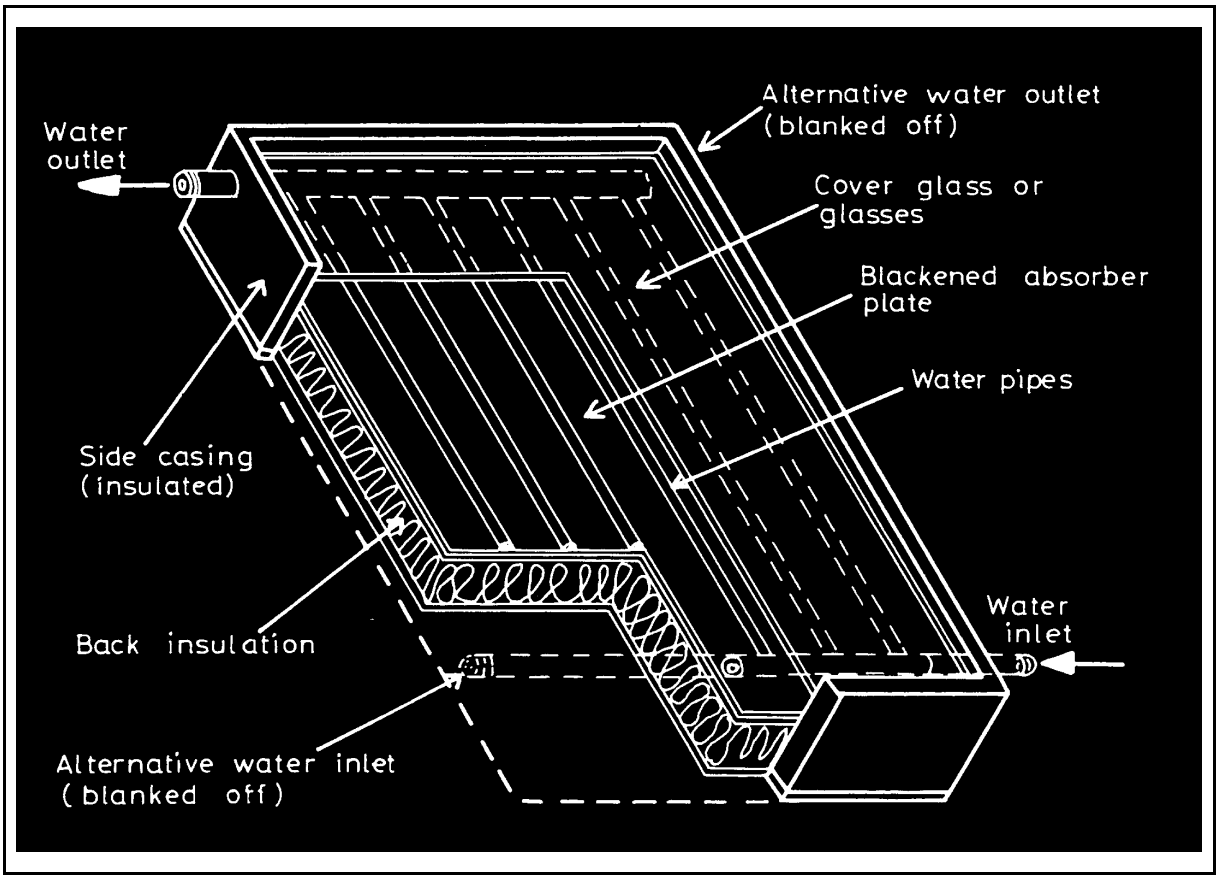


Absorber Plate: Usually made of copper, steel or plastic (Madsen, Goss 1981). The surface is covered with a flat black material of high absorptance. For metallic absorbers, the material may be simply black paint, or a selective coating that maximises absorptance of solar energy and minimises radiation from the plate.

Flow Network: The flow network conducts working fluid through the collector. The network usually consists of a number of parallel tubes attached to the underside or as an integral part of the absorber which acts as a fin for the tube. Tube diameters and spacing are an important part of collector design.

The tubes manifold into headers at the top and bottom of the panel. In a two phase collector, saturated liquid in the bottom of the panel is boiled, and saturated vapour exits through the top header. Most panels operate with a low (approximately atmospheric) internal pressure with a single phase working fluid. Sealed panels with a two phase working fluid must withstand the vapour pressure of the working fluid under stagnation[2] conditions as well as that at low temperatures which usually

[2]Stagnation Temperature - The maximum temperature whereby the heat loss from the

restricts two phase collectors to shell and tube varieties.

panel is equivalent to the heat gain. The efficiency of the panel is zero.

Cover plate: To reduce convective and radiative heat losses from the absorber, one or two transparent covers are generally placed above the absorber plate. The cover plate(s) should have high transmittance ($\tau$) and should not deteriorate with time. Glass is used typically ($\tau \approx$ 85-92%) but a number of plastics such as Tedlar (DuPont) or Polyvinyl Fluoride ($\tau \approx$ 93%) can be cheaper and lighter than glass with a higher transmittance arising from reduced thickness. These plastics often, however, degrade with long term exposure to UV radiation and/or heat.

Although increasing the number of cover plates reduces heat losses, each transparent cover reduces the radiation incident on the collector by at least 10%. Single glazed collectors will usually outperform double-glazed collectors at low and medium temperatures up to 100°C. For some low temperature applications such as in swimming pool heating, collectors are usually left open to obtain maximum efficiency and reduce cost.

Enclosure and Insulation: The collector enclosure is usually made from steel, aluminium or fibreglass composite, sealed to keep out water. Parasitic heat losses from the back and sides of the collector can be reduced by a nonflammable, preferably closed cell packing such as fibreglass.

#### 2.1.3.1.1 Collector Performance

The thermal performance of a collector is well documented and can be calculated from a first-law energy balance i.e.

| | | | |
|---|---|---|---|
| Useful Energy Collected | = | Energy Absorbed by | - Heat Loss to Collector Plate Surroundings |

$$q_u = I_c A_c (\tau\alpha)_s - U_c A_c (T_{cp} - T_a)$$

Or in Algebraic form:

where: $q_u$ = rate of useful energy gain (W)

$A_c$ = area of collector plate ($m^2$)

$I_c$ = global insolation on collector plate ($W/m^2$)

$\tau_s$ = net solar transmittance of glazing

$\alpha_s$ = solar absorptance of collector plate

$U_c$ = overall heat loss coefficient ($W/m^{2\circ}C$)

$T_{cp}$ = average collector plate surface temperature (°C)

$T_a$ = ambient air temperature (°C)

Hence for optimum performance a designer must maximise $(\tau\alpha)_s$ and minimise $U_c$ , often a compromise is required. These parameters can be determined analytically but are typically determined by experiment.

Thermal efficiency of the collector $\eta_c$ can be derived from equation 2.1, it is defined

$$\eta_c = \frac{q_u}{A_c.I_c} = (\tau\alpha)_s - U_c(T_{cp}-T_a)OVERI_c$$

as the ratio of useful energy collected to the total insolation on the collector aperture. The term $(\tau\alpha)_s$ is the optical efficiency of the collector and is the limiting factor on the maximum energy absorption possible.

$$\eta_c = A - \frac{B(T_{cp}-T_a)}{I_c}$$

Equation 2.2 is often written in the general form:
where A and B are constants specific to collector design. Equation 2.3 is commonly known as the HWB (Hottel, Whillier, & Bliss) equation after the main contributors to its derivation.

Equation 2.3 is commonly represented graphically as in *Figure 2.4* which shows performance characteristics for a number of different collector designs.

For an in-depth analysis of collector design refer; Kreith & Kreider, “Principles of Solar Engineering” (1978) and/or Duffie & Beckman, “Solar Energy Thermal Processes” (1974), as good introductory texts. Higher level analysis can be found in a multitude of published papers (for example, Ransmark 1978).

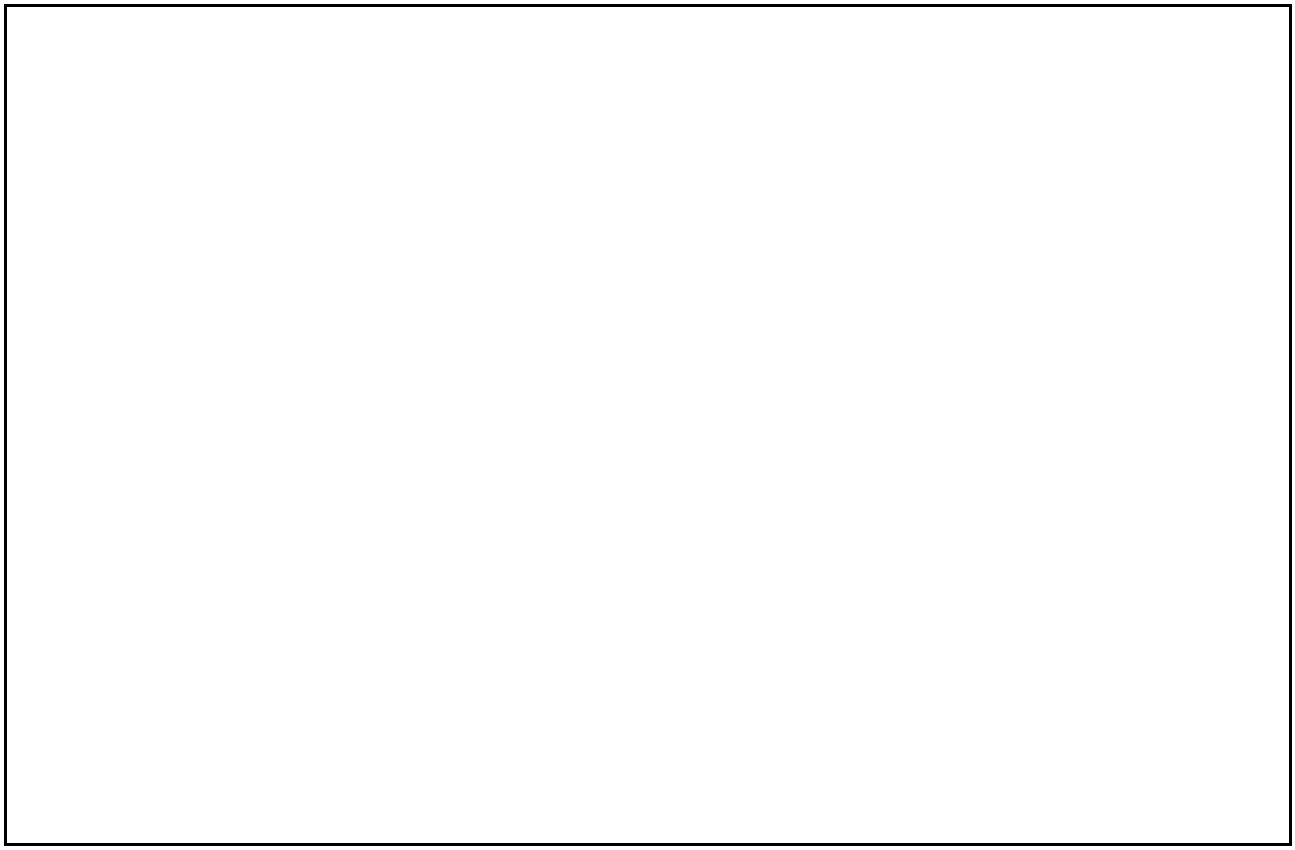

### 2.1.3.2 Single phase vs two phase collector systems

In a single phase solar collector installation, energy is extracted from the solar collector using a heat transfer fluid. A single phase fluid is circulated around the solar

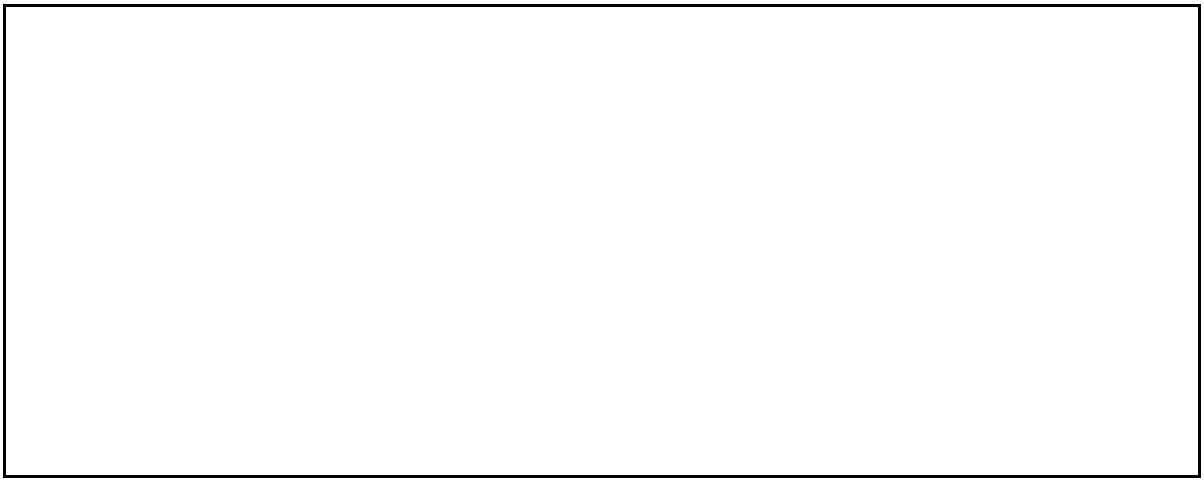

collector and secondary heat exchanger as shown in *Figure 2.5*.

This isolates the working fluid from the collector when the working fluid is highly corrosive or at high pressures or prone to freezing and ensures the collector can never run dry. It does however have a number of disadvantages:-

- The extra cost of the heat-exchanger

- Thermal losses in the heat-exchanger
- Additional cost of a circulation pump

A number of the larger, high temperature solar thermal installations reviewed justify this configuration because of the excessive working fluid vapour pressures. For smaller installations it is more economical to run at lower pressures, eliminating the heat-exchanger and circulation pump by using a two phase collector where the working fluid is boiled within the panels flow network. System design and working fluid selection should ensure panel damage cannot occur, particularly if the circulation of working fluid ceases.

A single-glazed two phase flat plate shell and tube collector with selective surface (giving high efficiency over the 50-70°C operating range) was considered the best alternative for the solar pump. These collectors have the advantages mentioned above of:

1. being able to utilise diffuse solar radiation,
2. not requiring continued re-orientation and tracking of the sun,
3. low cost and
4. minimal maintenance requirements.

Performance may be enhanced by the addition of plane reflectors along each edge.

A number of additional factors must be considered for any solar installation, these include:

- Thermal stress and fatigue
- Equilibrium temperatures under stagnation conditions can bring high temperatures and, in charged two phase collectors, high pressures if not allowed to exhaust.
- Low temperatures can cause extensive damage to the flow network if the working fluid is allowed to freeze.
- Cost. In the selection of a collector for an application, primary consideration must be given to the ultimate cost of the delivered energy. For example, an evacuated tube or double glazed collector would be prohibitively expensive for use as a swimming pool heating system.

- Corrosion created by different materials in electrical contact.
- Cleanliness of Cover Plate. Thermal performance can be severely affected by buildup of grime and dust or internal condensation.
- Environment. The cover plate and enclosure must be strong enough to withstand wind, rain, hail and snow.
- Installation, Shipping and Handling costs are generally high due to size and construction of flat plate solar collectors.
- Lifetime. Most commercially made collectors have a lifetime of 10-30 years with minimum degradation of thermal performance.
- Collector Angle. Axis parallel to sun's movement i.e. east/west and tilt approximately equivalent to the location's latitude.

## 2.2 Water Pumps

Water can be pumped by a number of different methods. The mechanism resulting in fluid displacement is generally:

1. Volumetric displacement (Positive displacement)
2. Dynamic addition of Kinetic Energy (Rotating/Impulse)
3. Electromagnetic force / special effect.

**1. Positive displacement pumps** lift a given volume of fluid every cycle mechanically or by the use of another fluid, by the application of force to a moveable boundary in an enclosed fluid containing volume. Generally they are suited to moving relatively low volumes at high pressure and can be divided into two main classes, reciprocating and rotary.

**Reciprocating pumps** include piston, plunger diaphragm (e.g. bellows) and inertia types, tube or vapour (e.g. Savoy pump). **Rotary pumps** can be of single or multiple rotor varieties and include gear, Archimedean screw, vane, cam, lobe, chain and bucket (dragon spine), progressing cavity.

Positive displacement pumps are self-priming and can generally pass solids in suspension, they can displace fluids of extremely high or extremely low viscosity.

**2. Dynamic pumps** continuously add kinetic energy to a fluid such that on discharge where velocities reduce the pump produces a pressure increase. Dynamic or kinetic pumps can be divided into two classes, centrifugal and regenerative.

**Centrifugal pumps** include radial, axial and mixed flow units. **Regenerative pumps** are also known as turbine or peripheral pumps.

Dynamic pumps are generally suited to high volume, low head applications but depending on design can perform reasonably well at higher heads. They are not self-priming so either need regular priming or to be submerged or partially submerged in the pumped fluid.

Other methods of pumping include electromagnetic, gas lift, jet ejector/venturi pump, hydraulic ram (water hammer pump).

Considerable literature is available on pump types and theory (Goetz 1990, Karassik et al 1986). Typically pumps give better discharge head than suction. This is due to the low pressures that generate the suction causing vaporization of the pumped fluid entering the pump. Vapour bubbles carried into the pump with the liquid collapse on discharge to a higher pressure causing noise, vibration, and erosion. Commonly known as cavitation, significant reductions in performance result.

The most versatile of pumping devices are those that up to the point of cavitation are insensitive to head requirements. Some pump's designs are limited to handling pure discharge head, with very limited or no suction capacity or vice versa.

Halcrow and Partners (1983) have looked extensively at a number of different pump types for solar water pumping applications. Typical solar water pumping installations use centrifugal units operating at around 72% for low heads 2 to 10 meters, or 60-65% for multistaged units pumping higher heads. This study, however, deals mainly with photovoltaic systems or thermodynamic systems in excess of 1 kW (hydraulic) where

rotodynamic pumps provide the most convenient form of energy conversion, and concludes that progress in small scale solar-thermal systems is slow.

For thermal systems less than 100 W (hydraulic) the use of rotodynamic pumps is less desirable with rotational bearing surfaces requiring lubrication and increased mechanical complexity resulting in possibly higher frictional losses. Under low levels of insolation a low power thermal rotodynamic system may have difficulty developing sufficient temperature and pressure to pump, with the rotor spinning for long periods of time on start-up dissipating energy against fluid viscosity.

For a rotodynamic system with water-lubricated bearings, periods of dry-running inevitably cause bearing damage, control equipment may be required to prevent the pump running dry or unprimed, as pump may easily lose its prime during periods of inactivity.

The ideal simple, small-scale, low cost, low maintenance solar-thermal water pump would therefore have no rotating or wearing components. It would operate automatically in a stand-alone fashion, remaining inoperative until adequate driving force (boiler pressure) was available and be self starting and self priming.

Pump type thus has been selected to be a direct acting diaphragm pump. A diaphragm type piston has pressurised working fluid on one side displacing working fluid on the other. Pumps of this style are commercially available as pneumatically powered diaphragm pumps manufactured by Wilden Pump & Engineering, and Warren Rupp (seen in *Figures 2.6 and 2.7*).

These pumps are typically double-acting (duplex) and can operate for very long periods of time dry over a wide range of operating pressures between the static water head and the limit of air supply pressure. They have excellent discharge characteristics with suction limited by the displacer's return mechanism (this may be a spring in a single

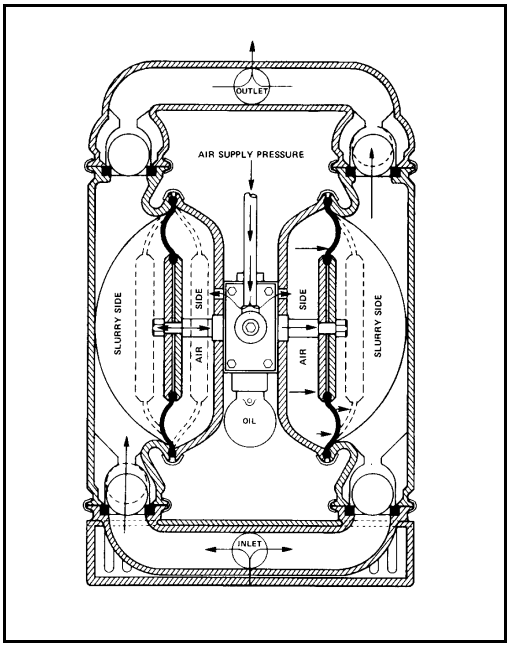


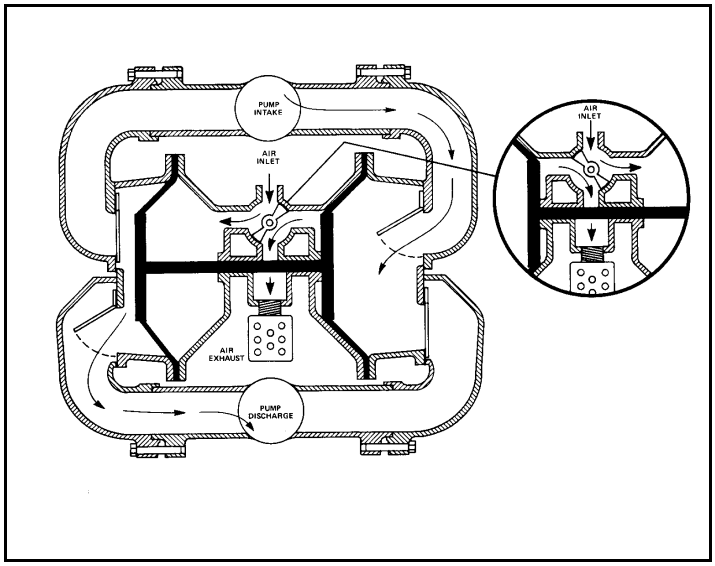


acting machine or air in the opposing chamber in the duplex machine) and the diaphragm deflection arising from the pressure differential across the flexible diaphragm. Suction ability can be improved by constraining the diaphragm to minimise deflections, for example by minimising the flexible area of the diaphragm.

## 2.3 Using Solar Energy to Pump Water

A number of different systems have been proven to utilise solar energy successfully for the purpose of water displacement. Of the man-made systems, mechanical energy for pumping is derived from two different energy conversion processes:

1- **Solar-Electric-Mechanical**

2- **Solar-Thermal-Mechanical**

### 2.3.1 Photovoltaic Water Pumping Systems

These systems are widely available commercially and a number of extensive studies

have covered their use in under-privileged countries (Halcrow & Partners 1983/4). These systems are generally costly; the cheapest Onga Sunmaster submersible pump available in Australasia pumps 200 litres per hour vertically through 7.6 meters (4.2 W hydraulic power) using a 48 Watt panel and costs $3,850 plus freight and GST (shown schematically in *Figure 2.8*).

Photovoltaic systems typically consist of a crystalline silicon photovoltaic array(s), sophisticated electronic control equipment possibly including tracking, electric motor and water pump.

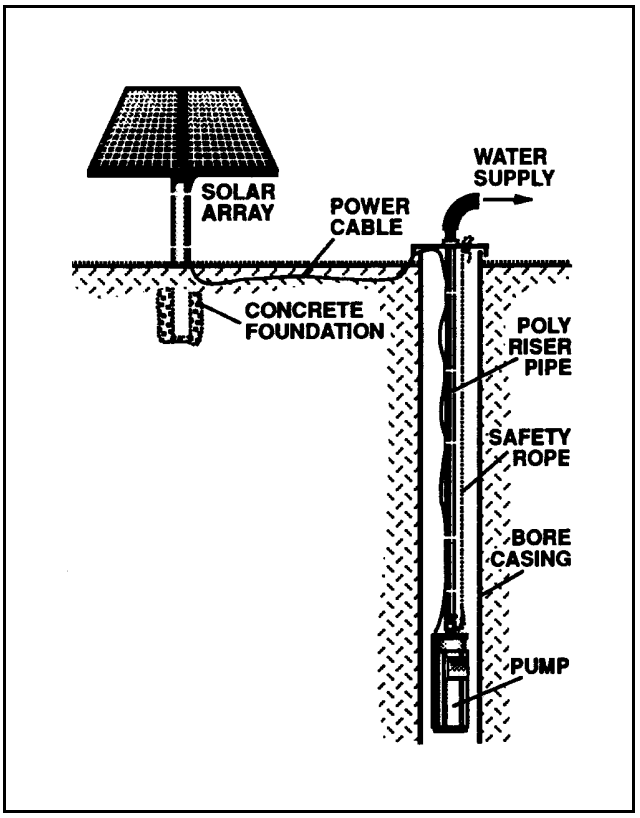


Photovoltaic panels are covered in Section 2.1.2.

The electronic control equipment may consist of a solar tracking system giving typically one but maybe two dimensional alignment for daily, weekly and monthly variations in the sun position. In *Figure 2.2* it can be seen that there is a maximum power point at the knee of the V-I curve for the array. This point is usually incompatible with the requirements of the electric motor, pump and load resulting in poor efficiency. Impedance matching devices, power maximisers or maximum power point trackers (MPPT) act as power (DC - AC) converters and are used to regulate voltage and current output in such a way that the panel is operating at maximum efficiency for any input insolation while correct motor voltage is maintained. Excess array voltage is converted to useful motor current. If correct motor conditions cannot be met under low input levels the controller will shut the system down. Batteries can also be used to condition power, operating at a fixed voltage, however they are costly, have a short operational life, and require regular maintenance.

Electric motors are typically permanent magnet DC motors, brushed or unbrushed.

Some larger units use AC motors because of the greater available range and lower cost. Brushed DC motors generally require new brushes every 2000-4000 hours (1-2 years for a solar pump).

Two different types of pump are commonly used in solar systems:

Centrifugal

- Designed for fixed head, flow increases with rotational speed. - Variations in efficiency occur with changing heads and rotational speed.
- Not self-priming therefore better suited to submerged or floating pump/motor sets.

Positive displacement pumps

- Flow is almost independent of head but proportional to speed
- Efficiency increases with increasing head. More efficient than centrifugal pumps at high heads.
- Self priming with good suction and discharge characteristics.

Self-priming is an essential feature of solar pumps due to the frequent number of unattended starts which occur daily or throughout the day as a result of cloud variations.

Provided water-lubricated motor/pump sets are not allowed to run dry, maintenance of PV pumping systems is low with well-developed proven and reliable components making up the system, however, 5-10 yearly replacement of the arrays and the high initial capital cost make these units unattractive for many ideal applications.

### 2.3.2 Solar-Thermal Water Pumping Systems

Three main components are required for a solar thermal water pump:

1. **Solar Collector** - responsible for the conversion of incoming solar radiation to

heat.

2. **Heat engine** (or Prime Mover) - required to use available heat source with a corresponding heat sink to generate mechanical energy.

3. **Water pump** - converts mechanical energy from the prime mover to hydraulic energy of the desired pumped fluid.

Each process has individual characteristics which must be matched to obtain maximum benefit from the complete system.

Significant energy losses occur in the first two conversion processes which have mutually incompatible characteristics. Section 2.2 discussed the thermal efficiency of

$$\eta_c = A - \frac{B(T_{cp}-T_a)}{I_c}$$

a solar collector based on a first law analysis represented as Equation 2.3.
A, B are constants defining panel characteristics.

The second term in Equation 2.3 means that as the difference between collector plate temperature ($T_{cp}$) and ambient temp ($T_a$) increases panel efficiency ($\eta_c$) drops.

The efficiency of any heat engine operating between a temperature source $T_H$ and a

$$\eta_E = \frac{T_H - T_C}{T_H}$$

temperature sink $T_C$ has an upper limit equivalent to that of the Carnot cycle i.e.
As the temperature difference between the source and sink increases so engine efficiency ($\eta_E$) increases.

$$\eta_o = \eta_c . \eta_E$$

The overall system efficiency is a combination of $\eta_c$ and $\eta_E$ i.e.
It can be seen from *Figure 2.9* an optimum operating temperature exists for the pump

and prime-mover combination.

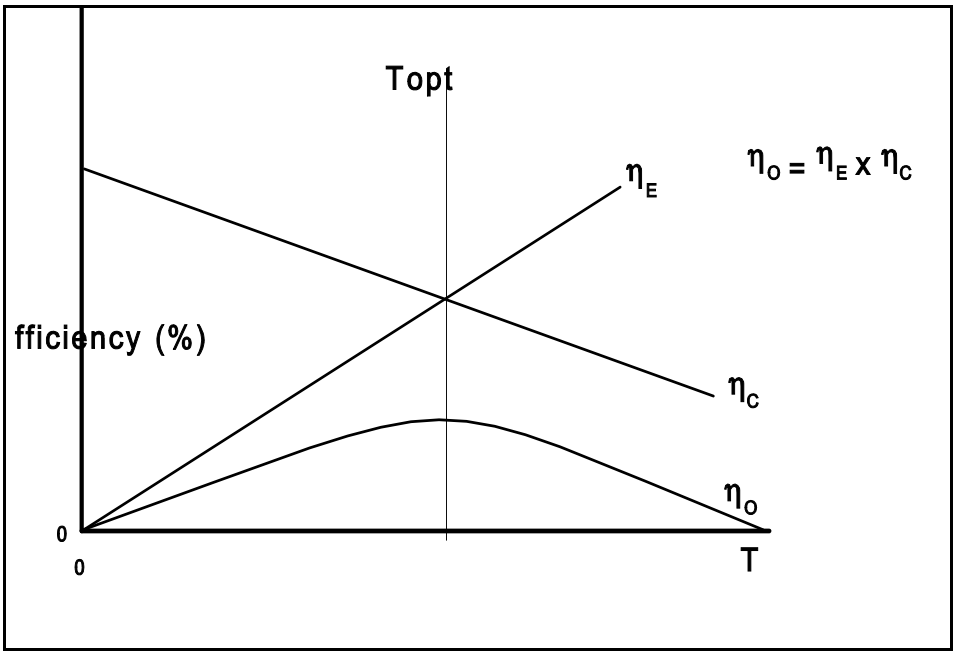


If $T_H$ is assumed to be $T_{cp}$ and $T_C$ is approximately $T_a$ then by differentiating Equation 2.5 with respect to $T_{cp}$ and equating to zero, maximum system efficiency occurs at a

$$T_{cp_{opt}} = \left[\frac{A}{B}.I.T_a + T_a^2\right]^{½}$$

panel temperature of:

Thus for an ordinary single glazed collector with A=0.88, B=7.6, for an insolation of 750W/m$^2$ and ambient temperature of 17°C Equation 2.6 gives:

$$\underline{T_{CP\ opt} = 57.6°C}$$

In reality, with the daily variation in irradiation and individual engine characteristics, the calculation of optimum system configuration for maximum daily performance is considerably more involved. Chapter 4 discusses the optimisation code written to simulate and determine the ideal system configuration.

The underlying trade-off is a financial one and increased overall efficiency can be obtained by increasing panel efficiency at higher temperatures. This requires the use

of concentrating collectors, solar tracking and high temperature materials all at higher cost. A larger system is required to reduce the invested dollar per unit hydraulic power. The challenge is to devise a system that pumps a useful volume of water (not an excess) while keeping cost per unit hydraulic power low. Obviously the system design is dependent on application. The Solar Panel has been discussed and was selected based on an available model matching the requirements of this study.

### 2.3.2.1. Types of Prime Mover

Different heat cycle engines (prime movers) were covered by Amor (1992). The principle of operation generally falls into one of three general categories:

1. Thermal Expansion of Solids. A number of different phenomena can be used to extract mechanical energy from thermal input :

a. Thermal expansion, (Beam et.al. 1973) whereby a stressed tube is heated on the compressed side and cooled on the side in tension around the circumference, this results in a turning moment. These devices are slow due to the limited rate of heat transfer with a low efficiency (the higher the stress the greater the efficiency but the greater the fatigue loadings).

b. Phase Change. Shape memory alloys, such as NITINOL, when appropriately treated undergo an unusual 'Marmen' cycle. The material changes shape depending on temperature as it moves between phases. Reasonable theoretical efficiencies have been reported for Marmen cycle engines, Mohomed (1979) predicts 9% when Carnot produces 20% but the low thermal diffusivity of the material requires small sections of considerable lengths.

A number of small engines have been built using the unusual characteristics of shape memory alloys. Tanaka (1992) reports on an engine with a calculated efficiency 20% of Carnot. Tong (1975) derives an equation for the theoretical efficiency of the Marmen cycle giving 20% when Carnot is 87%. Banks (1981) generates electricity using a simple solar collector and a 45 degree temperature difference. An estimated 3-4% efficiency was claimed less frictional losses (which would be considerable) when Carnot is 12%.

c. Differential Expansion, normally in the form of thin strips of metal with different rates of thermal expansion (typically Invar and Brass) bonded together to form bimetallic strips (Trihey, 1976). When heated the resulting deflection can be used to do work. A bimetallic water pump was suggested by Trihey but efficiency is inherently low because of high internal stresses within the prime mover (0.02% for a 170°K temperature difference (Amor 1992)).

d. Thermally contracting. Rubber is one of the few materials that contracts on heating. A number of small engines have been designed to heat and cool rubber in a cyclic process (Strong 1971). An engine of useful output would be large and costly again due to the low thermal diffusivity (4% of NITINOL) with an estimated upper efficiency of 0.2% (Amor 1992). Regular replacement of the rubber is necessary with oxidation and creep reducing performance.

Generally the low thermal difffusivity of solids result in large slow machines with a multitude of thin sections of the material and low efficiency.

2. Thermal expansion of liquids and gases. Among the many theoretical air standard cycles, devices operating on the Stirling and Brayton cycles are most commonly used in the thermal to mechanical energy conversion of solar irradiation (Capaldi 1981). Covered extensively in standard engineering thermodynamic texts, technical details of these cycles and engine operation will not be discussed.

Engines operating on these cycles are generally complex with high precision rotating components and seals. Financial viability of Stirling engines or Brayton cycle turbines therefore requires large systems with significant solar concentration to obtain the temperatures required to achieve appropriate efficiencies. Such machines generally vary between 1 kW to 50 kW and exist in a limited number of installations worldwide (covered by Halcrow and Partners (1983)).

The theoretical cycle efficiency of Stirling and Brayton cycle engines is given by:

$$\eta_S = \frac{T_{cp} - T_C}{C + T_{cp}}$$

$$\eta_B = 1 - \frac{T_C - T_{I1}}{T_{I2} - T_{cp}}$$

and

where: $T_{cp}$ = Hot temperature (°K)

$T_C$ = Cold Temperature (°K)

$T_{I1\&2}$ = Intermediate Temperatures (°K)

C = a factor depending on regeneration

For temperatures below 300°C the Brayton cycle efficiency would tend to zero because of internal inefficiencies. For the Stirling cycle, practical results indicate that efficiency drops off dramatically for source temperatures below 250°C (Capaldi 1981). Higher source temperature see ideal Stirling and Brayton efficiencies approaching that of the ideal Carnot cycle. Practical Stirling engines achieve at best about 50% of Carnot efficiency.

Small scale engines although feasible are too costly to manufacture to be viable.

One possible exception to the high cost of conventional Stirling machines, is the simple Fluidyne engine. This engine still undergoes a standard Stirling cycle but has minimal moving components due to a liquid piston arrangement seen in *Figure 2.10.*

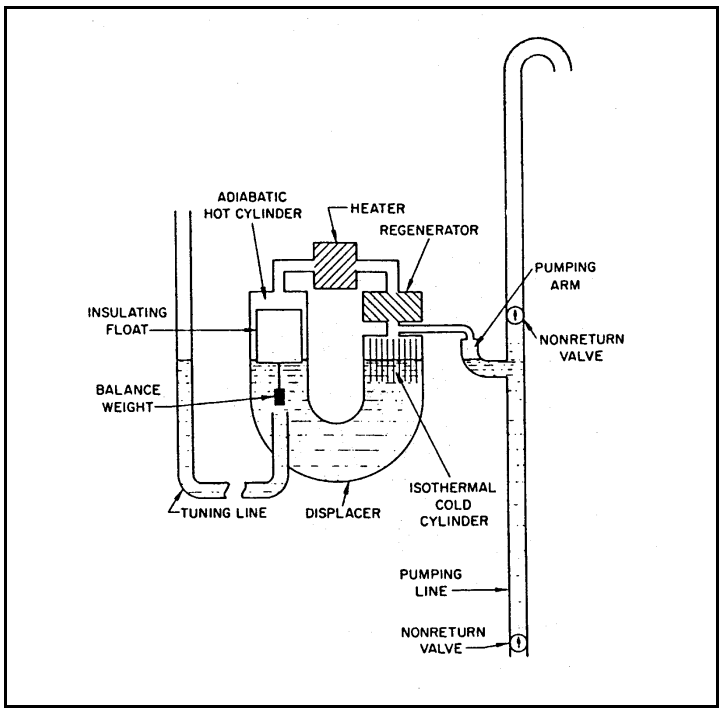


As the liquid in the U-tube oscillates, gas is displaced between the hot and the cold cavities, flowing through the regenerator, resulting in a change of gas volume. Coupled to a water column and a pair of one-way valves this phenomenon can be used to pump water. These engines have the advantages of low friction, simplicity, self-starting, and no sliding mechanical components, but operate at low pressure (therefore low head) and low frequency (low output). The pressure is determined by internal pressure variations, in turn dependent on the gas density; increasing gas density would force the liquid acting as the displacer out of the system. The frequency is determined by the natural frequency of the displacer, large displacer lengths are required to get usable displacements. Fluidyne pumps are therefore large, low power and low head devices, although a small number of prototypes have been built (West 1986). Walker (1985) covers a number of small novelty Fluidyne engines capable of water displacement.

3. Liquid/Vapour Heat Cycle Engines. By far the greatest number of prototype solar-thermal systems built to date use a Rankine or near Rankine cycle. The Rankine cycle theoretically and practically can have workable efficiencies at source temperatures below 100°C, making low cost, low concentration or flat plate solar collectors a suitable high temperature energy source.

The Rankine cycle is discussed in Chapter 3. However in simple terms, liquid/vapour cycle systems consist of a boiler which generates quantities of vapour by boiling a liquid working fluid. Pressure generated by the corresponding increase in volume is used in an engine to produce work. The exhaust is cooled in a condenser and the condensate returned to the high pressure boiler via a small feed-pump (illustrated in *Figure 2.11*).

In conventional Rankine systems the working fluid is water, the engine is a turbine, and a small volume of vapour is superheated and expanded isentropically (ideally) to produce work in a continuous flow process.

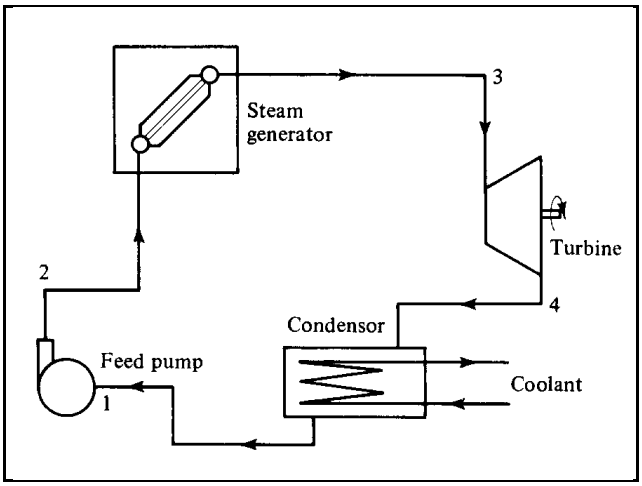


Simplified reciprocating engines executing discrete flow cycles similar to the Rankine cycle are common in small scale solar applications because of the potentially lower manufacturing costs, but are significantly less efficient.

The simplest engines are direct acting, the pressure of the working fluid acting directly on the pumped fluid isolated by a piston or diaphragm.

In a solar powered direct acting Rankine cycle engine the only inertial mechanism to ensure continued motion is that of the pumped fluid. If a displacement pump is in the process of self-priming or start-up this inertial mass is very small and stalling is highly likely especially under low levels of insolation. Thus the engine may induce a volume of working fluid with inadequate expansion potential to complete the cycle. This problem is commonly solved in these engines by having the expansion chambers open to the boiler throughout the induction stroke ensuring adequate pressure is available to complete the stroke. This means work is extracted from the cycle during the evaporation stage and not during the expansion stage. Work potential of the high pressure vapour is lost on exhaust. This cycle has been dubbed the "Modified Rankine cycle" and although of lower efficiency allows the design of a much simpler, more reliable prime mover.

The majority of work carried out by previous designers directs the development of small solar-thermal pumping systems toward third world or underprivileged countries. As a replacement to a village handpump or windmill it should at least meet the following criteria:

a - The United Nations Development Programme (UNDP) defined the Village Level

Operation and Maintenance (VLOM) scheme, outlined by Arlosoroff (1987) it specified pumps must incorporate the following features:

- Ease of maintenance
- Robustness
- Locally manufacturable from common materials
- Standardisation of components, operation and maintenance
- Low cost
- Reasonable discharge rate for effort involved (applies to handpumps)

b - Speidel (1978) adds for solar pumps:

- High efficiency
- Self-priming
- Freedom from maintenance
- Simple Construction
- Easily repaired
- Fabrication in user's country.

c - Boldt (1978):

- Without moving parts
- Low import share

d - Amor et al (1991) suggested:

- Equivalent work to pump which it would replace
- Appropriate technology
- Use of a non-CFC working fluid
- Use of working fluid above atmospheric pressures

e - Raine et al (1994) added:

- Adaptability for local solar radiation climates
- Condenser heat should be utilised to heat the pumped water where applicable

Much of these criteria apply to a unit designed for any purpose in any locality.

f - The author adds:-

- Use of nontoxic, non flammable working fluid
- Cheap to repair
- Waste heat should be used in any co-generation system, eg. space heating, water heating
- Self-starting

# CHAPTER 3 - Modelling of A Solar Thermal Engine

This chapter looks at the thermodynamic principles behind operation of the prime mover. It acts as a theoretical basis for the following chapter which discusses the modelling and optimisation of the collector, prime-mover and water pump combination.

The prime-mover executes a closed loop liquid-vapour cycle whereby an organic working fluid is circulated between a hot and a cold temperature source changing state in the process. Aside from system leakage, the mass of working fluid remains constant. The cycle resembles a Rankine cycle. It occurs as a batch rather than a continuous flow process and has been referred to as the "Modified" Rankine cycle or “Modified Organic Rankine Cycle” (MORC) where an organic working fluid is used.

## 3.1 Theoretical Rankine Cycle

The basic Organic Rankine cycle shown in *Figure 3.1*, is divided into four different processes and is carried out by four separate mechanical components.

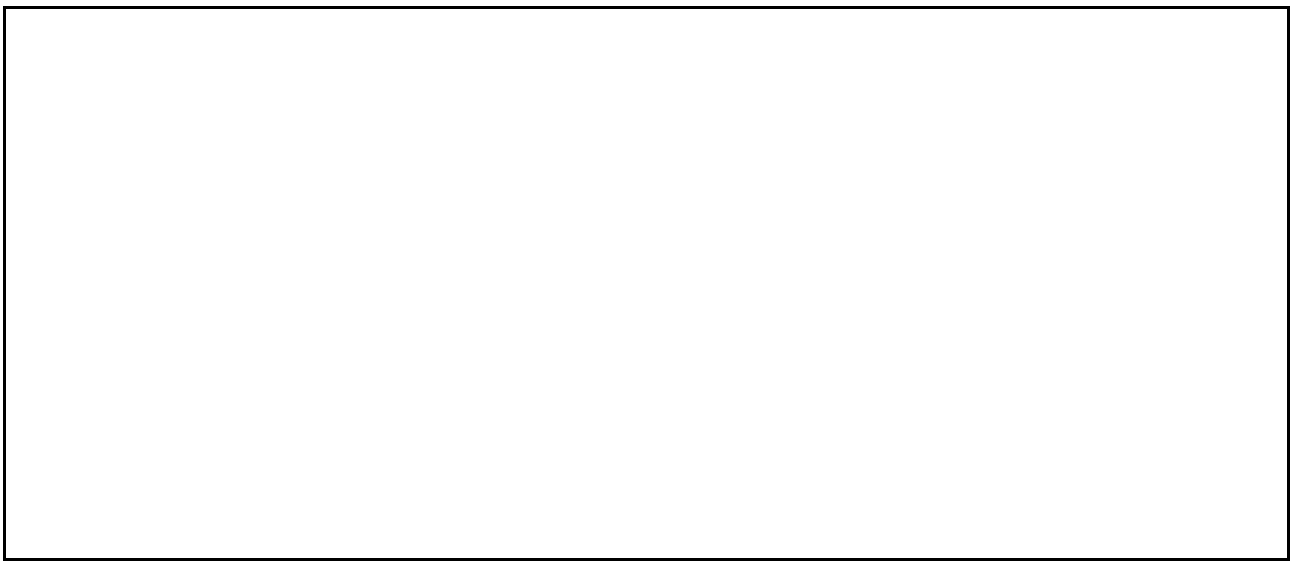

1-1A-2 - represents a constant pressure heating and occurs in a boiler (high temperature "source"). 1-1A is a temperature increase of the working fluid to a saturated liquid state. 1A-2 is a constant temperature change of phase to form high pressure saturated vapour. Applying the first law of thermodynamics for unit mass

$$q_{1\text{-}2} = q_{in} = h_2 - h_1$$

flow rate gives:

2-3 represents an isentropic expansion. During this stage work is extracted from the

$$w_{s_{2\text{-}3}} = -(h_3 - h_2)$$

cycle by an expander (typically a turbine). Work output is given by:

3-4 The wet vapour is condensed in a heat exchanger (low temperature "sink") to a

$$q_{3\text{-}4} = (h_4 - h_3)$$

saturated liquid state. The heat removed from the cycle is given by:

4-1 represents isentropic compression of the low temperature, low pressure saturated liquid in a small feed pump which returns the working fluid to the boiler. The work required during this stage is low as the saturated liquid is essentially incompressible.

$$w_{s_{4\text{-}1}} = -(h_1 - h_4) \approx -v_4(p_1 - p_4)$$

It can be shown (Karlekar 1983):

$$w_{cycle} = w_{s_{2\text{-}3}} + w_{s_{4\text{-}1}} = (h_2 - h_3) - (h_1 - h_4)$$

The net work of the cycle is:

$$\eta_{Rankine} = \frac{w_{cycle}}{q_{in}} = \frac{(h_2 - h_3) - (h_1 - h_4)}{(h_2 - h_1)}$$

and efficiency:

Rankine cycle efficiency is lower than the Carnot Efficiency for the same operating temperature limits:

$$\eta_{Carnot} = \frac{T_H - T_C}{T_H}$$

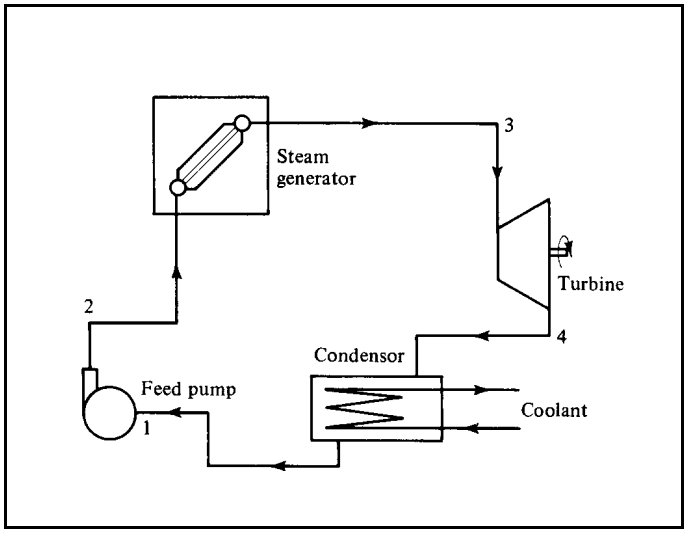


The components required to execute a Rankine cycle are illustrated in *Figure 3.2.* The thermodynamic state (Canjar 1967) of the working fluid in a system using n-Pentane and based on an ideal Rankine cycle operating between $T_H$ = 55.3°C and $T_C$ = 23°C, can be seen summarised in Table 3.1[1].

[1] The values in this table are read from a P-h diagram for n-Pentane and therefore may have small errors associated with their value.

# CHAPTER 4 - Computer Simulation and Optimisation

## The geometrical parameter optimisation and modelling of system operation.

Once the Solar Thermal Water Pump's (STWP) basic operation, configuration of ancillary components, and functional layout was defined as described in Chapters 2 and 3, it was necessary to further develop the theoretical understanding by creating a model to simulate the pump's operation. The model was to perform calculations of pump geometry to suit panel size, performance and insolation as well as to act as a performance basis against which operation of the working prototype could be compared. Presented in this chapter is an overview of simulation operation, rather than a line-by-line analysis of the code. It is important that the reader understand overall function before detailed analysis of the code presented in Appendix 3 can be undertaken.

The simulation was written in PC based Fortran initially by Amor (1992) but required extensive modification to simulate the double-acting configuration and to enhance reliability of operation. The simulation takes global position co-ordinates and, using solar panel characteristics, calculates the energy delivered to the working fluid based on quantities of direct and diffuse radiation, solar angle, reflective and convective losses and ambient temperature at 15 minute intervals for any specified day. It then optimises pump geometry and operating temperatures using multi-variable optimisation techniques, to achieve the maximum water flow for that day at the specified static water head. At the heart of the simulation, an iterative technique is used to balance energy flow on an incremental basis throughout the pump's cycle.

## 4.1 Program Structure

The methodology behind the simulation is shown in the flow diagram of *Figure 4.1.*

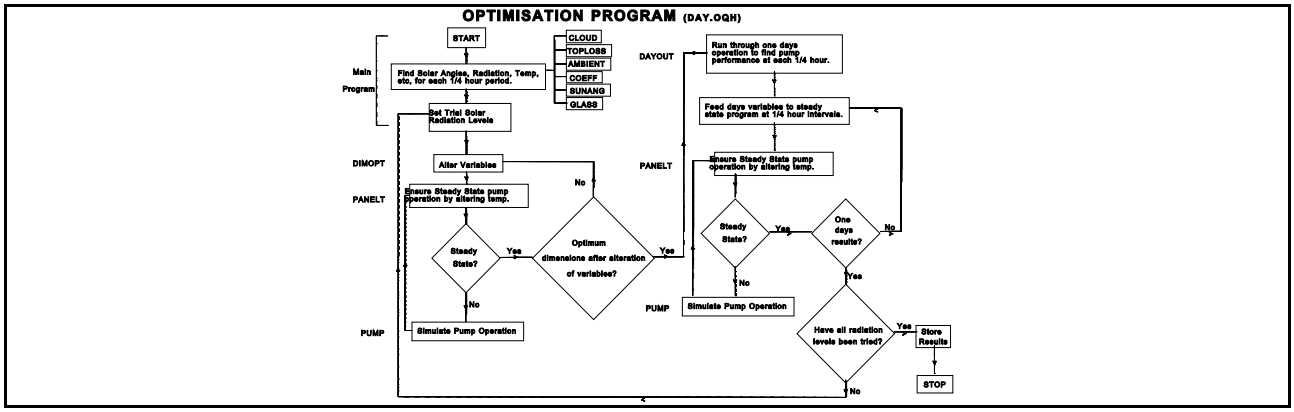


In the first stages of the program the parameters that undergo daily variation, and those associated with the collection of solar energy, are calculated between the hours of 4am. and 11.45pm. at 15 minute intervals. This section of the program was adapted from the work of Kysar (1988) who investigated the tracking of solar radiation and sunlight in rooms.

Maximum and minimum levels of daily insolation are used to set five different trial values of solar radiation equi-spaced between 150 W/m$^2$ above the minimum level, and 150 W/m$^2$ below the maximum level. The optimum pump geometry is based on maximum water output and is determined for these trial levels of insolation by altering the system temperature until the point where steady state operation is achieved. This steady state occurs when energy flows throughout the system balance based on a first law analysis. Once the optimum geometry is determined for that level of trial insolation, water output for one complete day of operation is calculated by the second stage of the program.

Once a complete day of pumping has been simulated for each of the 5 pumps optimised to operate at the trial levels of insolation, the water output for each is compared and the pump giving the greatest daily flow is recorded.

This approach considers that a system designed to operate at high levels of insolation will operate with high efficiency and a high flow-rate but for a short period of the day. Conversely a system optimised to operate at a low level of insolation will have a lower efficiency (low flow-rate) but operate for a greater period of the day. There exists an intermediate design optimum for the function:

$$\text{Water Output per Day} = \text{Mean Flow Rate during Operation} \times \text{Period of Operation}$$

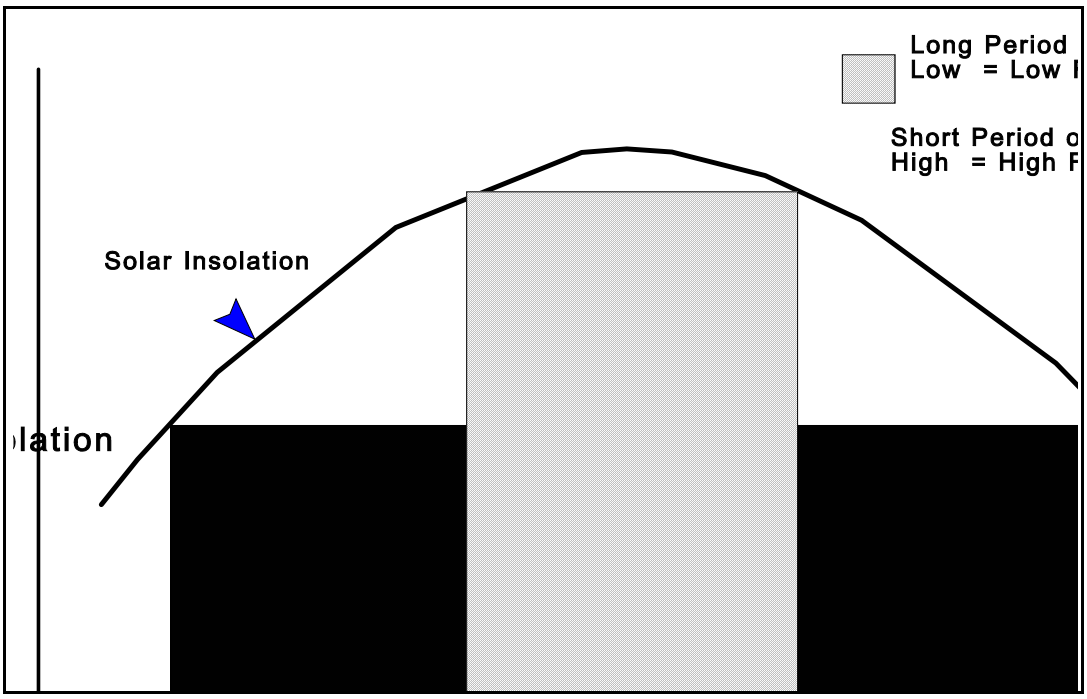


This can be seen pictorially in *Figure 4.2.*

Once the optimum set of pump parameters is determined, results of the complete day's pumping are stored.

Another feature of the simulation is the ability to skip the optimisation routine to determine daily performance for any specified pump geometry under non-optimal conditions.

This feature enables the researcher to manually investigate effects that variations in any geometric parameter set in the simulation (such as the static water head, intake or discharge pipe geometry, panel size, etc) will have on the performance of a specified pump as well as investigate its operation during different seasons of the year. The number of variables either set or calculated in the simulation is quite significant. The effect any one of these parameters has on pump performance is a study in its own right. A number of these as well as those optimised by the simulation have been studied to ensure correct operation of the routine (for results see Section 4.4).

The pump considered in this research has been optimised to lift water through a static

head of 6m during operation on a clear summer's day in Christchurch, New Zealand. Operation of this pump under static heads ranging from 2m to 9m is also considered.

## 4.2 The Sub-routines, Operation And Purpose

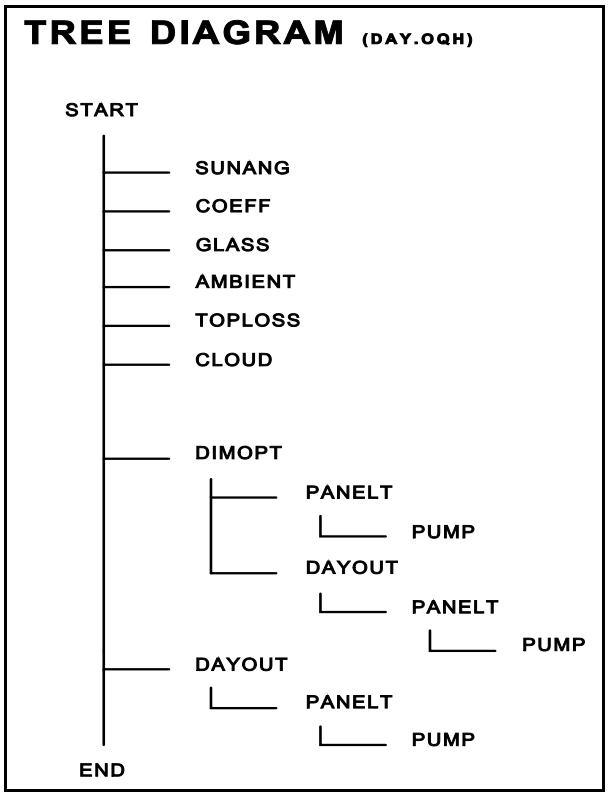


This section looks more closely at the operation of the model. It outlines the function of each of the routines that make up the simulation, the basis, assumptions and controls to which they work. The main program is responsible for setting initial variables and controlling the user interface. The tree diagram of *Figure 4.3* shows the layout of the subroutines called by the main program and in turn those nested within these subroutines. The first six subroutines determine environmental parameters at 15 minute intervals. Following this procedure, pump parameters, system operating conditions and pump operation are examined for each of the 5 trial levels of insolation discussed in the previous section, and daily output calculated. The last section records performance and operating conditions of the optimised pump for each 15 minute interval in the day.

### 4.2.1 Subroutine SUNANG

This subroutine calculates the altitude and azimuth angles of the sun at any point on the earth at any time of the year. The angle of incoming beam radiation is then calculated in terms of directional cosines u,v,w and is dependent on location, latitude, time of year (giving declination or angular position of the sun at solar noon with respect to the equator) and time of day.

For a discussion on the principles behind the sun's motion and positional calculations refer Kreider et.al. (1989).

### 4.2.2 Subroutine COEFF

This subroutine is essentially a coefficient look up table to allow the calculation of variations in radiation intensity resulting from the earth's elliptical orbit. The values

$$I = \frac{A}{e^{\frac{B}{\sin(alt)}}}$$

and equations were based on arguments presented in ASHRAE (1989) where:

where: A = apparent solar radiation at air mass = 0 ($W/m^2$)

B = atmospheric extinction coefficient

alt = solar altitude

I = Insolation ($W/m^2$)

Air mass is a term relating to the attenuation of radiation in the earth's atmosphere. Air mass = O refers to extraterrestrial radiation. Coefficients in the look-up table vary on a monthly basis but are adjusted within the main program by interpolation for the day of the month. The equation gives average radiation intensity for a cloudless day.

Values of diffuse radiation are calculated in the main program as a fraction of total radiation. This fraction is also sourced from the look-up table in subroutine COEFF and essentially is based on the clearness index (or cloudiness index in some texts). The clearness index is the ratio of terrestrial solar radiation to extraterrestrial radiation. It enables an estimate to be made of the monthly average of diffuse radiation as a portion of daily total radiation.

A hypothetical angle of incidence is calculated both for diffuse radiation from the sky incident on the collector and diffuse radiation reflected from the ground. The angle gives an effective beam radiation incidence angle for the diffuse component enabling calculations of effective radiation absorbed by the collector.

### 4.2.3 Subroutine GLASS

This subroutine calculates the amount of solar radiation transmitted and absorbed, rather than reflected, by the glass cover of the solar collector given the angle of incidence of beam radiation or the hypothetical angles of incidence for diffuse radiation.

Transmittance, reflectance and absorptance are functions of the incoming radiation and the thickness, refractive index and extinction co-efficient of the material. The refractive index, n, and the extinction co-efficient, K, are generally functions of the wavelength of the radiation. In this analysis however, all properties are assumed to be independent of wavelength. For glass covers this is an appropriate assumption. Absorptance and transmittance of energy into and through one or more glass covers is

$$\tau_r = \frac{1}{2}\left[\frac{1-r_\perp}{1+(2N-1)r_\perp} + \frac{1-r_|}{1+(2N-1)r_|}\right]$$

given by Equation 4.2 (Duffie and Beckman 1980):

where: $\tau_r$ = non reflected component of radiation

N = number of glass covers

$$=\frac{\sin^2(\theta_2-\theta_1)}{\sin^2(\theta_2+\theta_1)}$$

$r_\perp$ = perpendicular component of reflected unpolarised radiation

$$=\frac{\tan^2(\theta_2-\theta_1)}{\tan^2(\theta_2+\theta_1)}$$

$r_|$ = parallel component of reflected unpolarised radiation

where: $\theta_2$ = angle of refraction, and

$\theta_1$ = angle of incidence

of light through the glass

$$\frac{\sin\theta_2}{\sin\theta_1} = \frac{n_1}{n_2} \quad refractive\ index\ ratio$$

note, Snells Law:

The absorption of direct and diffuse radiation by the glass is allowed for with an absorption coefficient which takes into account the path length of the light through the cover. The remaining radiation is transmitted to the collector plate.

### 4.2.4 Subroutine AMBIENT

This routine maps the changes in ambient temperature as the day progresses. Given the average daily temperature range, average monthly temperature range and average maximum temperature for the hottest season for a location, it is possible to estimate average temperature for any particular day and superimpose hourly temperature variations to give the complete day's temperature map (Trewartha 1980). Although approximate, the method may be applied to most locations but will not account for climatic phenomenon such as monsoon seasons.

### 4.2.5 Subroutine TOPLOSS

Convective and radiative heat loss from the collector cover and body are a function of surface area and temperature differential. An overall loss co-efficient ($W/m^2K$) made up of a top loss co-efficient ($U_T$) and a back loss co-efficient ($U_b$) is calculated. Edge losses are small for well-designed collectors and in this analysis are neglected. For

$$U_b = \frac{k}{L}$$

the collector back, thermal losses are approximated by Equation 4.3:

where: k = Insulation conductivity (W/m.K)

L = Insulation thickness (m)

Convective and radiative losses from the collector cover are more complicated and have been modelled by numerous researchers. Garg (1984) compared a number of

different models and by tests run on an actual collector proposed the following set of

$$U_T = \left[ \frac{N}{\frac{c}{T_{p,m}} \left[ \frac{(T_{p,m}-T_a)}{N+f} \right]^e} + \frac{1}{h_w} \right]^{-1} + \frac{\sigma(T_{p,m}^2+T_a^2)(T_{p,m}+T_a)}{\left[ \frac{1}{d} + \frac{2N+f-1}{\varepsilon_g} + g - N \right]}$$

relations for the calculation of the top loss co-efficient.

$$c = \frac{204.429(\cos\beta)^e}{L^{0.24}}$$

$$d = \varepsilon_p+0.0425(1-\varepsilon_p)$$

$$e = 0.252$$

$$f = \left( \frac{a}{h_w} - \frac{30}{h_w^2} \right) \left( \frac{T_a}{316.9} \right) (1 + 0.091N)$$

$$g = 0$$

where:

and: $U_T$ = Top Loss Coefficient ($W/m^2K$)

N = number of glass covers

$\beta$ = collector tilt (degrees)

$\varepsilon_g$ = emittance of glass

$\varepsilon_p$ = emittance of plate

$T_a$ = ambient temperature (K)

$T_{p,m}$ = mean plate temperature (K)

$h_w$ = wind heat transfer coefficient ($W/m^2K$)

L = plate spacing (m)

$\sigma$ = Stefan Boltzman constant ($W/m^2K^4$)

The total heat loss co-efficient is taken as:

$$U_L = U_b + U_T \qquad (W/m^2K)$$

and heat loss:

$$Q_L = U_L.A_p$$

where: $A_p$ = surface area of collector cover
≈ surface area of collector back

### 4.2.6 Subroutine CLOUD

During periods of cloudiness, values of diffuse radiation increase as the direct radiation is blocked by cloud and scattered. Total energy absorbed by the collector plate is reduced during that period of cloud by a function of cloud coverage and cloud type.

Lestrade et al (1990) give values of insolation dependent on cloud cover and normalised to the calculated clear-sky global insolation. The code in this subroutine returns these values given a level of cloud cover.

Values of cloud cover are based on human estimation and corrected for cloud depth and viewer latitude by the simulation using a series of correction factors from Malberg (1973). The corrections compensate for the overestimates made from the viewer seeing the side of the cloud at low angles of inclination.

The period of equivalent cloudiness for each 15 minute interval is determined and used later in the simulation to determine pump downtime or reduced performance resulting from cloudy periods.

**At this point all of the above factors have been determined for each 15 minute period throughout the day. The code then begins the optimisation and system simulation procedures which are run for each of the five trial levels of insolation.**

### 4.2.7 Subroutine DIMOPT

This subroutine performs the multi-variable optimisation that determines the main

pump and prime mover dimensions for the geometry outlined in Chapter 2 ie:

1. Pump / vapour chamber outer diameter
2. Vapour chamber internal diameter (defined as a ratio of overall diameter) and
3. Pump / prime mover stroke.

From these values primary geometry is defined, the remaining geometry (components such as the diaphragm, feed pump, valve) can be related to, or calculated from the primary geometry.

The optimisation routine used is inefficient and crude but performs a reliable map of all combinations of the primary variables. The objective function (function to be optimised) is water output with the pump operating at the trial design insolation mentioned earlier. The water output is determined by a series of subroutines nested within this routine.

Sensible limits are placed on the variables and the solution area mapped with a coarse grid to minimise the number of iterations defining the locality of the maximum. The optimum set of variables (maximum value of the objective function) is obtained and a second finer mesh created around this first solution. With this second mesh outside diameter is defined to within 5mm, internal diameter ratio to within 1%, and stroke length to within 1mm of their respective optimum values. Results and performance for each iteration is displayed visually on screen.

The path to optimal geometry is deliberately biassed slightly by a requirement that a greater than 1% improvement in water output is necessary before the simulation will select a lesser preferred geometry. The bias preferences are toward a minimum pump overall diameter, maximum vapour chamber working area and maximum stroke.

The smallest pump diameter was desirable not only for minimising overall size but also vapour chamber surface area to minimise thermal losses to surroundings. The larger working area of the vapour chamber allows useful work to be done at lower operating pressures. To minimise effects of dead volumes within the vapour chamber and minimise vapour chamber surface to volume ratio, a bias is placed on a larger stroke. The effects of the bias can be seen in later sections.

Although time-consuming, this method of multi-variable optimisation proved totally reliable. Amor (1992) used an iterative technique which determined the most sensitive variable (that having the greatest effect on the objective function) which is then adjusted to produce the desired response. The next most sensitive variable is optimised and so on. It was found this method of optimisation was too easily fooled by localised maxima and the interrelationships between variables could not properly be accounted for.

**After optimum pump dimensions have been determined this routine then calls a further subroutine to calculate the full day's water output.**

### 4.2.8 Subroutine PANELT

Thermal equilibrium of the entire system with its surroundings occurs at one specific operating temperature. This energy equilibrium (or steady state temperature of operation) is determined by a three stage search which is the primary function of this routine. For a specified insolation, static head, and pump geometry, subroutine PANELT manipulates the simulation of the pump's operation. The energy flows are evaluated by a first law energy analysis based in subroutine PUMP, the results of which are

transferred back to subroutine PANELT for evaluation.

Upper and lower limits on operating temperature are set manually with flags to indicate if the energy balance is tending to a temperature outside the specified range. The first sweep across the temperature range defines the operating condition to within 5°K. The limits are automatically modified (range reduction) and the second sweep defines the temperature to 1°K. The final sweep gives solar collector temperature to 0.25°K (refer *Figure 4.4*). This is an exhaustive technique and is simply a single variable optimisation based on the same principle as the multi-variable

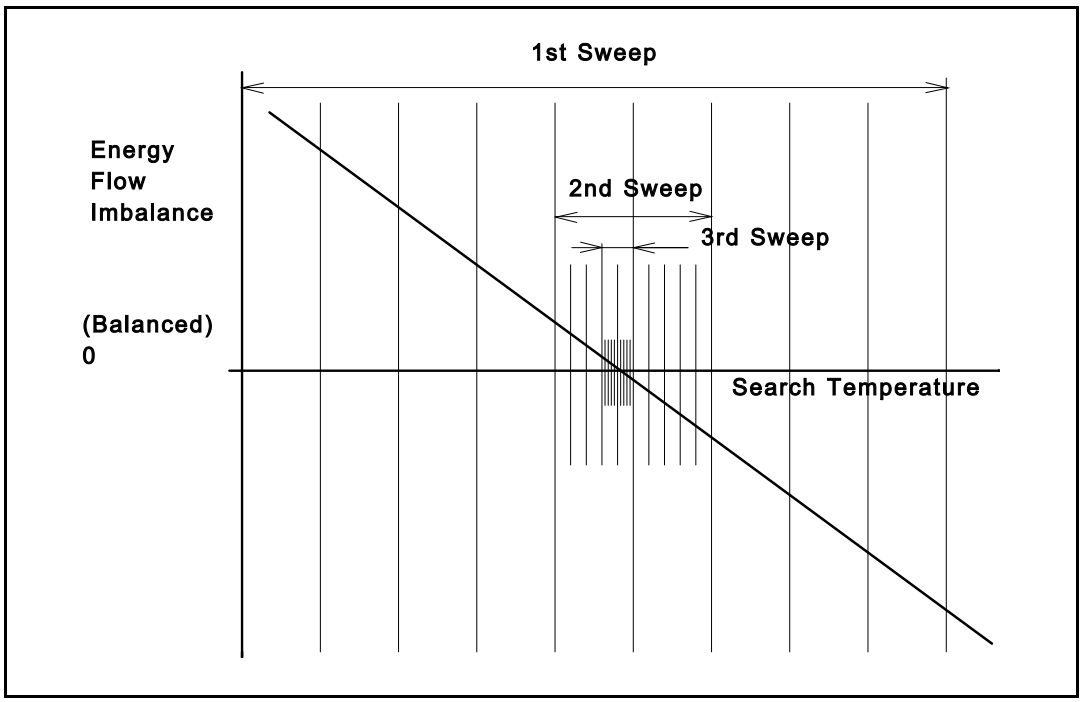


optimisation used in subroutine DIMOPT to determine pump geometry. The internal energy of the entire system is calculated by this routine for each different trial temperature based on the thermal mass of the working fluid (liquid and vapour), solar collector, pump and ancillary components which, under the steady state conditions remains relatively unchanged during the pump's cycle. The thermal inertia of the system is important during startup and for short periods of cloud during operation.

Flags are located in this routine to indicate if an adequate energy balance could not be found within programmed temperature limits. This may occur if, for example, there was a high rate of change of energy flow with small changes in temperature ie. a more accurate temperature definition would be required. A flag to indicate an inadequate thermal input for operation is also included.

### 4.2.9 Subroutine PUMP

This subroutine models the operation of the collector, prime mover and pump combination. Its primary function is to evaluate energy flows on a finite difference basis for a complete cycle of the pump (as described in Chapter 3) given input parameters of:

1. System internal energy (based on trial operating temperature)
2. Static suction and discharge heads
3. Pump geometry (outside diameter, vapour chamber inside diameter ratio and stroke length)
4. Ambient temperature (for that 1/4 hour of the day)
5. Panel operating temperature
6. Total radiation incident on the collector's absorber
7. Cloudiness factor

Other variables set within the subroutine include:

8. Length and diameter of waterside plumbing
9. Frictional loss co-efficient (k) of water flowing through pipes and fittings including entry and exit losses
10. Thermal mass of the constituent parts of the complete system

The subroutine initiates by calculating a number of simple geometric parameters based on these inputs for example:

water pipe area

radial length of diaphragm for the nominated stroke

effective working area of vapour and water chambers to account for the reduced displacement that occurs near the fixed region of the diaphragm

volumetric displacement in all chambers as a result of diaphragm inversion at the beginning and end of each stroke.

Inverting of the centre diaphragm counts as an irreversibility. In the diaphragm separating the vapour chamber and water chamber this inversion does useful work causing some displacement of the pumped fluid.

**4.2.9.1 Simulation of Energy Flow**

Three stages of prime mover operation are treated:

Stage 1 - Immediately prior to the control valve opening the vapour chamber to the high pressure vapour of the boiler, the vapour chamber is at condenser pressure (low vapour specific volume) and minimum internal volume. When the controlling valve opens, the incoming vapour must first pressurise the dead volume within the chamber and invert the centre diaphragm. The vapour/water chamber diaphragm may or may not invert depending on suction head and condenser pressure.

This first stage calculates the volume left within the vapour chamber and the mass of vapour required to both raise the pressure of this initial volume to operating pressure and invert the diaphragms. A small quantity of liquid must evaporate to do this. Pressure is calculated throughout the routine using the Antoine

$$\log_{10} P = A - \frac{B}{T+C}$$

Vapour Pressure Equation (Othmer, 1980).

where P = pressure (kPa)

T = temperature (°K)

A,B,C = fluid specific constants. For n-pentane:

A = 6.00122

B = 1075.78

C = - 39.94

Valid for the temperature range (220 to 330°K (-53 to 57°C)).

Work is done effectively expanding the system boundary. The useful work (inverting vapour/water chamber diaphragm) is calculated, the rest of this work is non-useful and results in no water output but requires energy - it is essentially flow work.

Stage 2 - The second stage of operation is where displacer motion occurs. The displacer's motion is tracked in 1/20 th second increments from minimum to maximum displacement. The dynamic[1] pressure of the induced and expelled water and that of the working fluid is calculated at the beginning of the increment and assumed constant for that increment. Balance of applied forces allows calculation of the acceleration of the displacer and mass of flowing water based on equations of motion. The induced mass of water accelerated from rest for that increment at the intake effectively increases dynamic pressure and reduces overall acceleration as its rate of change of momentum is higher than that of the mass already flowing in the system (unless of course the system is at startup from rest). Based on the acceleration of the displacer, its change in velocity and travel are calculated for that interval giving the corresponding change in velocity of the pumped fluid and displaced volume of water.

The limit of displacer acceleration and velocity is the point at which cavitation[2] occurs in the inducting side of the pump, a flag

[1]The dynamic pressure is based on static head, fluid velocity and frictional losses of the flowing water through pipework.

[2]Cavitation occurs when low suction pressures cause vaporisation of the pumped fluid.

is used to reject the combination of variables as cavitation can cause pump damage and inefficient operation.

The system pressure is recalculated every interval based on:

1. amount of system expansion (work)
2. heat flow into the working fluid from solar radiation
3. conduction through rubber diaphragms
4. convective and conductive losses from vapour chamber to water chamber
5. conductive and convective losses from the vapour chamber body to surroundings
6. convective and conductive losses to surroundings from the insulated copper pipe connecting the panel to the pump.

The last increment before the displacer reaches maximum travel is assessed as the fraction of a 1/20 th second interval required to complete the stroke.

Bubbles of vapour collapse when pressure rises rapidly.

Stage 3 - The final stage of operation, the exhaust and condensation stage of the cycle, was the most difficult to simulate. It was necessary to simplify the modelling of this stage until such a time as experimentation and analysis could be used to empirically define process dependencies. The parameter critical to the operation of the pump is the variation of pressure within with time P(t) in the exhausting chamber for the duration of the stroke. The relationship for P(t) was difficult to define due to the many factors affecting the changing pressure, namely:

1. vapour chamber volume
2. static water head*
3. solar insolation and panel efficiency*
4. valve orifice size and exhausting flow losses
5. internal volume of condenser and exhaust ducting
6. condenser area, construction and the rate of condensation
7. heat losses within pump
8. panel pressure/temperature*
9. condenser pressure/temperature (initial and time dependent variations)
10. valve leakage (high pressure to low pressure)
11. displacer speed, acceleration and dynamic water head*

*related variables

The instant the valve opens to exhaust the high pressure vapour, so too does it allow fresh high pressure vapour to enter the opposing (inducting) chamber. A time delay is assumed to occur at the end of the stroke during which the displacer remains stationary and the exhausting vapour is assumed to expand adiabatically into the condenser. Condensation then occurs until the pressure within the exhausting vapour chamber drops sufficiently low enough for the high pressure vapour in the inducting chamber to force displacer motion in the opposite

direction. During this delay it is assumed the pump ceases to lift water and that water velocity drops to zero for the beginning of the exhausting stroke. In reality this time delay would represent a period of rapid deceleration of the displacer. The valve should toggle just before the displacer reaches maximum travel.

Thus the assumed pressure profile in the exhausting chamber is shown in *Figure 4.5(a)*. The lower pressure of 90 kPa was an estimate of the mean pressure (Equation 4.6) of the vapour in the pump exhausting and condensing after the adiabatic expansion. The estimate was based on the working fluid dropping from a temperature of 54°C, to a mean effective condenser temperature of 23°C, and that the condenser volume is approximately equal to the full vapour chamber volume. *Figure 4.5(b)* shows a more probable pressure versus time distribution.

$$P_{mean} = \frac{1}{t_{stroke}} \int_{t_{beginning\ of\ displacer\ motion}}^{t_{end\ of\ stroke}} Pdt$$

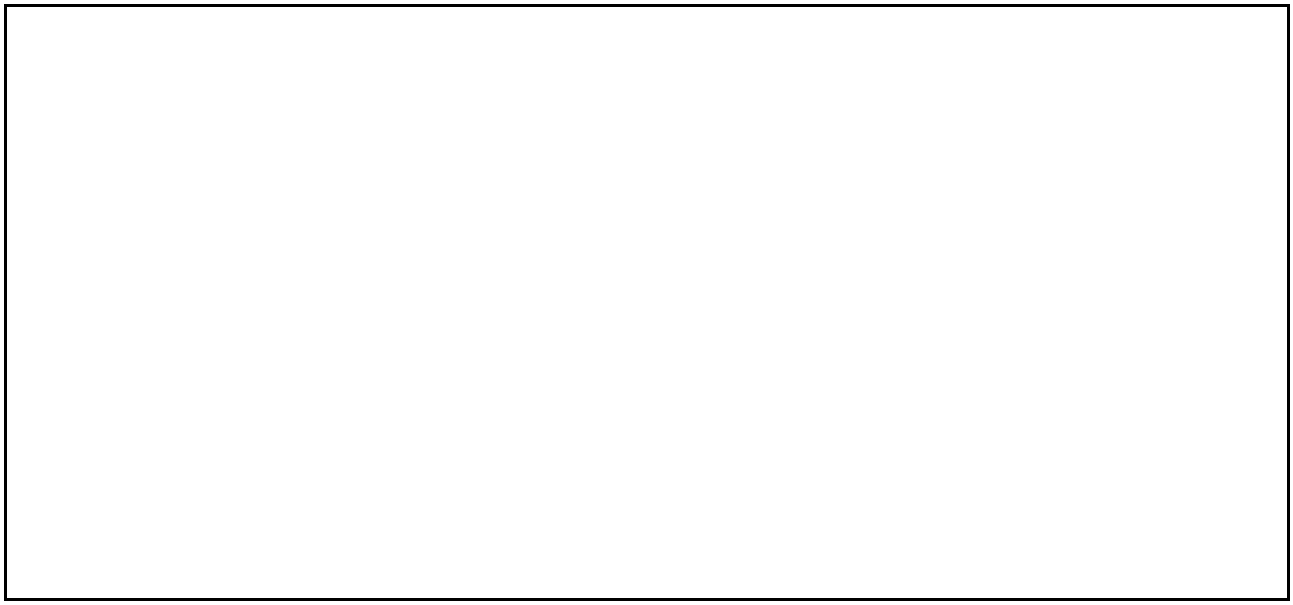

Displacer motion commences at the end of the time delay. Acceleration of the water in the inlet and discharge pipes is defined by Equation 4.7(a) and assumed constant for the 1/20 th second interval. Displacer acceleration is directly related assuming incompressible flow of the water, by the ratio given in

$$a_{water}=\frac{1}{\rho_w(l_1+l_0)}\begin{bmatrix} [P_{VC1}-P_{VC2}] & \frac{A_{VC}}{A_{WC}} & \\ -\rho_w & g & (,PREH,+,SUKH,) \\ - & \frac{1}{2}\rho_w V^2\sum(k_I+k_O) & \\ (,1,) & (,2,) & (,3,) \end{bmatrix} \quad (a)$$

$$: \qquad a_{displacer} = \frac{A_{pipe}}{A_{WC}} \quad a_{water} \qquad (b)$$

Equation 4.7(b).

where: $\rho_w$ = density of water (kg/m3)

$l_1$, $l_0$ = length of intake and discharge piping (m)

$\rho l$ $\propto$ mass of pumped water

$P_{VC1}$ = absolute pressure in filling chamber (Pa)

$P_{VC2}$ = absolute pressure in exhausting chamber

(Pa)

$A_{VC}$ = working area of vapour chamber ($m^2$)

$A_{WC}$ = working area of water chamber ($m^2$)

g = gravity ($m/s^2$)

PREH = static water head of discharge ($mH_2O$)

SUKH = static water head of suction ($mH_2O$)

V = average water velocity for interval (m/s)

$\Sigma(k_I+k_O)$ = sum of fluid flow losses

The first term (1) in Equation 4.7(a) represents the driving force on the displacer from the prime mover. The second term (2) is the force associated with the static water head and the third term (3) that of the dynamic water head. Note:

12. The force to accelerate the displacer is assumed negligible as its acceleration and mass is so much less than that of the pumped water.
13. The velocity used to determine the dynamic water head is the velocity reached at the end of the previous interval.
14. Conservation of momentum is used to apply a small iterative correction factor to the acceleration of Equation 4.7(a) to compensate for the induction and acceleration from rest of a new volume of water and corresponding discharge of the same volume of water.

The heat rejected to the condenser, rise in temperature of the cooling water and the change in internal energy of the system as the condensed fluid is returned to the collector is calculated. Feed pump work is assumed negligible for the cycle.

For each change that occurs during the execution of these stages the energy flow is summed in a piecewise integration for the entire cycle. Thus for the working fluid the first law of thermodynamics states:

$$\int_{cycle} \text{Heat absorbed} \; - \; \int_{cycle} \text{Losses} \; - \; \text{INTfrom}_{cycle} \; \text{Condensation} \; - \; \int_{cycle} \text{Work} \; = \; \Delta U_{cycle} \rightarrow$$

$$(,1,) \quad (,2,)(,3,) \quad (,4,) \quad (,5,) \quad 0$$

where: (1) is the transfer of solar energy to the working fluid in the solar collector

(2) includes cycle irreversibilities such as volumetric and uncontrolled heat losses

(3) is the heat removal from the working fluid in the condenser

(4) is the work done by the working fluid on the displacer (system boundary)

(5) is the change in total internal energy of the system.

For a system executing a thermodynamic cycle, steady state operation would require that the energy flows balance and term (5) be zero. Subroutine PANELT adjusts system operational temperature to satisfy this requirement.

#### 4.2.9.2 Cloudiness

The above routine simulates the operation of the panel, prime mover and pump combination for the 15 minute period being analysed. A final calculation carried out assesses the effect cloud has on the water output for that period. The level of cloudiness and consequent level of diffuse radiation during that period is calculated in the main program and subroutine CLOUD. The temperature to which the collector will fall is calculated in subroutine PUMP based on Equation 4.9 (Duffie 1980).

$$\frac{I-u_L(T_{C_f}-T_a)}{I-u_L(T_{C_i}-Tsuba)} = e^{-\left(\frac{A_P u_c \tau}{(mC)_e}\right)}$$

where:

| | | |
|---|---|---|
| I | = | Insolation ($W/m^2$) |
| $U_C$ | = | collector top loss coefficient ($W/m^2K$) |
| $A_p$ | = | collector area ($m^2$) |
| $(mC)_e$ | = | heat capacity of system (J/K) |
| $T_C$ | = | collector temperature (K) |
| $_i$ | = | initial |
| $_f$ | = | final |
| $T_a$ | = | ambient temperature (K) |
| $\tau$ | = | time of reduced insolation (s) |

The time required to reheat the collector to within 10% of operational temperature and time of reduced insolation is treated as downtime and the volume pumped for that 15 minute period is reduced accordingly.

### 4.2.10 Subroutine DAYOUT

Once subroutine PANELT determines the correct operating temperature for the particular set of geometric variables and subroutine DIMOPT has determined the optimum geometry for the particular trial insolation, subroutine DAYOUT uses subroutines PANELT and PUMP to calculate the performance and output of the system for each 15 minute interval in a complete day.

**The main program compares the water output from the complete day's pumping for each of the pump geometries optimised for each of the trial levels of insolation. The pump geometry that results in the greatest volumetric output for the day analysed is kept as the final output. The comparison is set up to prioritise the geometry that functions at low levels of insolation. The complete day's output is recalculated and stored. The Simulation code is presented in Appendix 3.**

## 4.3 Results From Computer Optimisation

The simulation was instructed to optimise pump dimensions for a system operating on a good summer's day in Christchurch, New Zealand, with the following parameters:

| | |
|---|---|
| Panel Area | 2.9 $m^2$ |
| Static Water head (H) | 6 $mH_2O$ |
| Pipe length (L) | 15 m |
| Pipe Diameter (D) | 40 mm |
| Frictional loss coefficient (k) | 10.1 (Intake → Discharge) |
| Cooling water temperature | 23°C |

These conditions were based on the assumption that the end use for this pump would be as a circulation device for the solar heating of a swimming pool. The static water head was based on a 5m vertical suction and 1m vertical discharge to simulate a pump located on a high roof near the pool and discharging into solar water heating panels. The design head is deliberately more than adequate to satisfy a typical installation of this type, the pump would also be suited to other applications. Due to the double acting configuration of the pump, the actual distribution of the suction and discharge heads has minimal theoretical effect on pump performance (except during cavitation). For example, similar performance would be expected with a 1m suction and 5m discharge head.

The optimised pump geometry (simulation output) for the above conditons was:

Pump Outside Diameter: 250 mm

Diameter ratio of:

**Error!**

0.25

giving:

Inside Diameter of Vapour Chamber 62.5 mm

Radial length of diaphragm 40 mm

giving:

Pump Stroke 50.9 mm

Optimised for a design Insolation 653.5 $W/m^2$

The pump operates for 9½ hours per day and displaces approximately 10.41 $m^3$ of water. The results of a full day's pumping are shown in Table 4.1.

Operation and Performance of the optimised pump under static heads ranging from 2.0m to 9.0m was then calculated for the same day. Daily averages for the same hours of operation are presented in Table 4.2.

# CHAPTER 5 - Prototype Design and Manufacture

Pump design alternatives were discussed in Section 2.6 - Conceptual Design. In summary, the system would operate on a modified organic Rankine cycle utilising flat plate solar collectors. A reciprocating double acting configuration was favoured with a mechanically activated pressure independent controlling valve. The feed pump would be incorporated into the unit and driven by the displacer movement. Rolling diaphragm seals were chosen for complete isolation of the working fluid. For versatility an external water-cooled condenser was desired.

This chapter looks at the main components that make up the Solar Thermal Water Pump (STWP), some design options and the final system configuration. Some design compromises were made in the fabrication of the prototype due to the lack of ready availability of some materials, expensive manufacturing techniques requiring moulding or press tools, or lack of developmental time to provide each individual component with the analysis, refinement and attention to detail desired.

A cross-section of the prime mover and pump combination can be seen in *Figure 5.1*.

Optimised geometrical parameters (refer Chapter 4) gave a pump working diameter (overall internal diameter) of 250mm, a vapour chamber OD of 250 mm and ID 62.5mm and stroke of 51 mm.

## 5.1 Valve

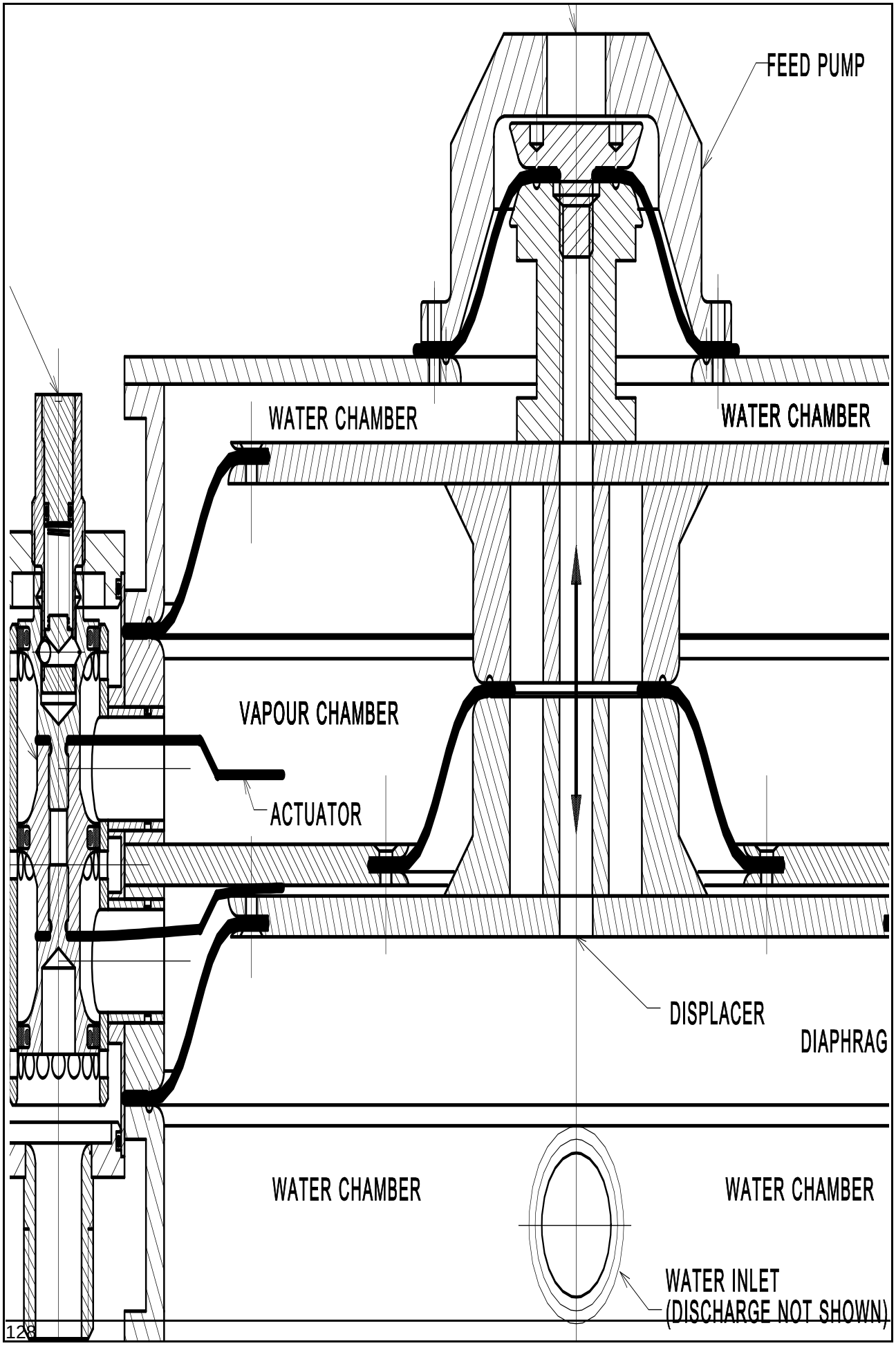
FEED PUMP
WATER CHAMBER
WATER CHAMBER
VAPOUR CHAMBER
ACTUATOR
DISPLACER
DIAPHRAG
WATER CHAMBER
WATER CHAMBER
WATER INLET
(DISCHARGE NOT SHOWN)

Of all components in the prime mover / pump mechanism the main controlling valve is the most complex both in design and function. In a double-acting arrangement the valve must alternate freely between allowing one chamber to exhaust whilst the other fills and vice versa when the displacer reaches the end of its stroke. It must be simple in design and to manufacture, have large flow areas to minimise fluid frictional losses, incorporate extremely good sealing with low friction seals and have a low actuation force. Preferably the valve should operate independently of operating pressures and toggle reliably with zero cross-over between exhaust and inlet ports. Some form of latching or detent is desirable to ensure the valve does not get stuck in any non-functional position. The moving parts within the valve should be capable of running unlubricated in the working fluid environment. All parts where possible should be designed for low precision, low technology manufacture to minimise component cost.

There have been a variety of methods used by previous designers of vapour actuated reciprocating pumps. A number use highly toleranced sliding metal to metal contact seals (Thureau et.al. 1976, Dorr Oliver 1972, Sharma 1980) in either rotating or reciprocating valves, others use polymer face seals (Xhi Chen et.al. 1985, Hamilton 1974, Amor 1992), flap seals (Umarov et.al. 1976), conical or ball seals (Lee 1957, Speidel 1977) or polymer radial seals (Kelsey 1974, Kishone et.al. 1986) which are either mechanically or pressure actuated. Of the literature sourced many authors fail to detail anything more than basic schematic drawings.

Of the many options considered, a mechanically actuated spool valve was considered the simplest configuration. A detailed cross-section of the valve can be seen in *Figure 5.2.*

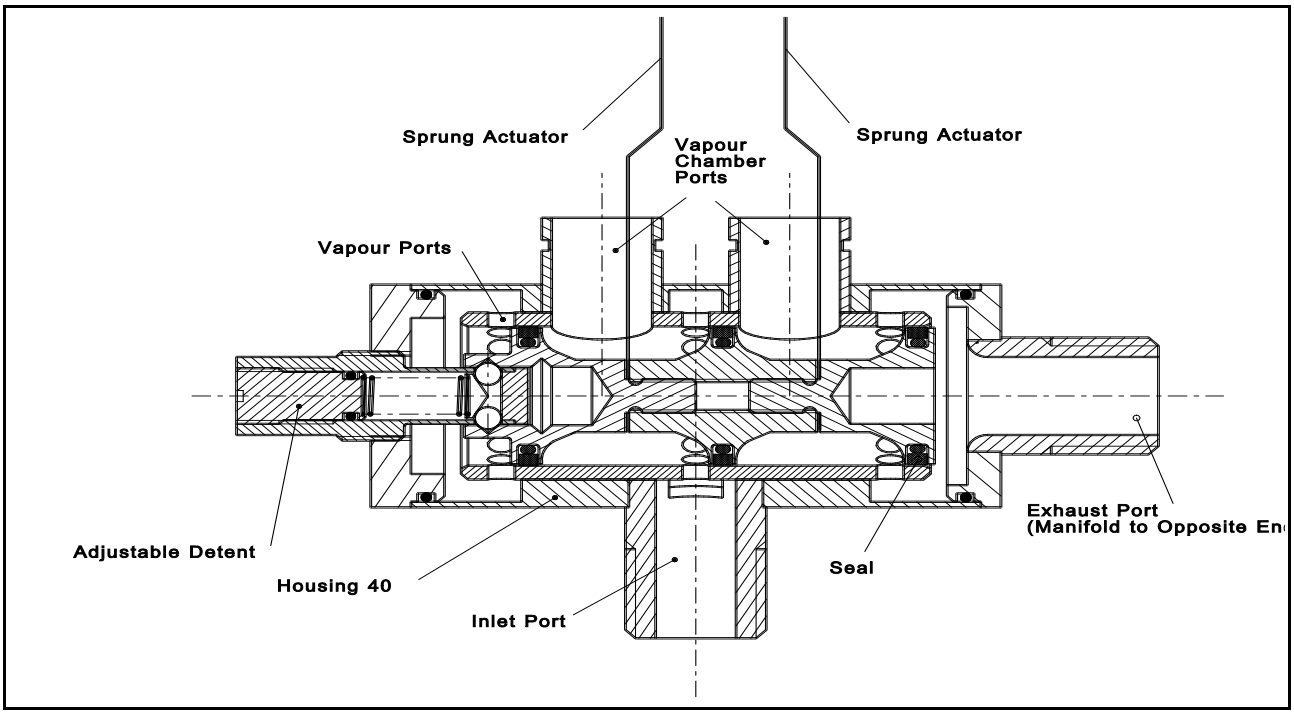


The valve body is made from 40mm square 304 grade stainless steel. A cylindrical brass sleeve is pressed into the centre. Sixteen 4mm vapour ports are drilled radially around each end of the sleeve and again in the middle prior to fitting.

The vapour is directed through toroidal cavities that form around these radial ports when the internal sleeve and housing are assembled.

These cavities and ports provide an equivalent flow area to a 16mm orifice to keep vapour velocities within the valve below 2.5m/s for a water flowrate less than 35 litres per minute. Vapour velocity is likely to be higher on exhaust and is dependent on water head as well as flow rate. This was the maximum flow area achievable without increasing valve stroke or internal diameter.

The central spool is made of three main components each locating one seal. The end pieces are located by an M6 thread and are assembled to the central piece from each end of the valve body. The pieces are shaped to direct vapour flow through the ports with minimum frictional loss and with minimum mass to keep reciprocating inertia low.

Vapour enters the valve through the middle inlet port and it is directed through either

the upper or lower vapour chamber port by the middle spool seal. While one chamber is filling, the opposing chamber is exposed to the condenser and is allowed to exhaust. The spools end seals isolate the high pressure inlet side from the low pressure exhaust side. The central spool toggles through 8mm of travel to alternate the intake and exhaust of vapour between opposing vapour chamber.

Vapour exiting the lower vapour chamber flows through the lower set of ports to the surrounding chamber and out the main exhaust port to the condenser. Vapour from the upper vapour chamber exits through the ports in the top of the sleeve to the surrounding chamber which is connected via a manifold (not visible in the cross section of *Figure 5.2*) to the lower chamber and main exhaust port.

As flow losses within the valve directly influence pump efficiency, it was important that attention be paid to vapour flow regimes and orifice restrictions. Standard pneumatic valves and actuators were considered unsuitable in this application. Pneumatic valves tend to have small flow orifices, high flow velocities and would require significant modification to meet the operation requirements and eliminate undesirable condensate buildup. Seal redesign and material replacement would be essential to ensure proper unlubricated function in the hydrocarbon vapour.

### 5.1.1 Spool Actuation

The spool is actuated by 0.7mm thick leaf springs clamped between the three spool components and extending through the vapour ports into the vapour chamber. The moving displacer extends the spring through a two stage curvature or double inflexion using the internal walls of the vapour chamber, depicted in *Figure 5.3.* This type of actuation maximises spring force and reduces non-axial loading on the spool.

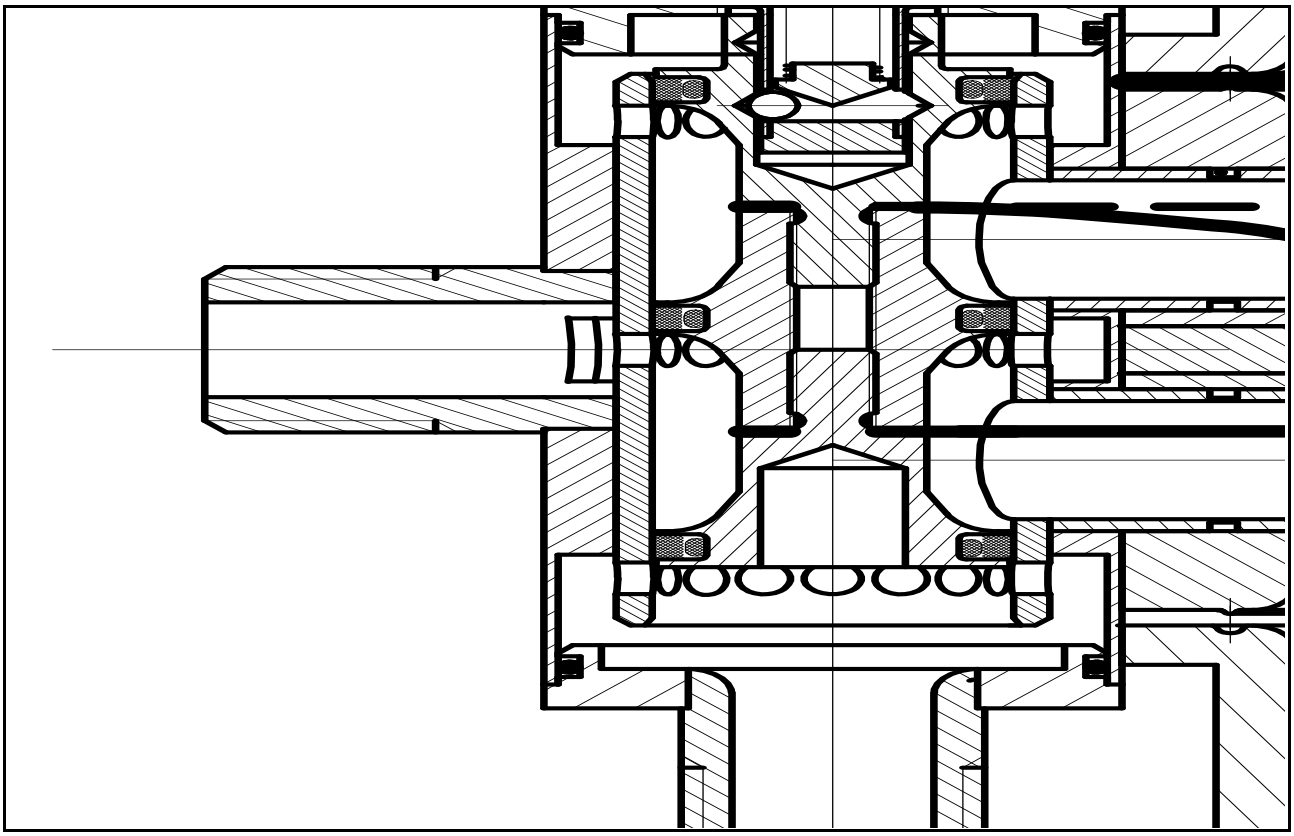

A detent located in the centre of one endcap of the valve has two opposing 4mm hardened steel balls which are sprung and locate in one of the two internal V-grooves found in the end of the spool. The function of the detent is to retain the spool in one position until enough potential energy has built in the actuating leaf spring to toggle the spool fully to the opposite position.

The detent is axially adjustable to allow initial alignment of the spool seal position with the vapour ports. Spring force on the detent balls can be increased or decreased by the adjustment of spring pre-load with a sealed plunger. This alters the release force of the detent balls in the spool grooves. The axial spring force applied by the spring is converted to radial force by a conical plunger acting on the balls which move perpendicular to the spool axis on a platform at the base of the detent, *Figure 5.4.*

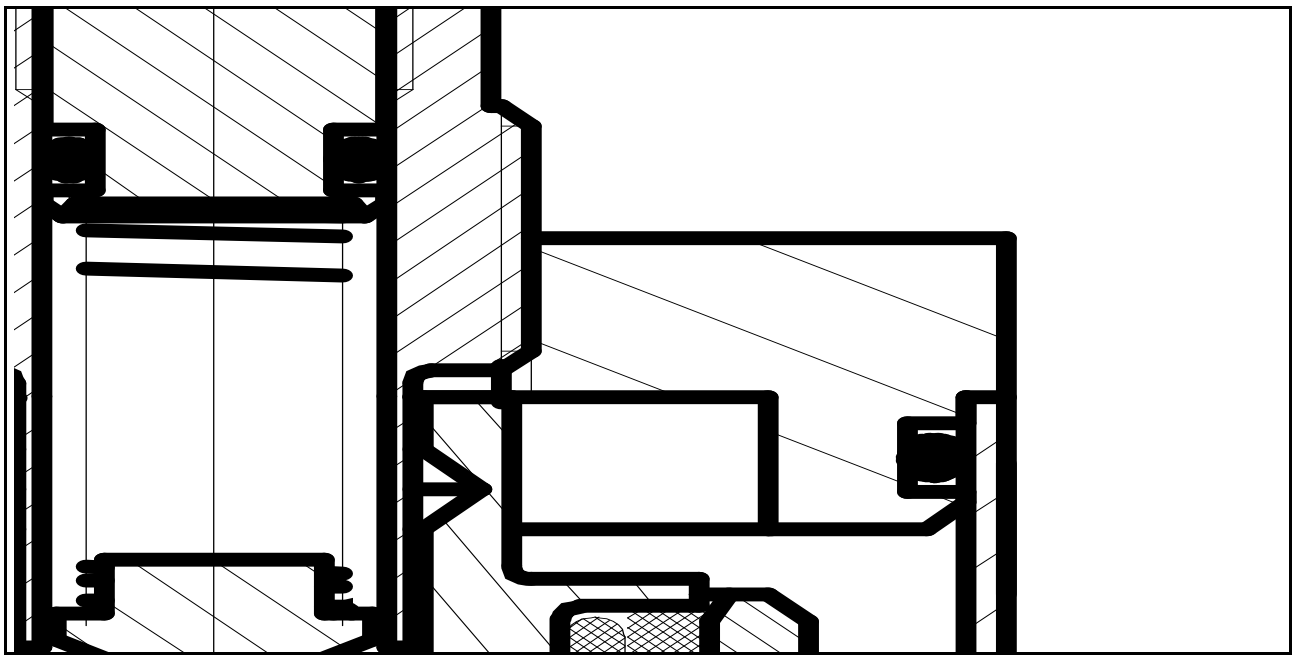

The geometry of the detent results in a slight asymmetry of toggle operation but it was considered the simplest, most compact design that was easily sealed and included external adjustment. Previous toggling designs have typically used either a "spring and latch" system similar to that just described or "bump and latch" systems where the displacer "knocks" the valve to its alternative position where it is held again by some form of detent. The bump and latch systems require some form of overcentre spring arrangement to assist valve motion past mid point (Thureau et.al. 1976, for example). Increased toggling reliability may be achieved by providing overcentre assistance to spring and latch systems (Sharma 1980, Malz Nominees 1975)

Other options included:

- Magnetic detent (Sharma 1980)
- Direct acting sprung ball detent (Kelsey 1974, Malz Nominees 1975, Zhi Chen 1985)
- Spring lever mechanism (Malz Nominees 1975, Thureau et.al. 1976)
- Pressure detent (Amor 1992, Speidel 1978, Hamilton 1974)
- or even some form of Belleville Washer

These options proved either difficult to adjust or unwieldy and complicated in design. Although unsuitable for the prototype, a simplified form of non-adjustable detent should prove adequate for mass produced items once the actuation force during

operation is determined.

### 5.1.2 Seals

Inadequate sealing within the valve will result in reduced performance (efficiency) or at worst pump failure. Direct leakage of the high pressure vapour across either the centre or one of the outer spool seals (depending on spool position) will result in higher condenser pressures and reduced pump capability. Excess condensate will form within the condenser. Should the rate of condensate formation exceed feed pump capacity eventually the condenser and pump will hydraulic.

Design is required not only to ensure the spool is an effective sealing mechanism but also to minimise loss of pressure during valve changeover. Any overlap of inlet and exhaust ports momentarily allows high pressure vapour to escape to the condenser. Excess overlap or a slow spool toggling motion would result in a significant loss of available work as well as the aforementioned problems relating to seal leakage.

To minimise overlap of inlet and exhaust ports, correct valve and seal geometry are required. Most elastomeric seals rely on relatively high differential pressures to cause deformation or extrusion (eg: O-ring seal) or high radial forces (eg: a lip seal) to provide the sealing force. High radial forces within the spool seals would result in high internal friction, requiring high actuation forces, possibly causing inadequate valve toggling and seal extrusion into the intake and discharge ports.
To eliminate port overlap a seal at least equivalent in width to the port diameter would be required. The result requiring a considerable spool stroke to clear the seal from either side of the ports. A slightly narrower but low friction seal was chosen as compromise, the low friction allowing rapid spool movement through a slightly shorter stroke.

Several double acting elastomeric seals were considered suitable for trial. These were all basically an elastomeric backed Teflon or lubricant impregnated Teflon, cap. The cap provides a wide rigid sealing area minimising port overlap and seal extrusion into the ports. The carbon filled PTFE chosen for the cap would give a low friction seal that was self lubricating, gave good sealing under low pressures, was resistant to

solvents and impervious to hydrocarbons (does not swell in hydrocarbon environments). Two other compounds were potentially better, Rulon A and Rulon J. Rulon™ is a harder compound with greater friction reducing additives but limited in availability. Direct acting metal seals were not considered due to high machining tolerances and high possibility of leakage.

The simplest form of seal consisted of a rectangular seal element backed by a standard nitrile O'ring acting as a radial spring (refer Appendix 9).

Complete Engineering drawings for valve components may be found in Appendix 5.

## 5.2 Pump Body

Designed for simplicity, the pump body consists of two central opposing vapour chambers and two outer opposing water chambers (see *Figure 5.1*). A central displacer reciprocates inside the chambers and is located and sealed by three radial diaphragms. The four internal chambers are separated by cast aluminium rings machined to give an inside diameter of 250 mm. A thermally insulating polymeric material such as nylon, polypropylene, acetyl, PVC or PTFE would have been preferred but suitable sections would generally require importation and/or unwarranted expenditure. Tooling for one-off injection moulding is also financially impractical.

Pressures within the chambers meant a 6mm thick mild steel central plate was required to separate vapour chambers. 4mm thick mild steel end plates house the water chambers. The displacer was made of two 6mm thick mild steel plates separated by a polypropylene central core 62mm in diameter. Mild steel, rather than stainless steel was used for these components for its low cost. It was considered suitable for the short term tests. A small diaphragm separating the vapour chambers is clamped between the core of the displacer and a clamping ring in the central plate. Two larger diaphragms separating the vapour chamber and water chambers are clamped to the displacer plates and seal between the aluminium body rings on a raised sealing lip. A central (10mm) through bolt locks the displacer components to the feed pump drive. 24, M4 studs that locate the four aluminium body rings, central

plate and two end plates are tightened to 4Nm. The joints between the central and end plates and the aluminium body rings are sealed by a Loctite™ flange sealant

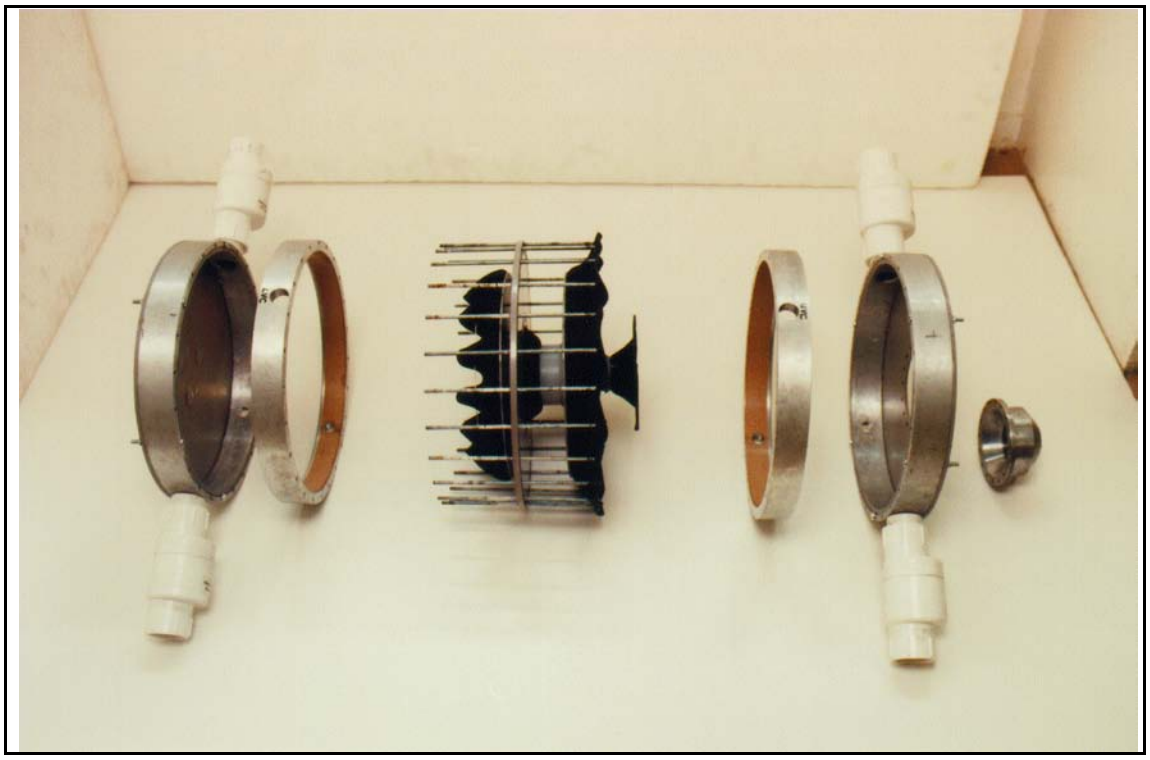

compound for simplicity. The pump simply concertinas as illustrated in *Plate 5.1.* The walls of the vapour chamber were lined with a fibreglass reinforced teflon to reduce thermal losses and cyclic condensation and re-evaporation effects[1]. Mild steel components were coated with a solvent resistant enamel paint.

Vapour enters and exits the two vapour chambers through two 15mm ports in the spool valve which is bolted to the side of the pump body. Water enters the two water chambers through two PVC one-way flap valves manifolded together to form the intake line and exits the chambers through a second pair of one-way valves (*Plate 5.2*).

[1] It was found under long term exposure to liquid Pentane, the adhesive back failed and the lining consequently removed.

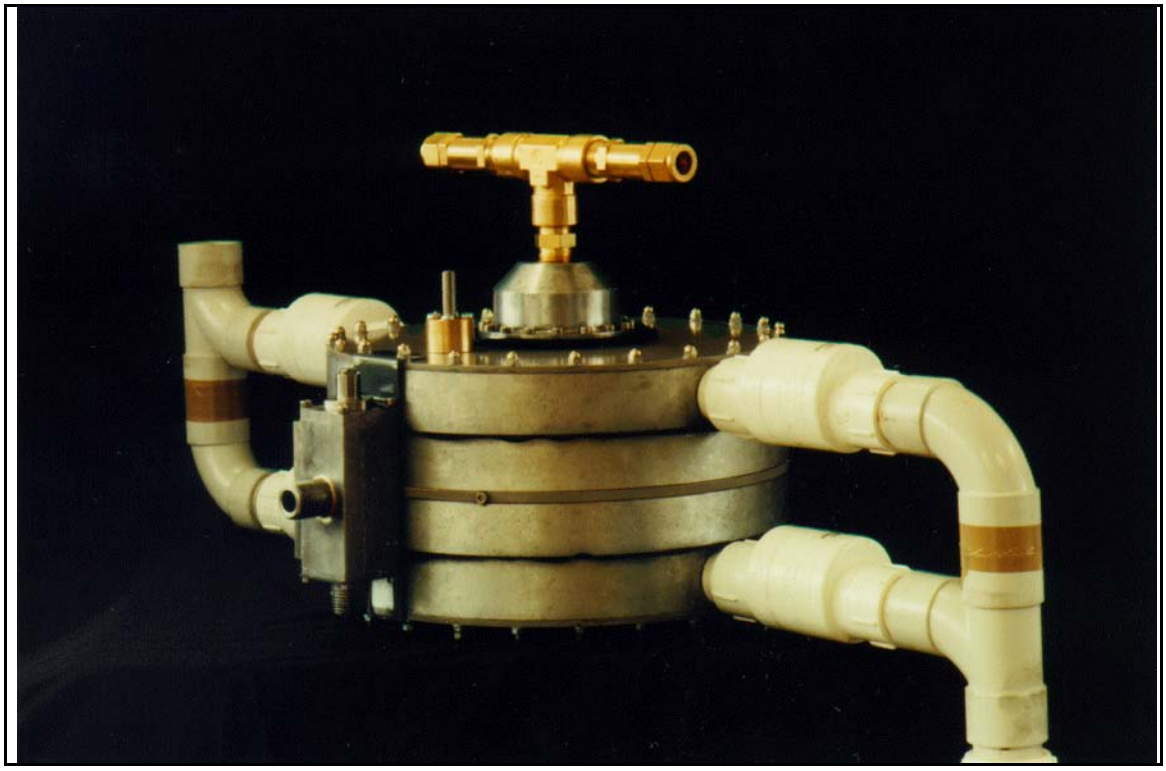

Full engineering drawings for the pump body may be found in Appendix 5.

## 5.3 Diaphragms

Correct sealing within the pump and ancillary components is essential to the long term operation of the solar thermal water pump. The system needs to be hermetically sealed to prevent loss of vacuum on the condensing side or loss of working fluid on the evaporating side. The diaphragms being a zero leakage device form an integral part of this seal preventing leakage of the working fluid into the water chambers or surroundings and the internal loss of high pressure vapour to the condenser across the central diaphragm. The former would cause the pump to eventually stall due to a lack of working fluid, the latter a reduction in efficiency or ineffective operation.

Considerable diaphragm flexing is a result of the large stroke (51mm) and small radial length (19.5mm). This is a design tradeoff for the need to minimise volumetric losses and irreversibilities which arise from vapour chamber dead volume and the ballooning and inversion of diaphragms during operation. A moulded or shaped convoluted or dished diaphragm is required that flexes rather than stretches to allow free displacer

movement, minimise internal stresses and losses to hysteresis and reduce diaphragm fatigue.

A feature of the double-acting design is that the pressure differential across the diaphragms is significantly lower than in the first prototype designed by Amor (1992). The worst case being the central diaphragm where, for the pump geometry chosen, at the design static water head of 6m$H_2O$ and maximum daily flow rate a pressure differential of 100kPa is predicted by the simulation outlined in Chapter 4. If the same pump was used to lift a 9m static head this differential could rise to 130kPa. Pressures in excess of 240kPa were expected for a suction head of 7.4m in the first prototype.

Many different materials are used in commercial diaphragm pumps, typically fabric reinforced synthetic rubbers such as neoprene, Buna N, butyl, Viton and Teflon. Natural rubber is still used in some applications. Reinforcing is required to prevent excessive deformation or ballooning and is usually cotton or rayon.

A number of alternatives were considered for the solar thermal water pump. The main difficulty with developing suitable prototype diaphragms was the inability to source small volume supplies of the uncured (or raw) materials for moulding. Of the cured materials natural rubber in either reinforced or non-reinforced forms was the most readily available but would degrade rapidly in the pentane environment. Neoprene and nitrile rubbers were also available in various fully cured forms and are resistant and durable. To obtain these materials in a mouldable, uncured state required a special one-off run by Skellerup Industrial, a local rubber manufacturer. Ideally these diaphragms should be moulded and reinforced nitrile rubber, however a thermoplastic elastomer or silicone rubber may also be suitable.

For the prototype pump, adequate diaphragms could be made from a soft 1.6mm thick reinforced nitrile rubber. Although already cured, enough stretch remained in the material to form a dished diaphragm which when clamped around the periphery a maintained the desired cupped profile. The three displacer diaphragms were made by this method, the central diaphragm is shown in *Plate 5.3.* A small amount of secondary set in the rubber was achieved by heating the clamped diaphragm in its

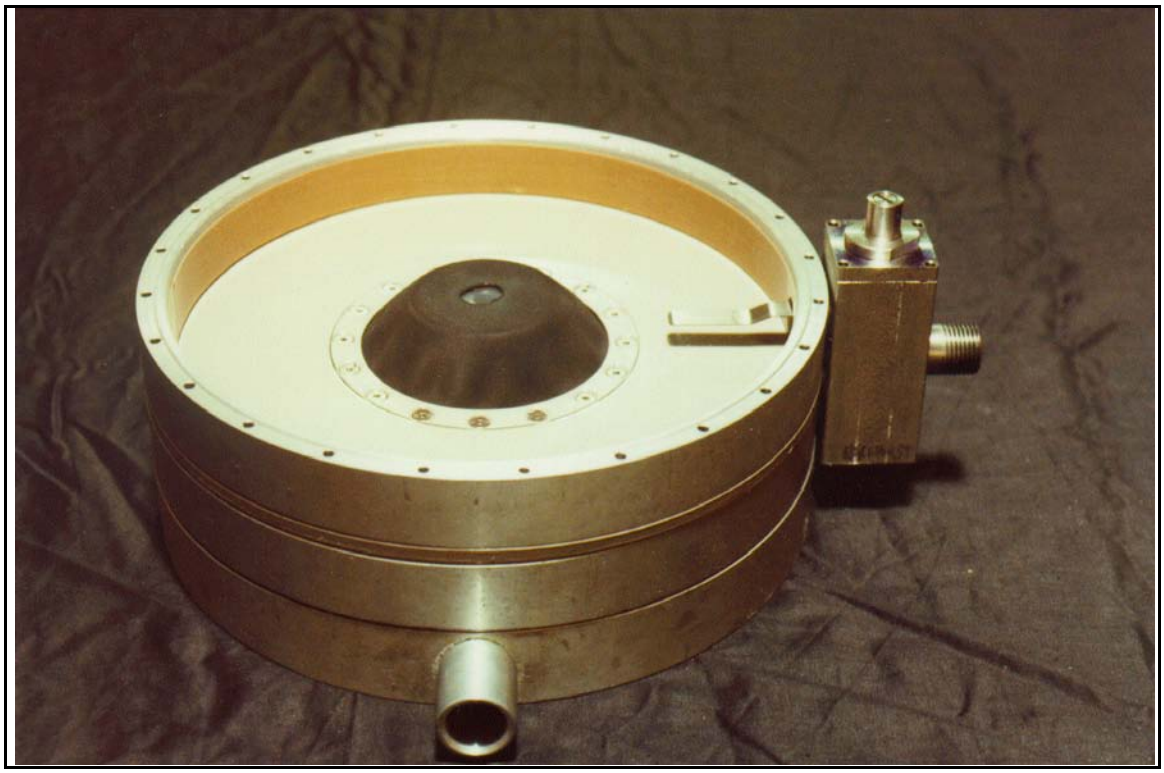

deformed state.

The feed pump diaphragm was too small to be made in this manner. A mould was made to stretch some raw 2mm non-reinforced nitrile. After curing for 20 minutes at 145°C it formed the top diaphragm shown in Plate 5.4. A rolling diaphragm would have been preferable for the feed pump but unsuitable. The varying water suction and water discharge conditions may result in a net alternating pressure across the diaphragm. A rolling diaphragm would invert and fail under these conditions.

Displacer guides could be omitted as forces on the displacer are uniform and axial, sufficient radial location is provided by the four working diaphragms.

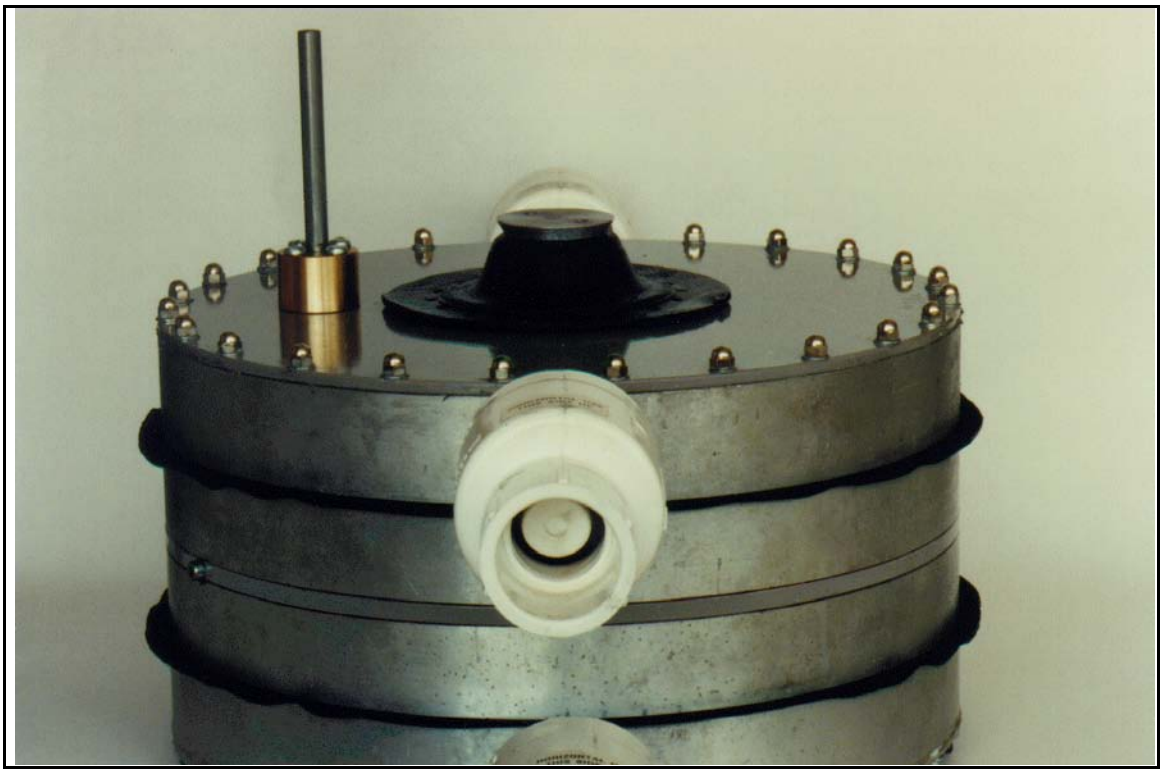

## 5.4 Condenser

Because of non-uniformity or batch nature of vapour flow, accurate calculations of condenser duty are difficult. The function of the condenser is to condense the working fluid vapour exiting the pump at a lower temperature (therefore pressure) than it was generated in the boiler. It thus provides the lower temperature/pressure reservoir and creates the pressure differential that is the basis for the systems operation.

Vapour-liquid condensers come in many different forms and can be air-cooled, liquid-cooled or liquid/vapour cooled (evaporative). The most obvious type of condenser for the STWP is a simple and preferably inexpensive unit that utilises the flow of the pumped liquid (water) for cooling. The high specific heat of most liquids means water-cooled condensers are considerably more compact and less expensive than other varieties. Suitable designs include a simple double pipe, immersed coiled tube, or basic shell and tube configuration.

Due to the fluctuating and pulsating vapour flow into, and condensate flow leaving the condenser, added complexity is introduced into calculations. An undersized condenser in terms of heat dissipation will result in higher exhaust pressures, reduced work outputs and higher boiler pressures. An undersized condenser in terms of internal volume will result in higher mean condenser pressures and reduced pump output. Ill-effects from oversizing condenser capacity are minimal. Cost and spatial concerns (eg. entry and exit points) provide the main design limitations. Thermodynamically, a large internal volume allows a more rapid pressure drop in the exhausting chamber (depending on valve restrictions) and a large surface area gives an increased rate of condensation improving pump performance by keeping condenser pressures low.

Sizing and analysis of the condenser began with considering film condensation on a vertical tube. By integrating the local convection co-efficient (a function of film thickness down the tube) an average convection heat transfer coefficient can be determined. By considering the maximum condenser loading and substituting relevant values for fluid properties, flow rates and expected operating temperatures, a simple formula was derived shown as Equation 5.1 (for a more detailed explanation refer Appendix 7). This enabled heat transfer calculations for the shell and tube

$$q_{Cond} = 13610.64\ n.\pi.OD.L^{3/4}$$

condenser with varying tube lengths, size and numbers.

where: $q_{cond}$ = heat capacity (W)

n = number of vertical tubes in the condenser

OD = tube outside diameter (m)

L = tube length (m)

and assuming:

- Minimal interaction on condensation rate with tube cluster
- Tube radius << film thickness
- Filmwise condensation
- Approximately steady flow
- Fluid properties are approximately constant
- Film flow is laminar

Ideally the pump's condenser should be a simple and cheap device such as a vertical or horizontal pipe/coil. For testing of the prototype an external condenser was chosen. For reduced plumbing and greater simplicity, an internal condensing coil may be incorporated into one of the pump's water chambers

A local manufacturer of oil and water heat exchangers produced a suitable unit containing 31 6.35mm OD tubes and 4 baffles in a 50mm OD shell. This exchanger was available in 150mm, 225mm, and 300mm lengths. For a duty of 2 kW Equation 5.1 predicts a required tube length of 147mm. As these units have low internal volumes (160ml for the 150mm and 240 ml for 225mm unit) the larger (225mm) exchanger was opted for, giving a higher rate of condensation to make up for the low internal volume.
As an added safety feature to the test setup, the duty of this condenser at approximately 2.78 kW would exceed the maximum electrical heat input achievable from a 10A mains socket of 2.3kW. Therefore cooling capacity exceeds heating capacity.

The condenser was positioned with the top inlet 0.5m above the exhaust from the pump. This allowed the condensate to gravity feed into the feed pump for improved priming. Under normal operating conditions any condensate forming within the pump should boil off during exhaust due to the lower condenser pressure. Condensate formation within exhaust ducting is negligible.

## 5.5 Feed Pump

The function of the feed pump is to return the condensate from the low pressure condenser to the high pressure solar panel or boiler.

The feed pump must have enough capacity to return condensate mass equivalent to the mass of vapour used in both vapour chambers as well as that formed by condensation on internal walls by cyclic heating processes and external heat losses. An undersized feed pump will result in condenser and pump flooding. An oversized

feed pump is necessary to ensure continued operation under various pump loads but requires a greater work input to drive. Approximately 20% more feed pump capacity was allowed in the prototype pump for condensation of vapour in excess of that directly consumed by pump displacement.

Various drive mechanisms were considered. The simplest coupled the feed pump directly to the displacer. The large stroke and small diameter of the feed pump causes considerable flexing of the diaphragm material which may reduce the long term integrity of diaphragm material. Increased diaphragm life mould be possible by decoupling the feed pump displacer from the main displacer with a punch drive mechanism and either a spring return or forced return as depicted in *Figure 5.5.* The

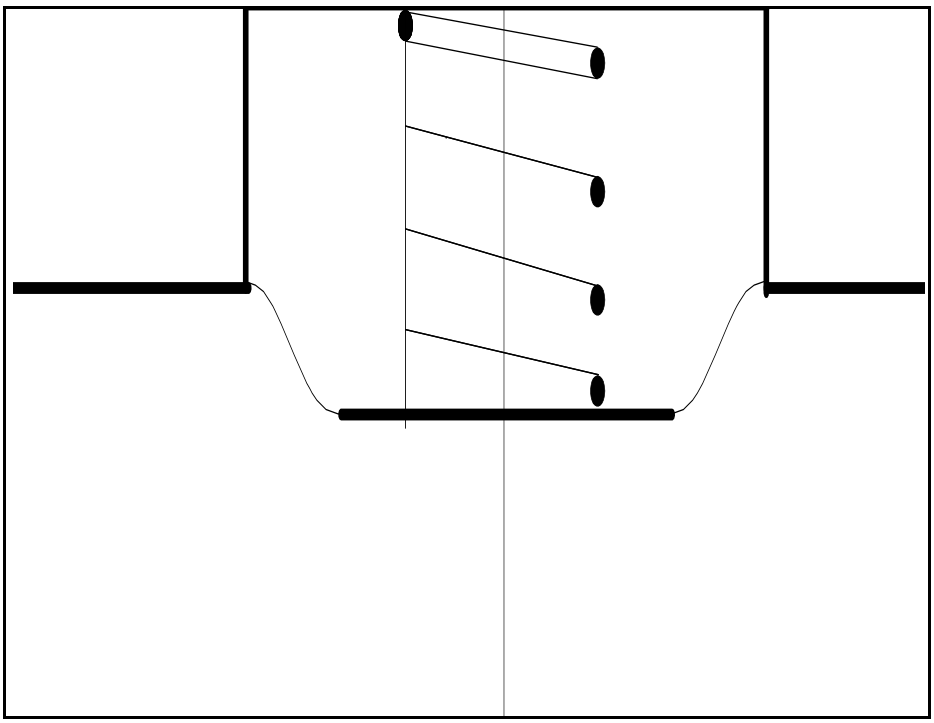

feed pump's larger diameter and shorter stroke would reduce diaphragm fatigue.

Two Nypro™ check valves with a _ psi crack pressure were tee-d into the top of the feed pump for flow control and self-priming.

The feed pump has a working diameter of 50mm, piston diameter of 30mm, with a stroke equivalent to main displacer stroke, a swept volume slightly less than 100ml was expected.

The prime mover and pump unit for the first and second prototype units can be seen in

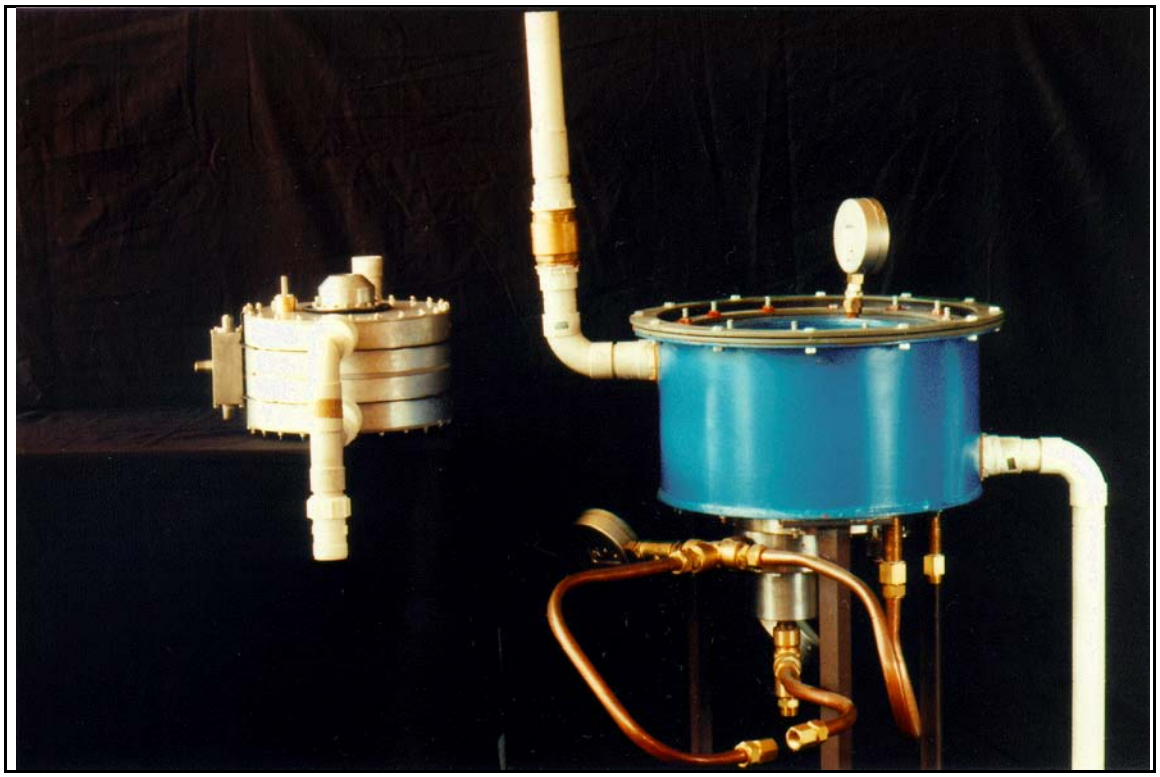

*Plate 5.5*.

## 5.6 Solar Panel

The design, characteristics and analysis of solar collectors is well documented in numerous books, papers and manufacturers' brochures. For this reason panel design and manufacture was considered outside the scope of this project. Two types of commercially available panel designs were to be used for testing. The first of these, a set of Colt panels, were already available in the department. These collectors are of a sheet and tube manifolded construction (Krieder et.al. 1989) with headers and four parallel risers suitable for the two phase working fluid. The 2.9 $m^2$ is made of four individual collectors connected in parallel by the direct coupling of top and bottom headers.

With a single glazing, minor damage, and an aged semi-selective coating these panels would be of moderate efficiency, less than that expected by the simulation. Further testing using a second set of panels with improved thermal insulation and

selective coating was intended should initial testing prove successful. The intended panels were those sold by Thermocell Inc., Christchurch.

Earlier sections have briefly discussed performance and efficiency of flat plate collectors. Operating at 54°C, 35°C above ambient, a panel efficiency of approximately 44% is expected by the model. Increasing collector area can compensate for lower efficiency panels. The different characteristics however will result in performance that differs from that simulated and will reduce the integrity of the thermodynamic optimisation.

It is worth noting that this system need not be limited to solar installations. This is essentially a temperature difference engine and should run adequately between any similar high temperature source and lower temperature sink. Changes of working fluid may be necessary if sink/source temperatures differ markedly from those expected in the solar installation. The high temperature source may well be fuel fired (eg. LPG, Diesel, Coal) but the type of system discussed in this research would be more appropriately used with low grade or waste heat sources. Waste process heat (hot gases, hot water or engine/generator exhaust), heat from decomposing waste matter, exothermic reactions, domestic fires/log burners, are all potential sources.

## 5.7 Ideas For Further Production

The prototype unit was fabricated from cheap, readily available materials, necessary to keep manufacturing costs realistic and to prevent long delivery delays. With batch or mass production of the parts that make up the unit, significant improvements could be made with material selection and fabrication techniques. Some minor design changes would also be appropriate.

The following sections discuss some of the considerations and compromises which developed during the manufacture and design of the prototype.

### 5.7.1 Solar Panel

It was intended the pump operate using standard commercially available solar collectors. The initial cost of this component is significantly higher than the cost of the pump itself. Material costs are low and significant reductions to the capital cost of the system may arise if the panels are included in the manufacture of the pump.

### 5.7.2 Pump, Prime Mover and Condenser

The physical pump configuration would need little modification for production. It has been designed for simplicity with the compact integration of the prime movers vapour chambers, and driven water chambers with one central moving displacer. Manufacture of moulded, cupped, reinforced diaphragms from a suitable elastomeric compound would be desirable.

Significant modifications may be made to material design and selection. Plastic moulding would allow a number of separate fabricated components to be combined and simplified. A variety of polymeric compounds were investigated for use in the prototype including nylon, polypropylene, acetyl, PVC or Teflon. Cost and/or availability of suitable sections for component fabrication was the major problem. Significant increases to efficiency may be obtained by reducing the thermal conductivity of body components to reduce internal condensation and external heat loss. The materials used in the prototype were those most easily and cheaply sourced (for example, the cast Aluminium body rings) and not necessarily ideal for use in a vapour engine of this type. For production models a number of improvements may be made, for example:

(i) Combining the main central disc and vapour chamber body rings into a single moulded polymeric component is an obvious improvement. The central disc will require strengthening to withstand operating pressures.
(ii) The central diaphragm could potentially be insert moulded with the central disc and body to further reduce part count.
(iii) The displacer could be made of two identical mouldings incorporating an insert moulded water chamber diaphragm and core bolted around the centre diaphragm.
(iv) Water chamber body rings and end plates should be a single pressed / formed

/ drawn sheet component, dished to improve strength, cosmetic appeal, reduce dead volumes, weight and cost.

(v) One way flap valves controlling water flow should be incorporated into the water chamber body or manifold rather than being separate and unnecessarily large items.

(vi) The spool valve housing may be injection moulded to reduce expensive fabrication cost and external heat loss.

(vii) The spool may be a moulded one piece item with the actuating fingers threaded into the spool stem, eliminating the need for a three piece spool.

(viii) The detent may be reduced to a single non-adjustable component (of a cupped Belleville washer form for example) which could assist spool motion with an overcentre action.

(ix) The feed pump may be incorporated into the displacer using the internal part of either the central vapour chamber or outer water chamber diaphragm as the feed pump diaphragm.

(x) A purpose built condensing unit could significantly reduce costs. The condenser may be considerably simpler than the shell and tube type selected for prototype testing, a simple double tube in the intake pipe, or coiled tube within the water chamber would be adequate.

(xi) Gravity feeding of the condenser from the prime mover exhaust and then onto the feed pump would be advantageous.

A number of other functional improvements are discussed in later chapters.

## 5.8 Prototype Costs

For the solar thermal water pump to be financially viable ideally it must be of comparable or lower capital cost than other water pumping options. In order to encourage further developmental interest and the potential for application in third world countries, the design of the prototype reflected this philosophy. Materials and processes specified in the fabrication were kept to low technology operations and low cost readily available products.

Retail costs (exclusive of GST) for the raw materials and components used in the

fabrication of the prototype are outlined below. All materials and components were sourced from local retail outlets with exception of the diaphragm material and working fluid. The modifications for production listed in section 5.7 would obviously alter costings. Labour was charged at $45 per hour including GST and includes machine running costs and overheads. With production quantities, manufacture and assembly times would drop significantly. For manufacture in developing countries with low or possibly intermediate technology manufacturing equipment, pump form and material selection would not be too dissimilar from that of the prototype but labour costs would be low. The simplicity of pump design allows complete assembly or disassembly in 1-2 hours.

Components were priced as follows:-

| | Material Cost | Labour |
|---|---|---|
| **Pump Body:** | | |
| - 4 Cast Aluminium Body Rings | | |
| @ $3.60/kg raw Al | | $ 9.00 ea |
| | | 2 hr ea |
| - Mild Steel Plate (cut cost) | | |
| 6mm Central Plate | | $10.29 |
| 2×6mm Displacer Plates | | $ 9.94 ea |
| 2×4mm End Plates | | $ 9.74 ea |
| - Polypropylene | | |
| φ100×120 @ $231/m | $27.50 | |
| - Aluminium Extrusion | | |
| φ100×60 + φ60×60 | | $58.60 |
| - M4 Threaded Rod | | |
| 24 Studs×155 long | | $ 2.00 ea |
| - Nuts, Bolts, Screws | $67.20 | |
| - 4 × Flap Valves | $25.70 ea | |
| - Water Chamber Manifolds | | $15.40 |
| - Labour | | |
| | | 28 hr |
| **Diaphragms:** | | |
| - 1.6mm reinforced nitrile rubber @ $54/m$^2$ | | |
| - 2 large | $ 5.20 ea | |
| | 0.25 hr ea. | |

- 1 small $ 1.70 0.25 hr

- 2mm unvulcanised nitrile rubber @ $324/m$^2$

- feed pump $ 3.60 0.5 hr

**Control Valve:**

- Stainless Steel
  - 40mm square section × 100 $19.00
  - φ30mm × 100 round bar $ 5.00
- Brass Sleeve
  - φ 30 OD tube × 100 long $ 8.00
- Seals
  - 3× Omniring piston seal $ 9.60 ea
  - 3× O-rings $ 5.00
- Springs
  - 2× Actuator Springs $ 1.00 ea
  - Coil Spring $ 0.50
- 2 × Ball Bearings φ4mm $ 0.50 ea
- Screws $ 4.00
- Labour

28 hr

**Fittings** (Prime Mover with external condenser and coupled to Solar Collector):

- Solar Collector/pump
  - Swagelock fittings $16.60
  - 2m ¾" Copper tube $19.30
- Pump/condenser
  - Swagelock fittings $31.70
  - ½m ¾" Copper tube $ 4.80
- Condenser/feed pump/solar collector
  - Swagelock fittings $48.90
  - 2×Nupro check valves _psi $32.00 ea
  - 2m ½" Copper tube $12.60
- Labour (assembly)

5 hr

**Fittings** (Water):

- 32mm PVC Waste pipe @ $4.80/m $28.80
- 2 × 90° Elbows $ 2.90 ea
- Labour (assembly)

0.5 hr

**Condenser:**

- Custom made
  - 2" OD × 9" Shell and Tube $190.00

**Solar Collectors:**

- 2.9m$^2$ Flat Plate, Sheet and Tube $1475.00

**Working Fluid:**

| | |
|---|---|
| - 4 litres n-Pentane @ $15/l | $60.00 |
| Total | |
| | $2452 |
| | 70.75 hr |

**Giving a total cost for the prototype of:**

| | |
|---|---|
| - Material cost | $2452 |
| - Labour[2] @ $45/hr | |
| | $3184 |
| **Total** | |
| | **≈ $5600** |

[2]Machining hours would see significant reduction with production manufacture

With batch or production manufacture it should be possible to reduce the capital cost of the complete system to significantly less than $2500. Significant savings are easily achievable with improved fabrication techniques to reduce the very high labour costs. Savings should also be sought in the cost of fittings, working fluid, solar collector, condenser and by designing for quantity manufacture. Incorporating items such as the flap valves into a moulding (for example) can reduce part count and the cost of purchasing these components.

A number of studies have been carried out concerning the viability of various pumping units for use in developing countries. The viability of any unit depends on a multitude of factors including the type and size of installation, demand, climate, lifestyle and attitude of local inhabitants. The size of the unit and demands on it dictate the level of technology associated with the system. For example using concentrating collectors with solar tracking allows higher temperatures to be achieved and higher Carnot efficiencies but at additional cost.

In direct competition to the solar thermal water pump would be the solar photo-voltaic water pump, windmill, petrol/diesel powered pump, handpump and where an electricity supply was available, electric powered pump.

With the exception of electric pumps, Amor (1992) compares the viability of the above systems, concluding that petrol centrifugal, solar thermal and wind were the most economic of systems next to the handpump. System viability is, however easily distorted by the varying emphasis placed on underlying factors such as labour costs (skilled/unskilled), convenience, climate etc. such that each installation should be considered on its own merit. A number of conflicting conclusions have been drawn by the viability studies examined.

Electric pumps would remain the most viable in Western countries where cheap sources of electricity can be obtained easily from national grid networks. The solar thermal water pump would certainly be well suited to a variety of niche markets, for both practical and novelty value. With changing attitudes and the increasing emphasis placed on global conservation and the use of sustainable / renewable energy sources, public pressure (for example, a forced pollution tax) will increasingly

diminish the higher capital cost of any "environmentally friendly" system. With increased production, manufacturing costs will undoubtedly drop, technology, efficiency and availability will also improve. The solar thermal water pumping system has the potential in the longer term to be a competitive market option.

# CHAPTER 6 - Pump Testing

Three initial stages of pump and system testing were envisaged:

- The first stage involved operating the pump on a pressure regulated compressed air supply to verify and refine pump operation.
- The second stage of testing involved coupling the pump to a simulated solar collector (or Pentane evaporator / boiler) to verify the thermodynamic cycle and system model.
- The third and final stage of testing would simply involve swapping the simulated solar boiler for 2.9 $m^2$ of flat plate solar collector to verify long term pump operation under solar radiation.

The problems that arose in the second stage of testing highlighted the need for some design modifications to be made to parts of the pump. Due to the lack of developmental time, the modifications and final stage of testing were not able to be carried out before the conclusion of the project.

This chapter describes the first two stages of testing, results, observations, problems, analysis, discussion and leads into the final concluding chapter which will discuss refinements to pump design to improve operation, reliability and efficiency.

## 6.1 Testing of Pump Operation on Compressed Air

The aim of this section of work was to check prototype operation, pump characteristics and capacity, limitations, areas of operational and design improvement and overall functionality. Results from this section also enabled verification and minor refinement of the computer simulation.

### 6.1.1 Compressed Air System

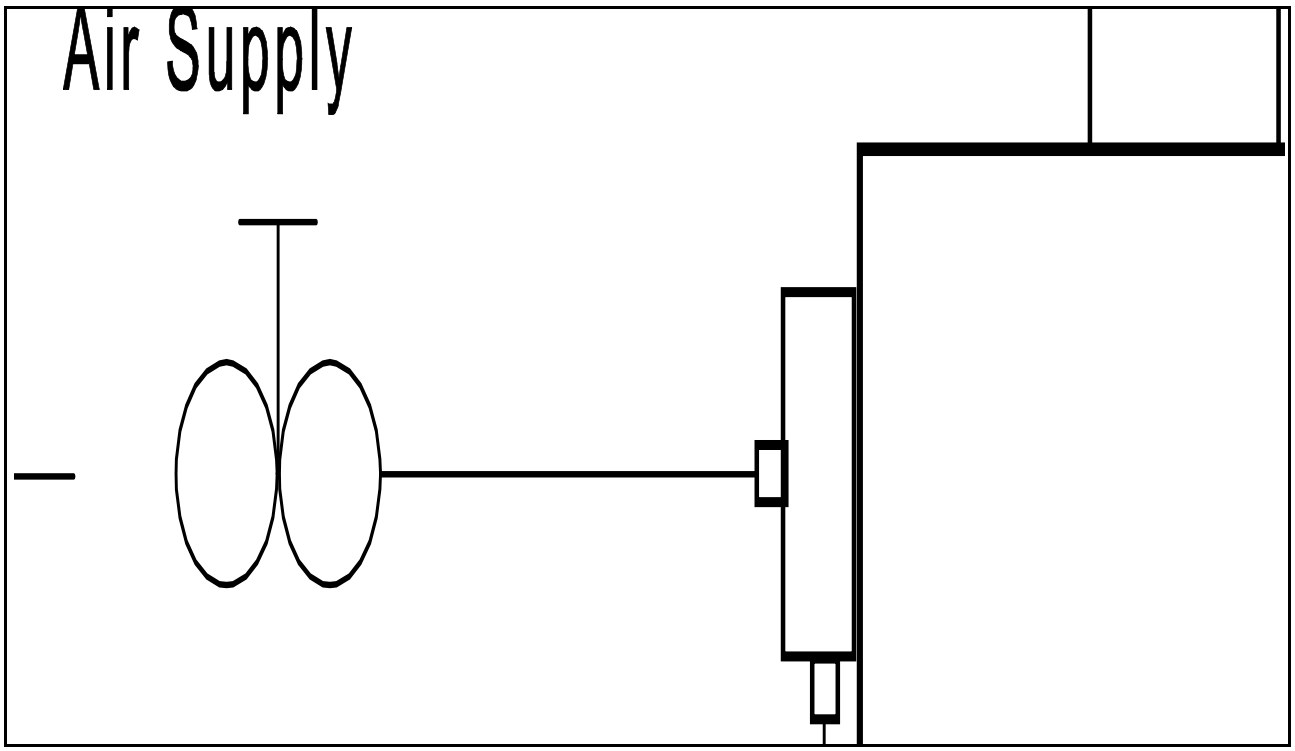


The system for testing the pump's operation on compressed air can be seen in *Figure 6.1*. The solar panel and high pressure Pentane vapour supply was simulated using a regulated compressed air supply and the pump allowed to exhaust to atmosphere.

Because of the nature of the pump's design, with the force driving the displacer arising from the pressure differential between the exhausting and inducting vapour chambers (solar panel and condenser pressures), comparisons to, and verification of, the model outlined in Chapter 4, could be achieved by altering the regulated air supply to compensate for condenser pressure and provide the same overall driving force as assumed in the model.

The supply of water consisted of a lower mains-fed reservoir. In order to maintain constant head this was fitted with a fixed head overflow from which a steady discharge was maintained. For testing heads up to 4.0m the reservoir was located on the solar deck giving 0.5m static suction head and up to 3.5m static discharge head using a variety of fixed pipe lengths. For test heads over 4.0m the lower reservoir was dropped below the level of the deck giving between 2.0 and 4.0m static suction heads and again from 0 to 3.5m static discharge head. Thus 7.5m total head was the maximum able to be tested, see *Plate 6.1.*

Flow rate was measured simply using a bucket and stopwatch technique. The measurement was made over approximately 5 full pumping cycles (10 strokes of the displacer) collecting 16-19 litres of water.

Pressure (gauge) of the regulated air supply was measured using a pressure transducer coupled to an amplifier and digital readout, in the form of an 'Airflow Digital Barometer DB1'. A standard analogue bourdon tube pressure gauge was used in parallel for verification.

### 6.1.2 Testing the Pump

Before actual testing began, the maximum volumetric displacement of all chambers was measured with a zero pressure differential acting across the diaphragms. This was to determine and enable calculations on the following aspects:

- operational stroke length (as opposed to the maximum available),
- effect of diaphragm ballooning on water/air displacement while operating and
- pumping efficiency ($E_p$, $\eta_p$)

Testing was carried out at fixed total heads of 2,3,4,5,6,7, and 7.5 meters for various operating pressures from the minimum and in excess of the maximum predicted by the simulation for daily operation.

Exhausting pressure (atmospheric / barometric) was measured and recorded before each test run. During testing the regulator was adjusted to provide the desired driving pressure and system allowed to reach steady state operation. Flow rate, stroke length, driving pressure, and cycle time were recorded. The regulator re-adjusted for the next setting and new measurements taken.

### 6.1.3 Results

After assembling the pump it was found that unloaded, the diaphragms constrained the pump's stroke to 47.5mm, lower than the designed stroke of 51mm. For a stroke of 47.5mm volumetric capacities of each chamber are listed in Table 6.1.

| Internal Pump Chamber (Refer Figure 2.30) | Volumetric Capacity |
|---|---|
| Upper Water Chamber | 1740 ± 10 ml |
| Lower Water Chamber | 1840 ± 10 ml |
| Upper Vapour Chamber | 1605 ±10 ml |
| Lower Vapour Chamber | 1605 ± 10 ml |
| Feed Pump | 94 ± 0.5 ml |

**Note**: The upper water chamber has less capacity than the lower water chamber due to the presence of the feedpump in the upper chamber reducing the working area of the displacer.

It was necessary to alter a number of physical variables in the computer simulation to account for physical differences in the test set-up and the set-up assumed in the initial optimisation. This meant the simulation was re-run for all heads with the "skip geometrical optimisation routine" option selected. These alterations were:

- Total intake / discharge pipe length: For a practical installation it was considered that a total length of pipework of 15 meters was appropriate for a pump lifting through a 6m static head. In the actual test set-up, total pipe length was virtually equivalent to the vertical head for tests below 4.0m. Above a 4.0m total head, 2.0m of additional horizontal pipe was required.
- Water pipe diameter: The simulation was run with the assumption that 40mm

PVC Waste pipe would be used for all water plumbing to minimise fluid velocity and frictional losses. Due to the compact pump geometry and manifold size, 32mm PVC Waste pipe was more convenient.

- Fitting losses: Due to the reduced plumbing in the test set-up fluid frictional losses in fittings (bends etc) was reduced in the intake pipeline from 5.3 to 4.4 times the square of fluid velocity. The discharge pipeline remained the same in the test rig as initially assumed in the simulation.

- Stroke length: As observed after the assembly of the pump, physical restrictions created by the diaphragms meant that the maximum pump stroke was 47.5mm instead of the predicted optimum of 51mm. This was a result of the techniques used to prototype the diaphragms.

- Pump Operation: It was observed during initial running of the pump on compressed air that the delay that occurs at the end of each stroke as the pressures in the vapour chambers change was significantly less than that estimated in the simulation. The time delay was reduced from approximately 1 second to 0.1 second. It was expected to be higher for operation on Pentane.

The simulation output for a day of operation lifting water through static heads ranging from 2 metres to 9 metres and incorporating the above changes can be seen in Appendix 4.

Performance of the pump during testing on regulated compressed air can be seen in Tables 6.2 to 6.8.

| Simulated | | Experimental Operation on Compressed Air | | | | | | | | | | |
|---|---|---|---|---|---|---|---|---|---|---|---|---|
| P (kPa) Boiler - Condenser | Flow Rate l/min | P (kPa) Supply - Ambient | Flow Rate l/min | Cycle Time s | Stroke Length mm | Water Vol per Cycle l | Calculated Output l | Displ of Diaph l | Air Vol per Cycle l | Work Input W | Pumping Work W | Efficiency % |
| | | 26.4 | 10.5 | | | | | | | | | |
| 26.7 | 21.5 | 26.8 | 14.0 | 16.84 | 43.5 | 3.93 | 3.30 | 0.63 | 3.57 | 5.7 | 4.6 | 80.6 |
| 29.6 | 27.4 | 30.0 | 24.0 | 9.00 | 44.3 | 3.60 | 3.36 | 0.24 | 3.23 | 10.8 | 7.9 | 72.8 |
| 31.3 | 30.4 | 31.5 | 30.8 | 7.20 | 44.0 | 3.70 | 3.34 | 0.36 | 3.33 | 14.6 | 10.1 | 69.1 |
| 32.9 | 32.9 | 32.5 | 35.4 | 6.50 | 45.1 | 3.84 | 3.42 | 0.41 | 3.46 | 17.3 | 11.6 | 66.9 |
| 34.0 | 34.6 | 34.0 | 36.6 | 6.16 | 45.9 | 3.76 | 3.48 | 0.27 | 3.38 | 18.6 | 12.0 | 64.2 |
| 34.2 | 34.8 | 34.4 | 39.3 | 5.74 | 44.9 | 3.76 | 3.41 | 0.35 | 3.39 | 20.3 | 12.9 | 63.3 |
| 34.9 | 35.8 | 34.4 | 39.7 | 5.36 | 44.0 | 3.55 | 3.34 | 0.21 | 3.18 | 20.4 | 13.0 | 63.6 |
| 34.9 | 35.8 | 35.0 | 42.9 | 5.10 | 45.6 | 3.65 | 3.46 | 0.19 | 3.27 | 22.4 | 14.0 | 62.6 |
| n/a | n/a | 39.5 | 50.0 | 4.30 | 45.9 | 3.58 | 3.48 | 0.10 | 3.20 | 29.4 | 16.4 | 55.6 |

| Simulated | | Experimental Operation on Compressed Air | | | | | | | | | | |
|---|---|---|---|---|---|---|---|---|---|---|---|---|
| P (kPa) Boiler - Condenser | Flow Rate l/min | P (kPa) Supply - Ambient | Flow Rate l/min | Cycle Time s | Stroke Length mm | Water Vol per Cycle l | Calculated Output l | Displ of Diaph l | Air Vol per Cycle l | Work Input W | Pumping Work W | Efficiency % |
| 37.7 | 20.1 | 37.5 | 11.8 | 17.74 | 43.5 | 3.49 | 3.30 | 0.19 | 3.13 | 6.6 | 5.8 | 87.6 |
| 38.9 | 22.6 | 39.0 | 18.2 | 11.68 | 44.3 | 3.55 | 3.36 | 0.19 | 3.18 | 10.6 | 8.9 | 84.2 |
| 40.0 | 24.9 | 40.0 | 22.9 | 9.26 | 44.0 | 3.53 | 3.34 | 0.19 | 3.17 | 13.7 | 11.2 | 82.1 |
| 40.7 | 26.2 | 41.0 | 29.4 | 7.28 | 44.3 | 3.56 | 3.36 | 0.20 | 3.20 | 18.0 | 14.4 | 80.0 |
| 42.8 | 29.6 | 43.3 | 35.8 | 6.12 | 44.4 | 3.65 | 3.37 | 0.28 | 3.28 | 23.2 | 17.6 | 75.6 |
| 43.8 | 31.4 | 43.5 | 34.9 | 6.22 | 44.5 | 3.61 | 3.38 | 0.24 | 3.24 | 22.7 | 17.1 | 75.4 |
| 44.7 | 32.4 | 44.5 | 36.9 | 5.82 | 44.2 | 3.58 | 3.35 | 0.22 | 3.21 | 24.6 | 18.1 | 73.7 |
| 45.7 | 33.8 | 45.3 | 39.9 | 5.54 | 44.3 | 3.68 | 3.36 | 0.32 | 3.32 | 27.1 | 19.6 | 72.2 |
| 45.9 | 34.1 | 45.8 | 37.4 | 5.78 | 45.0 | 3.60 | 3.42 | 0.19 | 3.23 | 25.6 | 18.3 | 71.7 |
| 47.1 | 35.6 | 47.5 | 44.5 | 4.92 | 44.8 | 3.65 | 3.40 | 0.25 | 3.27 | 31.6 | 21.8 | 69.0 |
| 48.1 | 36.9 | 48.0 | 46.3 | 4.60 | 45.5 | 3.55 | 3.45 | 0.10 | 3.17 | 33.1 | 22.7 | 68.6 |
| n/a | n/a | 49.8 | 50.0 | 4.40 | 43.8 | 3.67 | 3.32 | 0.35 | 3.31 | 37.4 | 24.5 | 65.6 |

| Simulated | | Experimental Operation on Compressed Air | | | | | | | | | | |
|---|---|---|---|---|---|---|---|---|---|---|---|---|
| P (kPa) Boiler - Condenser | Flow Rate l/min | P (kPa) Supply - Ambient | Flow Rate l/min | Cycle Time s | Stroke Length mm | Water Vol per Cycle l | Calculated Output l | Displ of Diaph l | Air Vol per Cycle l | Work Input W | Pumping Work W | Efficiency % |
| 49.1 | 19.6 | 49.4 | 18.2 | 11.30 | 42.0 | 3.42 | 3.19 | 0.23 | 3.07 | 13.4 | 11.9 | 88.5 |
| 51.1 | 23.6 | 51.0 | 20.1 | 10.48 | 43.8 | 3.51 | 3.32 | 0.19 | 3.15 | 15.3 | 13.2 | 85.8 |
| 52.3 | 25.8 | 52.5 | 27.3 | 7.80 | 43.4 | 3.55 | 3.29 | 0.25 | 3.19 | 21.5 | 17.9 | 83.2 |
| 53.4 | 27.5 | 53.4 | 33.8 | 6.02 | 42.1 | 3.39 | 3.20 | 0.19 | 3.04 | 27.0 | 22.1 | 81.9 |
| 54.3 | 28.9 | 54.0 | 34.0 | 6.40 | 44.0 | 3.63 | 3.34 | 0.29 | 3.26 | 27.5 | 22.3 | 80.8 |
| 56.7 | 32.2 | 56.0 | 37.6 | 5.74 | 43.7 | 3.60 | 3.32 | 0.28 | 3.23 | 31.6 | 24.6 | 77.9 |
| 56.7 | 32.2 | 56.4 | 41.2 | 4.96 | 42.4 | 3.41 | 3.22 | 0.19 | 3.05 | 34.7 | 26.9 | 77.6 |
| 57.4 | 33.2 | 57.9 | 40.8 | 5.20 | 44.0 | 3.54 | 3.34 | 0.20 | 3.17 | 35.3 | 26.7 | 75.6 |
| 57.4 | 33.2 | 58.0 | 42.6 | 5.08 | 43.6 | 3.61 | 3.31 | 0.30 | 3.25 | 37.1 | 27.9 | 75.2 |
| n/a | n/a | 58.5 | 44.7 | 4.64 | 42.3 | 3.46 | 3.21 | 0.25 | 3.10 | 39.1 | 29.2 | 74.7 |
| n/a | n/a | 62.0 | 51.3 | 4.22 | 44.0 | 3.61 | 3.34 | 0.27 | 3.24 | 47.6 | 33.5 | 70.4 |

| Simulated | | Experimental Operation on Compressed Air | | | | | | | | | | |
|---|---|---|---|---|---|---|---|---|---|---|---|---|
| P (kPa) Boiler - Condenser | Flow Rate l/min | P (kPa) Supply - Ambient | Flow Rate l/min | Cycle Time s | Stroke Length mm | Water Vol per Cycle l | Calculated Output l | Displ of Diaph l | Air Vol per Cycle l | Work Input W | Pumping Work W | Efficiency % |
| 58.7 | 14.0 | 60.0 | 12.8 | 13.85 | 37.5 | 2.96 | 2.85 | 0.11 | 2.65 | 11.5 | 10.5 | 91.4 |
| 62.9 | 22.2 | 62.9 | 19.6 | 9.41 | 37.9 | 3.08 | 2.88 | 0.20 | 2.76 | 18.5 | 16.0 | 86.9 |
| 63.1 | 22.5 | 63.9 | 24.3 | 7.56 | 38.2 | 3.06 | 2.90 | 0.16 | 2.75 | 23.2 | 19.9 | 85.6 |
| 65.3 | 25.6 | 65.0 | 29.7 | 6.26 | 38.4 | 3.10 | 2.91 | 0.18 | 2.78 | 28.9 | 24.3 | 84.1 |
| 65.6 | 26.0 | 65.5 | 30.7 | 6.07 | 38.7 | 3.10 | 2.94 | 0.17 | 2.78 | 30.0 | 25.1 | 83.5 |
| 66.6 | 27.3 | 67.0 | 33.1 | 5.71 | 39.2 | 3.15 | 2.98 | 0.17 | 2.82 | 33.2 | 27.1 | 81.7 |
| 67.5 | 28.3 | 67.3 | 33.4 | 5.65 | 39.0 | 3.15 | 2.96 | 0.19 | 2.82 | 33.6 | 27.3 | 81.2 |
| 68.8 | 29.9 | 69.0 | 37.5 | 5.02 | 39.0 | 3.13 | 2.96 | 0.17 | 2.81 | 38.6 | 30.6 | 79.3 |

| Simulated | | Experimental Operation on Compressed Air | | | | | | | | | | |
|---|---|---|---|---|---|---|---|---|---|---|---|---|
| P (kPa) Boiler - Condenser | Flow Rate l/min | P (kPa) Supply - Ambient | Flow Rate l/min | Cycle Time s | Stroke Length mm | Water Vol per Cycle l | Calculated Output l | Displ of Diaph l | Air Vol per Cycle l | Work Input W | Pumping Work W | Efficiency % |
| 71.0 | 15.9 | 71.0 | 14.0 | 13.53 | 38.7 | 3.15 | 2.94 | 0.22 | 2.83 | 14.9 | 13.7 | 92.3 |
| 72.1 | 18.2 | 71.8 | 15.9 | 11.87 | 40.1 | 3.14 | 3.04 | 0.09 | 2.80 | 17.0 | 15.6 | 91.8 |
| 72.4 | 18.5 | 72.5 | 16.9 | 11.14 | 39.1 | 3.13 | 2.97 | 0.16 | 2.81 | 18.3 | 16.6 | 90.6 |
| 73.5 | 20.5 | 73.0 | 21.1 | 9.15 | 39.1 | 3.21 | 2.97 | 0.25 | 2.89 | 23.1 | 20.7 | 89.7 |
| 73.7 | 20.8 | 73.5 | 21.6 | 8.83 | 39.4 | 3.18 | 2.99 | 0.19 | 2.86 | 23.8 | 21.2 | 89.3 |
| 74.6 | 22.1 | 74.0 | 18.4 | 10.36 | 39.0 | 3.17 | 2.96 | 0.21 | 2.84 | 20.3 | 18.0 | 88.6 |
| 74.9 | 22.6 | 75.0 | 20.6 | 9.32 | 39.6 | 3.19 | 3.01 | 0.19 | 2.86 | 23.1 | 20.2 | 87.5 |
| 75.8 | 23.8 | 75.5 | 24.2 | 7.95 | 39.2 | 3.21 | 2.98 | 0.23 | 2.88 | 27.4 | 23.8 | 86.8 |
| 76.0 | 24.1 | 76.0 | 26.0 | 7.42 | 39.6 | 3.21 | 3.01 | 0.20 | 2.88 | 29.5 | 25.5 | 86.3 |
| 76.9 | 25.2 | 76.0 | 28.1 | 7.09 | 39.5 | 3.32 | 3.00 | 0.32 | 2.99 | 32.1 | 27.6 | 85.9 |
| 77.1 | 25.6 | 77.0 | 29.5 | 6.53 | 39.6 | 3.21 | 3.01 | 0.20 | 2.88 | 33.9 | 28.9 | 85.2 |
| 78.0 | 26.7 | 77.5 | 30.1 | 6.78 | 40.1 | 3.40 | 3.04 | 0.36 | 3.07 | 35.1 | 29.5 | 84.2 |

| Simulated | | Experimental Operation on Compressed Air | | | | | | | | | | |
|---|---|---|---|---|---|---|---|---|---|---|---|---|
| P (kPa) Boiler - Condenser | Flow Rate l/min | P (kPa) Supply - Ambient | Flow Rate l/min | Cycle Time s | Stroke Length mm | Water Vol per Cycle l | Calculated Output l | Displ of Diaph l | Air Vol per Cycle l | Work Input W | Pumping Work W | Efficiency % |
| 81.7 | 14.5 | 81.5 | 17.5 | 10.83 | 39.3 | 3.16 | 2.98 | 0.18 | 2.83 | 21.3 | 20.0 | 94.0 |
| 82.9 | 16.7 | 82.5 | 19.6 | 9.57 | 38.7 | 3.12 | 2.94 | 0.18 | 2.80 | 24.2 | 22.4 | 92.8 |
| 83.2 | 17.3 | 83.0 | 20.5 | 9.27 | 39.2 | 3.17 | 2.98 | 0.19 | 2.84 | 25.5 | 23.5 | 92.2 |
| 84.3 | 19.2 | 84.5 | 22.3 | 8.46 | 38.8 | 3.14 | 2.94 | 0.19 | 2.81 | 28.1 | 25.5 | 90.6 |
| 85.6 | 21.1 | 85.0 | 22.1 | 8.70 | 39.4 | 3.21 | 2.99 | 0.22 | 2.88 | 28.2 | 25.3 | 90.0 |
| 85.6 | 21.1 | 85.0 | 22.7 | 8.33 | 39.1 | 3.15 | 2.97 | 0.18 | 2.83 | 28.9 | 26.0 | 90.1 |
| 85.8 | 21.4 | 85.0 | 23.1 | 8.34 | 39.2 | 3.20 | 2.98 | 0.23 | 2.88 | 29.3 | 26.4 | 89.9 |
| 85.8 | 21.4 | 85.5 | 23.4 | 8.18 | 38.9 | 3.19 | 2.95 | 0.24 | 2.87 | 30.0 | 26.8 | 89.4 |
| 85.8 | 21.4 | 85.5 | 23.5 | 8.01 | 39.7 | 3.13 | 3.01 | 0.12 | 2.80 | 29.9 | 26.8 | 89.8 |
| 86.7 | 22.6 | 86.0 | 25.9 | 7.46 | 40.0 | 3.22 | 3.04 | 0.18 | 2.88 | 33.2 | 29.6 | 89.1 |
| 86.7 | 22.6 | 86.0 | 26.7 | 7.13 | 38.8 | 3.17 | 2.94 | 0.22 | 2.85 | 34.4 | 30.5 | 88.9 |
| 87.0 | 23.1 | 87.0 | 27.4 | 6.97 | 40.4 | 3.19 | 3.07 | 0.12 | 2.85 | 35.6 | 31.4 | 88.2 |
| 87.0 | 23.1 | 87.0 | 27.5 | 6.91 | 39.5 | 3.17 | 3.00 | 0.17 | 2.84 | 35.8 | 31.5 | 88.0 |
| 88.0 | 24.3 | 88.0 | 30.4 | 6.35 | 39.7 | 3.22 | 3.01 | 0.20 | 2.89 | 40.0 | 34.8 | 86.9 |
| 88.2 | 24.5 | 88.5 | 32.2 | 6.08 | 41.0 | 3.26 | 3.11 | 0.15 | 2.92 | 42.5 | 36.8 | 86.7 |
| 88.2 | 24.5 | 90.5 | 34.6 | 6.02 | 40.5 | 3.47 | 3.07 | 0.39 | 3.13 | 47.1 | 39.6 | 84.0 |

| Simulated | | Experimental Operation on Compressed Air | | | | | | | | | | |
|---|---|---|---|---|---|---|---|---|---|---|---|---|
| P (kPa) Boiler - Condenser | Flow Rate l/min | P (kPa) Supply - Ambient | Flow Rate l/min | Cycle Time s | Stroke Length mm | Water Vol per Cycle l | Calculated Output l | Displ of Diaph l | Air Vol per Cycle l | Work Input W | Pumping Work W | Efficiency % |
| 85.8 | 10.3 | 86.0 | 17.7 | 10.92 | 38.0 | 3.22 | 2.88 | 0.34 | 2.91 | 22.9 | 21.7 | 94.9 |
| 87.9 | 15.4 | 87.5 | 18.7 | 9.78 | 38.5 | 3.05 | 2.92 | 0.13 | 2.73 | 24.4 | 23.0 | 93.9 |
| 88.2 | 15.9 | 88.5 | 18.7 | 9.87 | 38.1 | 3.08 | 2.89 | 0.19 | 2.76 | 24.8 | 23.0 | 92.7 |
| 89.4 | 18.1 | 89.0 | 22.7 | 8.32 | 39.0 | 3.15 | 2.96 | 0.19 | 2.82 | 30.2 | 27.8 | 92.2 |
| 89.6 | 18.4 | 89.5 | 23.3 | 7.92 | 38.5 | 3.08 | 2.92 | 0.16 | 2.76 | 31.2 | 28.6 | 91.7 |
| 89.6 | 18.4 | 90.0 | 23.9 | 7.69 | 38.0 | 3.07 | 2.88 | 0.18 | 2.75 | 32.2 | 29.4 | 91.1 |
| 89.7 | 18.5 | 90.0 | 25.2 | 7.61 | 38.6 | 3.19 | 2.93 | 0.26 | 2.87 | 34.0 | 30.9 | 90.9 |
| 90.5 | 19.9 | 90.5 | 25.5 | 7.22 | 38.6 | 3.06 | 2.93 | 0.13 | 2.74 | 34.4 | 31.2 | 90.8 |
| 90.5 | 19.9 | 91.0 | 25.2 | 7.39 | 38.5 | 3.10 | 2.92 | 0.18 | 2.78 | 34.2 | 30.9 | 90.2 |
| 91.8 | 21.7 | 91.0 | 25.9 | 7.34 | 38.6 | 3.16 | 2.93 | 0.23 | 2.84 | 35.3 | 31.7 | 90.0 |
| 91.8 | 21.7 | 91.0 | 25.9 | 7.40 | 39.0 | 3.19 | 2.96 | 0.23 | 2.87 | 35.3 | 31.7 | 90.0 |
| 91.8 | 21.7 | 91.5 | 27.6 | 7.00 | 40.2 | 3.22 | 3.05 | 0.17 | 2.88 | 37.7 | 33.8 | 89.7 |
| 92.0 | 22.0 | 92.5 | 28.4 | 6.53 | 38.1 | 3.09 | 2.89 | 0.20 | 2.78 | 39.4 | 34.9 | 88.6 |
| 93.0 | 23.2 | 93.0 | 29.4 | 6.40 | 39.1 | 3.14 | 2.97 | 0.17 | 2.82 | 40.9 | 36.1 | 88.2 |
| 93.3 | 23.6 | 93.0 | 31.0 | 6.01 | 38.2 | 3.10 | 2.90 | 0.20 | 2.79 | 43.1 | 38.0 | 88.1 |

To allow for comparison between actual and simulated performance Tables 6.2 - 6.8 also give the simulated output for the closest values of driving pressure.

## 6.1.4 Discussion on Compressed Air Operation

### 6.1.4.1 Observations Made During Operation

After some experimentation and refinement of the valve triggering mechanism the

pump's operation on compressed air was very encouraging. The pump cycled smoothly with a consistent discharge. The flow pulsed slightly at the end of each stroke but not enough to stop the flow of water. The flow performance indicated the inertial losses due to the acceleration and deceleration of water were much less significant in the double acting pump than any single acting design. As pump flow rate was increased output continuity improved. The simulation conservatively assumes water velocity at the beginning of each stroke is essentially zero. At low flow rates this assumption has some validity, however with increasing flow, the simulation is likely to underestimate pump performance. For a closed system (cycling a fixed volume of working fluid) the speed of displacer reversal is dependant on the pressure changes within the boiler and condenser when the valve changes. The pressure stability is primarily a function of the thermal inertia of the system and working fluid, dead volume in pump chambers, amount of valve leakage, and speed of exhaust and condensation. Stroke reversal may be slower on Pentane due to the above factors and thus the assumption made in the simulation will have greater validity.

The system was found to be highly sensitive to supply pressure variations. Approximately 1 kPa increase in supply pressure at a 6 metre static water head will increase flow by approximately 2.5 litres per minute. A 1 kPa increase in pressure corresponds to a 0.2°C increase in system temperature !

The one-way flap valves controlling water flow functioned well at all heads and flow rates. There was no noticeable leakage under static loads meaning the pump would keep its prime for long periods. Although the positive displacement pump is self priming, startup of an unprimed unit lifting water through a high static suction head or long length of intake pipe may be unreliable should the condenser temperature rise too high before the pumped cooling water can aid condensation.

At high static heads (7.5m $H_2O$) and high flow rates (30 l/m) the 4mm thick steel covers sealing the water chambers showed noticeable deflection as the chamber alternated between suction and discharge. Although the pump still functioned well during testing, this operation exceeds the design limits of the system and the physical limits of

the pumps components. Redesign of the pump's water chambers would be necessary to reduce losses and component fatigue if the pump were to be operated continuously at this loading. The worst loading condition occurs during suction when the end plates are subject to atmospheric pressure plus the dynamic suction head. A pressure differential of 200 kPa on the 4mm thick end plates results in a stress of 146 MPa and a deflection of 0.6 mm.

The operation of the detent was observed to cause some problems in the function of the pump. At very low speeds and high static loading the pump's valve would toggle correctly in one direction but would fail to toggle or would not latch correctly in the other direction. The design of the detent results in some asymmetry of operation i.e. the release force of the detent differs slightly depending on the direction of movement of

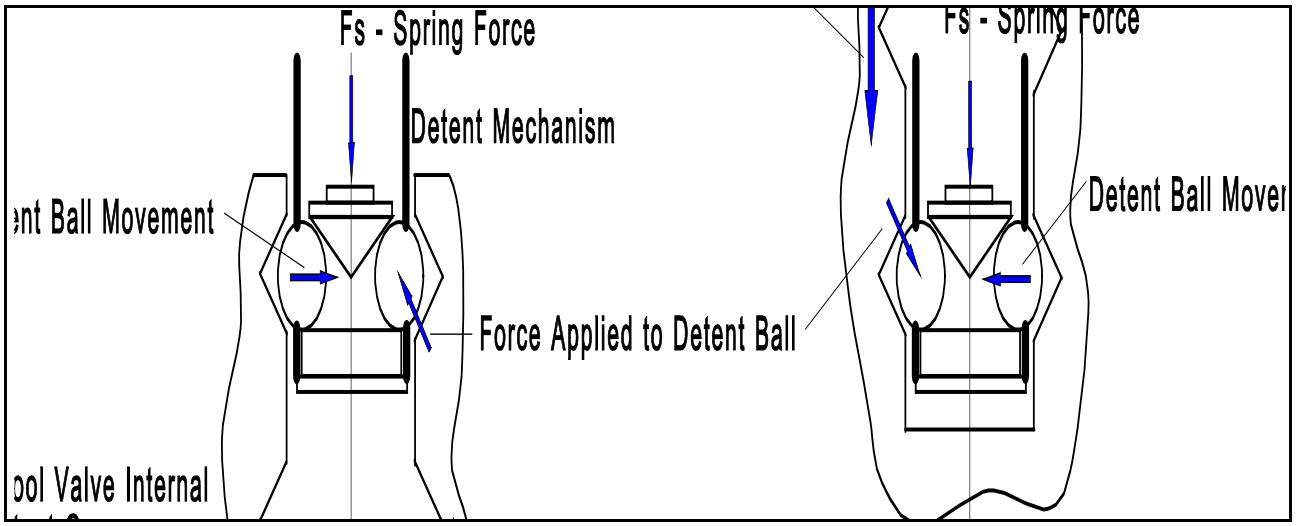


the spool valve.

*Figure 6.2* shows the operation of the detent. In order to release, the detent balls must slide on the detent plunger and end cap. The frictional force resisting the inward movement of the balls varies depending on the direction of spool movement. This problem was only apparent at higher static loadings (>4.5m$H_2O$) when the increased operating pressures resulted in greater friction of the spool seals. At greater flow rates the pump functioned correctly.

Reliable operation of the pump at high heads on solar energy would be compromised

by incorrect detent function. Redesign of the sprung actuators helped compensate for the asymmetric detent function however redesign of the detent itself would be required to eliminate improper operation and very low flow rates.

### 6.1.4.2 Pump Performance - Analysis of Results

Tables 6.2 - 6.8 show the pump performance on compressed air compared to the simulated performance on Pentane for a given pressure differential (driving pressure less exhaust pressure). The entries in these tables show:

- Simulated operation of the system on Pentane showing driving pressure differential (boiler pressure (abs.) less condenser pressure (abs.)) and corresponding predicted water flow rate.

- Compressed air driving pressure differential (air supply pressure (abs.) less exhaust pressure (abs.)) and the corresponding measured water flow rate.

- Mean Pump cycle time. The time for the pump to execute one complete downward stroke plus one complete upward stroke i.e. one complete cycle.

- Measured pump stroke during operation. Stroke length is related to the operation of the main valve. The main valve is triggered by displacer position. It can be seen that stroke length is relatively consistent up to 5m static head when some modifications were made to the triggering mechanism which resulted in a reduced stroke. The length of stroke of the actual unit is less than the design optimum of 52mm due to the inability to form the diaphragms in the prototype unit. The diaphragms restricted pump stroke to a maximum of 47.5mm. This is further reduced by the valve triggering mechanism.

- Average actual water output (litres) per pump cycle. Water volume per cycle of a fully primed pump is also a function of stroke length. If the pump is improperly primed or there exists an air bubble within the water chamber the air will compress and decompress. A drop in water volume per cycle would be observed with increasing flow rate due to the greater pressure variations within

the water chamber.

- Calculated water output per pump cycle based on stroke length with no diaphragm inversion. The calculated output with no diaphragm displacement indicates how much water would be displaced for the measured stroke for that trial with rigid diaphragms.

- Additional volume of pumped water due to the inversion of the pump's diaphragms. The difference between predicted output and the actual output per cycle gives the volumetric displacement of water due to the displacement of the pump's diaphragms. The variation observed in these values result from the cumulative error in the measurements of stroke length as well as water flow rate per cycle. This error is estimated at ±0.2 litres.
- The calculated volume of air used per cycle is based on stroke length and the volumetric displacement due to the inversion of the pumps diaphragms in the calculated in the previous column. Note: the additional volume of air used to invert the central (small) diaphragm is treated as insignificant in this calculation.

- The work input based on air pressure and calculated air flow rate.

- The work output based on water head and the water flow rate.

- The corresponding pumping efficiency of the unit.

The graphs of flow rate versus operating pressure can be seen *Figures 6.3 - 6.9*.

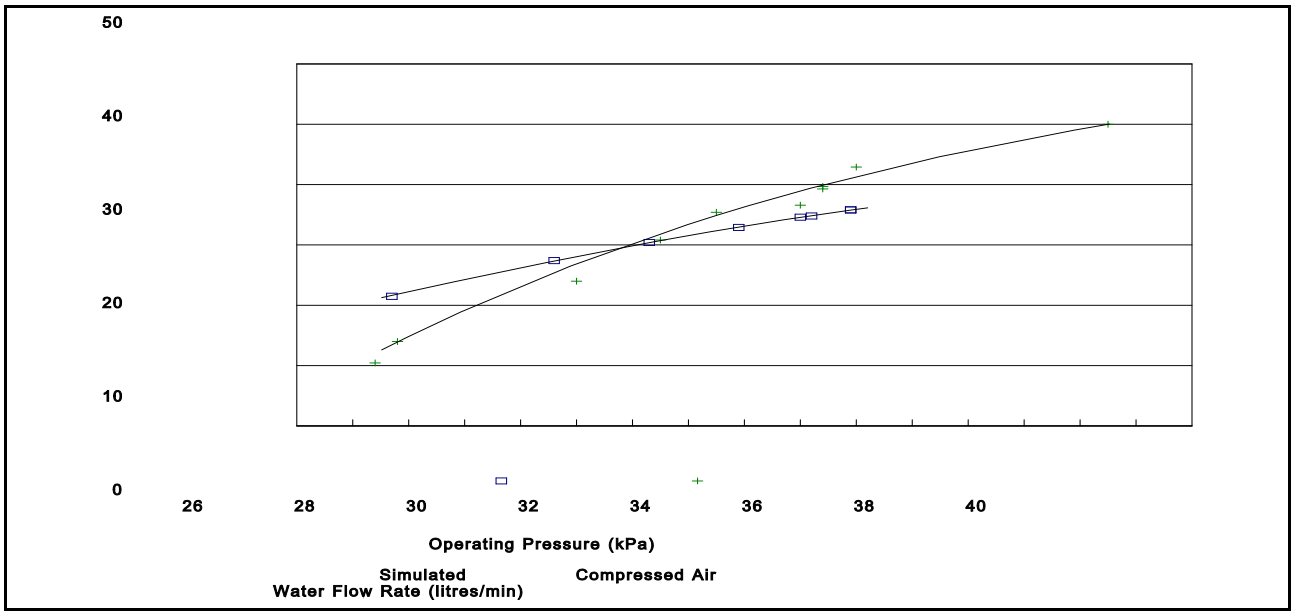
50
40
30
20
10
0
26
28
30
32
34
36
38
40
Operating Pressure (kPa)
Simulated
Compressed Air
Water Flow Rate (litres/min)

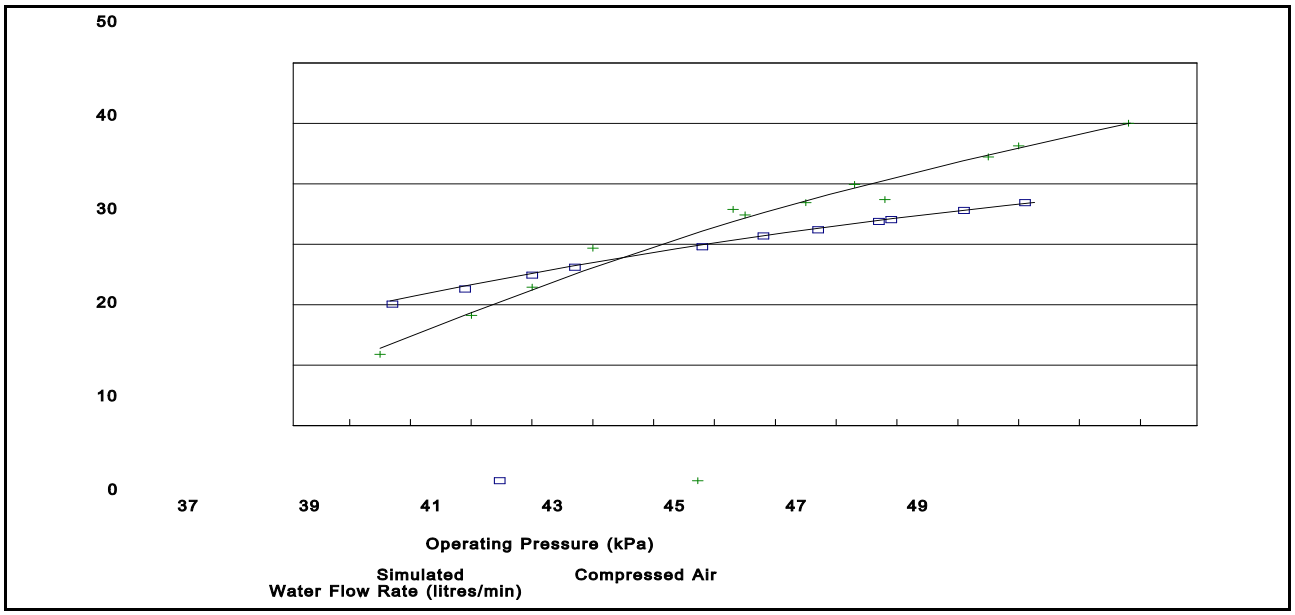
50
40
30
20
10
0
37
39
41
43
45
47
49
Operating Pressure (kPa)
Simulated
Compressed Air
Water Flow Rate (litres/min)

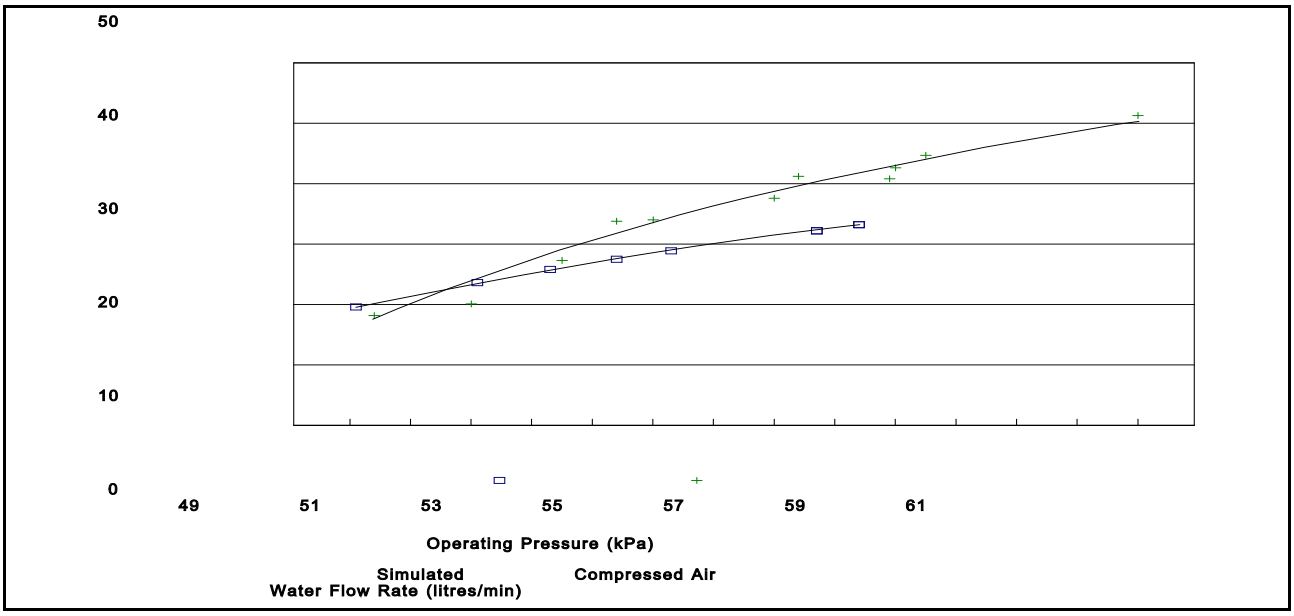
50
40
30
20
10
0
49
51
53
55
57
59
61
Operating Pressure (kPa)
Simulated
Water Flow Rate (litres/min)
Compressed Air

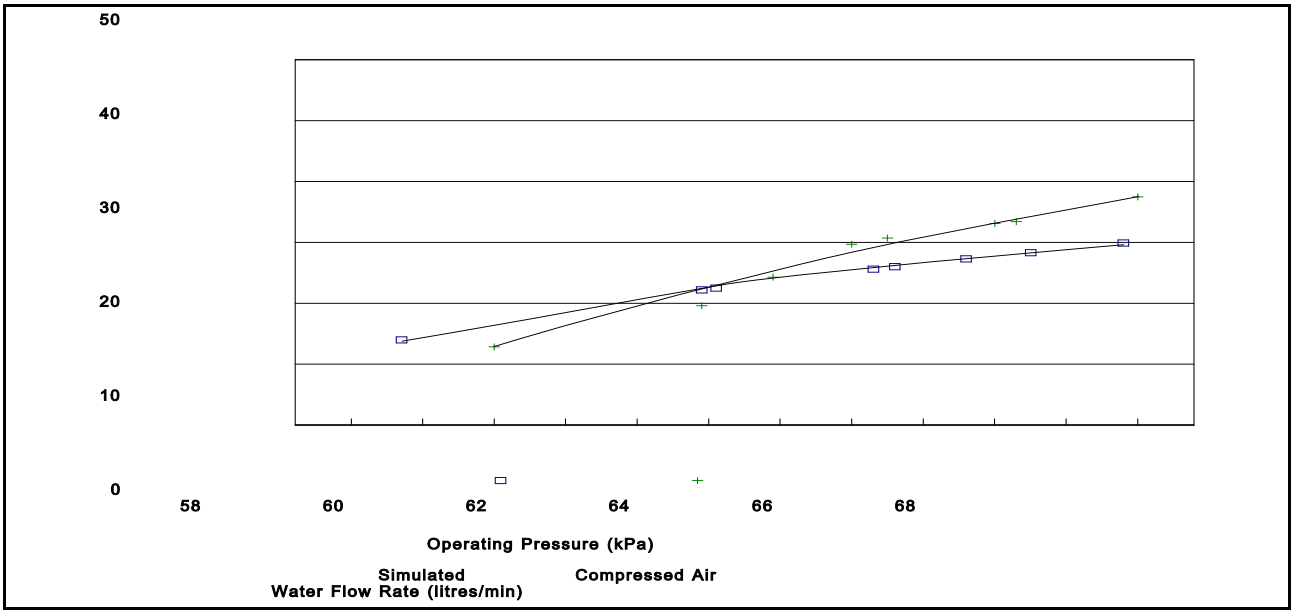
50
40
30
20
10
0
58
60
62
64
66
68
Operating Pressure (kPa)
Simulated
Water Flow Rate (litres/min)
Compressed Air

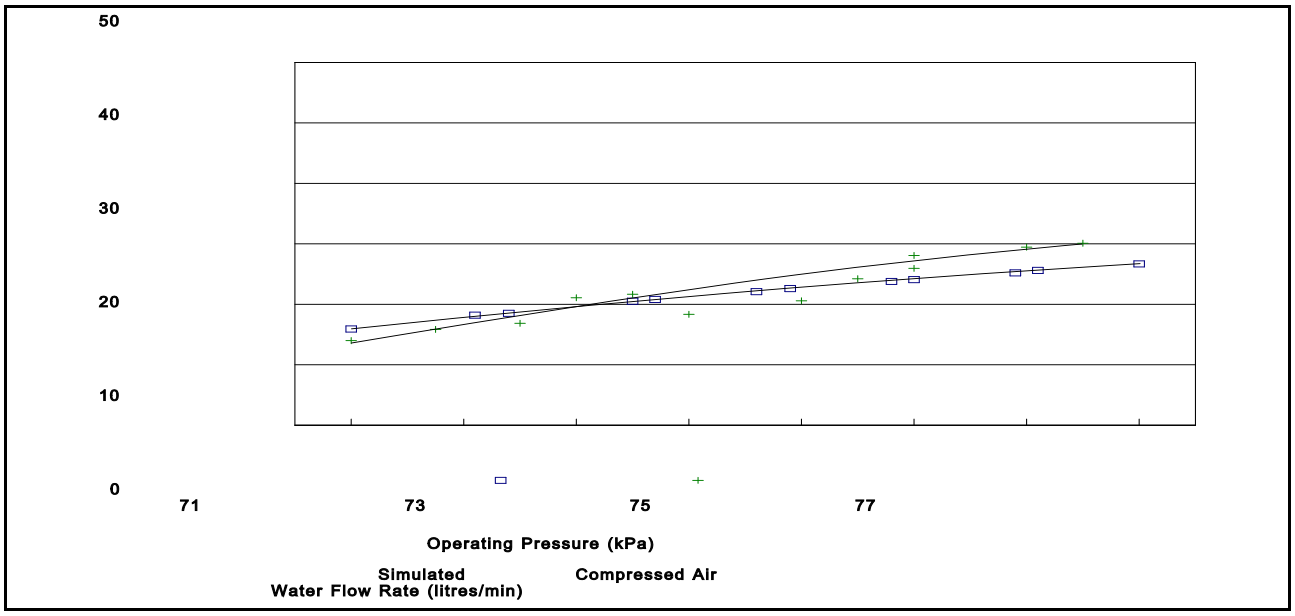
50
40
30
20
10
0
71
73
75
77
Operating Pressure (kPa)
Simulated
Water Flow Rate (litres/min)
Compressed Air

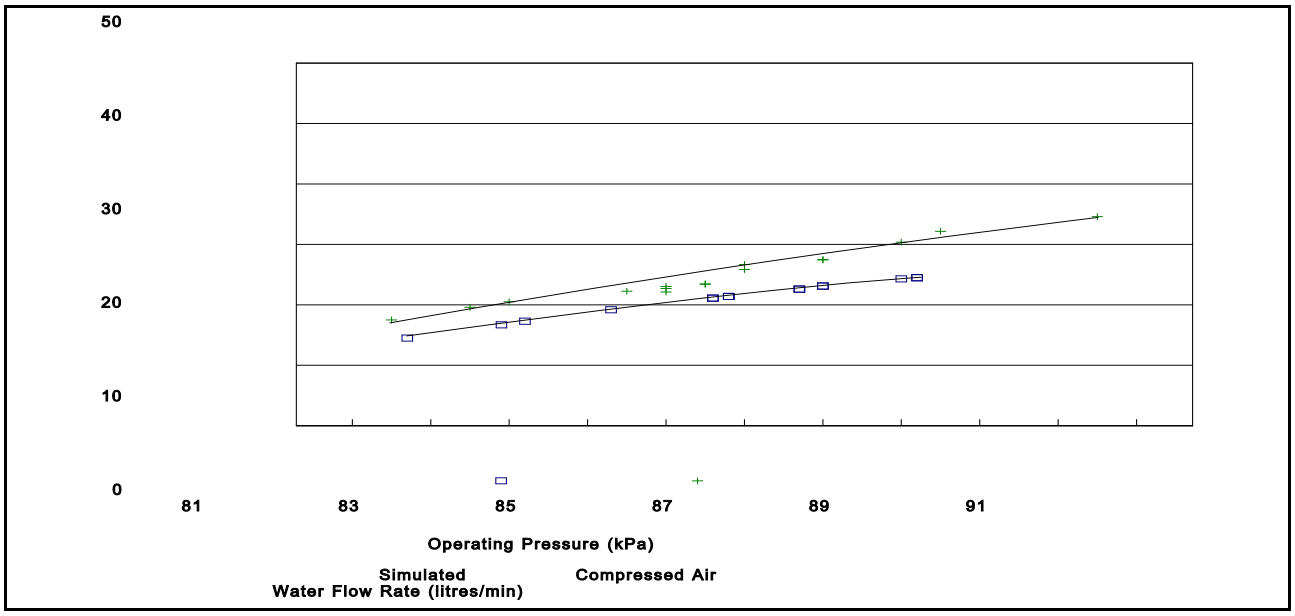
50
40
30
20
10
0
81
83
85
87
89
91
Operating Pressure (kPa)
Simulated
Water Flow Rate (litres/min)
Compressed Air

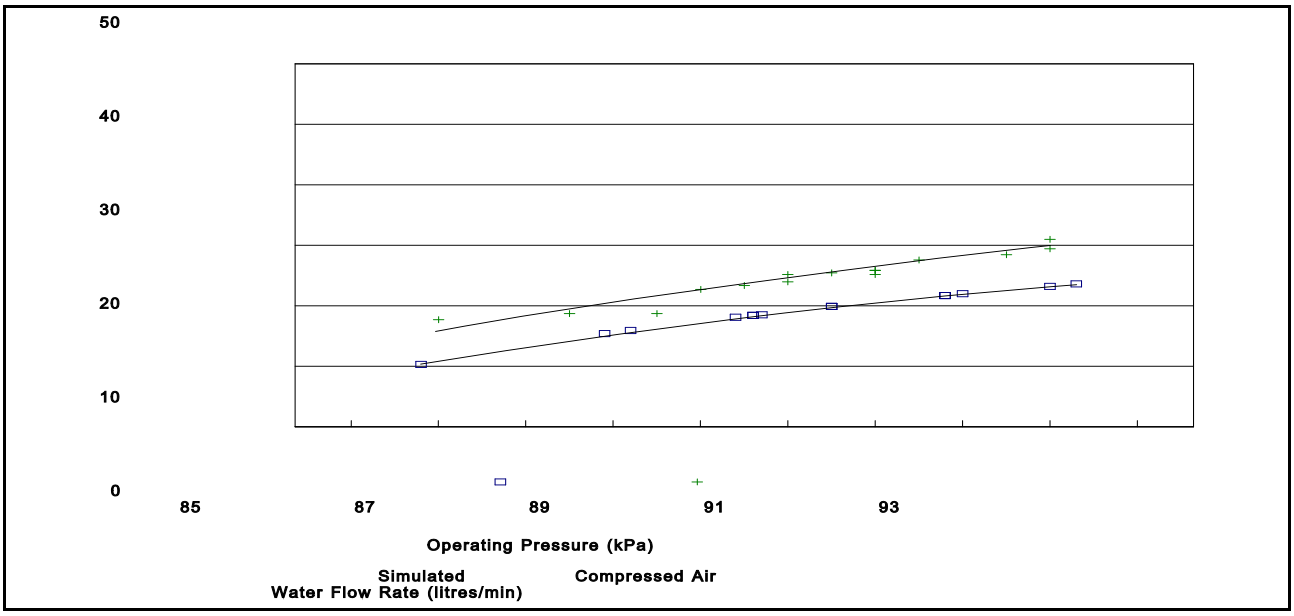


In general the output predicted by the simulation is a very good approximation to the actual output recorded. The observed discrepancies were:

1. At low flow rates the simulation tends to overpredict the water output from the pump.
2. As static head increases the degree by which the simulation overestimates flow at low flow rates tends to reduce.
3. As operating pressure increases the simulation begins to underestimate flow.

The first two observations can be explained by the fact that the simulation ignores all mechanical losses within the pump. The assumption was made that these mechanical losses would be small in comparison to other losses when the pump is operating around its design water head of 6m. At low heads the energy that is required to overcome mechanical losses and cycle the pump forms a greater proportion of the total energy requirement than at higher heads or at higher flow rates. As head or flow rate increases the discrepancy can be seen to reduce. Mechanical losses considered here are the rolling resistance of the diaphragm, operation of the spool valve and gravitational force on the displacer (although the additional pressure required to move the displacer during the upward stroke appears as a negative pressure during the downward stroke, there must still be sufficient system pressure to effect the upward stroke).

The following explanations have been proposed for the observation that at higher flow

rates the simulation tends to underestimate flow:

1. Inertia of the flowing water results in an initial flow velocity at the start of each stroke. The simulation assumes that the pump pauses at the end of each stroke and that the water comes to rest before starting the next stroke. It was observed that the pause at the end of each stroke was negligible and that the pulsations in flow were not significant enough to cause the discharge to stop. The initial flow velocity will increase with increasing flow rate resulting in a greater output than predicted by the simulation.

2. The simulation overestimating losses that are a function of fluid velocity (pipe and fitting losses).

3. Also proposed was that as flow rate is increased the momentum of the pumped water increases. The momentum of the flowing water may actually draw additional water into or through the pump giving a higher flow rate than expected. This third theory is not supported well either by the observation that the pause at the end of each stroke is negligible or by the results that show the difference between the theoretical volume of water pumped per cycle and the actual volume of water pumped per cycle does not increase as flow rate increases. The difference is primarily due to the inversion of the diaphragms within the pump at the end of each stroke.

Further experimentation and measurements of precise flow velocity as a function of displacer position would be required to quantify which in particular of the first two theories had the greater effect on pump output.

Flow rates up to 50 litres per minute (at a static head of 4 metres) were tested. At greater loads the maximum flow rate was reduced so as not to overload the pump's components. At the maximum flow rate cycle time is approximately 4 seconds and the mean displacer speed is approximately 20 mm/s. A low displacer speed results from the simulation optimising the pump's geometry to maximise the work output per cycle. A large displacer moving slowly is more efficient than a small displacer moving

rapidly. Given a fixed stroke length, the small displacer will also cycle more often for

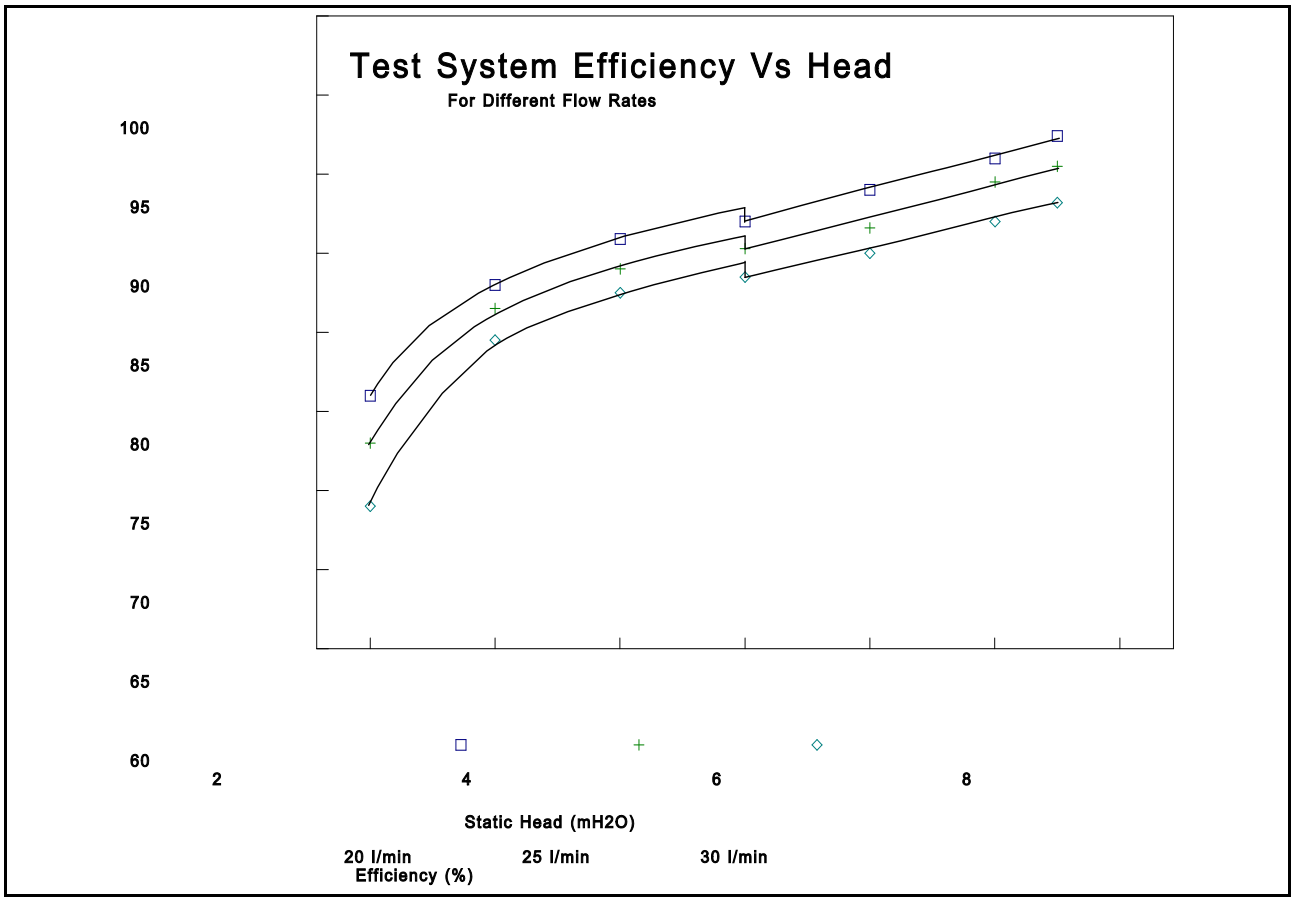


the same flow. Losses are induced at the end of each cycle.

*Figure 6.10* shows system efficiency versus static head for three different flow rates. It can be seen that:

4. As static head is increased pumping efficiency increases. This is a characteristic of displacement pumps which are more efficient at high heads and low flow rates. A smaller percentage of input work is being used to overcome mechanical losses. Also as head increases the pumped fluid increases potential energy (output work) with additional fluid frictional losses resulting only from the increased length of water pipe. Efficiency will drop off rapidly with head as cavitation begins to occur in the intake pipe.

5. The drop in efficiency at the 5 metre working head is due to the additional

fittings and intake pipe required to test heads greater than 4 metres in the test rig.

6. System efficiency increases with reduced flow rate. At higher flow rates more energy is lost to fluid friction (a function of fluid velocity) causing a reduction in useful work output as a percentage of work input.

7. The system efficiency drops off rapidly at lower heads as a smaller percentage of input work is used to increase the potential energy of the fluid and more is used simply to overcome the mechanical and frictional losses.

*Figure 6.11* shows the system efficiency versus flow rate for the design working head of 6m $H_2O$. It can again be seen the effect of increasing flow rate causing a reduction in efficiency. The average daily flow rate predicted by the simulation is 17.8 litres per minute with a maximum flow of 27 litres per minute reaching a maximum flow during the day of 27 litre per minute. It can be seen that for a typical day's operation the pumping efficiency of the unit will remain above approximately 86%. As the flow rate exceeds the design expectation the efficiency of the unit drops. If higher flow rates were required further optimisation of the pump components and pumping system to reduce flow and fitting losses would be recommended. The diameter and design of the water chambers would also require changing to reduce water flow velocity.

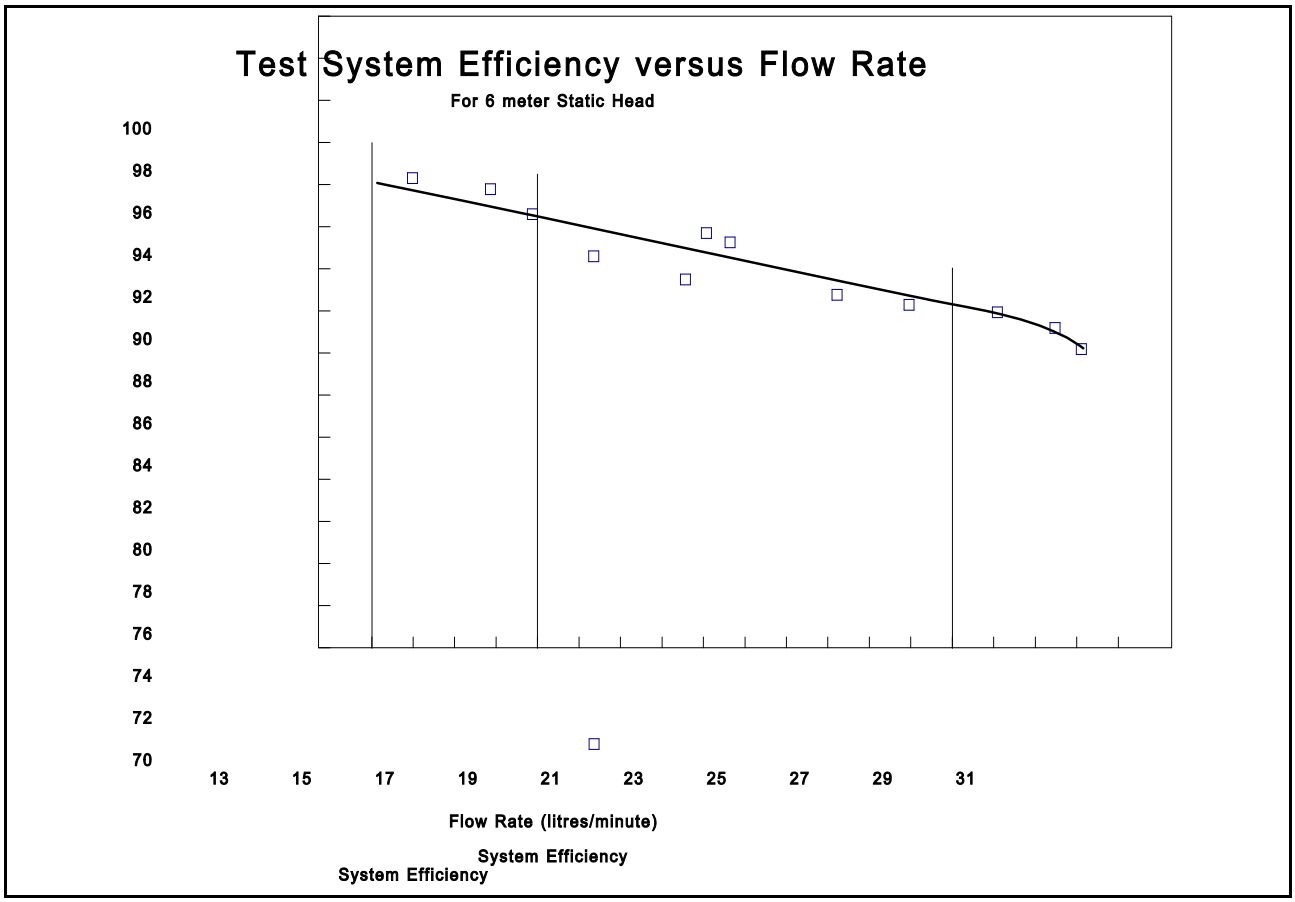


The results for the compressed air testing of Amor's (1991) single acting pump can be seen in Table 6.9. The driving Pressures are considerably higher and flow rates considerably lower than those of the double acting design. The optimisation of the double acting design resulted in a lower operating pressure differential but higher working fluid flow rate than that of the single acting unit. The lower operating pressure results in lower collector temperature and corresponding greater collector efficiency. The very low flow rates observed with the single acting design were a result of the very slow exhaust / delivery stroke and lower pumping efficiency of this configuration.

| Static Water Head ($m.H_2O$) | Driving Pressure (kPa) | Flowrate (litres/min) |
|---|---|---|
| 1.8 | 177 | 12.7 |
| 2.3 | 184 | 11.5 |
| 2.8 | 190 | 9.6 |
| 4.6 | 177 | 10.7 |
| 6.9 | 177 | 8.8 |
| 7.9 | 190 | 6.9 |

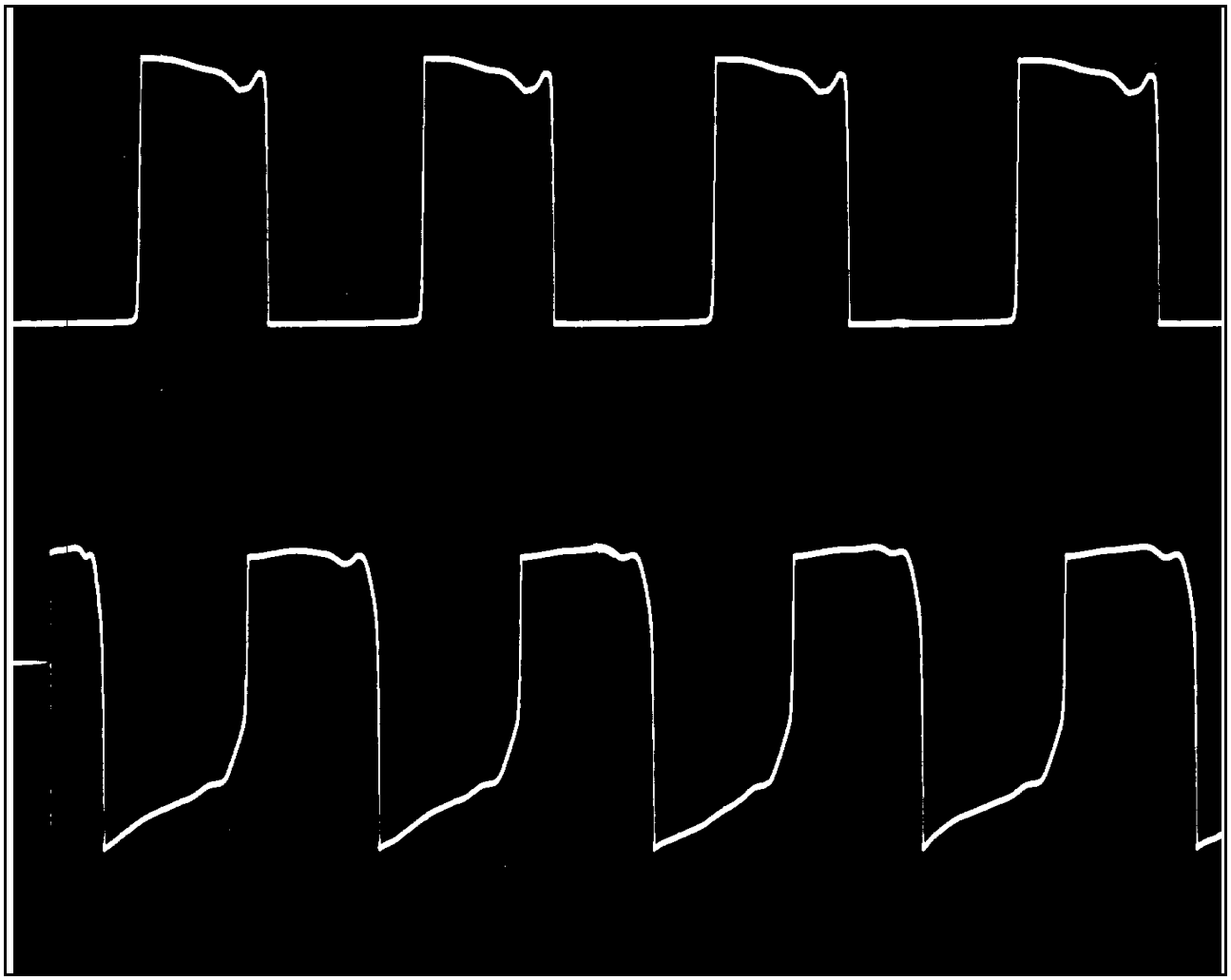

*Figure 6.12(a)* shows the pressure variations within the lower vapour chamber of the pump as it is cycled on compressed air and exhausts to atmosphere. The suction head of the pump is 0.5m and the discharge head is 1.5m giving a total head of 2m. At the beginning of the cycle the valve opens the vapour chamber to the high pressure air supply. The pressure within the vapour chamber rises rapidly to approximately 126 kPa (absolute) as the displacer decelerates (moving in the upward direction) the pressure drops to approximately 124 kPa while the displacer stops and ramps gradually to approximately 127 kPa as the displacer is accelerated in the downward direction. At the end of the stroke the main valve toggles to exhaust the chamber to atmosphere. At this point there is a rapid drop in pressure to 102 kPa. The almost instantaneous drop in pressure indicates that the flow losses within the main valve are small.

*Figure 6.12(b)* shows the pump cycling air in a closed loop system not open to

atmospheric pressure. A small air pump was used to extract air from the condenser and pressurise the boiler. The air pressure within the vapour chamber again rises rapidly as the vapour chamber fills and the displacer decelerates. Similarly the small drop in pressure is observed as the displacer stops and changes direction. The pressure in the boiler and vapour chamber drops off as the cycle progresses as the small air pump is not capable of maintaining the high pressure and flow rate as it extracts air and reduces the pressure in the condenser. At the end of the stroke when the valve toggles the vapour chamber exhausts rapidly to the condenser until both the vapour chamber and the condenser and the condenser are at a pressure equilibrium. The pressure drop is more gradual as the small air pump extracts the air from the condenser.

After approximately 40 hours of use on compressed air the pump was dismantled and the pump's components examined prior to operation on Pentane. There was no observable degradation of any of the pump's diaphragms nor any signs of rubbing contact or wear of the diaphragm on the perimeter clamps. Very minor corrosion of the aluminium and painted surfaces was observed in the water chambers but none in either the vapour chambers or the feed pump. The pump was reassembled and sealed with Loctite™ 515 Master gasket for the next stage of experimentation.

## 6.2 Testing of Pump Operation on Heated n-Pentane

The aim of this part of the experiment was to test the pumping system in a manner identical to that expected under solar conditions. Results from this testing would give greater understanding of pump thermodynamics and flow processes, operational problems and reliability, performance and efficiency. Further recommendations to pump hardware, design and theoretical system modelling may then be made to further refine on the work of this research.

### 6.2.1 Test System

The test set-up can be seen in *Plates 6.2 & 6.3*. *Plate 6.2* shows components located outside on the solar deck, Level Two, Department of Mechanical Engineering, University of Canterbury. *Plate 6.3* shows the mains powered control and measuring

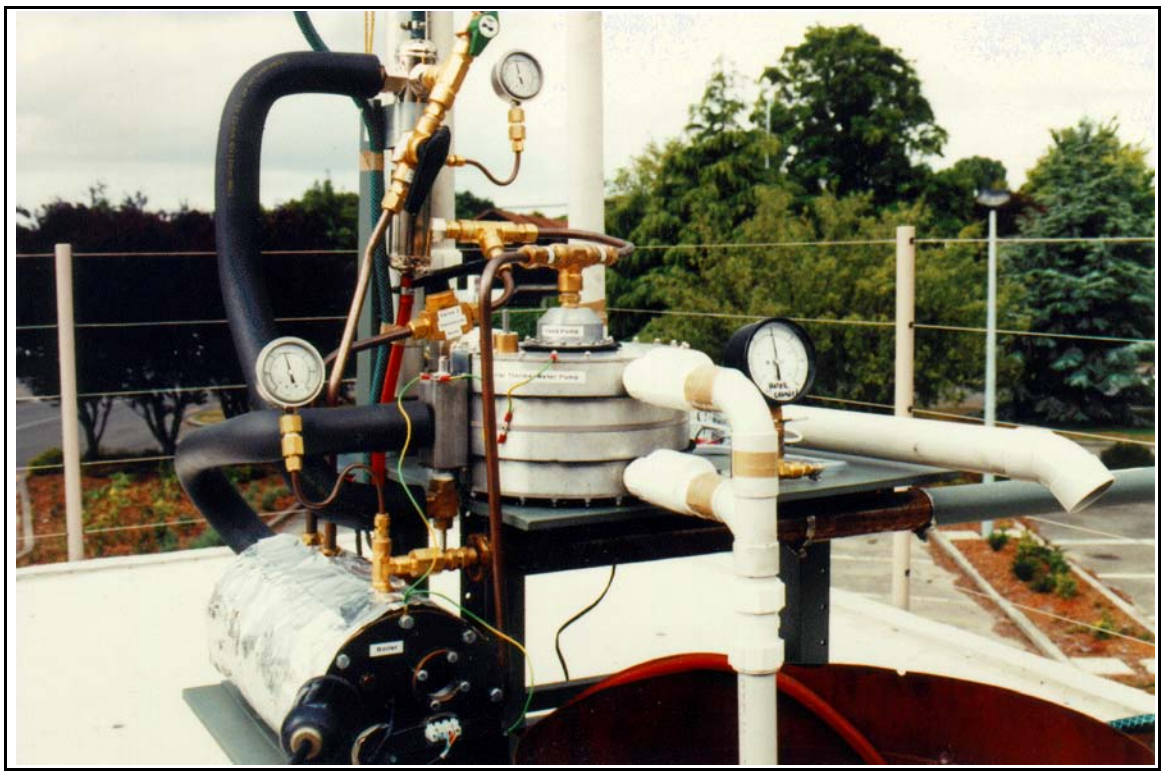

equipment located in the solar control room.

To get accurate and controllable heat input to the working fluid, solar heating was simulated by two electric water heating elements inside a 6 litre pressure vessel. This allowed electrical heat input (W) to be read directly off a Yokogawa 2433 clip on AC power meter. Electrical power could be adjusted via a 2kW Variac. By taking into account the minor heat loss from the boiler, the energy input to the 4 litres of working fluid could be determined and, after taking into account the corresponding collector efficiency, compared directly to an equivalent level of solar insolation or simulation result.

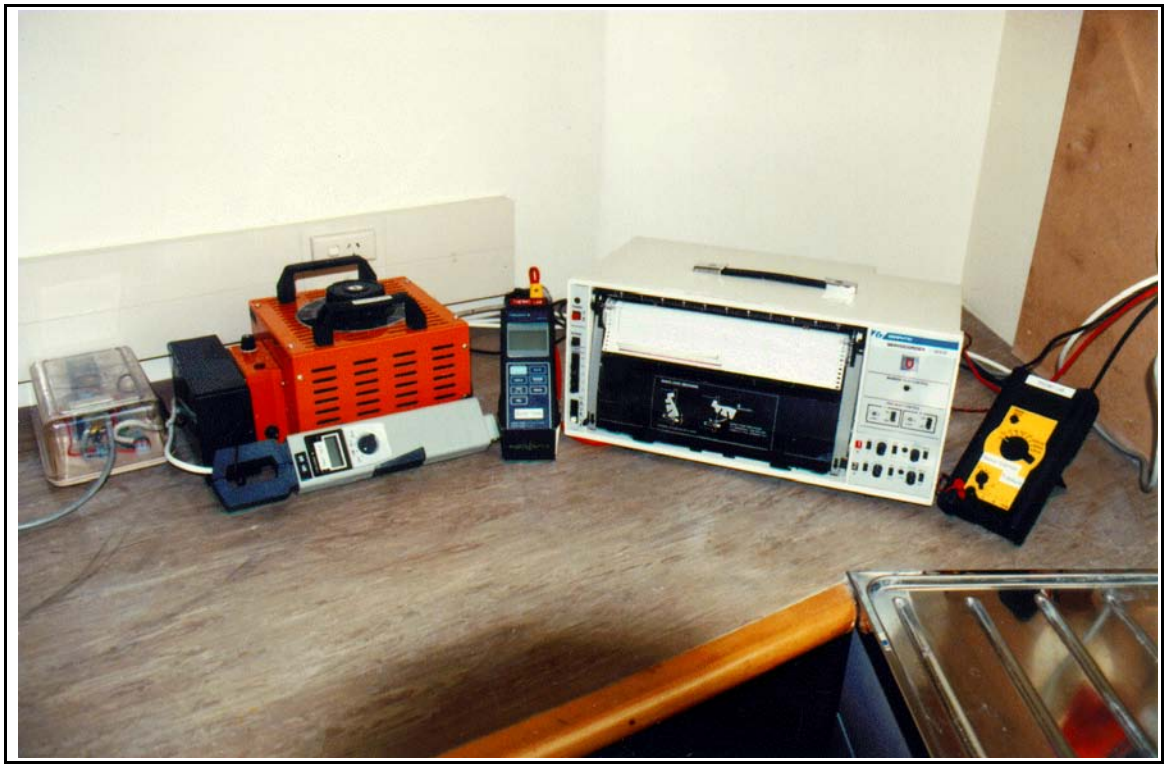

The pump was directly coupled to the boiler output via a 3/4" copper tube insulated[1] to reduce condensation of the saturated vapour. The circumference of the boiler was insulated with fibreglass backed aluminium, the ends left uninsulated for the safety reasons discussed in Section 6.2.2.

Exhaust from the pump was fed directly into the top of the shell and tube condenser located 500mm above the pump exhaust. The height of the condenser was to ensure gravity priming of the feed pump with condensate should the feed pump have less than satisfactory suction capacity. In the test arrangement the condenser was cooled by the water flowing from the mains into the lower pumping reservoir. The condenser outlet (lower tapping) fed through the feed pump back to the boiler.

[1] Centurylon AP701, foam insulator.

Pressure readings were read from bourdon tube gauges located on the boiler, condenser, and lower water chamber. All gauges read from -100 to +100 kPa with a claimed accuracy of 1%. The boiler and condenser gauges gave damped readings of working pressures, the water chamber gauge gave undamped dynamic readings of total suction lift ($h_s$) and total discharge head ($h_d$) during operation. Accurate measuring and recording of pressure in the lower vapour chamber was made using a pressure transducer and signal conditioning amplifier with offset and gain control coupled to a 4 digit digital multimeter and Graphtec Servocorder (for recording). The pressure transducer was calibrated to give a 1000mV reading on the multimeter for a 1000mbar input and was accurate to ±2mbar for a 0 - 2000mbar range. The Servocorder enabled real time recording of pressure variations within the vapour chamber during both evaporation and condensation stages (intake and exhaust) of the pumps cycle.

A thermocouple located in the boiler enabled accurate measurement of the working fluid temperatures to ± 0.5°C. Flow measurement was again made using bucket and stopwatch techniques.

### 6.2.2 Boiling n-Pentane: Safety Aspects

The introduction of Occupational Health and Safety Regulations (OSH) meant that the boiling of a flammable liquid caused considerably more concern than initially indicated in the conceptual design stage of this project. Significant effort was required to minimise risks and maximise operator safety in order to gain approval to commence testing. In the literature cited there have been no concerns documented by previous researchers using the same working fluid. Final conclusions led to the following hardware and procedural modifications:

- Optical level cut-out: A solid state optical liquid level switch consisting of an integral photosensor and LED in a solvent resistant polysulphone housing was mounted in the boiler approximately 30mm above the heating elements. The sensor controlled a relay through which power to the Variac and heating elements was switched. This was to ensure that if the liquid Pentane level in

the boiler dropped below this point and risked exposing the elements, the elements would automatically turn off. A 10mm thick perspex window placed in the boiler enabled a visual indication of liquid level and fluid activity.

- Thermal fuses: Two single shot Microtemp™ thermal fuses were wired in series with the heating elements. The fuses were mounted in thin-walled stainless steel pockets immersed in the working fluid in the centre of the elements (see *Plate 6.4*). These fuses have two sprung contacts mounted in a low melting point wax. When external temperatures exceed the melting point of the wax the contacts separate. Two series wired fuses were used for increased safety and were designed to trigger at a temperature of 60°C. At 60°C the absolute saturated vapour pressure of the n-Pentane working fluid is 214kPa, 14kPa higher than the maximum pressure desired during testing at maximum load.

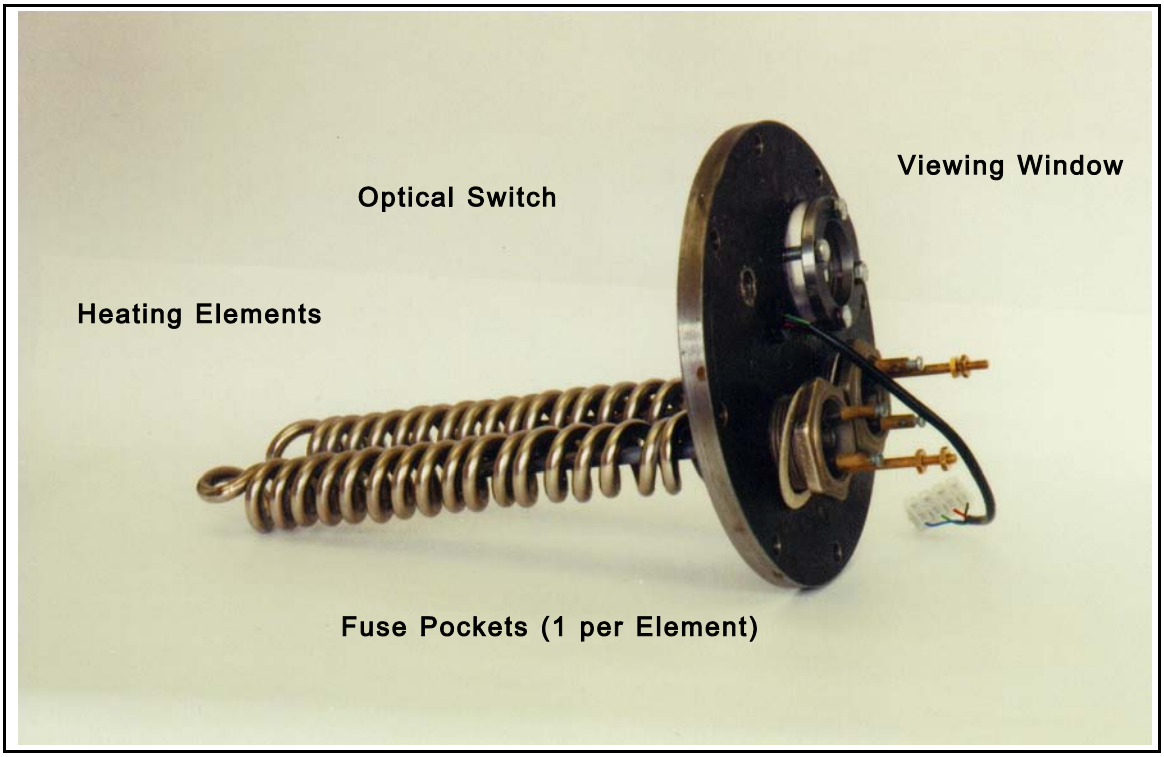


- Low watt density heating elements: It is essential that the temperature of any surface within the system is maintained well below the auto-ignition temperature of n-pentane at 309°C (BDH Data Sheets). Under normal evacuated conditions, ignition is not possible. If a connection or diaphragm

should fail which allows the introduction of air into the system, a high surface temperature will cause ignition and free burning of the fuel.

A number of methods for the safe heating of the fluid were considered. The most convenient method was to use two 1500 Watt low temperature water heating elements. This enabled direct electronic monitoring and measurement of power input. Each element was made of a 2 m length of 8 mm stainless steel Incaloy coiled to give an overall diameter of 38 mm and length of 280 mm. Total surface area for each element of $50 \times 10^{-3} m^2$ and Watt density of 3 $W/cm^2$ at 1500W. At rated power a surface temperature approximately 30°K above fluid temperature would result. In the test set-up two elements were wired in parallel and each run at less than half of rated power to further increase the safety margin.

The elements, optical switch and perspex viewing window can be seen mounted in the boiler endplate in *Plate 6.4.* A wiring diagram for the above electrical safety devices controlling input power to the heating elements can be seen in *Figure 6.13*. With a flash point of -48°C any likely sources of ignition (sparks, flames) both internal and external to the system had to be eliminated. The entire system was earthed to prevent static discharges. All electrical switching equipment with mechanical contacts was located inside the building. Only essential equipment was operated outside with the pump.

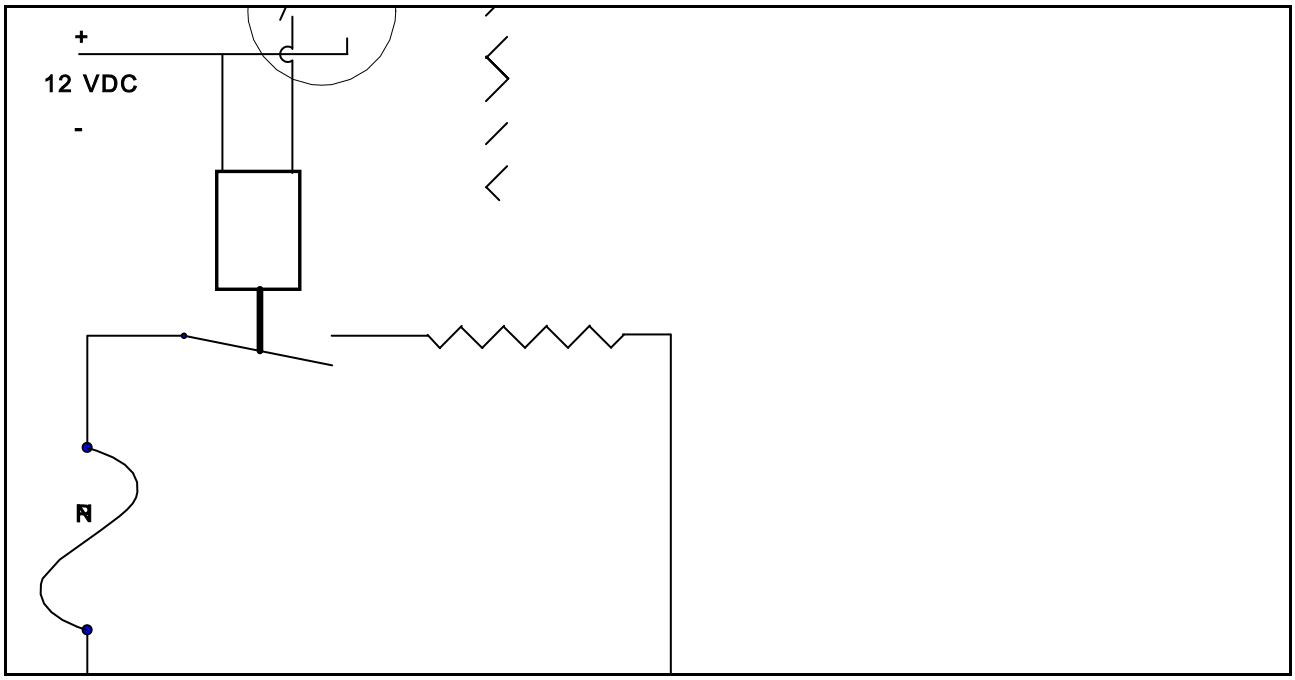


- Overpressure valve: To prevent pressure runaway should the pump fail a pressure relief valve was fitted to the boiler. The relief valve had a cracking pressure of 135kPa gauge corresponding to a working fluid temperature of 63°C (at which the thermal fuses would blow and prevent further heat input). A self draining chimney exhausted the vapour clear of the operator.

- Boiler bypass to condenser: To allow rapid pressure shut down of the system without loss of vapour to atmosphere two valved bypass lines were incorporated between the boiler and condenser. Opening these valves exposed high pressure Pentane vapour to the condenser. The condensate could gravity drain back to the boiler. This was the reason during the initial testing program to cool the condenser with a mains supplied water source rather than the water discharged by the pump.

The full liquid / vapour circuit for the Pentane can be seen in *Figure 6.14.*

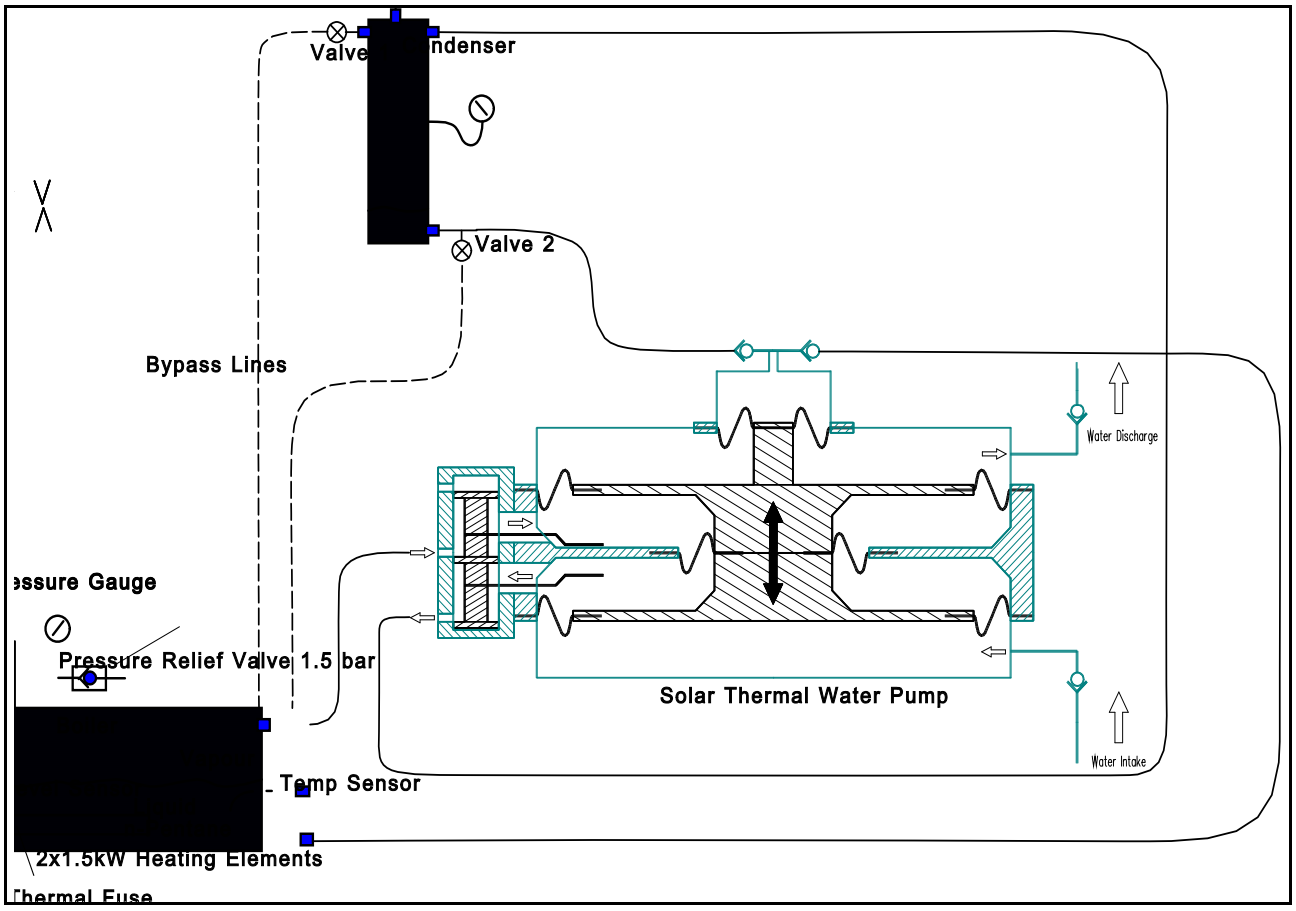


- Valves and fittings: All fittings and connections on the Pentane side of the system were of the Swagelock or Cajon brand, well known for their sealing reliability. The three valves on the system consisted of two Whitey ball valves and one Nupro plug valve. It was essential for all connections to be vacuum and pressure tight to prevent air leakage into the system or pentane leakage out. Where possible valve stems were kept on the atmospheric side of the valve seal.

- Fire Safety Equipment: Two 5½ kg Dry Chemical Fire Extinguishers were located in convenient positions around the rig. A $CO_2$ Extinguisher was also used to rapidly cool the boiler if necessary. For this reason the ends of the boiler were left uninsulated.

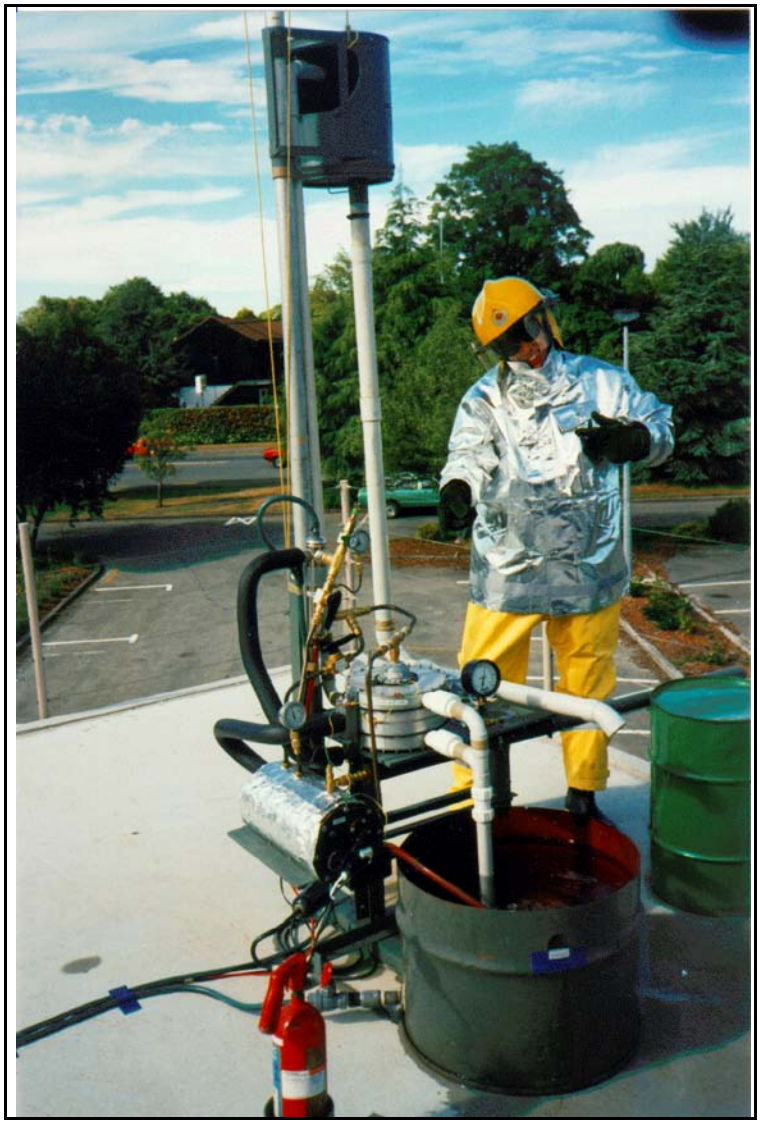

A full set of flame proof clothing was worn by each of the two operators. This included full level one fire fighting equipment (flame retardant cotton overalls, boots and gloves) and full level two equipment (flame proof overtrousers and cotton liner, flame proof aluminium jacket, cotton and woolen liners, helmet and face shield) seen in Plate 6.5. A safety screen was also nearby for the operator to seek refuge behind should a dangerous system state occur.

- Safety with Pentane: In order for a flammable liquid to burn, two conditions must be satisfied:

1. a correct fuel / air mix (for n-Pentane this ranges between 1.5% and 7.8% (Kirk.Othmer 1980) and
2. an ignition source.

Under normal circumstances in the STWP the n-Pentane is stored in an evacuated system with no internal sources of ignition. Heat is gently applied to the working fluid within the system, increasing the internal energy and exciting more molecules into the vapour state, an increase in pressure within the system results. Under these conditions there is no possibility of ignition. If the integrity of the systems seal is substandard or broken, two problems may arise: Leakage of air into the system only results in reduced performance of the condenser as there are no internal sources of ignition, the system will

still operate safely.

Due to the low viscosity of Pentane, leakage of vapour into the atmosphere is of greater concern should a sufficient concentration accumulate near an ignition source. For this reason all testing was carried out outside during periods of light breeze. Pentane vapour is heavier than air, requiring attention to low points such as drains. It was recommended that testing and experimentation be kept to a minimum. Full hazard data sheets for n-Pentane can be seen in Appendix 1.

### 6.2.3 Test Procedure

It was envisaged a short run of tests at heads ranging from 2 metres to 7.5 metres at 4 heat input levels of 1, 1.25, 1.5 and 1.75 kW be carried out to enable performance comparisons with compressed air results and the simulated output for a good summers day.

Before each run the system was thoroughly evacuated. A single vane Hitachi vacuum pump removed air from the highest level of the system (the condenser) pulling system pressure down to the point where the liquid Pentane (already loaded in the boiler) boiled, displacing the air. The exhaust from the vacuum pump was bubbled through liquid n-Pentane in order to ascertain when all air had been purged. Valves 1 and 2 were then closed (refer *Figure 6.14*) causing the vacuum pump to cycle the solar pump and exhaust air trapped within the pumps vapour chambers, this also served to prime the pump with water. Closing valve 3 sealed the system.

Two operators were required during testing. One responsible for the electronic control equipment inside the solar control room, one outside on the solar deck taking physical measurements from the pump.

Input was gradually increased from 0 W to the desired level over a five minute period. Desired readings for each head and heat input level was primarily the flow rate to enable pumping power and efficiency calculations. Also important were the boiler and condenser pressures, boiler temperature, pump cycle time and vapour chamber

pressure variations. These measurements could be extracted from the servocorder pressure trace and instruments described in Section 6.2.1. These readings would enable more detailed investigation of operational characteristics and a check on the validity of calculations within the pump simulation (PUMP) routine of the model. Detailed system operating procedure and practice can be found in Appendix 2.

### 6.2.4 Results

A number of attempts were made to achieve successful operation of the pump. Each time approximately 2 litres would be lifted 2m with 800-1000W of heat input before the pump stalled.

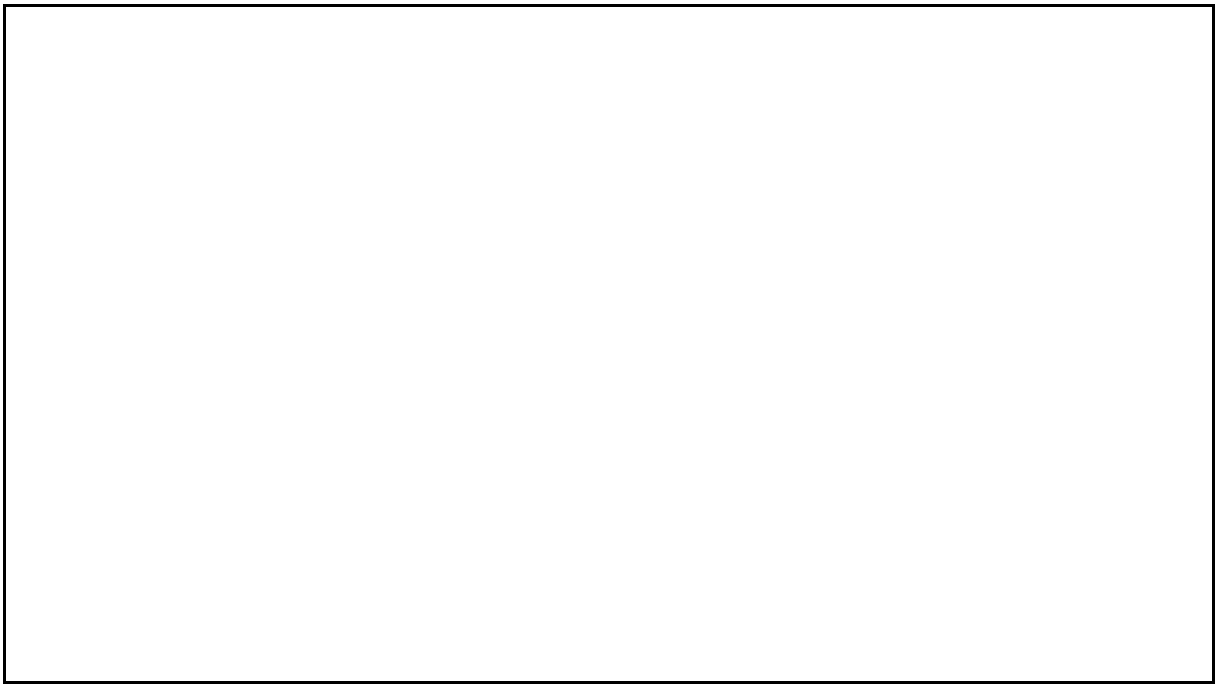

*Figure 6.15* shows the vapour chamber pressure trace (servocorder output) for one of these attempts. The trace shows the pressure building as the heat input is increased from zero to 800W during the later stages water is being lifted by the pump. The valve changes exposing the vapour chamber to the condenser resulting in the observed pressure drop. The pump continues to lift water being driven by the opposing vapour chamber. Shortly after this point the pump virtually stalls. The liquid Pentane level within the boiler was observed to drop significantly during this

startup time consequently the optical level sensor turned power off to the heating elements and testing could no longer continue. This occurred at a similar time to the pump stalling and indicated significant accumulation of condensate within the system.

Also noticeable after each test trial was the inadequate toggling of the main spool valve due to increased friction between spool seals and valve bore. This prevented the pump operating reliably and was verified by pressurising the boiler with compressed air following the test. Valve operation on air would gradually improve with time as the seals returned to their original state.

Other components operated well. Tests run on the condenser showed adequate cooling capacity although improvements may be made to pump operation by increasing its internal volume. The feed pump was tested using compressed air to positively pressurise the boiler (instead of high pressure vapour) causing the pump to cycle and pass water. The feed pump successfully drew liquid Pentane from a reservoir through a 0.5m static head, forcing it into the pressurised boiler. This procedure however could not verify the correct working capacity of the feed pump, although it was oversized in the design process to ensure the condenser never flooded under normal operation. Gauges and measuring equipment operated reliably and accurately and the arrangement functioned well as a testing rig.

### 6.2.5 Discussion based on Pentane Operation

As the results show, two problems occurred during the attempted operation of this pump which will require some design changes. Significant volumes of condensate were found to build within the initially cold vapour chamber on startup so that when the valve changed to fill the opposing chamber the pump would freely exhaust a small quantity of vapour then stall as it tried to force the liquid condensate through the valve, a significant flow restriction, and up 0.5m to the condenser.

At this point there was sufficient Pentane trapped in both pump chambers, condenser and feed pump to trigger the optical level cut-out and turn off the heating elements. Water was discharged from the pump fully during the first stroke and would stop part way through the second stroke indicating the point where condensate was being

forced through the valve.

In the initial design stages it was envisaged condensate formation within the pump due to heat losses would simply boil off when exposed to the lower pressure condenser (Bom 1993). This was included in the model and calculated in the simulation for the steady state operation of a pump already at operational temperatures. However, the significant volume of condensate that forms on start-up and its interaction with pump and prime mover operation, was not considered in sufficient detail during the design stage to realise the extent of the problem.

For example: to heat the metallic body surrounding the startup vapour chamber to a working temperature suitable to pump a 2m water head would require approximately 88 kJ of energy and result in the formation of over 410 ml of condensate. This constitutes in excess of 30% of the total internal volume of that chamber (for a 40mm stroke) and is a much higher volume than the spool valve could freely pass. This volume does not take into account the formation of condensate from thermal radiation through the displacer and diaphragms to the water mass, radiation to atmosphere, or conduction to other pump components.

Included in the model and computer simulation were the heat losses during steady state operation with all components at operating temperature. These losses included conduction and convection through the diaphragms and displacer to the water mass, losses to surroundings and other pump components and losses in associated pipework. Steady State losses amounted to 80 - 100W and resulted in the generation of less than 1.5ml of condensate per stroke.

Condensation buildup highlighted a number of points:

- The single acting feed pump operates once every cycle. The double acting pump fills one vapour chamber every stroke

# CHAPTER 7 - Conclusions and Recommendations

This research looked at the development of a small scale stand alone solar thermal engine designed to pump water.

The research was initially based on the work of Amor (1992) who developed a single acting prototype of limited success. In the course of the development, work by other researchers in this field was also studied resulting in a complete redesign of Amor's unit. A double acting design evolved that attempted to address all of the difficulties documented in previous works. The double acting design gave:

- Improved water flow characteristics resulting in less loss to water turbulence
- Improved suction lift characteristics as well as
- Improved discharge lift characteristics
- Reliable operation and start-up (a result of the double acting engine design)
- Reduced component stress (eg diaphragms)
- Optimised thermal operation of the engine and solar collector combination to suit any specified water head
- Optimised matching of engine and pump geometry
- Pressure independent operation of controlling valve and ancillary components
- Optimised system geometry to suit global location and season
- Simulated Operation of the Entire System

In the attempt to build a working and reliable, compact and viable solar thermal engine to pump water, this research unveiled many aspects worthy of further study. Although a pump was designed that exceeded expectation in terms of flow characteristics and operation on regulated air input, the pump failed to operate satisfactorily as a low temperature difference heat cycle engine.

Operation of engines similar in operating principle has been verified by previous researchers but none with the exception of Amor (1992) have attempted to optimise pump and panel operation to suit a specific designed water head. In most cases,

direct acting pumps have been designed with a 1:1 pressure ratio (ie. Working fluid pressure = total dynamic discharge or suction head). This means there is one static head where the solar pump and solar panel are operating at a maximum combined efficiency and corresponds to a head dependant on the working fluid (for n-Pentane this equated to approximately 9 metres). The intention of this research was, by including the ideas of previous designers, to design and build the ideal Solar Thermal Water Pump. With a small amount of additional development a successful unit based on this work is inevitable. Following is a brief overview of the work carried out subsequent to the study of previous publications in this field and the conclusions drawn from this research.

To begin with system thermodynamics were studied concluding that it is theoretically possible to obtain work from the "Modified Organic Rankine Cycle" the solar thermal engine executes, however inherent to the nature of the design, significant loss of exergy occurs when the working fluid is allowed to exhaust from the high pressure vapour chamber to the low pressure condenser.

A complex computer simulation initially developed by Amor was extensively re-written and improved for the new double acting design. The purpose of the simulation was not only to simulate system operation but also to optimise engine and pump geometry for the given conditions of location, time of year, desired water head and documented panel characteristics. The simulation allowed an initial study to be carried out to characterise system performance as well as provide a basis from which practical experimentation could begin. The optimisation of pump geometry is a combination of:

1. Achieving the correct pressure ratio to satisfy the load (total water head) whilst,
2. maintaining the optimum operating temperature for the collector and primer mover (engine) combination and,
3. minimising system losses (irreversibilities) for,
4. the range of atmospheric conditions experienced in the location and season of desired optimum operation.

It was also noted that significant improvements in overall energy usage (from less than 1% to approximately 24%) would be possible if the waste process heat could be used in a co-generative process such as water heating.

The simulation also showed that a pump optimised for a static water head of 6 metres ($H_2O$) would also give acceptable efficiency between 4 and 8 metres $H_2O$.

Simulation Recommendations. Further refinement of the computer model would be recommended, especially in the modelling of the exhaust (condensation) stroke of the pump's operation. Here a study of the actual performance of the system to better characterise the pressure variation within the exhausting chamber as the pump operates would be advantageous. Experiments could also be carried out to determine the effect condenser parameters have on a pump performance enabling the optimisation of condenser surface area, volume and location to be included in the simulation. Further development to the simulation in the longer term would be to include the optimisation of collector area to achieve a desired daily flow requirement. This routine could still perform a complete optimisation of pump geometry specific to the installation or simply select the most suited engine/pump from a range offered by the manufacturer.

Fabrication Recommendations. The development of the prototype unit involved many compromises that could be addressed in a production unit. The most significant of these from an efficiency viewpoint would be in the choice of materials. Thermally insulating polymeric materials such as nylon would result in reduced heat loss to the atmosphere and pumped water as well as reduced condensation/re-evaporation losses as the pump cycles. The use of polymeric materials would also allow several separate fabricated components in the prototype to be moulded as one. The use of insert moulding technology could also allow the diaphragms to be moulded into the displacer for improved sealing and simplicity.

The cost of the prototype unit was in the order of NZ$5000 (parts and labour). With batch and production manufacture the cost of the solar thermal system could be significantly less the NZ$2500, NZ$1500 of this being in the cost of the solar panels.

Testing of the prototype unit on compressed air showed the pump to function smoothly and reliably for the static water heads tested (from 2 to 7.5m $H_2O$). Flow rates in excess of 50 litres per minute were trialed with no observed difficulties. The double acting design resulted in a consistent and only slightly pulsed flow, indicating lower inertia losses than those present in single action designs. At high heads and very low flow rates the detent was observed to cause occasional problems with the function of the value. The valve would toggle correctly in one direction but fail to latch in the other. Future development should include refinement of the detent mechanism to improve the symmetry of operations as under these conditions the integrity of startup on Pentane could be compromised.

The performance of the pump on compressed air compared well to that expected from the results of the simulation. The minor discrepancies noted could be improved with the next iteration of the simulation and the inclusion of mechanical losses within the pump into the simulation. A study of flow velocity as a function of displacer position and speed would also be advantageous to the development of the simulation. This will enable a more accurate assessment of the water dynamics as the displacer changes direction.

The attempted operation on n-Pentane using a simulated solar collector was less successful than that on compressed air. The pump would displace approximately 2 litres of water before stalling. This corresponded to one full stroke of the displacer and part of the return stroke. It was observed that during startup a significant volume of condensate would form within the pump's vapour chamber, during the return stroke the pump would attempt to exhaust this condensate through the spool valve and stall. The low level sensor within the evaporator would then trigger and shut the system down as the volume of Pentane liquid left in the boiler lowered below a safe level. In the initial design stages it was envisaged that condensate formation within the pump would simply boil off during exhaust when exposed to the low pressure condenser. Cyclic condensation/re-evaporation during steady state operation was included in the simulation. Condensate formation during start-up was not considered in sufficient detail during the design stages of the development to realise the full extent of the

problem.
Also noted after each attempt at operation was the inadequate toggling of the main spool valve due to increased friction between spool seals and the valve bore.

Other components operated well. Tests carried out on the condenser showed adequate capacity although increasing its internal volume may improve pump operation by reducing the exhaust back pressure. The feed pump successfully transferred condensate from the low pressure condenser to the high pressure boiler[1]. The test setup and recording equipment operated reliably and accurately. Operation of the system and data acquisition proved simple and effective.

A possible area of concern with the STWP is the choice of working fluid. The system was optimised for the use of n-Pentane as the working fluid, although flammable n-Pentane was the most suitable of those fluids studied. The flammability of n-Pentane could be hazardous if not handled correctly or if the system leaked near any source of ignition. This may make the STWP undesirable to certain markets. n-Pentane does however have many properties in its favour for this application. It is the author's opinion that this issue is only of minor concern and that it should not prevent continuing research into the STWP.

The research and testing carried out on this pump shows the basic design to be good, resulting in even flow, excellent suction and discharge characteristics and potentially reliable operation. No fundamental changes to the design would be required.

As above however two main problems were encountered during trialing of the system on n-Pentane:

1. Formation of condensate within the vapour chamber during startup causing the pump to hydraulic during the exhaust stroke.

[1]This test was carried out using compressed air to cycle the pump.

2. Swelling of the nitrile O-rings backing the carbon filled teflon spool seals in the presence of large volumes of liquid condensate. The swelling of the O-rings resulted in increased friction between the spool and the bore of the valve preventing correct operation of the valve. It was noted that in the presence of Pentane vapour the spool valve functioned properly, it was only the presence of Pentane liquid that caused improper operation.

Also noted was some asymmetry in the operation of the detent that retains the spool valve in either of it's two operating locations. The spool would occasionally fail to toggle correctly in one direction. Once the detent failed to latch, the spool would float in between its two operating positions and eventually allow the high pressure supply to exhaust directly to the condenser.

Operational Recommendations. Although these problems did prevent the successful operation of the prototype on n-Pentane, with some minor modifications it is believed the STWP would operate successfully as intended.

1. The formation of condensate within the vapour chamber could be prevented if the pump is orientated such that the displacer reciprocates on a horizontal axis rather than the vertical axis. The spool valve should be located at the bottom of the pump and the pump should be located above the output of the solar panel. This allows any condensate formed within the vapour chamber to drain freely back to the boiler by gravity.

A further advantage to this configuration is that the vapour feed pipe to the pump's vapour chamber forms a heat pipe such that as the solar collector is heating at the beginning of the day the pump is also being heated prior to there being enough pressure to move the displacer.

The heat pipe effect is created when the liquid within the solar collector is heated and boils, it then rises into the pumps vapour chamber and condenses giving up its enthalpy of evaporation to the walls of the pump. The condensate runs back to the solar collector as more vapour rises to heat the pump. This would occur as a

continuous flow process as the system heats to operating temperature and continually as the unit operates.

The design of the system to utilise this form of heat transfer would be simpler and more efficient than any alternative option such as a pressure dependant startup valve that only allows vapour to enter the pump when the collector has reached operating pressure (with obvious operational drawbacks), or alternative means of heating the vapour chamber.

Initially the displacer was intended to reciprocate about a vertical axis. This was to help prevent side loading on the diaphragms and non-axial movement of the displacer without the use of displacer guides. After the prototype was completed, the rigidity of the four diaphragms within the pump as designed was significantly greater than expected and more than sufficient to guide and support the displacer while it reciprocates about a vertical or horizontal axis.

Although the internal design of pump's vapour and water chambers would not require modification, the pump should be reassembled to orientate the water outlet towards the top of the pump and inlet at the bottom to prevent an airlock forming in the water chambers as this will significantly decrease performance.

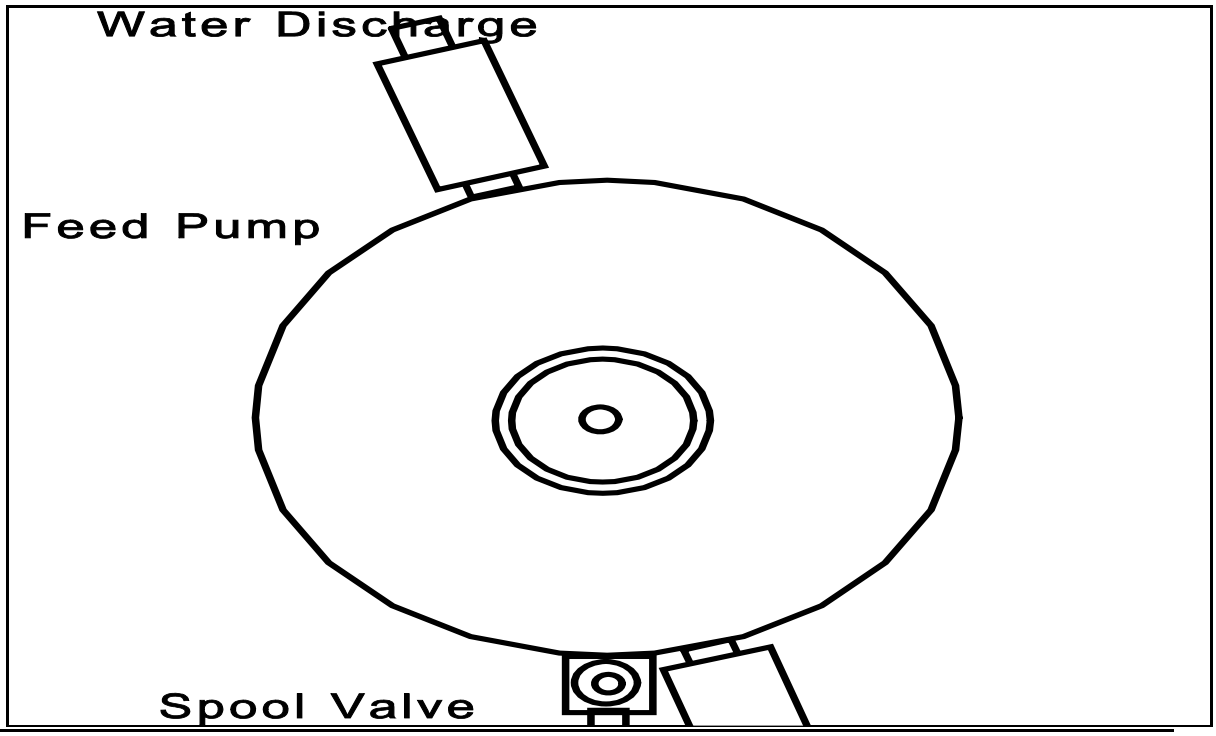

This would be simple to do with the current prototype and would require no part modifications. The location of the main controlling valve would prevent optimum positioning of the inlet port but the orientation shown in *Figure 7.1* would be adequate to continue.

The design of the feed pump, with the single axial port giving both inlet and discharge, would require modification. The port should be shifted to the top of the feed pump to prevent an airlock forming (*Figure 7.1*).

2. Incorrect toggling of the spool valve may be remedied by the previous modification. It was observed that in the presence of Pentane vapour the spool would still function correctly. It was only when the valve was flooded with quantities of condensate that the spool would fail to toggle its full travel to the opposite detent position. When the spool was immersed in condensate the O-rings backing the teflon seals would swell and increase the friction between the seals and the bore. There is inadequate energy stored in the actuators to overcome this friction and still force the spool to travel the 8mm required to latch in its alternative position.

By allowing the condensate to drain freely back to the evaporator rather than collect in the vapour chamber and spool valve, the swelling of the seals may not be sufficient to cause the unit to fail in this manner. This theory must be supported by adequate experimentation. Should the valve continue to function erratically, following are some additional modifications to the mechanism.

a. The first modification recommended would be to modify the o-ring that backs each of the PTFE seals of the spool. The function of the o-ring is to act as a radial spring that pre-loads the PTFE seal against the bore with enough pressure to seal. At the time of selection it was believed that the nitrile o-ring would not be subjected to sufficient quantities of Pentane, nor that they would swell to an extent that would prevent correct operation of the valve.

An alternative form of seal pre-load could be considered however the simplest option would be to select an o-ring of a material that was dimensionally stable in the presence of hydrocarbon fluid (possibly Hytrel or Viton).

b. The clearance between the seals and the bore could be increased reducing the pre-load the O-rings have on the PTFE seals, or alternatively reducing the diameter of the seal ring groove in the spool.

Although this will result in reduced sealing force at low pressure, inherent to the design of the seal is a second pressure dependant sealing mechanism. The inner of the surface PTFE seal is exposed to operating pressures meaning that as the pressure across the seal rises the sealing face is forced harder against the bore. This increases the sealing force and therefore seal friction however with the pump already operating, actuation forces on the spool are higher.

The critical point for sealing is as the pressure is building enough to start the pump, displacer motion is gradual and the actuation forces on the spool are low. The sealing pre-load need only be sufficient to ensure that the valve does not leak under low startup pressures.

The author believes that the above recommendations will eliminate the problems experienced with the valve. The following suggestions (in an order of increasing complexity) are some further ideas to refine the mechanism. These ideas involve greater design changes but may be necessary should the valve continue to cause operational problems:

c. Alternative lower friction seals could be investigated.

d. The detent design could be improved such that it was entirely symmetrical in its operation. Although, more advantageous to the operation of the valve would be to provide an over-centring action that assisted the spool to move to its correct position.

e. The diameter of the four orifices around the bore of the spool valve could be reduced. This would eliminate the small amount of port crossover between the inlet and the exhaust ports as the spool toggles between positions and prevent the spool from resting in a position that allows vapour to flow from the boiler directly to the condenser. The stroke (travel) of the spool could also be reduced with the reduced port size to reduce the work required of the actuator springs to toggle the spool.

f. The final suggestion would be to improve/redesign the actuator mechanism, to allow a greater build-up of potential energy before the detent released the spool. This could also require a higher detent force which would be achieved simply by using four detent balls (rather than two) in the current design and/or by increasing the spring force on the detent balls.

With the pump operating successfully on the simulated solar collector (Pentane boiler) no further difficulties would be envisaged by the replacement of the boiler with the solar collector (stage 3 of the testing program outlined in Chapter 6).

Longer Term Recommendations. With the completion of the modifications suggested to ensure reliable operation of the Solar Thermal Water Pump, extensive field trialing would be recommended to ascertain the long term integrity of all components. A study based on data obtained from the operation would be useful to further refine the simulation and theoretical modelling of the system. Further field trialing of the unit in applications such as a circulation pump for a swimming pool, or as a water supply in a third world environment would be useful in gaining commercial interest and funding for further development and a final design iteration before the unit could be manufactured and marketed commercially.

# References


Amor, M.R. (1992) A Solar-Thermal Water Pump.
Thesis in Mechanical Engineering. University of Canterbury. 1992.

Arlosoroff, S. Tschannerl, G. et al. (1987)
Community Water Supply - The Handpump Option.
United Nations Development Program. Nov 1987.

ASHRAE (1989) 1989 Fundamentals Handbook (SI).
American Society of Heating and Refrigeration Engineers. 1989

BDH Data Sheets n-Pentane.
BDH Chemicals (NZ) Ltd. On-Line Reference. Chemistry Department. University of Canterbury

Beam, R. Jedlicka, J. (1973) A Solar Engine Using the Thermal Expansion of Metals.
Solar Energy. Vol. 15 pg. 133-142. 1973.

Bhattacharyga, T.K. Ramachandra, S. et al. (1978)
Low Temperature Bellow Actuated Solar Pump.
Proceedings of ISES Congress 1978. Vol. 3 pg. 2118-2121. 1978.

Boldt,J. (1977) Solar Powered Water Pump for the Rural Third World.
Solar Energy, International Progress. Vol. 3. Report No 780667. 1977.

Bom (1993) Energy Losses Through Entrance Condensation in Small Vapour Engines.
Solar Energy. Vol. 50 no. 3 pg 223-228. Pergamon Press Ltd. 1993.

B.P. (1990) B.P. Statistical Review 1990.
Corporate Communications Services, 1990.

Brown, M.W. (1990) Seals and Sealing Handbook.
3rd Edition, Elsevier Science Publishers Ltd. England. 1990.

Burgess, P. Prynn, P. (1985)
Solar Pumping in the Future - A Socio-economic Assessment.
The Economics of Technology Change 1985. CSP Economic Publications.

Burton, R. (1982) A Solar Powered Diaphragm Pump.
Solar Energy. Vol. 31 no. 5 pg. 523-525. 1983.

Canjar, L.N. Manning, F.N. (1967)
Thermodynamic Properties & Reduced Correlations for Gases.
Gulf Publishing Co. 1967.

Capaldi, B. (1981) Solar Mechanical Converters.
The Energy Journal. May 1981.

Cattaneo, G. Cortesi, P. Arcella, V. (1983)
The Solar Pump.

Solar 83, International Solar Energy Symposium. Pg 821-828. 1983.

Chadwick, D.G. (1980) Heat Powered Water Pump.
United States Patent No. 4197060. 1980.

Dorr Oliver Inc. (1972) Diaphragm Pump.
United States Patent No. 1344576. 1972.

Duffie, J.A. Beckman, W.A. (1974)
Solar Energy Thermal Processes.
John Wiley and Sons. 1974.

Duffie, J.A. Beckman, W.A. (1980)
Solar Engineering of Thermal Processes.
John Wiley and Sons. 1980.

Garg, H.P. Datta, G. (1984) Top Loss Calculation for Flat Plate Solar Collectors.
Solar Energy. Vol. 31 no. 1 pg 141-143. 1984.

Goetz P.W.(Editor in Chief) The New Encyclopaedia Britannica.
15th Edition, Encyclopaedia Britannica Inc, Chicago. 1990.

Gribik, J.A. Osterle, J.F. (1984)
The Second Law of Solar Energy Conversion.
Journal Solar Energy Engineering. Vol. 106. 1984.

Halcrow, W. & Partners. Intermediate Technology Ltd (1984)
Handbook on Solar water Pumping.
UNDP Project GLO/80/003, World Bank, Reading and Swindon, UK. Feb 1984.

Halcrow, W. & Partners. Intermediate Technology Ltd (1983)
Small Scale Solar Powered Pumping Systems: The Technology, its Economics and Advancement.
Main Report, UNDP Project GLO/80/003, World Bank.
London, Swindon and Reading, UK. June 1983.

Halcrow, W. & Partners. Intermediate Technology Ltd (1983)
Small Scale Solar Powered Pumping Systems: The Technology, its Economics and Advancement.
Main Report Supporting Document 1, UNDP Project GLO/80/003, World Bank.
London, Swindon and Reading, UK. June 1983.

Hamilton, T.W. (1974) Novel Design for a Diaphragm Pump.
The Consulting Engineer. Vol. 38 no. 8 pg 70. August 1974.

Hedley, D. (1986) World Energy - The Facts and the Future.
2nd Edition, Euromonitor Publications, 1986.

Howel, Y. Bereny, J.A. (1979)
Engineers Guide to Solar Energy.
Solar Energy Information Services (SEIS), 1979.

Janna, W.S. (1986) Engineering Heat Transfer.
Van Nostrand Reinhold (International). 1986.

Jeter, S.M. (1980) Maximum Conversion Efficiency for the Utilisation of Direct Solar Radiation.
Solar Energy. Vol. 26 pg 231-236. 1981.

Jordan, D. (1988) Solar (Photovoltaic) Systems
SAE-A Journal May/June 1988. Pg 23-30. 1988.

Karassik, I.J. Krutzsch, W.C. Fraser, W.H. Messina, J.P. (1986)
Pump Handbook.
2nd Edition, McCraw Hill. 1986.

Karlekar, B.V. (1983) Thermodynamics for Engineers.
Prentice-Hall International Editions. 1983.

Kelsey, C.G. (1974) Vapour Power Generating Unit.
Australian Patent No. 75389/74. 1974.

Kimura, K. Stephenson, D.G. (1969)
Solar Radiation on Cloudy Days.
ASHRAE Transactions. Vol. 75 no. 1 pg 227-234. 1969.

Kishore, V.V.N. Ghandi, M.R. et al. (1986)
Development of a Solar (Thermal) Water Pump Prototype - An Indo-Swiss Experience.
Solar Energy. Vol. 39 no. 3 pg 257-265. 1986.

Kreider, J.F. Hoogendoorn, C.J. Kreith, F. (1989)
Solar Design. Components, Systems, Economics.
Hemisphere Publishing Corporation. 1989.

Kreith, F. Kreider, J.F. (1978)
Principles of Solar Engineering.
Hemisphere Publishing Corporation. 1978.

Kysar, J.K. (1988) A Program That Finds The Sunlit Patch Inside a Room.
Thesis in Mechanical Engineering. University of Canterbury. 1988.

Landsberg, P.T. Tonge, G. (1979)
Thermodynamics of the Conversion of Diluted Radiation.
Journal of Physics A. Math. Gen. Vol. 12 no. 4 pg 551-562. 1979.

Lee, W.C. (1957) Solar Thermostat Control Unit.
United States Patent No. 2928606. March 1960.

Lestrade, P.J. Acock, B. Trent, T. (1990)
The Effect of Cloud Layer Plane Albedo on Global and Diffuse Radiation.
Solar Energy. Vol. 44 no. 2 pg 115 - 121. 1990.

MacCracken, C.D. (1959) Liquid Heating Systems.
United States Patent No. 2918219. 1959.
MacCracken, C.D. (1960) Vapour Actuated Pump System.
United States Patent No. 2927434. 1960.

Madsen, P. Goss, K. (1981) Report on Non-Metallic Solar Collectors.
Solar Age. Jan 1981 pg 28-32. 1981.

Malberg, H. (1973) Comparison of Mean Cloud Cover Obtained by Satellite Photographs and Ground Based Observation Over Europe and the Atlantic.
Monthly Weather Review. Vol. 101 no. 12 pg 893-897. 1973.

Malz Nominees Pty. (1975) Pumps.
Australian Patent No 12116/76. 1975.

McNelis, B. (Editor) (1982) Solar Refrigeration and Water Pumping for Developing Countries - An Introduction.
UK-ISES Conference Proceedings SE for Developing Countries - Refrigeration and Water Pumping. 1982.

Mohomed, H.A. (1979) Thermal Conversion Efficiency of an Ideal Thermoelastic Marmem Cycle.
Journal of Material Science 1979. Vol. 14 pg 1339-1343. 1979.

Moore, T. (1992) High Hopes for High Power Solar.
EPRI Journal, Dec. 1992 pg 17-25. 1992.

Othmer, K. (1980) Encyclopaedia of Chemical Technology 3rd Edition.
Vol 12 pg 919 - 925. Wiley Interscience. 1980.

Parrott, J.E. (1978) Theoretical Upper Limit on the Conversion of Solar Energy.
Solar Energy. Vol. 21 no. 3 pg 227. 1978.

Parrott, J.E. (1979) Letters to the Editor.
Solar Energy. Vol. 22 pg 572-573. 1979.

Petela, R. (1964) Exergy of Heat Radiation.
Journal of Heat Transfer, May 1964 pg 187-192. 1964.

Press,W.H. (1976) Theoretical Maximum for Energy from Direct and Diffuse Sunlight.
Nature. Vol. 264 pg 734-735. Dec 23/30 1976.

Pytlinski, J.T. (1978) Solar Energy Installations for Pumping Irrigation Water.
Solar Energy. Vol. 21 pg 255-262. Pergamon Press Ltd. 1978.

Raine, J.K. Foster D.R. Amor, M.A. (1994)
Development of Single and Double Acting Solar Thermal Water Pumps.
Proceedings IPENZ Annual Conference. IPENZ. Feb 1994.

Raine, J.K. Foster D.R. Amor, M.A. (1994)
Computer Simulation and Test-Bed Performance of Single and Double-Acting Solar Thermal Water Pumps.
IPENZ Transactions EMCh. Vol. 21 no. 1 pg 10-18. Nov 1994.

Ransmark, S.E. (1978) Flat Plate Solar Collectors.
International Symposium Workshop on Solar Energy, Caino, Egypt 1978.
Solar Energy, International Progress pg 187-214. 1978.

Rao, D.P. Rao, K.S. (1976) Solar Water Pump for Lift Irrigation.
Solar Energy. Vol. 18 pg 405-411. 1976.

Rao, D.P. Soin, R.S. (1978) Solar Water Pump.
Proceedings of ISES Congress 1978. Vol. 3 pg 1905-1916. 1978.

Saidov, M.S. (1990) Nonsingle-Crystal Silicon and Conversion of Solar Energy.
Applied Solar Energy. Geliotekhnika. Vol.26 no. 6 pg 38-46. 1990.

Sharma, M.P. Singh,G. (1980)
A Low Lift Solar Water Pump.
Solar Energy. Vol. 25 pg 273-278. 1980.

Serpone, N. Lawless, D. Terzian, R. (1992)
Solar Fuels: Status and Perspectives.
Solar Energy. Vol. 49 no. 4 pg 221-234. 1992

Spanner, D.C. (1964) Introduction to Thermodynamics.
Academic Press. New York. 1964.

Speidel, K. (1977) A Simple Water Pump, Powered by Solar Energy.
Solar Energy, International Progress. Vol. 3 pg 1748-1761. 1977.

Strong, C.L. (1971) Some Delightful Engines Driven by the Heating of Rubber Bands.
Scientific American. April 1971.

Stubbs, H.P. (1979) Vapour Operated Motor.
Australian Patent No. 29601/77. 1979.

Tanaka, M. (1992) Shape Memory Alloy Engine.
IECEC 1992. Vol. 3 pg 3.87-3.91. 1992.

Thureau, P. Bremont, M. (1976)
Pumping System using Solar Energy.
United States Patent No. 3937599. 1976.

Tong, H.C. Wayman, C.M. (1975)
Thermodynamic Considerations of Solid State Engines Based on Thermoelastic Martensitic Transformations and the Shape Memory Effect.
Metallurgical Transactions A. Vol. 6A pg 29-32. Jan 1975

Trewartha, G.T. Horn, L.H. (1980)
An Introduction to Climate 5th Edition.
McGraw Hill. 1980.

Trihey, J.M. (1976) Low Energy Thermally Driven Pump.
Australian Patent No. 12116/76. 1976.

Umarov, G.Y. Alimov, A.K. et al. (1976)
Solar Water Lifting Unit with Diaphragm Pump.
Gelioteknika. Vol. 12 no. 6 pg 82-83. 1976.

Wakao, N. Tanisho, S. Liu, H.Z. (1984)
Liquid Pumps Driven by Temperature Difference Between Two Waters or Temperature Variations in the Environment.
Journal of Chemical Engineering of Japan. Vol. 17 no. 5 pg. 538-541. 1984.

Walker, J. (1985) Experiments with the External Combustion Fluidyne Engine Which Has Liquid Pistons.
The Amateur Scientist, April 1985. pg 108-114. 1985.

West, C.D. (1986) Principles and Applications of Stirling Engines.
Van Nostrand Reinhold Co. Inc. 1986.

Zhi-chen, H. Xin-zhong, X. (1985)
Optimum Design and Tests for a Small Solar Pump.
Solar and Wind Energy Applications - International Conference - Papers.
pg 245-250. 1985.

# Appendix 1

# n-Pentane Data Sheets

**A) Properties of Pentane**

**B) BDH Hazard Data Sheets**

**C) Pressure Enthalpy Diagram for n-Pentane**

## A) Properties of n-Pentane

| **Property** | |
|---|---|
| Molecular Weight | 72.151 |
| Density (at 1atm, 273.15K) kg/$m^{-3}$ | 645.5 |
| Normal Freezing Point °K | 143.429 |
| Normal Boiling Point °K | 309.224 |
| Water Solubility at 25°C, g Pentane per 100kg Water | 9.9 |
| Spontaneous Ignition Temperature in Air °K | 557.0 |
| Flash Point °K | 233.0 |
| Critical Point<br>Pressure Mpa<br>Temperature °K<br>Density kg/$m^3$<br>Volume $m^3$/mol<br>Compressibility Factor | <br>3.369<br>469.7<br>231.9<br>$304x10^{-6}$<br>0.262 |
| Heat of Combustion kJ/mol (at 298K)<br>Liquid<br>Gas | <br>3245<br>3272 |
| Heat of Fusion kJ/kg | 115.9 |
| Heat of Vaporisation kJ/kg | 355.6 |
| Entropy of Fusion kJ/mol.K | $5.852x10^{-2}$ |
| Entropy of Vaporisation kJ/mol.K | $8.335x10^{-2}$ |
| Antione Vapour Pressure Equation<br>$Log_{10}$Pressure(kPa) = A - B/(Temperature (K) +C)<br>A<br>B<br>C<br>T (max) K<br>T (min) K | <br><br>6.00122<br>1075.78<br>-39.94<br>330<br>220 |
| Dielectric Constant | 1.843 |
| Surface Tension mN/m<br>At 20°C<br>At 30°C | <br>16.00<br>14.95 |
| ASTM Octane number<br>Research<br>Engine | <br>61.8<br>63.2 |
| Flammability Limits Vol %<br>Lower<br>Upper | <br>1.5<br>7.8 |

Information extracted from Kirk.Othmer (1980)

**B) BDH Hazard Data Sheets**

| | |
|---|---|
| Product: | **n-Pentane** (Including Pentane for lamp) |
| CAS Number: | 109-66-0 |
| Product Codes: | 10360-15334-29451-29751-29857 |

HAZARD IDENTIFICATION

Symbols: F Phrases: R11

S9-16-23-29-33

TRANSPORT INFORMATION

Hazard Class: 3.1 UN Number: 1265 Pkg Group: I

COMPOSITION

Hydrocarbon solvent

REGULATORY INFORMATION

Not implemented

PHYSICAL AND CHEMICAL PROPERTIES

Description: Colourless liquid, characteristic odour

Melting Pt: -130 °C Boiling Pt: 36 °C Specific Gravity: 0.63

Solubility in Water: Practically insoluble

Vapour Pressure: 400 mmHg at 19 °C

Vapour Density: 2.48 (air=1)

FIRE AND EXPLOSION HAZARD

Highly flammable

Vapour/air mixture explosive

Flash Point: -48 °C

Explosive Limits: lower 1.4 upper 8 (%)

Auto-Ignition Temperature: 309 °C

FIREFIGHTING MEASURES

Foam, dry powder, carbon dioxide or vaporising liquids

STABILITY AND REACTIVITY

Stability: Stable

Reaction with Water: None

Other Known Hazards: Can react vigorously with oxidising materials

Avoid Contact With: Water (No) Acids (No) Bases (No)
Oxidisers (Yes) Combustibles (No)

HEALTH HAZARDS May be harmful by ingestion and inhalation. Degreases. Irritating to skin and eyes. Vapour may irritate respiratory system, and is narcotic in high concentrations.

TOXICOLOGICAL INFORMATION

Toxicity Data: No Data

Carcinogenicity: No evidence of carcinogenic properties

Mutagenicity/Teratogenicity: No evidence of mutagenic or teratogenic effects

FIRST AID MEASURES

Eyes: Irrigation thoroughly with water for at least 10 minutes. OBTAIN MEDICAL ATTENTION.

Lungs: Remove from exposure, rest and keep warm. In severe cases obtain medical attention.

Skin: Wash off skin thoroughly with water. Remove contaminated clothing and wash before re-use. In severe cases, OBTAIN MEDICAL ATTENTION.

Mouth: Wash out mouth thoroughly with water and give plenty of water to drink. OBTAIN MEDICAL ATTENTION.

ACCIDENTAL RELEASE MEASURES

Precautions: Shut off all sources of ignition
Inform others to keep at a safe distance
Wear appropriate protective clothing

Absorb on an inert absorbent, transfer to container and arrange removal by disposal company. Wash site of spillage thoroughly with water and detergent. For large spillages liquids should be contained with sand or earth and both liquids and solids transferred to salvage containers. Any residues should be treated as for small spillages.

If material has entered surface drains it may be necessary to inform local authorities, including fire service if flammable.

DISPOSAL

Dispose of through local authorities if appropriate facilities are available, otherwise pass to a chemical disposal company.

EXPOSURE CONTROLS AND PERSONAL PROTECTION

UK Exposure Limits: OES, mg/$m^3$ (long Term 8hr TWA) - 1800

Respirator: Self-containing breathing apparatus

Ventilation: Fume-cupboard, flameproof

Gloves: Nitrile

Eye Protection: Goggles or face shield

Other Measures: Plastic apron, sleeves, boots if handling large quantities

ECOLOGICAL DATA

Not implemented

STORAGE AND HANDLING

Special Requirements

As required by the Petroleum Act 1928 and the Highly Flammable Liquids and Liquefied Petroleum Gases Regulations 1972. In accordance with HSE guidance not CS17. Take precautions against static discharges.

This is only an extract of the available information for the above product.

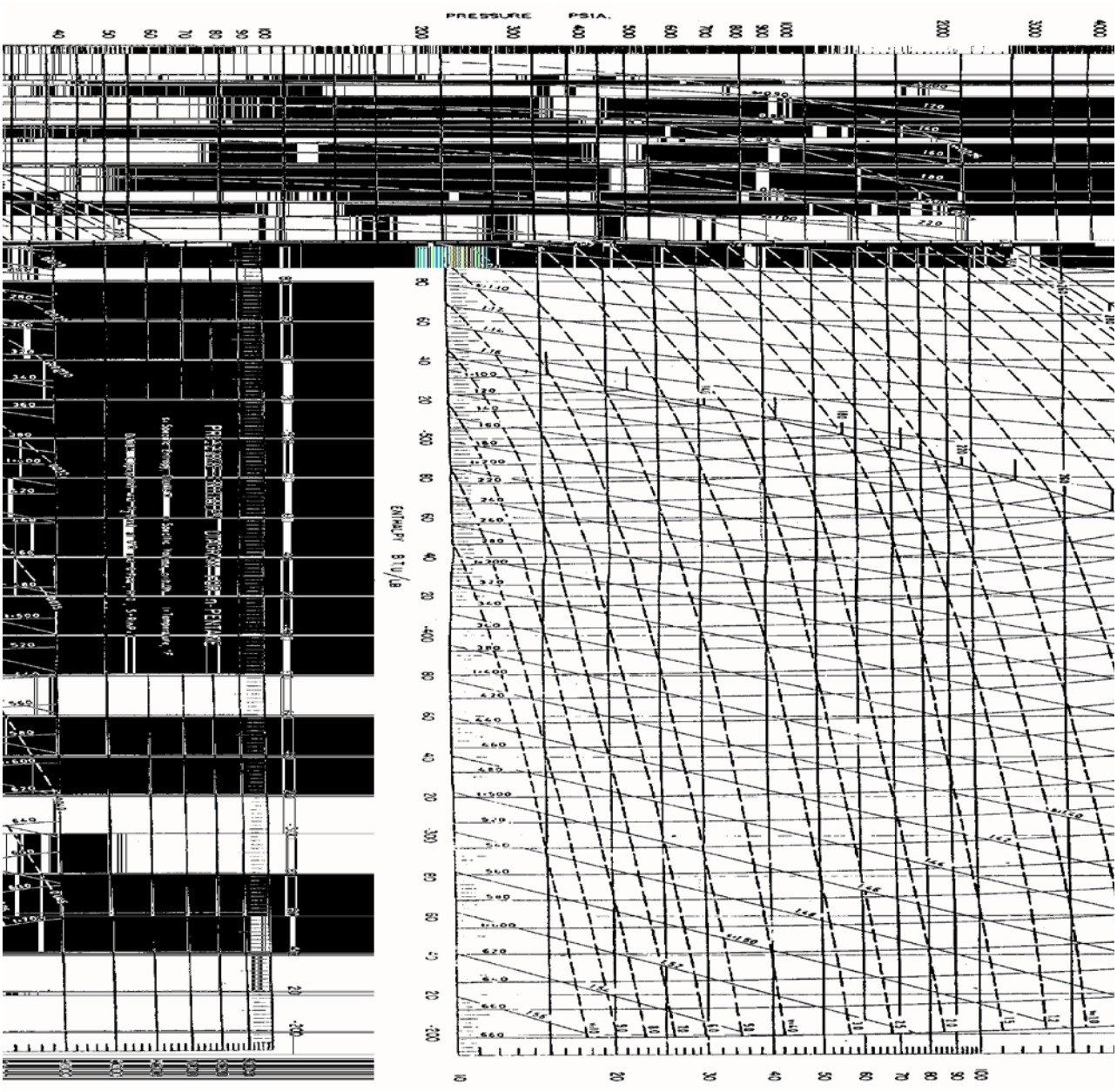
PRESSURE PSIA.
ENTHALPY BTU/LB

# Appendix 2

# Testing Procedure (Simulated Evaporator)

---

**Where Necessary Refer to Chapter 6 for System and Component Descriptions**

---

## TESTING PROCEDURE FOR SOLAR THERMAL WATER PUMP OPERATING ON A SIMULATED SOLAR BOILER

## LOADING PENTANE AND PURGING SYSTEM OF AIR

1. Load 4 litres of n-Pentane into boiler through filler plug (1/4"BSPT Plug). Usual safety precautions for the handling of flammable liquids apply.

2. With valves 1,2 and 3 fully open, depressurise system with vacuum pump to the point where Pentane vapour is being generated by boil off, the vapour will start to replace the air within the system. This can be determined by bubbling the discharge from the vacuum pump through liquid Pentane, when bubbles cease Pentane vapour is being discharged (Note: Pentane vapour is considerably heavier than air). This should also correspond with the vapour pressure of Pentane at the ambient temperature.

3. Close valve 1 to allow vapour to be drawn through condenser (should have already been purged).

4. Partially close valve 2 to allow slow operation of pump for a couple of cycles to purge pump chambers.

5. Close valve 3 and remove vacuum pump.

The system is now sealed and ready for action, to maintain system vacuum do not open valve 3 unless you intend to repeat this procedure.

If it observed that small volumes of air maybe leaking into the system, i.e. a gradual loss of vacuum, this procedure should be repeated before each testing session. If large volumes of air are being induced, dismantle defective seal and replace.

## OPERATING THE PUMP

- Do not smoke while testing unless you can't help it, i.e. you just got toasted.

- Initial testing - manually prime pump to avoid unknown behaviour when

self-priming.

- Gradually apply heat using the Variac on low setting (as read off the power meter) and increase gently when system temperature starts to rise to desired heat input as indicated by the power meter.

- Allow system to reach stable operation i.e. stable temperature of liquid in boiler.

- Begin taking measurements when this point is reached (estimated time 10-15 minutes).

- If pump should stop because of incorrect valve operation, attempt restart by operating valve with manual valve actuator, pump may restart with no further problems. (Note: once the pump has been correctly set up the valve and pump operation should be 100% reliable).

## SYSTEM SHUTDOWN

- Under no circumstances should valve 3 be opened when system is in operation, this will cause mixing of air with Pentane vapour inside and outside the system and the formation of explosive mixtures.

- Under normal conditions turning off the heating elements will cause pump to gradually come to a stop and system to de-pressurise.

- More rapid shut-down (under normal conditions) for impatient operators can be achieved by opening valves 1 and 2 starting with valve 1.

- System heating will automatically shut down if a 60°C temperature limit is exceeded or if liquid Pentane level drops to below optical switch ie system losing Pentane.

- Should more rapid shut-down be desired under other than normal conditions a $CO_2$ fire extinguisher can be used on the exposed parts of the boiler to rapidly cool and depressurise system.

- Overpressure relief valve will exhaust an over-pressurised system should death of the operator, pump failure and failure of other safety measures occur. Note keep clear of exhausting vapour, it will be hot and if ignition should occur even hotter.

- If a system failure should occur, eg. broken or loose fitting allowing vapour leakage, operator should seek immediate safety behind safety shield and if able cool system with fire extinguisher, Second operator should shut down heating elements if safety devices haven't already triggered.

- If fire should start seek immediate shelter if able.

## SOLAR THERMAL WATER PUMP

### Operator Tasks:

**Operator 1** - Responsible for taking measurements listed below and is located outside on the solar deck with the pump. This operator must wear full level 1 fire fighting equipment (flame retardant cotton overalls, boots and gloves) and overtop, level 2 fire fighting equipment (flame proof overtrousers and cotton liner, flame proof jacket, cotton and woollen liners, helmet and face shield). He/she must also be familiar with the use of both fire extinguishers which are to be on hand and be prepared to take immediate refuse behind the protective screen should a dangerous system state occur eg rapid leakage of high pressure Pentane vapour. This operator should stay inside or behind the protective screen whilst system is being powering up and until such a time as stable operation is achieved. If problems with valve operation should occur on start-up and manual toggling of the valve is required this operator is permitted to do so whist maintaining utmost caution. If operator starts to feel dehydrated he/she should seek liquid refreshment under no circumstances should fire fighting equipment be doused in water to cool operator as a fire ball will quickly boil the water and cause severe burns.

### Readings to be taken:

1. Boiler pressure readings; mean and variation (min/max)
2. Condenser pressure readings; mean and variations (min/max)
3. Water chamber pressure readings during suction and discharge periods of the cycle; mean and variation
4. Flow rate using bucket and stopwatch method
5. Cycle time or time for 10 strokes (5 cycles)
6. Stroke length (if possible)

**Operator 2** - Responsible for taking measurements listed below and is located inside of the solar deck exit with the pump controlling equipment. This operator must wear full level 1 fire fighting equipment (flame retardant cotton overalls, helmet and face shield (gloves and boots optional)). This operator should not be tempted to join operator 1 outside or assist in combatting a system failure but must maintain a careful vigil on system performance as indicated by corresponding meters and gauges and system operation and safety on deck. He/she should be prepared to shut the system down immediately a problem is noticed or when indicated to do so by operator 1. Under no circumstances should operator 2 take his job lightly or lose concentration as

the life of operator 1 may depend on his/her actions or lack of action.

**Readings to be taken:**

Set desired heat input and record

Boiler temperature from thermocouple

Vapour Chamber pressure from voltage readout on multimeter (1 V = 1 bar absolute); mean, max. and min.

Turn on chart recorder whilst flow measurement is being taken and mark approx. beginning and end of flow measurement test as well as recorder settings (chart speed and input sensitivity), date, time, ambient pressure, water head, empty bucket mass, test mass and time (hence flow)

Note: until system integrity is verified and confidence in its operation is gained these cautions must be adhered to. These may be modified at a later stage to reflect the systems true hazard potential likely to be considerably less significant than allowed for in the recommendations for preliminary testing.

## SOLAR THERMAL WATER PUMP

### Experimental Measurements
### Operator 1 - Outside on Solar Deck

Date: .....

Time: .....

Test Number: .....

Head (m $H_2O$): .....

Heat Input approx (W): .....

Boiler Pressure kPa (≈mean, max., min.)

..... ..... .....

Condenser Pressure kPa (≈mean, max., min.)

..... ..... .....

Water Pressure (kPa)

-Induction (≈mean, max., min.)

..... ..... .....

-Discharge (≈mean, max., min.)

..... ..... .....

Flow Rate:

-Time (s) .....

-Test Mass (include bucket mass) (kg) .....

-Bucket Mass (kg) .....

## SOLAR THERMAL WATER PUMP

### Experimental Measurements
### Operator 2 - Inside on Control Desk

Date: .....

Time: .....

Test Number: .....

Ambient Pressure (kPa abs): .....

Ambient Temperature (°C): .....

Head (m $H_2O$): .....

Exact Heat Input (W): .....

Boiler Temperature (°C): .....

Vapour Chamber 2 Pressure (kPa abs):

-Filling (boiler)

.....

-Exhausting (condenser)

.....

Start chart recorder on signal from operator 1 and signal when operating

Mark when flow measurement started and finished on edge of lineflow ...

Stop recording after approx 5 more cycles

Mark test no on lineflow ...

Chart Speed (mm/min): .....

Input Sensitivity (V for full range): .....

# Appendix 3

# Computer Simulation and Optimisation Routine

```
WATFOR-77 V3.1 Copyright WATCOM Systems Inc. 1984,1989   94/10/05 08:50:25

      C                SOLAR THERMAL WATER PUMP
      C            OPTIMISATION AND SIMULATION PROGRAMME
      C          OPERATING THROUGH A DAILY CYCLE WITH INTERMITTENT
      C          CLOUD COVER AND WITH n-PENTANE AS THE WORKING FLUID


      C     SETTING VARIABLE TYPES

      IMPLICIT REAL(A-T)
      IMPLICIT INTEGER(W-Z)
      INTEGER MONNUM,DAYNUM,I,N,LSIGN,R
      REAL LATDEG,ORIENT,U,V,W,SOLRAD,COLALT,P(80),WATOUT,FLOW(80)
      REAL HERP,SRADSK,SRADGR,FSS,FSG,TRANS,SORB,THICK,MAXRAD
      REAL TLOW,DULAST,TOGLAST,PLTEMP1,PLTEMP2,PLTEMP3,CPL,CPM,CPG
      REAL MM,ML,MG,HFG,TET,CC(80),DIFF(80),BET(80),DIF
      REAL HR(80),TORADD(80),TORAD(80),ABCOEF,HOUR,WPMM,NUMB,COLAZI
      REAL MONTH,BETA,A,B,C,D,E,F,UTL,UBL,MAXT,THERCO,PRESETS
      REAL DFLOW,ONE,ZER,TOR,OMTOR,GOLD,VALTOR,VALOMTOR,RI,VIL,CU,CV,CW
      REAL RA,RL,DIA,ALTIT(80),DU,TOG,TOT,CU2,CV2,CW2
      REAL DIAM,RATI,RLEN,LIN,SUKH,PREH,CONDV,CONDA,SPRF,ATEMP
      REAL SOAD(80),HEP(80),AS(80),BB(80),EE(80),UIN,VALOUT(80)
      REAL DAYDIF,SEADIF,TAMB,EMITP,EMITG,OUTCON,TA,TEMSYS(80),INCWT(80)
      CHARACTER STRING(38)*120


      C    INPUT THE STRING OF QUESTIONS

      STRING(1) =  'WHICH HEMISPHERE (1=NORTH OR (-1)=SOUTH)?'
      STRING(2) =  'LATITUDE IN DEGREES (0 TO 90)?'
      STRING(3) =  'WHAT IS THE MONTH (1 TO 12)?'
      STRING(4) =  'WHAT IS THE DAY OF THE MONTH?'
      STRING(5) =  'LOCAL SOLAR TIME (24 HOUR/DECIMAL FORMAT)?'
      STRING(6) =  'WHAT IS THE COLLECTORS ALTITUDE ANGLE?'
      STRING(7) =  'WHAT IS THE COLLECTORS AZIMUTH ANGLE?'
      STRING(8) =  'HOW MANY GLASS PANELS DOES THE COLLECTOR HAVE?'
      STRING(9) =  'WHAT IS THE REFRACTIVE INDEX FOR THE GLASS?'
      STRING(10)=  'WHAT IS THE ABSORPTION COEFFICIENT OF THE GLASS?'
      STRING(11)=  'WHAT IS THE GLASS THICKNESS? (M)'
      STRING(12)=  'WHAT IS THIS COMPUTATION RUN NUMBER?'
      STRING(13)=  'WHAT IS THE MAXIMUM AVERAGE MAXIMUM TEMPERATURE IN
     .THE HOTTEST SEASON? (C)'
      STRING(14)=  'WHAT IS THE RANGE OF DAILY TEMPERATURES?     ie
     .AVERAGE DAILY MAXIMUM MINUS AVERAGE DAILY MINIMUM'
      STRING(15)=  'WHAT IS THE RANGE OF SEASONAL TEMPERATURE VARIATION?
     . ie HOTEST AVERAGE MAX MINUS COOLEST AVERAGE MAX OVER THE YEAR'
      STRING(16)=  'WHAT IS THE SPACING BETWEEN THE GLASS PLATES? (M)'
      STRING(17)=  'WHAT IS THE GLASS PLATES EMITTANCE?'
      STRING(18)=  'WHAT IS THE PLATES EMITTANCE?'
      STRING(19)=  'WHAT IS THE PLATE TEMPERATURE? (C)'
      STRING(20)=  'WHAT IS THE OUTER CONDUCTIVITY?'
      STRING(21)=  'CONDUCTIVITY OF THE BACK INSULATION?'
      STRING(22)=  'THICKNESS OF BACK INSULATION? (M)'
      STRING(23) =  'assumed atmospheric temperature'
      STRING(24) =  'Initial pump diameter'
      STRING(25) =  'diameter ratio'
      STRING(26) =  'initial rubber length'
      STRING(27) =  'lower input power'
      STRING(28) =  'upper input power'
      STRING(29) =  'suction head'
      STRING(30) =  'pressure head'
      STRING(31) =  'condenser volume'
      STRING(32) =  'condenseer area'
      STRING(33) =  'spring force'
      STRING(34) =  'DID YOU MAKE AN ERROR? (1=YES) RE-ENTER ALL VALUES'
      STRING(35) =  'WOULD YOU LIKE TO CHANGE FROM THE PRESET VALUES?
     .1.0=YES   2.0=NO'
       MONTH=W
      STRING(36) =  'WOULD YOU LIKE TO EXIT 1=NO, 2=YES'
      STRING(37) =  'CLOUDINESS (0-1)'
      STRING(38) =  'TOTAL SOLAR RADIATION'

      C    ENTER SOME DEFAULT RESPONSES

    9 LSIGN=-1
      LATDEG=43
      W=3
      X=1
      HOUR=4
      COLALT=56
      COLAZI=2
      N=2
      REFG=1.586
      ABCOEF=.04
      THICK=.001
      NUMB=123
      MAXT=23
      DAYDIF=10
      SEADIF=10
      SPACE=.004
      EMITG=.84
      EMITP=.80
      PTEMP=68
      OUTCON=25
      THERCO=.06
      THICKB=.03
      DIAM=0.2
      RATI=0.5
      RLEN=.04
      LIN=300
      UIN=800
      SUKH=4.5
      PREH=3.5
      CONDV=0.3E-3
      CONDA=0.1
      SPRF=300
      ATEMP=17
      VALTO=0
      VALOMTO=0
      MAXRAD=0
      TSR=1.68E7
      CLO=0.5
      PI=3.141592654


      C    OPTION TO CHANGE FROM DEFAULT VALUES

   11 WRITE(*,*) STRING(35)
      READ(*,*) PRESETS
      IF(PRESETS.NE.1)GOTO320
      C
      C    HEMISPHERE CHECK
      C
   40 WRITE(*,*) STRING(1),LSIGN
      READ(*,*) LSIGN
      IF(LSIGN.NE.1) THEN
         LSIGN=-1
      ENDIF
      C    CHECK THE LATITUDE
      WRITE(*,*) STRING(2),LATDEG
      READ(*,*) LATDEG
      C
      C    CHECK VALUES FOR THE MONTH
      C
      WRITE(*,*) STRING(3),W
      READ(*,*) W
      MONNUM=W
```

```
      C   CHECK THE DAY OF MONTH
      C
  107       WRITE(*,*) STRING(4),X
  108       READ(*,*) X
  109       DAY = X
  110       DAYNUM = X
      C
      C   CHECK SOLAR TIME
      C
  111       WRITE(*,*) STRING(5),HOUR
  112       READ(*,*) HOUR
      C
      C   CHECK THE COLLECTORS ALT + AZI ANGLES
      C
  113       WRITE(*,*) STRING(6),COLALT
  114       READ(*,*) COLALT
      C
  115       WRITE(*,*) STRING(7),COLAZI
  116       READ(*,*) COLAZI
      C
      C   GET THE NUMBER OF GLASS PANES
      C
  117       WRITE(*,*) STRING(8),N
  118       READ(*,*) N
      C
      C   GET THE REFRACTIVE INDEX FOR GLASS
      C
  119       WRITE(*,*) STRING(9),REFG
  120       READ(*,*) REFG
      C
      C   GET THE ABSORPTION COEFF FOR THE GLASS
      C
  121       WRITE(*,*) STRING(10),ABCOEF
  122       READ(*,*) ABCOEF
      C
      C   GET THE GLASS THICKNESS
      C
  123       WRITE(*,*) STRING(11),THICK
  124       READ(*,*) THICK
      C
      C   GET THE RUN NUMBER
      C
  125       WRITE(*,*) STRING(12),NUMB
  126       READ(*,*) NUMB
      C
      C   MAXIMUM TEMP
      C
  127       WRITE(*,*) STRING(13),MAXT
  128       READ(*,*) MAXT
      C
      C   DAILY TEMP DIFF
      C
  129       WRITE(*,*) STRING(14),DAYDIF
  130       READ(*,*) DAYDIF
      C
      C   SEASONAL TEMP DIFF
      C
  131       WRITE(*,*) STRING(15),SEADIF
  132       READ(*,*) SEADIF
      C
      C   DISTANCE BETWEEN PLATES
      C
  133       WRITE(*,*) STRING(16),SPACE
  134       READ(*,*) SPACE
      C
      C   GLASS EMITANCE
      C
  135       WRITE(*,*) STRING(17),EMITG
  136       READ(*,*) EMITG
      C
      C   PLATE EMITTANCE
      C
  137       WRITE(*,*) STRING(18),EMITP
  138       READ(*,*) EMITP
      C
      C   PLATE TEMPERATURE
      C
  174       WRITE(*,*) STRING(23),ATEMP
  175       READ(*,*) ATEMP
      C
      C   CLOUD COVER
  139       WRITE(*,*) STRING(19),PTEMP
  140       READ(*,*) PTEMP
  141       PTEMP=PTEMP+273
      C
      C   OUTWARD CONDUCTIVITY OF GLASS - AIR INTERFACE
      C
  142       WRITE(*,*) STRING(20),OUTCON
  143       READ(*,*) OUTCON
      C
      C   CONDUCTIVITY OF BOTTOM INSULATION
      C
  144       WRITE(*,*) STRING(21),THERCO
  145       READ(*,*) THERCO
      C
      C   THICKNESS OF BACK INSULATION
      C
  146       WRITE(*,*) STRING(22),THICKB
  147       READ(*,*) THICKB
      C
      C   DIAMETER
      C
  148       WRITE(*,*) STRING(24),DIAM
  149       READ(*,*) DIAM
      C
      C   RATIO
      C
  150   250 WRITE(*,*) STRING(25),RATI
  151       READ(*,*) RATI
  152       IF(RATI.LE.0.OR.RATI.GT.3) THEN
  153          GOTO250
  154       ENDIF
      C
      C   RUBBER LENGTH
      C
  155   260 WRITE(*,*) STRING(26),RLEN
  156       READ(*,*) RLEN
  157       IF(RLEN.LT.0.OR.RLEN.GT.1) THEN
  158          GOTO260
  159       ENDIF
      C
      C   LOWER ENERGY IN
      C
  160       WRITE(*,*) STRING(27),LIN
  161       READ(*,*) LIN
      C
      C   UPPER ENERGY IN
      C
  162       WRITE(*,*) STRING(28),UIN
  163       READ(*,*) UIN
      C
      C   SUCTION HEAD
      C
  164       WRITE(*,*) STRING(29),SUKH
  165       READ(*,*) SUKH
      C
      C   PRESSURE HEAD
      C
  166       WRITE(*,*) STRING(30),PREH
  167       READ(*,*) PREH
      C
      C   CONDENSER VOLUME
      C
  168       WRITE(*,*) STRING(31),CONDV
  169       READ(*,*) CONDV
      C
      C   CONDENSER AREA
      C
  170       WRITE(*,*) STRING(32),CONDA
  171       READ(*,*) CONDA
      C
      C   SPRING FORCE
      C
  172       WRITE(*,*) STRING(33),SPRF
  173       READ(*,*) SPRF
      C
      C   ASSUMED ATMOSPHERIC TEMPERATURE
      C
      C
  176       WRITE(*,*) STRING(37),CLO
  177       READ(*,*) CLO
      C
```

```
C   TOTAL SOLAR RADIATION
C
      WRITE(*,*) STRING(38),TSR
      READ(*,*) TSR
C
C   ERROR RECOVERY
C
      WRITE(*,*) STRING(34)
      READ(*,*) ERR
      IF(ERR.EQ.1)THEN
         GOTO11
      ENDIF
C
320 CLOSE(1)
      IF(PRESETS.NE.1) THEN
         PTEMP=PTEMP+273
         DAY = X
         MONTH=W
         MONNUM=W
         DAYNUM = X
      ENDIF
C
C   FIND THE ALTITUDE AND AZIMUTH ANGLES WITH A SUBROUTINE
C
C
      LATDEG=LATDEG*LSIGN
      LATRAD=LATDEG*PI/180.0
C
C   WORKING OUT VARIABLES FOR THE WHOLE DAY, IE. 80 * .25 HOUR STEPS
C
340 DO 46 I=1,80
C
      WRITE(*,*)'COLLECTING DATA FOR EACH 1/4 HOUR PERIOD, ',I
       CALL SUNANG(LATRAD,MONNUM,DAYNUM,HOUR,BETA,GAMMA,U,V,W)
C
         ALTIT(I)=W*(-1)
         IF(ALTIT(I).LT.0)THEN
            ALTIT(I)=0
         ENDIF
         IF(W.GE.0) THEN
            TORAD(I)=0
            TORADD(I)=0
            SOAD(I)=0
            DIFF(I)=0
            HR(I)=HOUR
            HOUR=HOUR+.25
            GOTO46
         ENDIF
C
C    INTERPOLATING THE VALUES FOR THE CONSTANTS TO FIND SOLAR RADIATION
INTENSITY
C
         IF (ABS(DAY-21).EQ.(DAY-21)) THEN
            GOTO44
         ENDIF
         CALL COEFF(MONTH,A,B,E)
         F=E
         C=A
         D=B
         MONTH=MONTH-1
         CALL COEFF(MONTH,A,B,E)
         A=C+((21-DAY)/30)*(A-C)
         B=D+((21-DAY)/30)*(B-D)
         E=F+((21-DAY)/30)*(E-F)
         MONTH=MONTH+1
         GOTO42
44    CALL COEFF(MONTH,A,B,E)
         C=A
         D=B
         F=E
         MONTH=MONTH+1
         CALL COEFF(MONTH,A,B,E)
         A=A+((30-(DAY-21))/30)*(C-A)
         B=B+((30-(DAY-21))/30)*(D-B)
         E=E+((30-(DAY-21))/30)*(F-E)
C
         CALL TOPLOSS(TA,SPACE,EMITP,N,OUTCON,EMITG,PTEMP,COLALTR,
     *UTL)
C
C   ACCOUNT FOR BOTTOM LOSS (SIDE LOSSES IGNORED)
C
         MONTH=MONTH-1
C
C   SOLAR RADIATION INTENSITY AT A NORMAL TO THE DIRECTION OF THE RAYS
C
42    SOLRAD=A/(EXP(B/SIN(BETA)))
C
C   DIFFUSE SOLAR RADIATION FROM THE SKY
C
         WPMM=0
         GLASSORB=0
         COLALTR=COLALT*PI/180.0
         COLAZIR=COLAZI*PI/180.0
C
         FSS=(1+COS((PI/2)-COLALTR))/2
         SRADSK=E*SOLRAD*SIN(BETA)*FSS
C   ACCOUNT FOR TRANSMITANCE AND ABSORBANCE IN GLASS
         HERP=59.68-.1388*(COLALT)+.001497*(COLALT)**2
         HERPR=HERP*PI/180.0
         CALL GLASS(N,TRANS,TRINT4,SORB,HERPR,ABCOEF,REFG)
         TRANS1=TRINT4*SRADSK
         SORB1=SORB*SRADSK
         WPMM=WPMM+TRANS1
         GLASSORB=GLASSORB+SORB1
C
C   DIFFUSE SOLAR RADIATION REFLECTED FROM THE GROUND
C
         FSG=1-FSS
         SRADGR=.2*FSG*(SOLRAD*SIN(BETA)*(E+SIN(BETA)))
C   ACCOUNT FOR TRANSMITANCE AND ABSORBANCE IN GLASS
         HERP=90.0-.5788*(COLALT)+.002693*(COLALT)**2
         HERPR=HERP*PI/180.0
         CALL GLASS(N,TRANS,TRINT5,SORB,HERPR,ABCOEF,REFG)
         TRANS2=TRINT5*SRADGR
         SORB2=SORB*SRADGR
         WPMM=WPMM+TRANS2
         GLASSORB=GLASSORB+SORB2
C
C   COLLECTOR DIRECTION CALCULATIONS
C
         CU=COS(COLAZIR)*COS(COLALTR)
         CV=SIN(COLAZIR)*COS(COLALTR)
         CW=SIN(COLALTR)
C
C   ANGLE BETWEEN NORMAL TO COLLECTOR AND SUNS RAYS
C
         CU2=CU**2
         CV2=CV**2
         CW2=CW**2
         HERPR=ACOS((CU*U+CV*V+CW*W)/(SQRT(U*U+V*V+W*W)*
     *SQRT(CU2+CV2+CW2)))
         CU=SQRT(CU)
         CV=SQRT(CV)
         CW=SQRT(CW)
         HERPR=PI-HERPR
C
C    CALL A PROGRAMME TO FIND THE TOTAL DIRECT SOLAR RADIATION ON THE
SURFACE
C    BEHIND THE GLAZING
C   ACCOUNTING FOR TRANSMITANCE AND ABSORBANCE IN GLASS
C
         CALL GLASS(N,TRANS6,TRINT,SORB,HERPR,ABCOEF,REFG)
         TRANS3=TRANS6*SOLRAD*COS(HERPR)
         SORB3=SORB*SOLRAD*COS(HERPR)
         WPMM=WPMM+TRANS3
         GLASSORB=GLASSORB+SORB3
C
C
C   FIND TA (AMBIENT TEMP) FOR ANY PLACE AT ANY TIME OF ANY DAY
C
         CALL AMBIENT(HOUR,DAYNUM,LSIGN,DAYDIF,SEADIF,MAXT,
     *TAMB,LATDEG)
         TA=TAMB+273.0
C
C   HEAT LOSS THROUGH GLAZING (TOP LOSS)
C   FIND ULT (TOP LOSS COEFF) INCLUDING RADIATIVE LOSSES
         UBL=THICKB*THERCO
         UTL=UTL+UBL
C
C   TOTAL HEAT LOSS
C
         QLOSS=UTL*(PTEMP-TA)
```

```
C
C    CLOUDINESS CALCULATIONS
C    CORRECTION FOR CLOUDINESS OBSERVATION
C
280      CG=CLO
281      CS=.965*CG-.12
C
C    CALCULATE DIFFUSE RADIATION LEVEL DURING CLOUDY PERIOD
C
282      FICTOR=ABS(SIN((HOUR-6)*PI/12))
283      CC(I)=(CG*FICTOR+CS*(1-FICTOR))+.24-.0018*LATDEG
284      CD=CC(I)
285      CALL CLOUD(CD,DIF)
286      DIFF(I)=DIF
C
C   CHECH NOS
C
287          SOAD(I)=SOLRAD
288          HEP(I)=QLOSS
289          AS(I)=TAMB
290          BB(I)=UTL-UBL
291          EE(I)=UBL
292          BET(I)=BETA
C
293          HR(I)=HOUR
294          TORADD(I)=WPMM
295          TORAD(I)=SOAD(I)*COS(HERPR)
296          HOUR=HOUR+.25
297          IF(TORAD(I).GT.MAXRAD)THEN
298              MAXRAD=TORAD(I)
299          ENDIF
300     46 CONTINUE


301      IF(MAXRAD.GT.UIN)THEN
302          UIN=MAXRAD
303      ENDIF
C
C    CLOUDINESS CALCULATIONS TO FIND PERIOD OF CLOUDINESS PER .25 HOUR
C
304      DU=0
305      TOT=0
306      TOG=TSR
307      DO 1357 T=0,15
308          TOGLAST=TOT
309          TOT=0
310          DO 1337 I=1,80
311              TOT=TOT+(SOAD(I)*ALTIT(I)*(15-T)*60+DIFF(I)*SOAD(I)*T*60)
312              IF(I.EQ.80.AND.TOT.LT.TSR)THEN
313                  GOTO1358
314              ENDIF
315  1337     CONTINUE
316  1357 CONTINUE
317  1358 T=T-(1-((TOGLAST-TSR)/(TOGLAST-TOT)))


C    ALLOW USER TO SKIP OPTIMISATION AND CALCULATE OUTPUT FOR A GIVEN
C    PUMP GEOMETRY

318      WRITE(*,*)'DO YOU WISH TO SKIP OPTIMISATION AND CALCULATE OUTPUT'
319      WRITE(*,*)'FOR DEFAULT DIMENSIONS? (1=YES, 2=NO)'
320      READ(*,*)R
321      IF(R.EQ.1)THEN
322          WRITE(*,*)'TYPE IN PUMP DIAMETER (m),'
323          READ(*,*)DIA
324          WRITE(*,*)'TYPE IN INNER DIAMETER TO OUTER DIAMETER RATIO,'
325          READ(*,*)RA
326          WRITE(*,*)'TYPE IN DIAPHRAGM RADIAL LENGTH (m),'
327          READ(*,*)RL
328          GOTO 8500
329      ENDIF

379      WRITE(*,*)UIN
380      IF(VALTOR.GT.(.99*TOR))THEN
381          TOR=VALTOR
382          RI=UIN
383          DIA=DIAM
384          RA=RATI
385          RL=RLEN
386      ENDIF
387      UIN=UIN-GOLD
C
C   RUN THROUGH OPTIMISATION ROUTINE FOR 5 DIFFERENT RADIATION
C   CONDITIONS AND PUT RESULTS ON DISC
C
330      TOR=0.0
331      RI=0.0
332      DIA=0.0
333      RA=0.0
334      RL=0.0
335      GOLD=(UIN-100-(LIN+100))/4
336      UIN=UIN-100

337      WRITE(*,*)'CALLING DIMOPT 1ST'

338      OPEN(4,FILE='C:\USERS\DANS\OUTPUT\OUTPUT1.DAT',STATUS='UNKNOWN')

339      CALL DIMOPT(UIN,PREH,SUKH,DIAM,RATI,RLEN,ATEMP,SPRF,CONDA,CONDV,
     *AS,TORAD,VALTO,UIN,VALTOR,DIFF,UTL,T)

340      CLOSE(4,STATUS='KEEP')

341      OPEN(4,FILE='A:\RESULT1.DAT',STATUS='UNKNOWN')
342      WRITE(4,50) DIAM,RATI,RLEN,CONDV
343      WRITE(4,55) PREH,SUKH,ATEMP,VALTOR,UIN
344      CLOSE(4,STATUS='KEEP')
345      WRITE(*,*)UIN
346      IF(VALTOR.GT.TOR)THEN
347          TOR=VALTOR
348          RI=UIN
349          DIA=DIAM
350          RA=RATI
351          RL=RLEN
352      ENDIF
353      UIN=UIN-GOLD

354      WRITE(*,*)'CALLING DIMOPT 2'

355      OPEN(4,FILE='C:\USERS\DANS\OUTPUT\OUTPUT2.DAT',STATUS='UNKNOWN')

356      CALL DIMOPT(UIN,PREH,SUKH,DIAM,RATI,RLEN,ATEMP,SPRF,CONDA,CONDV,
     *AS,TORAD,VALTO,UIN,VALTOR,DIFF,UTL,T)

357      CLOSE(4,STATUS='KEEP')

358      OPEN(4,FILE='A:\RESULT2.DAT',STATUS='UNKNOWN')
359      WRITE(4,50) DIAM,RATI,RLEN,CONDV
360      WRITE(4,55) PREH,SUKH,ATEMP,VALTOR,UIN
361      CLOSE(4,STATUS='KEEP')
362      WRITE(*,*)UIN
363      IF(VALTOR.GT.(.99*TOR))THEN
364          TOR=VALTOR
365          RI=UIN
366          DIA=DIAM
367          RA=RATI
368          RL=RLEN
369      ENDIF
370      UIN=UIN-GOLD

371      WRITE(*,*)'CALLING DIMOPT 3'

372      OPEN(4,FILE='C:\USERS\DANS\OUTPUT\OUTPUT3.DAT',STATUS='UNKNOWN')

373      CALL DIMOPT(UIN,PREH,SUKH,DIAM,RATI,RLEN,ATEMP,SPRF,CONDA,CONDV,
     *AS,TORAD,VALTO,UIN,VALTOR,DIFF,UTL,T)

374      CLOSE(4,STATUS='KEEP')

375      OPEN(4,FILE='A:\RESULT3.DAT',STATUS='UNKNOWN')
376      WRITE(4,50) DIAM,RATI,RLEN,CONDV
377      WRITE(4,55) PREH,SUKH,ATEMP,VALTOR,UIN
378      CLOSE(4,STATUS='KEEP')

388      WRITE(*,*)'CALLING DIMOPT 4'

389      OPEN(4,FILE='C:\USERS\DANS\OUTPUT\OUTPUT4.DAT',STATUS='UNKNOWN')

390      CALL DIMOPT(UIN,PREH,SUKH,DIAM,RATI,RLEN,ATEMP,SPRF,CONDA,CONDV,
     *AS,TORAD,VALTO,UIN,VALTOR,DIFF,UTL,T)

391      CLOSE(4,STATUS='KEEP')
```

```
      OPEN(4,FILE='A:\RESULT4.DAT',STATUS='UNKNOWN')
      WRITE(4,50) DIAM,RATI,RLEN,CONDV
      WRITE(4,55) PREH,SUKH,ATEMP,VALTOR,UIN
      CLOSE(4,STATUS='KEEP')
      WRITE(*,*)UIN
      IF(VALTOR.GT.(.99*TOR))THEN
         TOR=VALTOR
         RI=UIN
         DIA=DIAM
         RA=RATI
         RL=RLEN
      ENDIF
      UIN=LIN+100

      WRITE(*,*)'CALLING DIMOPT 5'

      OPEN(4,FILE='C:\USERS\DANS\OUTPUT\OUTPUT5.DAT',STATUS='UNKNOWN')

      CALL DIMOPT(UIN,PREH,SUKH,DIAM,RATI,RLEN,ATEMP,SPRF,CONDA,CONDV,
     *AS,TORAD,VALTO,UIN,VALTOR,DIFF,UTL,T)

      CLOSE(4,STATUS='KEEP')

      OPEN(4,FILE='A:\RESULT5.DAT',STATUS='UNKNOWN')
      WRITE(4,50) DIAM,RATI,RLEN,CONDV
      WRITE(4,55) PREH,SUKH,ATEMP,VALTOR,UIN
      CLOSE(4,STATUS='KEEP')
      WRITE(*,*)UIN
      IF(VALTOR.GT.(.99*TOR))THEN
         TOR=VALTOR
         RI=UIN
         DIA=DIAM
         RA=RATI
         RL=RLEN
      ENDIF
C
C   RUN THROUGH OPTIMUM TO GIVE VALUES OF PERFORMANCE FOR EACH .25 HOUR
C
      WRITE(*,*)'CALLING DAYOUT TO FIND OUTPUT FOR OPTIMUM RESULTS'
      WRITE(*,*)'FROM MAIN PROGRAM'
 8500 CALL DAYOUT(PREH,SUKH,DIA,RA,RL,INCWT,TEMSYS,CONDV,AS,TORAD,VALOUT,
     .WATOUT,P,DIFF,UTL,T)
         DFLOW=0
         DO 1820 I=1,80
            IF(P(I).LE.0.0.OR.VALOUT(I).LE.0.0)THEN
               VALOUT(I)=0.0
               P(I)=0.0
               GOTO1822
            ENDIF
            FLOW(I)=VALOUT(I)*20.0*1000*60/P(I)
            VALOUT(I)=VALOUT(I)*18000.0/P(I)
 1822       DFLOW=VALOUT(I)+DFLOW
 1820 CONTINUE
C
C   OUTPUT THE OPTIMUM PUMPS RESULTS TO FILE ON DISC A
C
 2010 OPEN(4,FILE='A:\RESULTS.DAT',STATUS='UNKNOWN')
      WRITE(4,43) NUMB,LATDEG,MONTH
      WRITE(4,45) DAY,COLAZI,COLALT
      WRITE(4,52)
      WRITE(4,50) DIA,RA,RL,CONDV
      WRITE(4,53)
      WRITE(4,51) PREH,SUKH,ATEMP,DFLOW,RI
      WRITE(4,47)
      DO 49 I = 1,80
       P(I)=P(I)/20.0
       WRITE(4,48) HR(I),TORAD(I),TEMSYS(I),AS(I),INCWT(I),
     . FLOW(I),P(I)
   49 CONTINUE
   43 FORMAT(1X,'RUN NO =',F5.0,'     LAT = ',F6.2,'    MONTH = ',F5.0)
   45 FORMAT(1X,'DAY = ',F5.0,'    COLAZI = ',F6.2,'    COL ALT = ',F5.2)
   47 FORMAT(2X,'HOUR   RADIATION SYST   AMBT WATERDT L/MIN   TIME/STROKE')
   48 FORMAT(2X,F5.2,2X,F6.1,2X,F7.2,2X,F5.1,2X,F5.3,2X,F8.3,2X,F7.2)
   52 FORMAT(1X,'DIAM=',2X,'RATIO=',2X,'RLEN=',2X,'MAXTRA=')
   50 FORMAT(1X,F6.4,2X,F6.4,2X,F6.4,2X,F6.4)
   51 FORMAT(1X,F4.1,2X,F4.1,2X,F5.1,2X,F5.2,2X,F6.1)
   55 FORMAT(1X,F4.1,2X,F4.1,2X,F5.1,2X,F5.1,2X,F6.1)
   53 FORMAT(1X,'PREH=',2X,'SUKH=',2X,'ATEMP=',2X,'1 DAYS OUTPUT'
     .,2X,'DESIGN RADIATION')
      CLOSE(4,STATUS='KEEP')
C
C   CHECK TO SEE IF USER WANTS TO USE PROGRAM AGAIN
C
      WRITE(*,*)'OPTIMISATION IS FINISHED'
      WRITE(*,*)'IF YOU WISH TO USE THE COMPUTER, PLEASE TYPE'
      WRITE(*,*)'ANY NUMBER EXCEPT 1, THEN ENTER TWICE,'
      WRITE(*,*)'ONCE BACK IN WATFOR TYPE QUIT, THEN ENTER'
      WRITE(*,*)'REMOVE FLOPPY, LOGOUT, AND REBOOT'
      WRITE(*,*) STRING(36)
      READ(*,*) AGAIN
      IF(AGAIN.EQ.1)THEN
         GOTO 9
      ENDIF
      STOP
      END
```

```
      SUBROUTINE CLOUD(CC,DIFF)

      IMPLICIT NONE
      REAL CC,DIFF
C
C  LOOK UP TABLE FOR DIFFUSE FACTOR VERSUS CLOUD COVER
C
      IF(CC.GE.0.AND.CC.LT..5)DIFF=.2
      IF(CC.GE..5.AND.CC.LT.1.5)DIFF=.26
      IF(CC.GE.1.5.AND.CC.LT.2.5)DIFF=.32
      IF(CC.GE.2.5.AND.CC.LT.3.5)DIFF=.35
      IF(CC.GE.3.5.AND.CC.LT.4.5)DIFF=.38
      IF(CC.GE.4.5.AND.CC.LT.5.5)DIFF=.41
      IF(CC.GE.5.5.AND.CC.LT.6.5)DIFF=.45
      IF(CC.GE.6.5.AND.CC.LT.7.5)DIFF=.46
      IF(CC.GE.7.5.AND.CC.LT.8.5)DIFF=.47
      IF(CC.GE.8.5.AND.CC.LT.9.5)DIFF=.45
      IF(CC.GE.9.5.AND.CC.LE.10)DIFF=.43
      RETURN
      END
```

```
485         SUBROUTINE DAYOUT(PREH,SUKH,DIAM,RATI,RLEN,INCWT,TEMSYS,
           *MAXTRA,AS,TORAD,ILUT,WATOUT,IP,DIFF,UTL,TIME)

486         IMPLICIT NONE
487         REAL DIAM,RATI,RLEN,SUKH,PREH,MAXTRA,TEMSYS(80),INCWT(80),AB,P
488         REAL IP(80),ILUT(80),AS(80),TORAD(80),DIFF(80),WATOUT
489         REAL LUT,TORAE,UTL,TIME,SPRF,CONDA
490         INTEGER I
        C
        C     SUBROUTINE TO WORK THROUGH ONE DAYS WATER PUMPING IN .25 HOUR
INTERVALS
        C
491         WATOUT=0
492         DO 3050 I=1,80
493            IF(TORAD(I).LE.200)THEN
494               ILUT(I)=0
495               IP(I)=0
496               GOTO3050
497            ENDIF
498            WRITE(*,*)I
499            TORAE=TORAD(I)
500            AB=AS(I)

501         WRITE(*,*)'CALLING PANELTD FROM DAYOUT'

502            CALL PANELTD(TORAE,PREH,SUKH,DIAM,RATI,RLEN,AB,SPRF,CONDA,
           *    MAXTRA,LUT,P,DIFF,UTL,TIME)
503            WATOUT=LUT
504            ILUT(I)=LUT
505            IP(I)=P
506            INCWT(I)=SPRF
507            TEMSYS(I)=CONDA
508   3050 CONTINUE
509         RETURN
510         END
```

```
      SUBROUTINE DIMOPT(WIN,PREH,SUKH,DIAM,RATI,RLEN,ATEMP,SPRF,CONDA,
     *MAXTRA,AS,TORAD,WATOUT,RI,DFLOW,DIFF,UTL,TIME)

      IMPLICIT NONE
      REAL DIAM,RATI,RLEN,SUKH,PREH,MAXTRA,ATEMP,SPRF,CONDA
      REAL DFLOW,VALOUT(80),OP(80),P,P2,DIFF(80),UTL,TIME
      REAL AS(80),TORAD(80),MAXOUT,WATOUT,WIN,INCWT(80),TEMSYS(80)
      REAL LUT,RI,CAV,EGAIN,CAVIT,EGAINO
      REAL DIA,RAT,RLE,MAXDIA,MINDIA,MAXRAT,MINRAT,MAXRLE,MINRLE
      REAL INCDIA,INCRAT,INCRLE,SWT,SL,WTI,THS
      INTEGER L,M,N,Q,D,R,RL,I,z
C
C     SEARCH PROGRAMME FOR OPTIMUM VARIABLE VALUES
C
      MAXOUT=0.0
      WATOUT=0.0

C     SETTING GLOBAL MAP VARIABLE LIMITS

      MAXDIA=0.35
      MINDIA=0.15
      MAXRAT=0.8
      MINRAT=0.2
      MAXRLE=0.06
      MINRLE=0.015
      L=4
      M=12
      N=9
      Q=1

C     SETTING INCREMENTION VALUES

  100 INCDIA=(MAXDIA-MINDIA)/L
      INCRAT=(MAXRAT-MINRAT)/M
      INCRLE=(MAXRLE-MINRLE)/N

C     PERFORM COMPLETE VARIABLE COMBINATION MAP TO DETERMINE THE POINT
C     WHERE PUMP SIZING WOULD RESULT IN MAXIMUM WATER OUTPUT

      DO 1000 D=1,L+1
         DIA=MINDIA+INCDIA*(D-1)

            DO 1100 R=1,M+1
               RAT=MINRAT+INCRAT*(R-1)

      WRITE(*,*)' Diameter   Ratio    Rlen    Operating Temp      Egain
     .Output   Stroke Time'
      WRITE(4,*)' Diameter   Ratio    Rlen    Operating Temp      Egain
     .Output   Stroke Time'

                  DO 1200 RL=1,N+1
                     RLE=MAXRLE-INCRLE*(RL-1)
C                     WRITE(*,*)'DIAM,RATI,RLEN,'
C                     write(*,*)DIA,RAT,RLE
                     CALL PANELT(WIN,PREH,SUKH,DIA,RAT,RLE,ATEMP,SPRF,
     .                    CONDA,MAXTRA,LUT,P,DIFF,UTL,TIME,CAV,EGAIN)

      WRITE(*,93)DIA,RAT,RLE,CONDA,20*EGAIN/P,LUT,P/20
      WRITE(4,93)DIA,RAT,RLE,CONDA,20*EGAIN/P,LUT,P/20
   93 FORMAT(1X,F6.3,3X,F6.4,2X,F6.4,4X,F8.2,5X,F8.3,5X,F8.7,2X,F8.5)

                     IF((0.99*LUT).GT.MAXOUT)THEN
                        WRITE(*,*)'
     .                       IMPROVEMENT'
                        WRITE(4,*)'
     .                       IMPROVEMENT'
                        DIAM=DIA
                        RATI=RAT
                        RLEN=RLE
                        MAXOUT=LUT
                        WTI=SPRF
                        SWT=CONDA
                        SL=MAXTRA
                        THS=P/20
                        CAVIT=CAV
                        EGAINO=EGAIN
                     ENDIF
 1200             CONTINUE
C     CALCULATE FINAL PUMPS PERFORMANCE OVER A WHOLE DAY

      WRITE(*,*)'CALLING DAYOUT TO WORK OUT OVERALL OUTPUT FOR A DAY'
 1100       CONTINUE
 1000 CONTINUE

C    CURRENT STATUS OUTPUT FOR INQUISITIVE OPERATORS

      WRITE(*,*)'1st(coarse) or 2nd(fine) Mapping',Q
      WRITE(*,*)'Operational Insolation,',RI
      WRITE(*,*)'Incremental Diameter Variation,',INCDIA
      WRITE(*,*)'Water Flow Rate m3/s,',MAXOUT
      WRITE(*,*)'Time for 1/2 stroke,s,',THS
      WRITE(*,*)'Energy Imbalance (J,W)',EGAINO,EGAINO/THS
      WRITE(*,*)'Optimum Outer Diameter / Ratio,',DIAM,RATI
      WRITE(*,*)'Optimum Rubber diaphragm radial length,',RLEN
      WRITE(*,*)'Stroke Length,',SL
      WRITE(*,*)'Discharge / Suction Heads,',PREH,SUKH
      WRITE(*,*)'Cavitation Occurence (0=no)',CAVIT
      WRITE(*,*)'System Working Temp (K)',SWT
      WRITE(*,*)'Water Temperature Increase,',WTI
      WRITE(*,*)'Ambient Temperature,',ATEMP
      WRITE(*,*)
      WRITE(*,*)'          PLEASE DO NOT INTERRUPT THIS COMPUTER'
      WRITE(*,*)'        MULTI-VARIABLE OPTIMISATION IS IN PROGRESS'

      IF(DIAM.EQ.MAXDIA)WRITE(*,*)'MAXDIA LIMIT SET TOO LOW ON PASS',Q
      IF(DIAM.EQ.MINDIA)WRITE(*,*)'MINDIA LIMIT SET TOO HIGH ON PASS',Q
      IF(RATI.EQ.MAXRAT)WRITE(*,*)'MAXRAT LIMIT SET TOO LOW ON PASS',Q
      IF(RATI.EQ.MINRAT)WRITE(*,*)'MINRAT LIMIT SET TOO HIGH ON PASS',Q
      IF(RLEN.EQ.MAXRLE)WRITE(*,*)'MAXRLE LIMIT SET TOO LOW ON PASS',Q
      IF(RLEN.EQ.MINRLE)WRITE(*,*)'MINRLE LIMIT SET TOO HIGH ON PASS',Q

C     OUTPUT STATUS TO DISK

      WRITE(4,*)'1st(coarse) or 2nd(fine) Mapping',Q
      WRITE(4,*)'Operational Insolation,',RI
      WRITE(4,*)'Incremental Diameter Variation,',INCDIA
      WRITE(4,*)'Water Flow Rate m3/s,',MAXOUT
      WRITE(4,*)'Time for 1/2 stroke,s,',THS
      WRITE(4,*)'Energy Imbalance (J,W)',EGAINO,EGAINO/THS
      WRITE(4,*)'Optimum Outer Diameter / Ratio,',DIAM,RATI
      WRITE(4,*)'Optimum Rubber diaphragm radial length,',RLEN
      WRITE(4,*)'Stroke Length,',SL
      WRITE(4,*)'Discharge / Suction Heads,',PREH,SUKH
      WRITE(4,*)'Cavitation Occurence (0=no)',CAVIT
      WRITE(4,*)'System Working Temp (K)',SWT
      WRITE(4,*)'Water Temperature Increase,',WTI
      WRITE(4,*)'Ambient Temperature,',ATEMP
      WRITE(4,*)
      WRITE(4,*)'          PLEASE DO NOT INTERRUPT THIS COMPUTER'
      WRITE(4,*)'        MULTI-VARIABLE OPTIMISATION IS IN PROGRESS'

      IF(DIAM.EQ.MAXDIA)WRITE(4,*)'MAXDIA LIMIT SET TOO LOW ON PASS',Q
      IF(DIAM.EQ.MINDIA)WRITE(4,*)'MINDIA LIMIT SET TOO HIGH ON PASS',Q
      IF(RATI.EQ.MAXRAT)WRITE(4,*)'MAXRAT LIMIT SET TOO LOW ON PASS',Q
      IF(RATI.EQ.MINRAT)WRITE(4,*)'MINRAT LIMIT SET TOO HIGH ON PASS',Q
      IF(RLEN.EQ.MAXRLE)WRITE(4,*)'MAXRLE LIMIT SET TOO LOW ON PASS',Q
      IF(RLEN.EQ.MINRLE)WRITE(4,*)'MINRLE LIMIT SET TOO HIGH ON PASS',Q

c     read(*,*)z

C     PERFORM REDUCED INCREMENT LOCAL MAPPING AROUND OPTIMUM POINT

      IF(Q.EQ.1)THEN
         MAXDIA=DIAM+0.05
         MINDIA=DIAM-0.05
         MAXRAT=RATI+0.06
         MINRAT=RATI-0.06
         MAXRLE=RLEN+0.007
         MINRLE=RLEN-0.007
         L=20
         M=12
         N=14
         Q=2
         GOTO 100
      ENDIF

c     read(*,*)z

      WRITE(*,*)'FROM DIMOPT'

 4000 CALL DAYOUT(PREH,SUKH,DIAM,RATI,RLEN,INCWT,TEMSYS,MAXTRA,AS,TORAD,
```

```
     .VALOUT,WATOUT,OP,DIFF,UTL,TIME)
626          DFLOW=0
627          DO 1820 I=1,80
628            IF(TORAD(I).LE.200)THEN
629              VALOUT(I)=0.0
630              OP(I)=0.0
631              GOTO1822
632            ENDIF
633            VALOUT(I)=VALOUT(I)*18000/OP(I)
634  1822        DFLOW=DFLOW+VALOUT(I)
635  1820 CONTINUE
636       WRITE(*,*)'One Days Water Output m3',DFLOW
637       WRITE(4,*)'One Days Water Output m3',DFLOW
638       RETURN
639       END
```

```
      SUBROUTINE PANELT(TORAD,PREH,SUKH,DIAM,RATI,RLEN,ATEMP,SPRF,CONDA,
     *CONDV,LUT,P,DIFF,UTL,TIME,CAV,EGAINO)
      IMPLICIT NONE
      INTEGER IS,K,N,J,C
      REAL PREH,SUKH,DIAM,RATI,RLEN,ATEMP,SPRF,CONDA,CONDV
      REAL CPM,CPL,CPG,MM,ML,HFG,MG,WROUT,M
      REAL EGAINT,LUT,P,TORAD,P1,EGAIN,EGAINO
      REAL DIF,UTL,TIME,DIFF(80),SUM,SPCVOL,TEMP
      REAL INC,OT,TRIALT,HT,LT,TOR
      REAL CAV,SPR,CONA,CONV,WROU,PT
      DOUBLE PRECISION TET
C
C     CONTROL PROGRAM FOR PUMP SIMULATION ROUTINES INCLUDING SEARCH TO
C     FIND STEADY STATE OPERATING TEMPERATURE
C     ALSO DEALS WITH SOME OF THE FAILURE SCENARIOS.
C     PUMPS PERFORMANCE CALCULATED OVER A WHOLE DAYS INPUT CONDITIONS
C
      WROUT=0.0
      P1=0.0
      EGAINT=0.0
      CPM=460.0
      CPL=2470.0
      CPG=1810.0
      MM=46.4
      ML=5.6
      HFG=330000.0

      K=0
      SUM=0.0
      DO 1000 IS=1,80
        IF(DIFF(IS).NE.0.0)THEN
          SUM=SUM+DIFF(IS)
          K=K+1
        ENDIF
1000  CONTINUE
        DIF=SUM/K

      OT=0.0
      HT=90.0
      LT=40.0
      N=10
      C=1
      M=1.0E10

1010  INC=(HT-LT)/N

      DO 1020 J=1,N+1
        TRIALT=HT-INC*(J-1)
        MG=3.5E-3/SPCVOL(TRIALT)
        TET=(TRIALT+273)*(CPM*MM+CPL*ML+CPG*MG)+HFG*MG
        CALL PUMP(TET,PREH,SUKH,DIAM,RATI,RLEN,ATEMP,SPR,CONA,
     .       CONV,TORAD,WROU,PT,TRIALT,EGAIN,P1,DIF,UTL,TIME)

          IF(ABS(EGAIN).LE.M)THEN
            M=ABS(EGAIN)
            EGAINO=EGAIN
            OT=TRIALT
            SPRF=SPR
            CONDA=CONA
            CONDV=CONV
            WROUT=WROU
            P=PT
            CAV=P1
          ENDIF
1020  CONTINUE

          IF(OT.EQ.HT)WRITE(*,*)'UPPER TEMP LIMIT TOO LOW',C
          IF(OT.EQ.LT)WRITE(*,*)'LOWER TEMP LIMIT TOO HIGH',C

      IF(C.EQ.1)THEN
        HT=OT+5.0
        LT=OT-5.0
        N=10
        C=2
        GOTO 1010
      ENDIF
      IF(C.EQ.2)THEN
        HT=OT+1.0
        LT=OT-1.0
        N=8
        C=3
        GOTO 1010
      ENDIF

      IF(20*M/P.GT.50)THEN
C       WRITE(*,*)'THERMAL STABILITY NOT DETERMINED'
        WROUT=0.0
        GOTO 3000
      ENDIF

      IF(P.EQ.2001)THEN
        WRITE(*,*)'INSUFFICIENT HEAT INPUT TO OPERATE'
        WROUT=0.0
      ENDIF

3000  LUT=20.0*WROUT/P
      RETURN
      END
```

```
      SUBROUTINE PANELTD(TORAD,PREH,SUKH,DIAM,RATI,RLEN,ATEMP,SSPRF,CONDA,
     *CONDV,LUT,P,DIFF,UTL,TIME)

      IMPLICIT NONE
      INTEGER DUMY,CUN,DUM,CON,I,K
      REAL TORAD,PREH,SUKH,DIAM,RATI,RLEN,ATEMP,SPRF,CONDA,CONDV,LUT,P
      REAL CPM,CPL,CPG,MM,ML,HFG,GOLD,ONE,ZER,TOR,OMTOR,MG,WROUT
      REAL EGAINT,EGAINOMT,DIF,UTL,TIME,P1,DIFF(80),SUM
      DOUBLE PRECISION TET,TEO
C
C     CONTROL PROGRAM FOR PUMP SIMULATION ROUTINES INCLUDING GOLDEN SECTION
C     SEARCH TO FIND STEADY STATE OPERATING TEMPERATURE, ALSO DEALS WITH
C     SOME OF THE FAILURE SCENARIOS. PUMPS PERFOMANCE CALCULATED ON INPUT
C     CONDITITONS
C
C      RATI=1.67
C      RLEN=.02
C      DIAM=.24
C      CONDA=.4
C      CONDV=.002
      DUMY=0
      CUN=0
      DUM=0
      CON=0
      WROUT=0.0
      P1=0.0
      EGAINT=0.0
      EGAINOMT=0.0
      CPM=460
      CPL=2470
      CPG=1810
      MM=46.4
      ML=5.6
      HFG=330000
      GOLD=1/((1+(5**.5))/2)
      ONE=85
      ZER=30
      TOR=(ONE-ZER)*GOLD+ZER
C      TOR=68.5
      MG=3.5E-3*(1/(.5279-5.68E-3*TOR))
      TET=(TOR+273)*(CPM*MM+CPL*ML+CPG*MG)+HFG*MG

      K=0
      SUM=0.0
      DO I=1,80,1
         IF(DIFF(I).NE.0.0)THEN
           SUM=SUM+DIFF(I)
           K=K+1
         ENDIF
      ENDO
         DIF=SUM/K

C      WRITE(*,*)'CALLING PUMP 1 FROM PANELTD'

      CALL PUMP(TET,PREH,SUKH,DIAM,RATI,RLEN,ATEMP,SPRF,CONDA,CONDV,
     *TORAD,WROUT,P,TOR,EGAINT,P1,DIF,UTL,TIME)
C      WRITE(*,*)'1',P1,P
      OMTOR=(ONE-ZER)*(1-GOLD)+ZER
      MG=3.5E-3*(1/(.5279-5.68E-3*OMTOR))
      TEO=(OMTOR+273)*(CPM*MM+CPL*ML+CPG*MG)+HFG*MG

C      WRITE(*,*)'CALLING PUMP 2 FROM PANELTD'

      CALL PUMP(TEO,PREH,SUKH,DIAM,RATI,RLEN,ATEMP,SPRF,CONDA,CONDV,
     *TORAD,WROUT,P,OMTOR,EGAINOMT,P1,DIF,UTL,TIME)
C      WRITE(*,*)'2',OMTOR
      IF(WROUT.EQ.0.AND.P.EQ.2001)THEN
         DUM=1
      ENDIF

      if(p.eq.4000)goto5070

5210  IF(ABS(EGAINT).LE.ABS(EGAINOMT).OR.DUM.EQ.1)THEN
         DUM=0
         CUN=CUN+1
         ZER=OMTOR
         OMTOR=TOR
         TEO=TET
         ENDIF
      IF(WROUT.EQ.0)THEN
         CON=CON+1
      EGAINOMT=EGAINT
      TOR=(ONE-ZER)*GOLD+ZER
      MG=3.5E-3*(1/(.5279-5.68E-3*TOR))
      TET=(TOR+273)*(CPM*MM+CPL*ML+CPG*MG)+HFG*MG

C     WRITE(*,*)'CALLING PUMP 3 FROM PANELTD'

      CALL PUMP(TET,PREH,SUKH,DIAM,RATI,RLEN,ATEMP,SPRF,CONDA,CONDV
     *,TORAD,WROUT,P,TOR,EGAINT,P1,DIF,UTL,TIME)
C     WRITE(*,*)'3',TOR,EGAINT,P,P1
      IF(WROUT.EQ.0.AND.P.EQ.4001)THEN
         CON=CON+1
         DUM=1
         WRITE(*,*)'DEAD ROOSTER1'
         DUMY=DUMY+1
         IF(DUMY.GT.15)THEN
            WROUT=0
            GOTO5070
         ENDIF
         GOTO5220
      ENDIF
C     IF(CUN.GT.15.AND.ABS(EGAINT).GT.50)THEN
C        WROUT=0
C        GOTO5070
C     ENDIF
      IF(WROUT.EQ.0.AND.P.EQ.2001)THEN
         CON=CON+1
         DUM=1
         GOTO5210
      ENDIF
      IF(WROUT.EQ.0.AND.P.NE.2001)THEN
         CON=CON+1
         DUM=1
         GOTO5220
      ENDIF
       IF(ABS(TOR-OMTOR).LT.0.10)THEN
         GOTO5070
       ENDIF
      GOTO5210
     ENDIF
5220 IF(ABS(EGAINT).GT.ABS(EGAINOMT).OR.DUM.EQ.1)THEN
      DUM=0
      CUN=CUN+1
      ONE=TOR
      TOR=OMTOR
      TET=TEO
      EGAINT=EGAINOMT
      OMTOR=(ONE-ZER)*(1-GOLD)+ZER
      MG=3.5E-3*(1/(.5279-5.68E-3*OMTOR))
      TEO=(OMTOR+273)*(CPM*MM+CPL*ML+CPG*MG)+HFG*MG

C     WRITE(*,*)'CALLING PUMP 4 FROM PANELTD'

      CALL PUMP(TEO,PREH,SUKH,DIAM,RATI,RLEN,ATEMP,SPRF,CONDA,
     *CONDV,TORAD,WROUT,P,OMTOR,EGAINOMT,P1,DIF,UTL,TIME)
C     WRITE(*,*)'4',OMTOR,EGAINOMT,P,P1
     ENDIF
C     IF(CUN.GT.15.AND.ABS(EGAINOMT).GT.50)THEN
C      WROUT=0
C      GOTO5070
C     ENDIF
     IF(CON.EQ.CUN.AND.CON.GT.10)THEN
      WROUT=0
      GOTO5070
     ENDIF
      IF(ABS(TOR-OMTOR).LE.0.10)THEN
       GOTO5070
      ENDIF
      IF(WROUT.EQ.0.AND.P.EQ.4001)THEN
         CON=CON+1
         DUM=1
         WRITE(*,*)'DEAD ROOSTER2'
         DUMY=DUMY+1
         IF(DUMY.GT.15)THEN
            WROUT=0
            GOTO5070
         ENDIF
         GOTO5210
      DUM=1
      GOTO5210
     ENDIF
```

```
836         GOTO5210
837   5070 LUT=WROUT
838            WRITE(*,*)'OPERATING TEMP FROM PANELTD & EGAIN',TOR,EGAINT
839         RETURN
840         END
```

```
841       SUBROUTINE PUMP(INTEIN,PREH,SUKH,DIAM,RATI,RLEN,ATEMP,INCRWT,
         .TK,MAXTRA,TORAD,WATER,P,STEMP,EGAIN,P1,DIF,UTL,TIME)

842       IMPLICIT NONE
843       REAL PI,G
844       PARAMETER (PI=3.141592654,G=9.81)
845       REAL DIAM,RATI,HFG,ATEMP,TORAD
846       REAL LI,LO,SUMKI,SUMKO,APIPE,RLEN,DGAP,MAXTRA,ODIAM,IDIAM,OD,ID
847       REAL WCAREA,VCAREA,APANEL,VOLI,VOLO,MM,ML,MG,CPM,CPL,CPG
848       REAL STEMP,ATMOS,PW,WATERT,TK,DEDVOL,VCGM,VCENGY,PREVC1,PREVC2
849       REAL P,V,V1,WATER,VOLG,MIN,PIN,SUKH,PREH,INCR,CONVOL
850       REAL MASGVC,CLOSS,MASSW,INCRWT,TMSC,DRIG,DRAG,DOOG,PLTEMP1
851       REAL UTL,DIF,OFF,TIME,TIME2,TIME3,EGAIN,a,p1,PREE,TINT,td
852       DOUBLE PRECISION INTEIN,THETA,RADIUS,AREA,NETOTE,VOLINC
853       DOUBLE PRECISION MGINC,TRAVEL,GASVOL,WATVOL,TRAV,GAIN,ACCELW
854       REAL SPCVOL,TEMP



      C   Diam refers to outside diameter of vapour chamber, rati*diam=inside
      C   diameter of vapour chamber, dgap is diaphragm working radius

      C   Setting geometric parameters
855   100 LI=6.5
856       LO=3.5

      c   sumki was 5.3 li=sukh+2 for increased suction heads
857       SUMKI=4.4

858       SUMKO=4.8

859       APIPE=PI/4*(32.5E-3*32.5E-3)

860       DGAP=2*RLEN/PI-6E-3
861       MAXTRA=4*RLEN/PI
862       ODIAM=DIAM
863       IDIAM=RATI*DIAM
864       OD=ODIAM-DGAP
865       ID=IDIAM+DGAP

866       WCAREA=PI/4*OD*OD

867       VCAREA=PI/4*(OD*OD-ID*ID)
868       APANEL=2.9

      C   Geometry resulting from diaphragm changing shape
869       THETA=(6-(6*DGAP+18E-3)/(RLEN-1.5E-3*PI))**0.5
870       RADIUS=1/THETA*(RLEN-1.5E-3*PI)
871       AREA=RADIUS*RADIUS*(THETA-SIN(THETA))
872       VOLI=PI*ID*AREA
873       VOLO=PI*OD*AREA

      C   Setting material properties
874       MM=46.4
875       CPM=460.0
876       CPL=2470.0
877       CPG=1810.0
878       HFG=330000.0
879       ML=5.6
880       MG=3.5E-3/SPCVOL(STEMP)
881       ATMOS=101.3E3
882       PW=1000.0
883       WATERT=296.0
884       EGAIN=0.0
885       GAIN=0.0
886       NETOTE=0.0

      C   VALVE OPENS TO DEFLATED VAPOUR CHAMBER - CALC NEW GAS VOL, CALC
      C   ENERGY IN SYSTEM, CALC NEW SYSTEM TEMP
887       TK=STEMP+273.0



888       NETOTE=INTEIN
889       DEDVOL=VCAREA*5E-3 + 0.5*10E-3*10E-3*PI*(OD + ID)
      C    write(*,*)'tk-watert/2',((tk+watert)/2)
      C    VCGM=DEDVOL/SPCVOL(WATERT-273.0)
      C    MG=MG+VCGM
      C    VCENGY=VCGM*(CPG*WATERT + HFG)

      C   CAVITATION CALCULATION
925       MIN=PW*APIPE*LI
      C    NETOTE=INTEIN+VCENGY-VCGM*CPG*(TK-WATERT)
      C    EGAIN=VCENGY-VCGM*CPG*(TK-WATERT)
      C    TK=(NETOTE-HFG*MG)/(CPM*MM+CPL*ML+CPG*MG)


      C   HIGH PRESSURE VAPOUR STARTS TO FILL CHAMBER BY LIQUID EVAPORATION
      C   BEFORE THE PISTON STARTS TO MOVE, INNER DIAPHRAGM WILL INVERT
      C   USING SOME ENERGY FOR NO WATER OUTPUT,OUTER DIAPHRAGM WILL INVERT
      C   AND RESULT IN SOME WATER OUTPUT AND SOME VAPOUR WILL BE USED TO
      C   REPRESSURISE THE VAPOUR CHAMBER.
      C   CALC SYSTEM PRESSURE (IE VC1 PRESSURE) AT THE END OF THESE
      C   INTERMEDIATE EFFECTS TO FIND PRESSURE AT THE BEGINNING OF PUMPING
      C   (PISTON DISPLACEMENT)

890       VOLINC=VOLO+VOLI
891       PREE=133.322*10**(6.8643-1070.62/(TK-40.304))
892       MGINC=VOLINC/SPCVOL(TK-273)+DEDVOL/SPCVOL(TK-273)
         .-DEDVOL/SPCVOL(WATERT-273)
893       MG=MG+MGINC
894       ML=ML-MGINC
895       GAIN=-PREE*(VOLINC+DEDVOL*(1-SPCVOL(TK-273)/SPCVOL(WATERT-273)))
      C     write(*,*)'GAIN',Pree,volinc,dedvol,tk,watert,GAIN
896       EGAIN=EGAIN+GAIN
897       NETOTE=NETOTE+GAIN
898       TK=(NETOTE-HFG*MG)/(CPM*MM+CPL*ML+CPG*MG)

      C     write(*,*)'tk3 after expanding diaphragms and addition of vc'
      C     write(*,*)'gas',tk

899       PREVC1=133.322*10**(6.8643-1070.62/(TK-40.304))
      C   ASSUME VC2 PRESSURE REMAINS AT AN AVERAGE THROUGHOUT STROKE
900       PREVC2=90E3
901       TINT=273.0+34.0

      C   RUN THROUGH PUMP TRAVEL MAINTAINING FORCE EQUILIBRIUM FOR EACH
      C   1/20TH SEC INTERVAL

902       P=0.0
903       P1=0.0
904       V=0.0
905       TRAVEL=0.0
906       GASVOL=0.0
907       ACCELW=0.0
908       MGINC=0.0
909       WATER=VOLO

910   1000 IF (TRAVEL.LT.MAXTRA) THEN
911       P=P+1.0
912       IF(P.GT.2000)GOTO1020
913       V1=V

      C   WORK OUT ENERGY GAIN IN SOLAR PANEL, NEW SYSTEM TEMP AND PRESSURE

914       GAIN=1.0/20.0*((0.6625-3.98*(TK-ATEMP-273)/TORAD)*APANEL*TORAD
         .-50.0*(TK-ATEMP-273)*PI*OD*RLEN
         .-49.0*(TK-ATEMP-273)*PI/4*((ODIAM-2*DGAP)**2-IDIAM**2)
         .-0.18*(TK-ATEMP-273))

915       EGAIN=EGAIN+GAIN
916       NETOTE=NETOTE+GAIN
917       TK=(NETOTE-HFG*MG)/(CPM*MM+CPL*ML+CPG*MG)
918       PREVC1=133.322*10**(6.8643-1070.62/(TK-40.304))

      C   WATER ACCELERATION FROM EQUATIONS OF MOTION

919       ACCELW=1.0/(PW*(LI+LO))*((PREVC1-PREVC2)*VCAREA/WCAREA
         .-PW*G*(PREH+SUKH)-0.5*PW*V*V*(SUMKI+SUMKO))
      C   write(*,*)'tk,prevc1,prevc2,vcarea,wcarea,v,accelw,egain'
      C   write(*,*)tk,prevc1,prevc2,vcarea,wcarea,v,accelw,egain

      C   WATER VELOCITY IN PIPE AT END OF INTERVAL (FROM MMTM CONSERVATION)

920       V=V1+ACCELW/20.0
921       V=(LI+LO)/(V/20.0+(LI+LO))*V
922       ACCELW=20.0*(V-V1)
      C   Negative velocities impossible
923       IF(V.LE.0.0)V=0.0
924       if(v.eq.0.0)goto1000
926       PIN=ATMOS-(PW*G*SUKH)-(0.5*PW*V*V*SUMKI)-(MIN*ACCELW/APIPE)
927       IF(PIN.LT.2500)THEN
      C     WRITE(*,*)'CAVITATION ALERT !??'
```

```
C          V=V1
C          P=3000
C          WATER=0.0
C          GOTO2000
928          ACCELW=(ATMOS-PIN-PW*G*SUKH-0.5*PW*V*V*SUMKI)*APIPE/MIN
929          V=V1+ACCELW/20
930          V=((LI+LO)/(V/20+(LI+LO)))*V
931          P1=2001
932        ENDIF

C     WATER VOLUME PUMPED IN 1/20 SEC INTERVAL
933        WATVOL=1.0/20.0*(V+V1)/2*APIPE
934        WATER=WATER+WATVOL
c       write(*,*)'watvol,water,travel,p,gain,egain'
c       write(*,*)watvol,water,travel,p,gain,egain



C     PISTON TRAVEL AND GAS VOLUME USED
935        TRAV=WATVOL/WCAREA
936        TRAVEL=TRAVEL+TRAV
937        VOLG=TRAV*VCAREA
938        MGINC=VOLG/SPCVOL(TK-273)
939        MG=MG+MGINC
940        ML=ML-MGINC
941        GAIN=-pw*apipe*(v+v1)*(g*(preh+sukh)/40+(li+lo)*(v-v1)/2)
c         WRITE(*,*)'GAIN',GAIN
942        EGAIN=EGAIN+GAIN
943        NETOTE=NETOTE+GAIN
944        GASVOL=GASVOL+VOLG
945        TK=(NETOTE-HFG*MG)/(CPM*MM+CPL*ML+CPG*MG)



c       IF(V.EQ.0.0)GOTO1000


C     FOR LAST INCREMENT OF PUMP TRAVEL

946        ELSE

947        INCR=(MAXTRA-(TRAVEL-TRAV))/TRAV
948        WATER=WATER-(1-INCR)*WATVOL
949        TRAVEL=MAXTRA
950        P=P+(INCR-1)
951        NETOTE=NETOTE-(1-INCR)*GAIN
952        EGAIN=EGAIN-(1-INCR)*GAIN
953          mg=mg-mginc*(1-INCR)
954          gasvol=gasvol-volg*(1-INCR)
955        GOTO 1010

956        ENDIF

957        GOTO 1000

C     TIME DELAY (td) AT THE END OF STROKE WHILE VC1 EVACUATES AND VC2
C      FILLS, 0.1 SECOND IS GIVEN AS AN APPROXIMATION.

958   1010 td=2.0
959        P=P+td

C     ASSUME CONDENSED VAPOUR IS PUMPED BACK INTO THE PANEL DURING THIS
C     TIME AND THAT THE HEAT LOST IN CONDENSER IS REMOVED FROM SYSTEM
C     ENERGY

960        CONVOL=GASVOL+VOLINC
961        MASGVC=CONVOL/SPCVOL(TK-273)
962        GAIN=-MASGVC*(CPG*(TK-TINT)+HFG+CPL*(TINT-WATERT))
C       WRITE(*,*)'GAIN IN CONDENSER',GAIN
963        NETOTE=NETOTE+GAIN
964        EGAIN=EGAIN+GAIN
965        ML=ML+MASGVC
966        mg=mg-masgvc
967        TK=(NETOTE-HFG*MG)/(CPM*MM+CPL*ML+CPG*MG)

C     ENERGY GAIN IN SOLAR PANEL WHILE ABOVE FACTORS ARE GOING ON

968        GAIN=1.0/20.0*td*TORAD*APANEL*(0.6625-3.98*(TK-ATEMP-273)/TORAD)
969        NETOTE=NETOTE+GAIN
970        EGAIN=EGAIN+GAIN
971        TK=(NETOTE-HFG*MG)/(CPM*MM+CPL*ML+CPG*MG)

C     CALCULATE WATER TEMP RISE ASSUMING 100% EFF HEAT EXCHANGER

972        CLOSS=MASGVC*(CPG*(TK-TINT)+HFG+CPL*(TINT-WATERT))
973        MASSW=WATER*PW
974        INCRWT=CLOSS/(MASSW*4182)

975   1020   IF(P.EQ.2001)WATER=0.0

C     DOWN TIME DUE TO CLOUD COOLING OF PANEL AND REDUCED OUTPUT

976        TMSC=CPM*MM+CPL*ML+CPG*MG

977        DRIG=EXP((-1)*UTL*TIME*60/(TMSC/APANEL))
978        DRAG=DIF*TORAD-UTL*(STEMP-ATEMP)
979        PLTEMP1=ATEMP+((-1)/UTL)*((-1)*DIF*TORAD+(DRIG*DRAG))
980        IF(PLTEMP1.GE.STEMP)THEN
981          OFF=TIME/15.0
982          GOTO2000
983        ENDIF
984        DOOG=(TORAD-UTL*(STEMP-ATEMP))/(TORAD-UTL*(PLTEMP1-ATEMP))
985        IF(DOOG.LE.0.0)THEN
986          OFF=1.0
987          GOTO2000
988        ENDIF
989        TIME2=TMSC*(-1)*LOG(DOOG)/(UTL*APANEL)
990        TIME3=TIME*60+TIME2
991        OFF=TIME3/(15*60)
C         WRITE(*,*)'OFF RESET TO ZERO?? OFF,TIME,2,3'
C         WRITE(*,*)OFF,TIME,TIME2,TIME3
C         WRITE(*,*)'ATEMP,PLTEMP1,STEMP,TK,INCRWT'
C         WRITE(*,*)ATEMP,PLTEMP1,STEMP,TK,INCRWT

992          OFF=0.0

c       write(*,*)'off time',off

993   2000 WATER=WATER*(1-OFF)
994        RETURN
995        END



996        REAL FUNCTION SPCVOL(TEMP)

C     Returns approximate specific gas volume at specified temperature
C     (C) by approximating ranges of temperatures with linear functions
C     accurate to within 5%

997        IF (TEMP.LT.0.0)WRITE(*,*)'TEMP IS LT 0.0 DEGREES CENT'
998        IF (TEMP.GE.0.0.AND.TEMP.LE.38)SPCVOL=0.8546-(14.59E-3*TEMP)
999        IF (TEMP.GT.38.AND.TEMP.LE.60)SPCVOL=0.5300-(6.125E-3*TEMP)
1000       IF (TEMP.GT.60.AND.TEMP.LE.100)SPCVOL=0.3344-(2.946E-3*TEMP)
1001       IF (TEMP.GT.100)WRITE(*,*)'TEMP IS GT 100 DEGREES CENT'
1002       RETURN
1003       END
```

```
      SUBROUTINE SUNANG(LATRAD,MONTH,DAY,HOUR,BETA,GAMMA,U,V,W)

      IMPLICIT NONE
      INTEGER MONTH,DAY,TOTOMN(12)
      REAL DAYOFY,HOUR,LATRAD,ALT,AZI,LSTRAD,DECRAD,BETA,GAMMA,PI
      REAL U,V,W,DUM,DOM,SEC
      PARAMETER ( PI = 3.141592654 )
C
C   THIS PROGRAM WILL DETERMINE THE ALTITUDE AND AZIMUTH ANGLES
C   OF THE SUN AT ANY POINT ON THE EARTH AT ANY TIME OF THE YEAR.
C
C             REQUIRED ARGUMENTS:
C                LATRAD -- LATITUDE ANGLE IN RADIANS.   THE NORTHERN
C                     HEMISPHERE ANGLES ARE POSITIVE AND THE SOUTHERN
C                     HEMISPHERE ANGLES ARE NEGATIVE.   THE ABSOLUTE
C                     VALUE OF THE LATITUDE MUST BE LESS THAN OR EQUAL
C                     TO PI/2.
C                MONTH -- THE VALID RANGE OF INPUTS ARE 1 THROUGH 12.
C                DAY -- THE VALID RANGE CORRESPONDING TO EACH MONTH.
C                     NOTE THAT 29 FEBRUARY IS NOT AN OPTION.
C                LST -- LOCAL STANDARD TIME.   THE VALID RANGES ARE
C                     BETWEEN 00.00 AND 24.00.   NOTE THAT FRACTIONS
C                     OF HOURS ARE TO BE EXPRESSED IN DECIMAL FORM.
C
C             RETURNED ARGUMENTS:
C                ALT -- THE ALTITUDE ANGLE IN RADIANS MEASURED FROM
C                     THE LOCAL HORIZON.
C                AZI -- THE AZIMUTH ANGLE IN RADIANS MEASURED
C                     CLOCKWISE FROM TRUE NORTH.
C
C
C
C   THIS IS A LIST OF THE NUMBER OF DAYS UNTIL A GIVEN MONTH
C
      TOTOMN(1)=0
      TOTOMN(2)=31
      TOTOMN(3)=59
      TOTOMN(4)=90
      TOTOMN(5)=120
      TOTOMN(6)=151
      TOTOMN(7)=181
      TOTOMN(8)=212
      TOTOMN(9)=243
      TOTOMN(10)=273
      TOTOMN(11)=304
      TOTOMN(12)=334
C
C   FIND DAY OF THE YEAR
C
      DAYOFY=TOTOMN(MONTH)+DAY
C
C   CALCULATE THE AZIMUTH AND ALTITUDE ANGLES
C
      LSTRAD = (HOUR-12.0)*PI/12.0
C
      DECRAD = SIN((DAYOFY-81.5)*2*PI/365.0)*0.410152
C
      DUM=(COS(LATRAD)*COS(LSTRAD)*COS(DECRAD)+SIN(LATRAD)*SIN(DECRAD))
      IF(DUM.GT.1)THEN
         DUM=1
         WRITE(*,*)'SUNANG ALMOST AT ERROR'
      ENDIF
      BETA = ASIN(DUM)
C
      DOM=(SEC(BETA)*(COS(LATRAD)*SIN(DECRAD)-COS(DECRAD)*SIN(
     *LATRAD)*COS(LSTRAD)))
      IF(DOM.GT.1)THEN
         WRITE(*,*)'SUNANG ALMOST AT ERROR'
         DOM=1
      ENDIF
      GAMMA = ACOS(DOM)
C
C   THIS CORRECTS FOR THE FACT THAT THE EQUATIONS RETURN THE AZIMUTH
C   ANGLES MEASURED CLOCKWISE FROM TRUE NORTH BETWEEN SOLAR NOON AND
C   SOLAR MIDNIGHT.
C
      IF(LSTRAD.GT.0.0) THEN
         GAMMA = 2*PI-GAMMA
      ENDIF
C
      ALT = BETA
      AZI = GAMMA
      IF(AZI.LE.0)THEN
         WRITE(*,*)'SUNANG ALMOST AT ERROR'
         GOTO 1234
      ENDIF
C
      AZI=AZI+INT((ABS(AZI)-AZI)/2/AZI+.1)*2*PI
C
 1234 U=-COS(AZI)*COS(ALT)
      V=-SIN(AZI)*COS(ALT)
      W=-SIN(ALT)
C
      RETURN
      END
C


      REAL FUNCTION SEC(BETA)
C
C   THIS RETURNS THE SECANT OF THE ANGLE BETA
C   IF THE ANGLE IS PI/2 OR 3*PI/2 THEN A VAL OF 64000.0
C   IS RETURNED.
C
      PARAMETER(PI=3.1415927)
      IF(BETA.EQ.(PI/2.0).OR.BETA.EQ.(3.0*PI/2.0)) THEN
         SEC = 64000.0
      ELSE
         SEC = 1.0/COS(BETA)
      ENDIF
      RETURN
      END
```

```
      SUBROUTINE COEFF(MONTH,A,B,E)

      IMPLICIT NONE
      REAL A,B,E,MONTH
C
C     GIVES COEFFICIENTS FOR THE EQUATIONS USED IN THE MAIN PROGRAMME
C
      IF(MONTH.EQ.0) GOTO130
      IF(MONTH.EQ.1) GOTO20
      IF(MONTH.EQ.2) GOTO30
      IF(MONTH.EQ.3) GOTO40
      IF(MONTH.EQ.4) GOTO50
      IF(MONTH.EQ.5) GOTO60
      IF(MONTH.EQ.6) GOTO70
      IF(MONTH.EQ.7) GOTO80
      IF(MONTH.EQ.8) GOTO90
      IF(MONTH.EQ.9) GOTO100
      IF(MONTH.EQ.10) GOTO110
      IF(MONTH.EQ.11) GOTO120
      IF(MONTH.EQ.12) GOTO130
      IF(MONTH.EQ.13) GOTO20
   20 A=1230
      B=.142
      E=.058
      GOTO140
   30 A=1215
      B=.144
      E=.060
      GOTO140
   40 A=1186
      B=.156
      E=.071
      GOTO140
   50 A=1136
      B=.180
      E=.097
      GOTO140
   60 A=1104
      B=.196
      E=.121
      GOTO140
   70 A=1088
      B=.205
      E=.134
      GOTO140
   80 A=1085
      B=.207
      E=.136
      GOTO140
   90 A=1107
      B=.201
      E=.122
      GOTO140
  100 A=1151
      B=.177
      E=.092
      GOTO140
  110 A=1192
      B=.160
      E=.073
      GOTO140
  120 A=1221
      B=.149
      E=.063
      GOTO140
  130 A=1233
      B=.142
      E=.057
      GOTO140
  140 RETURN
      END
```

```
      SUBROUTINE GLASS(N,TRANS,TRINT,SORB,HERP,ABCOEF,REFG)
C
C   THIS FINDS THE SOLAR RADIATION TRANSMITTED TO A ONE METER SQUARE
C     SURFACE BEHIND A CERTAIN AMONT OF GLASS AT A CERTAIN ANGLE (SPECIFIED)
C
      IMPLICIT NONE
      INTEGER N
      REAL IDASH,RP,RS,TRINT,TRANS,SORB,HERP,ABCOEF,REFG
C
C   NON REFLECTED COMPONENT
C
      IDASH=ASIN(SIN(HERP)/REFG)
      RP=((TAN(HERP-IDASH))**2)/(((TAN(HERP+IDASH))**2)*2)
      RS=((SIN(HERP-IDASH))**2)/(((SIN(HERP+IDASH))**2)*2)
      TRINT=.5*(((1-RP)/(1+(2*N-1)*RP))+((1-RS)/(1+(2*N-1)*RS)))
C
C   ABSORPTANCE COMPONENT
C
      TRANS=TRINT*((1-ABCOEF)**N)
      SORB=TRANS-TRINT
      RETURN
      END
```

```
      SUBROUTINE AMBIENT(HOUR,DAYNUM,LSIGN,DAYDIF,SEADIF,MAXT,
     *TAMB,LATDEG)

      IMPLICIT NONE
      INTEGER DAYS,DAYNUM,LSIGN
      REAL HOUR,DAYDIF,SEADIF,MAXT,TAMB,LATDEG,MMEAN,TSEA,PI
      REAL PVESIZ,NVESIZ,PVEHEI,DAYSPV,DAYSNV
      PI=3.141592654
C
C  DAILY VARIATIONS DUE TO THE SEASONS (IGNORING RAINY SEASONS)
C
      MMEAN=MAXT-SEADIF/2-DAYDIF/2
C
C  FOR N + S AND LAT GE 23.5 DEGREES
      IF(LSIGN.EQ.-1.AND.LATDEG.GE.23.5) THEN
          TSEA=MMEAN+SEADIF*(COS((DAYNUM-11)*2*PI)/265)/2
          GOTO50
      ENDIF
      IF(LSIGN.EQ.1.AND.LATDEG.GE.23.5) THEN
          TSEA=MMEAN-SEADIF*(COS((DAYNUM-11)*2*PI)/265)/2
          GOTO50
      ENDIF
C
C  FOR N + S AND LAT LT 23.5 DEG
C
      PVESIZ=.5*LATDEG/23.5
      NVESIZ=PVESIZ-1
      PVEHEI=PVESIZ*SEADIF
      DAYSPV=182*LATDEG/23.5+182
      DAYSNV=365-DAYSPV
      IF(LSIGN.EQ.1)THEN
          IF(DAYNUM.LT.182)THEN
              DAYS=182+DAYNUM
          ENDIF
          IF(DAYNUM.GE.182)THEN
              DAYS=DAYNUM-182
          ENDIF
      ENDIF
      IF(LSIGN.EQ.-1)THEN
          DAYS=DAYNUM
      ENDIF
      IF(DAYS.LE.(DAYSPV/2))THEN
          TSEA=MMEAN+(SEADIF-(PVEHEI/2)+(PVEHEI/2)*(COS(DAYS/(DAYSPV/2))
     **PI+PI))/2
      ENDIF
      IF((365-DAYS).LE.(DAYSPV/2))THEN
          TSEA=MMEAN+(SEADIF-(PVEHEI/2)+(PVEHEI/2)*(COS((DAYS-365)/
     *(DAYSPV/2))*PI+PI))/2
      ENDIF
      IF(DAYS.GT.(DAYSPV/2).AND.DAYS.LT.(365-DAYSPV/2))THEN
          TSEA=MMEAN+SEADIF*COS((DAYS-DAYSPV/4)*2*PI/(DAYSNV+DAYSPV/2))
     */2
      ENDIF
C
C  NOW ADD THE HOURLY VARIATION TO THE DAILY MEAN
C
   50 IF(HOUR.LT.6) THEN
          TAMB=TSEA+DAYDIF*COS(PI-((6-HOUR)*PI/16))/2
      ENDIF
      IF(HOUR.GE.6.AND.HOUR.LE.14) THEN
          TAMB=TSEA+DAYDIF*COS(((HOUR-6)*PI/8)-PI)/2
      ENDIF
      IF(HOUR.GT.14) THEN
          TAMB=TSEA+DAYDIF*COS((HOUR-14)*PI/16)/2
      ENDIF
      RETURN
      END
```

```
1191        SUBROUTINE TOPLOSS(TA,SPACE,EMITP,N,OUTCON,EMITG,PTEMP,COLALTR,
           *UTL)

1192        IMPLICIT NONE
1193        INTEGER N
1194        REAL UTL,TA,SPACE,EMITP,OUTCON,EMITG,PTEMP,COLALTR,STEF,PI
1195        REAL F,C,D
1196        PI=3.141592654
      C
      C   FINDS THE TOP LOSS COEFFICIENT FOR A FLAT PLATE COLLECTOR
      C
1197        STEF=5.6697E-08
1198        F=(9/OUTCON-30/(OUTCON**2))*(TA/316.9)*(1+.091*N)
1199        D=EMITP+.0425*N*(1-EMITP)
1200        C=204.429*((COS(PI/2-COLALTR))**.252)/(SPACE**.24)
1201        UTL=(((N/(C/PTEMP*(((PTEMP-TA)/(N+F))**.252))+1/OUTCON))**(-1))
           *+(STEF*(PTEMP**2+TA**2)*(PTEMP+TA))/(1/D+(2*N+F-1)/EMITG-N)
1202        RETURN
1203        END
```

# Appendix 4
# Simulation Output

**A) Simulation results for one days operation of the system optimised for a static water head of 6 m$H_2O$ but lifting water through varying static water heads (refer to Chapter 4).**

**B) Simulation results for one days operation of the selected pump design lifting water through varying static water heads operating as per the test setup (refer to Chapter 6).**

| Time of Day | Insolation W/sq.m | System Temp deg K | Ambient Temp deg C | Increased Water Temp deg K | Flow Rate l/m | Time for Stroke s | System Pressure kPa(abs) | Panel Efficiency % | Heat Input W |
|---|---|---|---|---|---|---|---|---|---|
| 7.25 | 274.7 | 313.27 | 12.8 | 0.245 | 3.71 | 17.77 | 116688.6 | 26.5 | 796.6 |
| 7.50 | 337.8 | 313.51 | 13.1 | 0.247 | 7.74 | 9.98 | 117618.0 | 34.0 | 979.6 |
| 7.75 | 400.5 | 313.73 | 13.4 | 0.248 | 10.45 | 7.99 | 118475.0 | 39.1 | 1161.5 |
| 8.00 | 462.3 | 314.18 | 13.7 | 0.251 | 14.15 | 6.17 | 120243.2 | 42.6 | 1340.7 |
| 8.25 | 522.4 | 314.90 | 14.1 | 0.256 | 17.77 | 4.92 | 123114.8 | 45.1 | 1515.0 |
| 8.50 | 580.4 | 315.62 | 14.5 | 0.261 | 20.46 | 4.27 | 126039.5 | 47.0 | 1683.2 |
| 8.75 | 635.9 | 316.58 | 14.9 | 0.268 | 23.28 | 3.75 | 130022.7 | 48.3 | 1844.1 |
| 9.00 | 688.5 | 317.47 | 15.3 | 0.275 | 25.44 | 3.43 | 133802.0 | 49.4 | 1996.7 |
| 9.25 | 737.8 | 318.24 | 15.8 | 0.281 | 27.04 | 3.23 | 137139.9 | 50.4 | 2139.6 |
| 9.50 | 783.7 | 318.96 | 16.3 | 0.287 | 28.39 | 3.08 | 140319.2 | 51.2 | 2272.7 |
| 9.75 | 825.8 | 319.85 | 16.8 | 0.295 | 29.91 | 2.92 | 144327.5 | 51.8 | 2394.8 |
| 10.00 | 864.0 | 320.58 | 17.3 | 0.302 | 31.02 | 2.82 | 147680.9 | 52.3 | 2505.6 |
| 10.25 | 897.9 | 321.26 | 17.7 | 0.308 | 32.00 | 2.73 | 150858.4 | 52.7 | 2603.9 |
| 10.50 | 927.5 | 321.98 | 18.2 | 0.315 | 32.97 | 2.65 | 154280.1 | 53.0 | 2689.8 |
| 10.75 | 952.6 | 322.43 | 18.7 | 0.319 | 33.54 | 2.61 | 156448.9 | 53.4 | 2762.5 |
| 11.00 | 973.1 | 322.64 | 19.2 | 0.322 | 33.80 | 2.58 | 157469.0 | 53.8 | 2822.0 |
| 11.25 | 988.8 | 323.14 | 19.6 | 0.327 | 34.42 | 2.54 | 159918.5 | 54.0 | 2867.5 |
| 11.50 | 999.7 | 323.19 | 20.0 | 0.327 | 34.47 | 2.54 | 160165.0 | 54.2 | 2899.1 |
| 11.75 | 1005.8 | 323.60 | 20.4 | 0.332 | 34.94 | 2.50 | 162197.8 | 54.3 | 2916.8 |
| 12.00 | 1007.0 | 323.60 | 20.8 | 0.332 | 34.94 | 2.50 | 162197.8 | 54.5 | 2920.3 |
| 12.25 | 1003.2 | 323.60 | 21.1 | 0.332 | 34.94 | 2.50 | 162197.8 | 54.5 | 2909.3 |
| 12.50 | 994.7 | 323.36 | 21.4 | 0.329 | 34.67 | 2.52 | 161005.5 | 54.7 | 2884.6 |
| 12.75 | 981.2 | 323.14 | 21.7 | 0.327 | 34.42 | 2.54 | 159918.5 | 54.7 | 2845.5 |
| 13.00 | 963.1 | 322.92 | 21.9 | 0.324 | 34.14 | 2.56 | 158837.1 | 54.7 | 2793.0 |
| 13.25 | 940.2 | 322.47 | 22.0 | 0.320 | 33.59 | 2.60 | 156642.8 | 54.6 | 2726.6 |
| 13.50 | 912.8 | 322.02 | 22.2 | 0.315 | 33.02 | 2.65 | 154472.0 | 54.6 | 2647.1 |
| 13.75 | 881.0 | 321.53 | 22.2 | 0.311 | 32.38 | 2.70 | 152134.6 | 54.4 | 2554.9 |
| 14.00 | 845.0 | 320.74 | 22.3 | 0.303 | 31.27 | 2.79 | 148423.8 | 54.3 | 2450.5 |
| 14.25 | 804.9 | 320.13 | 22.2 | 0.298 | 30.34 | 2.88 | 145606.7 | 53.9 | 2334.2 |
| 14.50 | 761.0 | 319.40 | 22.2 | 0.291 | 29.17 | 3.00 | 142289.9 | 53.6 | 2206.9 |
| 14.75 | 713.5 | 318.64 | 22.2 | 0.285 | 27.82 | 3.14 | 138899.2 | 53.2 | 2069.2 |
| 15.00 | 662.6 | 317.69 | 22.2 | 0.277 | 25.90 | 3.37 | 134749.2 | 52.7 | 1921.5 |
| 15.25 | 608.8 | 316.79 | 22.1 | 0.270 | 23.83 | 3.67 | 130906.8 | 52.1 | 1765.5 |
| 15.50 | 552.3 | 316.07 | 22.0 | 0.265 | 21.86 | 4.00 | 127894.6 | 51.1 | 1601.7 |
| 15.75 | 493.6 | 315.18 | 22.0 | 0.258 | 18.88 | 4.63 | 124245.9 | 50.0 | 1431.4 |
| 16.00 | 433.0 | 314.69 | 21.9 | 0.255 | 16.84 | 5.19 | 122271.8 | 48.1 | 1255.7 |
| 16.25 | 371.2 | 314.01 | 21.8 | 0.250 | 13.06 | 6.69 | 119572.8 | 45.7 | 1076.5 |
| 16.50 | 308.7 | 313.68 | 21.7 | 0.248 | 10.43 | 8.29 | 118279.8 | 41.8 | 895.2 |
| 16.75 | 246.5 | 313.30 | 21.5 | 0.245 | 4.72 | 16.90 | 116804.4 | 35.9 | 714.9 |
| Average | 726.8 | 318.93 | 19.2 | 0.290 | 25.69 | 4.45 | 140875.9 | 49.8 | 2107.6 |
| Maximum | 1007.0 | 323.60 | 22.3 | 0.332 | 34.94 | 17.77 | 162197.8 | 54.7 | 2920.3 |

| Time of Day | Insolation W/sq.m | System Temp deg K | Ambient Temp deg C | Increased Water Temp deg K | Flow Rate l/m | Time for Stroke s | System Pressure kPa(abs) | Panel Efficiency % |
|---|---|---|---|---|---|---|---|---|
| 7.25 | 274.7 | 316.48 | 12.8 | 0.268 | 2.20 | 26.01 | 129603.2 | 21.8 |
| 7.50 | 337.8 | 316.55 | 13.1 | 0.268 | 3.42 | 21.12 | 129896.7 | 30.4 |
| 7.75 | 400.5 | 316.79 | 13.4 | 0.270 | 8.22 | 9.72 | 130906.8 | 36.0 |
| 8.00 | 462.3 | 317.07 | 13.7 | 0.272 | 11.45 | 7.40 | 132093.0 | 40.1 |
| 8.25 | 522.4 | 317.52 | 14.1 | 0.276 | 14.98 | 5.83 | 134016.8 | 43.1 |
| 8.50 | 580.4 | 318.19 | 14.5 | 0.281 | 18.41 | 4.75 | 136921.2 | 45.2 |
| 8.75 | 635.9 | 318.68 | 14.9 | 0.285 | 20.34 | 4.30 | 139076.1 | 47.0 |
| 9.00 | 688.5 | 319.40 | 15.3 | 0.291 | 22.70 | 3.85 | 142289.9 | 48.3 |
| 9.25 | 737.8 | 320.13 | 15.8 | 0.298 | 24.68 | 3.54 | 145606.7 | 49.3 |
| 9.50 | 783.7 | 320.74 | 16.3 | 0.303 | 26.16 | 3.34 | 148423.8 | 50.3 |
| 9.75 | 825.8 | 321.53 | 16.8 | 0.311 | 27.83 | 3.14 | 152134.6 | 51.0 |
| 10.00 | 864.0 | 322.02 | 17.3 | 0.315 | 28.77 | 3.04 | 154472.0 | 51.6 |
| 10.25 | 897.9 | 322.70 | 17.7 | 0.322 | 29.98 | 2.91 | 157761.4 | 52.1 |
| 10.50 | 927.5 | 323.18 | 18.2 | 0.327 | 30.79 | 2.84 | 160115.7 | 52.5 |
| 10.75 | 952.6 | 323.59 | 18.7 | 0.332 | 31.43 | 2.78 | 162148.0 | 52.9 |
| 11.00 | 973.1 | 323.91 | 19.2 | 0.335 | 31.91 | 2.74 | 163748.0 | 53.3 |
| 11.25 | 988.8 | 324.31 | 19.6 | 0.340 | 32.50 | 2.69 | 165765.0 | 53.5 |
| 11.50 | 999.7 | 324.59 | 20.0 | 0.343 | 32.89 | 2.66 | 167188.2 | 53.7 |
| 11.75 | 1005.8 | 324.60 | 20.4 | 0.343 | 32.89 | 2.66 | 167239.2 | 53.9 |
| 12.00 | 1007.0 | 324.76 | 20.8 | 0.345 | 33.13 | 2.64 | 168056.9 | 54.0 |
| 12.25 | 1003.2 | 324.53 | 21.1 | 0.342 | 32.80 | 2.66 | 166882.4 | 54.2 |
| 12.50 | 994.7 | 324.59 | 21.4 | 0.343 | 32.89 | 2.66 | 167188.2 | 54.2 |
| 12.75 | 981.2 | 324.31 | 21.7 | 0.340 | 32.51 | 2.69 | 165765.0 | 54.2 |
| 13.00 | 963.1 | 324.15 | 21.9 | 0.338 | 32.26 | 2.71 | 164955.9 | 54.2 |
| 13.25 | 940.2 | 323.86 | 22.0 | 0.335 | 31.85 | 2.74 | 163497.2 | 54.0 |
| 13.50 | 912.8 | 323.43 | 22.2 | 0.330 | 31.17 | 2.80 | 161352.6 | 53.9 |
| 13.75 | 881.0 | 322.87 | 22.2 | 0.324 | 30.27 | 2.89 | 158592.2 | 53.7 |
| 14.00 | 845.0 | 322.43 | 22.3 | 0.320 | 29.51 | 2.96 | 156448.9 | 53.5 |
| 14.25 | 804.9 | 321.74 | 22.2 | 0.313 | 28.24 | 3.09 | 153133.0 | 53.1 |
| 14.50 | 761.0 | 321.02 | 22.2 | 0.306 | 26.77 | 3.26 | 149731.0 | 52.7 |
| 14.75 | 713.5 | 320.54 | 22.2 | 0.301 | 25.67 | 3.40 | 147495.6 | 52.1 |
| 15.00 | 662.6 | 319.81 | 22.2 | 0.295 | 23.85 | 3.66 | 144145.5 | 51.5 |
| 15.25 | 608.8 | 318.96 | 22.1 | 0.288 | 21.30 | 4.10 | 140319.2 | 50.7 |
| 15.50 | 552.3 | 318.47 | 22.0 | 0.283 | 19.54 | 4.47 | 138149.4 | 49.3 |
| 15.75 | 493.6 | 317.92 | 22.0 | 0.279 | 17.15 | 5.09 | 135745.0 | 47.8 |
| 16.00 | 433.0 | 317.24 | 21.9 | 0.274 | 13.16 | 6.64 | 132817.2 | 45.7 |
| 16.25 | 371.2 | 317.02 | 21.8 | 0.272 | 11.40 | 7.64 | 131880.6 | 42.4 |
| 16.50 | 308.7 | 316.74 | 21.7 | 0.270 | 7.91 | 10.37 | 130695.9 | 37.8 |
| 16.75 | 246.5 | 316.52 | 21.5 | 0.268 | 3.22 | 22.59 | 129770.9 | 30.7 |
| Average | 726.8 | 320.84 | 19.2 | 0.306 | 23.49 | 5.50 | 149385.4 | 48.4 |
| Maximum | 1007.0 | 324.76 | 22.3 | 0.345 | 33.13 | 26.01 | 168056.9 | 54.2 |

| Time of Day | Insolation W/sq.m | System Temp deg K | Ambient Temp deg C | Increased Water Temp deg K | Flow Rate l/m | Time for Stroke s | System Pressure kPa(abs) | Panel Efficiency % | Heat Input W |
|---|---|---|---|---|---|---|---|---|---|
| 7.25 | 274.7 | 319.50 | 12.8 | 0.292 | 2.12 | 22.33 | 142740.8 | 17.4 | 796.6 |
| 7.50 | 337.8 | 319.56 | 13.1 | 0.293 | 3.53 | 18.82 | 143011.8 | 26.8 | 979.6 |
| 7.75 | 400.5 | 319.79 | 13.4 | 0.295 | 7.85 | 9.68 | 144054.5 | 33.1 | 1161.5 |
| 8.00 | 462.3 | 319.86 | 13.7 | 0.295 | 9.05 | 9.06 | 144373.0 | 37.7 | 1340.7 |
| 8.25 | 522.4 | 320.13 | 14.1 | 0.298 | 12.20 | 7.03 | 145606.7 | 41.1 | 1515.0 |
| 8.50 | 580.4 | 320.57 | 14.5 | 0.302 | 15.61 | 5.60 | 147634.5 | 43.6 | 1683.2 |
| 8.75 | 635.9 | 321.02 | 14.9 | 0.306 | 18.00 | 4.85 | 149731.0 | 45.5 | 1844.1 |
| 9.00 | 688.5 | 321.70 | 15.3 | 0.312 | 20.86 | 4.19 | 152942.4 | 46.9 | 1996.7 |
| 9.25 | 737.8 | 322.02 | 15.8 | 0.316 | 21.99 | 3.97 | 154472.0 | 48.3 | 2139.6 |
| 9.50 | 783.7 | 322.64 | 16.3 | 0.322 | 23.91 | 3.65 | 157469.0 | 49.3 | 2272.7 |
| 9.75 | 825.8 | 323.18 | 16.8 | 0.327 | 25.41 | 3.44 | 160115.7 | 50.2 | 2394.8 |
| 10.00 | 864.0 | 323.63 | 17.3 | 0.332 | 26.50 | 3.30 | 162347.3 | 50.9 | 2505.6 |
| 10.25 | 897.9 | 324.31 | 17.7 | 0.340 | 28.01 | 3.12 | 165765.0 | 51.4 | 2603.9 |
| 10.50 | 927.5 | 324.76 | 18.2 | 0.345 | 28.92 | 3.02 | 168056.9 | 51.8 | 2689.8 |
| 10.75 | 952.6 | 325.04 | 18.7 | 0.348 | 29.45 | 2.97 | 169495.2 | 52.3 | 2762.5 |
| 11.00 | 973.1 | 325.31 | 19.2 | 0.351 | 29.96 | 2.92 | 170891.1 | 52.7 | 2822.0 |
| 11.25 | 988.8 | 325.52 | 19.6 | 0.354 | 30.34 | 2.88 | 171982.9 | 53.0 | 2867.5 |
| 11.50 | 999.7 | 325.70 | 20.0 | 0.356 | 30.64 | 2.85 | 172923.0 | 53.2 | 2899.1 |
| 11.75 | 1005.8 | 325.93 | 20.4 | 0.359 | 31.04 | 2.82 | 174130.0 | 53.4 | 2916.8 |
| 12.00 | 1007.0 | 325.93 | 20.8 | 0.359 | 31.04 | 2.82 | 174130.0 | 53.6 | 2920.3 |
| 12.25 | 1003.2 | 325.93 | 21.1 | 0.359 | 31.04 | 2.82 | 174130.0 | 53.6 | 2909.3 |
| 12.50 | 994.7 | 325.70 | 21.4 | 0.356 | 30.64 | 2.85 | 172923.0 | 53.7 | 2884.6 |
| 12.75 | 981.2 | 325.75 | 21.7 | 0.357 | 30.75 | 2.84 | 173184.9 | 53.7 | 2845.5 |
| 13.00 | 963.1 | 325.48 | 21.9 | 0.353 | 30.27 | 2.89 | 171774.6 | 53.6 | 2793.0 |
| 13.25 | 940.2 | 325.08 | 22.0 | 0.348 | 29.53 | 2.96 | 169701.5 | 53.5 | 2726.6 |
| 13.50 | 912.8 | 324.80 | 22.2 | 0.345 | 29.00 | 3.01 | 168261.8 | 53.3 | 2647.1 |
| 13.75 | 881.0 | 324.36 | 22.2 | 0.340 | 28.10 | 3.11 | 166018.4 | 53.1 | 2554.9 |
| 14.00 | 845.0 | 323.91 | 22.3 | 0.335 | 27.14 | 3.22 | 163748.0 | 52.8 | 2450.5 |
| 14.25 | 804.9 | 323.36 | 22.2 | 0.329 | 25.84 | 3.38 | 161005.5 | 52.3 | 2334.2 |
| 14.50 | 761.0 | 322.91 | 22.2 | 0.325 | 24.68 | 3.54 | 158788.1 | 51.8 | 2206.9 |
| 14.75 | 713.5 | 322.43 | 22.2 | 0.320 | 23.28 | 3.75 | 156448.9 | 51.1 | 2069.2 |
| 15.00 | 662.6 | 321.75 | 22.2 | 0.313 | 21.02 | 4.16 | 153180.6 | 50.3 | 1921.5 |
| 15.25 | 608.8 | 321.29 | 22.1 | 0.309 | 19.25 | 4.54 | 150999.8 | 49.1 | 1765.5 |
| 15.50 | 552.3 | 320.75 | 22.0 | 0.303 | 16.59 | 5.27 | 148470.4 | 47.7 | 1601.7 |
| 15.75 | 493.6 | 320.30 | 22.0 | 0.299 | 13.78 | 6.34 | 146387.6 | 45.9 | 1431.4 |
| 16.00 | 433.0 | 320.08 | 21.9 | 0.297 | 12.06 | 7.25 | 145377.6 | 43.1 | 1255.7 |
| 16.25 | 371.2 | 319.81 | 21.8 | 0.295 | 8.74 | 9.60 | 144145.5 | 39.4 | 1076.5 |
| 16.50 | 308.7 | 319.59 | 21.7 | 0.293 | 4.38 | 17.69 | 143147.5 | 34.2 | 895.2 |
| 16.75 | 246.5 | 319.59 | 21.5 | 0.293 | 4.41 | 14.64 | 143147.5 | 25.7 | 714.9 |
| Average | 726.8 | 322.79 | 19.2 | 0.325 | 21.46 | 5.72 | 158531.1 | 46.9 | 2107.6 |
| Maximum | 1007.0 | 325.93 | 22.3 | 0.359 | 31.04 | 22.33 | 174130.0 | 53.7 | 2920.3 |

| Time of Day | Insolation W/sq.m | System Temp deg K | Ambient Temp deg C | Increased Water Temp deg K | Flow Rate l/m | Time for Stroke s | System Pressure kPa(abs) | Panel Efficiency % |
|---|---|---|---|---|---|---|---|---|
| 7.25 | 274.7 | 322.59 | 12.8 | 0.322 | 3.93 | 8.93 | 157225.7 | 12.9 |
| 7.50 | 337.8 | 322.37 | 13.1 | 0.319 | 3.56 | 16.96 | 156158.4 | 23.5 |
| 7.75 | 400.5 | 322.45 | 13.4 | 0.320 | 5.33 | 13.54 | 156545.8 | 30.4 |
| 8.00 | 462.3 | 322.49 | 13.7 | 0.320 | 6.11 | 12.96 | 156739.9 | 35.4 |
| 8.25 | 522.4 | 322.86 | 14.1 | 0.324 | 11.47 | 7.27 | 158543.2 | 39.0 |
| 8.50 | 580.4 | 323.14 | 14.5 | 0.327 | 14.19 | 6.10 | 159918.5 | 41.8 |
| 8.75 | 635.9 | 323.36 | 14.9 | 0.329 | 15.79 | 5.53 | 161005.5 | 44.1 |
| 9.00 | 688.5 | 323.86 | 15.3 | 0.335 | 18.60 | 4.70 | 163497.2 | 45.7 |
| 9.25 | 737.8 | 324.31 | 15.8 | 0.340 | 20.58 | 4.25 | 165765.0 | 47.1 |
| 9.50 | 783.7 | 324.53 | 16.3 | 0.342 | 21.41 | 4.08 | 166882.4 | 48.4 |
| 9.75 | 825.8 | 325.07 | 16.8 | 0.349 | 23.32 | 3.75 | 169649.9 | 49.3 |
| 10.00 | 864.0 | 325.48 | 17.3 | 0.353 | 24.56 | 3.56 | 171774.6 | 50.0 |
| 10.25 | 897.9 | 325.92 | 17.7 | 0.359 | 25.80 | 3.39 | 174077.4 | 50.6 |
| 10.50 | 927.5 | 326.24 | 18.2 | 0.363 | 26.61 | 3.28 | 175767.0 | 51.2 |
| 10.75 | 952.6 | 326.65 | 18.7 | 0.368 | 27.58 | 3.17 | 177950.2 | 51.6 |
| 11.00 | 973.1 | 326.69 | 19.2 | 0.368 | 27.67 | 3.16 | 178164.3 | 52.1 |
| 11.25 | 988.8 | 326.96 | 19.6 | 0.372 | 28.28 | 3.09 | 179614.7 | 52.4 |
| 11.50 | 999.7 | 327.13 | 20.0 | 0.374 | 28.65 | 3.05 | 180532.6 | 52.7 |
| 11.75 | 1005.8 | 327.36 | 20.4 | 0.377 | 29.14 | 3.00 | 181780.1 | 52.8 |
| 12.00 | 1007.0 | 327.36 | 20.8 | 0.377 | 29.14 | 3.00 | 181780.1 | 53.0 |
| 12.25 | 1003.2 | 327.36 | 21.1 | 0.377 | 29.14 | 3.00 | 181780.1 | 53.1 |
| 12.50 | 994.7 | 327.13 | 21.4 | 0.374 | 28.65 | 3.05 | 180532.6 | 53.2 |
| 12.75 | 981.2 | 327.20 | 21.7 | 0.375 | 28.79 | 3.04 | 180911.5 | 53.1 |
| 13.00 | 963.1 | 326.92 | 21.9 | 0.371 | 28.20 | 3.10 | 179399.3 | 53.0 |
| 13.25 | 940.2 | 326.65 | 22.0 | 0.368 | 27.58 | 3.17 | 177950.2 | 52.9 |
| 13.50 | 912.8 | 326.48 | 22.2 | 0.366 | 27.18 | 3.22 | 177042.5 | 52.6 |
| 13.75 | 881.0 | 325.97 | 22.2 | 0.359 | 25.91 | 3.37 | 174340.6 | 52.3 |
| 14.00 | 845.0 | 325.75 | 22.3 | 0.357 | 25.34 | 3.45 | 173184.9 | 51.9 |
| 14.25 | 804.9 | 325.31 | 22.2 | 0.351 | 24.06 | 3.63 | 170891.1 | 51.4 |
| 14.50 | 761.0 | 324.80 | 22.2 | 0.345 | 22.40 | 3.90 | 168261.8 | 50.8 |
| 14.75 | 713.5 | 324.36 | 22.2 | 0.340 | 20.74 | 4.21 | 166018.4 | 50.0 |
| 15.00 | 662.6 | 323.91 | 22.2 | 0.335 | 18.80 | 4.65 | 163748.0 | 49.0 |
| 15.25 | 608.8 | 323.59 | 22.1 | 0.332 | 17.18 | 5.09 | 162148.0 | 47.6 |
| 15.50 | 552.3 | 323.19 | 22.0 | 0.328 | 14.64 | 5.97 | 160165.0 | 45.9 |
| 15.75 | 493.6 | 322.91 | 22.0 | 0.325 | 12.42 | 7.04 | 158788.1 | 43.7 |
| 16.00 | 433.0 | 322.64 | 21.9 | 0.322 | 9.20 | 9.28 | 157469.0 | 40.8 |
| 16.25 | 371.2 | 322.47 | 21.8 | 0.320 | 6.10 | 13.21 | 156642.8 | 36.6 |
| 16.50 | 308.7 | 322.40 | 21.7 | 0.320 | 4.49 | 16.10 | 156303.6 | 30.5 |
| 16.75 | 246.5 | 322.35 | 21.5 | 0.319 | 3.15 | 17.76 | 156061.6 | 21.3 |
| Average | 726.8 | 324.83 | 19.2 | 0.347 | 19.63 | 5.97 | 168590.0 | 45.5 |
| Maximum | 1007.0 | 327.36 | 22.3 | 0.377 | 29.14 | 17.76 | 181780.1 | 53.2 |

| Time of Day | Insolation W/sq.m | System Temp deg K | Ambient Temp deg C | Increased Water Temp deg K | Flow Rate l/m | Time for Stroke s | System Pressure kPa(abs) | Panel Efficiency % | Heat Input W |
|---|---|---|---|---|---|---|---|---|---|
| 7.25 | 274.7 | 325.63 | 12.8 | 0.355 | 3.28 | 6.17 | 172557.0 | 8.5 | 796.6 |
| 7.50 | 337.8 | 324.97 | 13.1 | 0.348 | 2.46 | 22.06 | 169134.7 | 20.5 | 979.6 |
| 7.75 | 400.5 | 325.05 | 13.4 | 0.348 | 4.45 | 15.30 | 169546.8 | 27.8 | 1161.5 |
| 8.00 | 462.3 | 325.09 | 13.7 | 0.349 | 5.32 | 14.34 | 169753.0 | 33.2 | 1340.7 |
| 8.25 | 522.4 | 325.25 | 14.1 | 0.351 | 8.55 | 9.51 | 170580.2 | 37.2 | 1515.0 |
| 8.50 | 580.4 | 325.48 | 14.5 | 0.354 | 11.66 | 7.27 | 171774.6 | 40.2 | 1683.2 |
| 8.75 | 635.9 | 325.69 | 14.9 | 0.356 | 13.94 | 6.26 | 172870.7 | 42.6 | 1844.1 |
| 9.00 | 688.5 | 325.97 | 15.3 | 0.359 | 15.97 | 5.47 | 174340.6 | 44.5 | 1996.7 |
| 9.25 | 737.8 | 326.25 | 15.8 | 0.363 | 17.65 | 4.95 | 175820.0 | 46.0 | 2139.6 |
| 9.50 | 783.7 | 326.65 | 16.3 | 0.368 | 19.71 | 4.43 | 177950.2 | 47.3 | 2272.7 |
| 9.75 | 825.8 | 326.96 | 16.8 | 0.372 | 21.09 | 4.14 | 179614.7 | 48.3 | 2394.8 |
| 10.00 | 864.0 | 327.37 | 17.3 | 0.377 | 22.65 | 3.86 | 181834.5 | 49.2 | 2505.6 |
| 10.25 | 897.9 | 327.65 | 17.7 | 0.381 | 23.61 | 3.70 | 183362.4 | 49.9 | 2603.9 |
| 10.50 | 927.5 | 327.85 | 18.2 | 0.384 | 24.29 | 3.60 | 184459.9 | 50.5 | 2689.8 |
| 10.75 | 952.6 | 328.13 | 18.7 | 0.388 | 25.13 | 3.48 | 186004.7 | 51.0 | 2762.5 |
| 11.00 | 973.1 | 328.30 | 19.2 | 0.390 | 25.62 | 3.41 | 186947.5 | 51.5 | 2822.0 |
| 11.25 | 988.8 | 328.54 | 19.6 | 0.394 | 26.27 | 3.33 | 188284.7 | 51.8 | 2867.5 |
| 11.50 | 999.7 | 328.81 | 20.0 | 0.398 | 26.99 | 3.24 | 189797.8 | 52.0 | 2899.1 |
| 11.75 | 1005.8 | 328.75 | 20.4 | 0.397 | 26.82 | 3.26 | 189460.7 | 52.3 | 2916.8 |
| 12.00 | 1007.0 | 328.75 | 20.8 | 0.397 | 26.82 | 3.26 | 189460.7 | 52.4 | 2920.3 |
| 12.25 | 1003.2 | 328.75 | 21.1 | 0.397 | 26.82 | 3.26 | 189460.7 | 52.5 | 2909.3 |
| 12.50 | 994.7 | 328.81 | 21.4 | 0.398 | 26.99 | 3.24 | 189797.8 | 52.5 | 2884.6 |
| 12.75 | 981.2 | 328.58 | 21.7 | 0.394 | 26.38 | 3.31 | 188508.3 | 52.5 | 2845.5 |
| 13.00 | 963.1 | 328.53 | 21.9 | 0.394 | 26.27 | 3.33 | 188228.8 | 52.4 | 2793.0 |
| 13.25 | 940.2 | 328.36 | 22.0 | 0.391 | 25.80 | 3.39 | 187281.1 | 52.1 | 2726.6 |
| 13.50 | 912.8 | 328.08 | 22.2 | 0.387 | 25.01 | 3.49 | 185728.1 | 51.9 | 2647.1 |
| 13.75 | 881.0 | 327.81 | 22.2 | 0.384 | 24.16 | 3.62 | 184240.0 | 51.5 | 2554.9 |
| 14.00 | 845.0 | 327.41 | 22.3 | 0.378 | 22.80 | 3.83 | 182052.1 | 51.1 | 2450.5 |
| 14.25 | 804.9 | 327.20 | 22.2 | 0.375 | 22.02 | 3.97 | 180911.5 | 50.4 | 2334.2 |
| 14.50 | 761.0 | 326.69 | 22.2 | 0.369 | 19.90 | 4.39 | 178164.3 | 49.8 | 2206.9 |
| 14.75 | 713.5 | 326.42 | 22.2 | 0.365 | 18.57 | 4.71 | 176722.9 | 48.8 | 2069.2 |
| 15.00 | 662.6 | 326.20 | 22.2 | 0.362 | 17.41 | 5.02 | 175555.1 | 47.6 | 1921.5 |
| 15.25 | 608.8 | 325.92 | 22.1 | 0.359 | 15.69 | 5.57 | 174077.4 | 46.1 | 1765.5 |
| 15.50 | 552.3 | 325.53 | 22.0 | 0.354 | 12.45 | 7.02 | 172035.1 | 44.2 | 1601.7 |
| 15.75 | 493.6 | 325.46 | 22.0 | 0.353 | 11.84 | 7.29 | 171670.4 | 41.7 | 1431.4 |
| 16.00 | 433.0 | 325.29 | 21.9 | 0.351 | 9.44 | 8.74 | 170787.4 | 38.3 | 1255.7 |
| 16.25 | 371.2 | 325.07 | 21.8 | 0.349 | 5.22 | 14.74 | 169649.9 | 33.8 | 1076.5 |
| 16.50 | 308.7 | 325.00 | 21.7 | 0.348 | 3.39 | 19.75 | 169289.2 | 27.2 | 895.2 |
| 16.75 | 246.5 | 324.93 | 21.5 | 0.347 | 1.85 | 25.09 | 168929.0 | 17.1 | 714.9 |
| Average | 726.8 | 326.85 | 19.2 | 0.371 | 17.80 | 6.79 | 179144.7 | 44.1 | 2107.6 |
| Maximum | 1007.0 | 328.81 | 22.3 | 0.398 | 26.99 | 25.09 | 189797.8 | 52.5 | 2920.3 |

| Time of Day | Insolation W/sq.m | System Temp deg K | Ambient Temp deg C | Increased Water Temp deg K | Flow Rate l/m | Time for Stroke s | System Pressure kPa(abs) | Panel Efficiency % |
|---|---|---|---|---|---|---|---|---|
| 7.25 | 274.7 | 328.15 | 12.8 | 0.389 | 0.84 | 5.87 | 186115.4 | 4.9 |
| 7.50 | 337.8 | 327.50 | 13.1 | 0.379 | 0.00 | 0.00 | 182542.7 | 17.5 |
| 7.75 | 400.5 | 327.48 | 13.4 | 0.379 | 1.51 | 42.49 | 182433.6 | 25.4 |
| 8.00 | 462.3 | 327.56 | 13.7 | 0.380 | 5.33 | 13.73 | 182870.2 | 31.1 |
| 8.25 | 522.4 | 327.60 | 14.1 | 0.381 | 6.04 | 13.09 | 183088.9 | 35.4 |
| 8.50 | 580.4 | 327.81 | 14.5 | 0.384 | 9.97 | 8.32 | 184240.0 | 38.6 |
| 8.75 | 635.9 | 328.07 | 14.9 | 0.387 | 13.20 | 6.49 | 185672.8 | 41.1 |
| 9.00 | 688.5 | 328.13 | 15.3 | 0.388 | 13.86 | 6.31 | 186004.7 | 43.2 |
| 9.25 | 737.8 | 328.53 | 15.8 | 0.394 | 16.85 | 5.19 | 188228.8 | 44.8 |
| 9.50 | 783.7 | 328.58 | 16.3 | 0.395 | 17.12 | 5.10 | 188508.3 | 46.3 |
| 9.75 | 825.8 | 328.98 | 16.8 | 0.400 | 19.38 | 4.51 | 190755.2 | 47.4 |
| 10.00 | 864.0 | 329.25 | 17.3 | 0.405 | 20.69 | 4.22 | 192283.5 | 48.3 |
| 10.25 | 897.9 | 329.52 | 17.7 | 0.409 | 21.87 | 4.00 | 193821.1 | 49.0 |
| 10.50 | 927.5 | 329.70 | 18.2 | 0.411 | 22.54 | 3.88 | 194851.4 | 49.7 |
| 10.75 | 952.6 | 329.97 | 18.7 | 0.416 | 23.55 | 3.71 | 196404.7 | 50.3 |
| 11.00 | 973.1 | 330.01 | 19.2 | 0.416 | 23.70 | 3.69 | 196635.6 | 50.8 |
| 11.25 | 988.8 | 330.25 | 19.6 | 0.420 | 24.49 | 3.57 | 198025.5 | 51.1 |
| 11.50 | 999.7 | 330.18 | 20.0 | 0.419 | 24.28 | 3.60 | 197619.4 | 51.4 |
| 11.75 | 1005.8 | 330.42 | 20.4 | 0.423 | 25.03 | 3.49 | 199014.6 | 51.6 |
| 12.00 | 1007.0 | 330.42 | 20.8 | 0.423 | 25.03 | 3.49 | 199014.6 | 51.8 |
| 12.25 | 1003.2 | 330.42 | 21.1 | 0.423 | 25.03 | 3.49 | 199014.6 | 51.8 |
| 12.50 | 994.7 | 330.42 | 21.4 | 0.423 | 25.03 | 3.49 | 199014.6 | 51.8 |
| 12.75 | 981.2 | 330.18 | 21.7 | 0.419 | 24.28 | 3.60 | 197619.4 | 51.9 |
| 13.00 | 963.1 | 330.02 | 21.9 | 0.416 | 23.70 | 3.69 | 196693.4 | 51.7 |
| 13.25 | 940.2 | 329.98 | 22.0 | 0.416 | 23.56 | 3.71 | 196462.4 | 51.4 |
| 13.50 | 912.8 | 329.74 | 22.2 | 0.412 | 22.70 | 3.85 | 195080.9 | 51.2 |
| 13.75 | 881.0 | 329.46 | 22.2 | 0.408 | 21.61 | 4.04 | 193478.6 | 50.8 |
| 14.00 | 845.0 | 329.29 | 22.3 | 0.405 | 20.88 | 4.19 | 192510.7 | 50.2 |
| 14.25 | 804.9 | 329.02 | 22.2 | 0.401 | 19.59 | 4.46 | 190981.1 | 49.5 |
| 14.50 | 761.0 | 328.75 | 22.2 | 0.397 | 18.13 | 4.82 | 189460.7 | 48.7 |
| 14.75 | 713.5 | 328.53 | 22.2 | 0.394 | 16.86 | 5.18 | 188228.8 | 47.7 |
| 15.00 | 662.6 | 328.36 | 22.2 | 0.391 | 15.70 | 5.57 | 187281.1 | 46.3 |
| 15.25 | 608.8 | 328.08 | 22.1 | 0.388 | 13.48 | 6.48 | 185728.1 | 44.7 |
| 15.50 | 552.3 | 327.86 | 22.0 | 0.384 | 11.03 | 7.92 | 184514.9 | 42.6 |
| 15.75 | 493.6 | 327.80 | 22.0 | 0.384 | 10.08 | 8.36 | 184185.0 | 39.8 |
| 16.00 | 433.0 | 327.58 | 21.9 | 0.381 | 5.99 | 13.37 | 182979.5 | 36.2 |
| 16.25 | 371.2 | 327.59 | 21.8 | 0.381 | 6.31 | 11.58 | 183034.2 | 31.1 |
| 16.50 | 308.7 | 327.45 | 21.7 | 0.379 | 1.12 | 55.06 | 182270.0 | 24.0 |
| 16.75 | 246.5 | 327.68 | 21.5 | 0.382 | 3.87 | 8.77 | 183526.7 | 12.7 |
| Average | 726.8 | 328.88 | 19.2 | 0.400 | 16.00 | 7.86 | 190261.4 | 42.7 |
| Maximum | 1007.0 | 330.42 | 22.3 | 0.423 | 25.03 | 55.06 | 199014.6 | 51.9 |

| Time of Day | Insolation W/sq.m | System Temp deg K | Ambient Temp deg C | Increased Water Temp deg K | Flow Rate l/m | Time for Stroke s | System Pressure kPa(abs) | Panel Efficiency % | Heat Input W |
|---|---|---|---|---|---|---|---|---|---|
| 7.25 | 274.7 | 330.74 | 12.8 | 0.429 | 0.00 | 0.00 | 200886.5 | 1.1 | 796.6 |
| 7.50 | 337.8 | 329.84 | 13.1 | 0.414 | 2.99 | 13.36 | 195655.6 | 14.7 | 979.6 |
| 7.75 | 400.5 | 329.81 | 13.4 | 0.414 | 1.07 | 56.13 | 195483.1 | 23.1 | 1161.5 |
| 8.00 | 462.3 | 329.92 | 13.7 | 0.415 | 5.79 | 12.09 | 196116.3 | 29.0 | 1340.7 |
| 8.25 | 522.4 | 329.96 | 14.1 | 0.416 | 6.57 | 11.66 | 196347.0 | 33.6 | 1515.0 |
| 8.50 | 580.4 | 330.02 | 14.5 | 0.417 | 7.82 | 10.38 | 196693.4 | 37.1 | 1683.2 |
| 8.75 | 635.9 | 330.23 | 14.9 | 0.420 | 11.32 | 7.44 | 197909.4 | 39.8 | 1844.1 |
| 9.00 | 688.5 | 330.41 | 15.3 | 0.423 | 13.42 | 6.45 | 198956.3 | 41.9 | 1996.7 |
| 9.25 | 737.8 | 330.46 | 15.8 | 0.424 | 13.95 | 6.26 | 199247.8 | 43.8 | 2139.6 |
| 9.50 | 783.7 | 330.63 | 16.3 | 0.427 | 15.39 | 5.68 | 200241.5 | 45.3 | 2272.7 |
| 9.75 | 825.8 | 330.90 | 16.8 | 0.431 | 17.32 | 5.04 | 201827.5 | 46.4 | 2394.8 |
| 10.00 | 864.0 | 331.14 | 17.3 | 0.435 | 18.74 | 4.66 | 203245.4 | 47.4 | 2505.6 |
| 10.25 | 897.9 | 331.19 | 17.7 | 0.436 | 18.97 | 4.61 | 203541.7 | 48.3 | 2603.9 |
| 10.50 | 927.5 | 331.35 | 18.2 | 0.439 | 19.87 | 4.40 | 204492.2 | 49.0 | 2689.8 |
| 10.75 | 952.6 | 331.62 | 18.7 | 0.444 | 21.19 | 4.12 | 206103.9 | 49.6 | 2762.5 |
| 11.00 | 973.1 | 331.85 | 19.2 | 0.448 | 22.20 | 3.94 | 207484.4 | 50.0 | 2822.0 |
| 11.25 | 988.8 | 331.86 | 19.6 | 0.448 | 22.20 | 3.94 | 207544.6 | 50.4 | 2867.5 |
| 11.50 | 999.7 | 331.90 | 20.0 | 0.449 | 22.37 | 3.91 | 207785.4 | 50.8 | 2899.1 |
| 11.75 | 1005.8 | 331.91 | 20.4 | 0.449 | 22.37 | 3.91 | 207845.7 | 51.0 | 2916.8 |
| 12.00 | 1007.0 | 332.14 | 20.8 | 0.453 | 23.29 | 3.75 | 209235.1 | 51.1 | 2920.3 |
| 12.25 | 1003.2 | 332.14 | 21.1 | 0.453 | 23.29 | 3.75 | 209235.1 | 51.2 | 2909.3 |
| 12.50 | 994.7 | 331.91 | 21.4 | 0.449 | 22.37 | 3.91 | 207845.7 | 51.2 | 2884.6 |
| 12.75 | 981.2 | 331.90 | 21.7 | 0.449 | 22.37 | 3.91 | 207785.4 | 51.2 | 2845.5 |
| 13.00 | 963.1 | 331.86 | 21.9 | 0.448 | 22.20 | 3.94 | 207544.6 | 51.0 | 2793.0 |
| 13.25 | 940.2 | 331.63 | 22.0 | 0.444 | 21.19 | 4.12 | 206163.7 | 50.7 | 2726.6 |
| 13.50 | 912.8 | 331.58 | 22.2 | 0.443 | 21.00 | 4.16 | 205864.5 | 50.4 | 2647.1 |
| 13.75 | 881.0 | 331.41 | 22.2 | 0.440 | 20.19 | 4.33 | 204849.5 | 49.9 | 2554.9 |
| 14.00 | 845.0 | 331.18 | 22.3 | 0.436 | 18.97 | 4.61 | 203482.4 | 49.4 | 2450.5 |
| 14.25 | 804.9 | 330.91 | 22.2 | 0.431 | 17.33 | 5.04 | 201886.5 | 48.6 | 2334.2 |
| 14.50 | 761.0 | 330.86 | 22.2 | 0.431 | 17.05 | 5.12 | 201592.0 | 47.6 | 2206.9 |
| 14.75 | 713.5 | 330.69 | 22.2 | 0.428 | 15.85 | 5.51 | 200593.1 | 46.5 | 2069.2 |
| 15.00 | 662.6 | 330.41 | 22.2 | 0.423 | 13.56 | 6.44 | 198956.3 | 45.1 | 1921.5 |
| 15.25 | 608.8 | 330.19 | 22.1 | 0.420 | 11.02 | 7.93 | 197677.3 | 43.3 | 1765.5 |
| 15.50 | 552.3 | 330.03 | 22.0 | 0.417 | 8.34 | 10.27 | 196751.2 | 41.0 | 1601.7 |
| 15.75 | 493.6 | 330.00 | 22.0 | 0.417 | 7.84 | 10.49 | 196577.9 | 38.0 | 1431.4 |
| 16.00 | 433.0 | 329.94 | 21.9 | 0.416 | 6.51 | 11.86 | 196231.7 | 34.0 | 1255.7 |
| 16.25 | 371.2 | 329.84 | 21.8 | 0.414 | 1.64 | 42.43 | 195655.6 | 28.7 | 1076.5 |
| 16.50 | 308.7 | 329.78 | 21.7 | 0.413 | 0.67 | 83.39 | 195310.7 | 21.0 | 895.2 |
| 16.75 | 246.5 | 330.27 | 21.5 | 0.421 | 2.95 | 6.66 | 198141.7 | 8.5 | 714.9 |
| Average | 726.8 | 330.88 | 19.2 | 0.431 | 14.39 | 10.25 | 201763.8 | 41.3 | 2107.6 |
| Maximum | 1007.0 | 332.14 | 22.3 | 0.453 | 23.29 | 83.39 | 209235.1 | 51.2 | 2920.3 |

| Time of Day | Insolation W/sq.m | System Temp deg K | Ambient Temp deg C | Increased Water Temp deg K | Flow Rate l/m | Time for Stroke s | System Pressure kPa(abs) | Panel Efficiency % |
|---|---|---|---|---|---|---|---|---|
| 7.25 | 274.7 | 333.55 | 12.8 | 0.490 | 0.00 | 0.00 | 217908.4 | -2.9 |
| 7.50 | 337.8 | 332.18 | 13.1 | 0.455 | 3.37 | 9.37 | 209477.5 | 12.0 |
| 7.75 | 400.5 | 332.03 | 13.4 | 0.452 | 2.94 | 18.73 | 208569.7 | 20.9 |
| 8.00 | 462.3 | 332.07 | 13.7 | 0.453 | 2.69 | 24.90 | 208811.5 | 27.2 |
| 8.25 | 522.4 | 332.12 | 14.1 | 0.453 | 3.58 | 20.78 | 209114.0 | 32.0 |
| 8.50 | 580.4 | 332.27 | 14.5 | 0.456 | 8.47 | 9.35 | 210023.6 | 35.5 |
| 8.75 | 635.9 | 332.30 | 14.9 | 0.457 | 8.99 | 9.20 | 210205.8 | 38.5 |
| 9.00 | 688.5 | 332.36 | 15.3 | 0.458 | 9.97 | 8.57 | 210570.7 | 40.8 |
| 9.25 | 737.8 | 332.52 | 15.8 | 0.461 | 12.37 | 7.06 | 211546.2 | 42.7 |
| 9.50 | 783.7 | 332.74 | 16.3 | 0.465 | 14.69 | 5.95 | 212893.0 | 44.2 |
| 9.75 | 825.8 | 332.79 | 16.8 | 0.466 | 15.06 | 5.80 | 213200.1 | 45.5 |
| 10.00 | 864.0 | 333.00 | 17.3 | 0.484 | 16.74 | 5.22 | 214493.2 | 46.6 |
| 10.25 | 897.9 | 333.05 | 17.7 | 0.484 | 17.04 | 5.13 | 214802.0 | 47.5 |
| 10.50 | 927.5 | 333.28 | 18.2 | 0.487 | 18.56 | 4.71 | 216226.7 | 48.2 |
| 10.75 | 952.6 | 333.23 | 18.7 | 0.486 | 18.18 | 4.81 | 215916.4 | 48.9 |
| 11.00 | 973.1 | 333.45 | 19.2 | 0.489 | 19.56 | 4.47 | 217284.4 | 49.4 |
| 11.25 | 988.8 | 333.50 | 19.6 | 0.489 | 19.78 | 4.42 | 217596.2 | 49.8 |
| 11.50 | 999.7 | 333.50 | 20.0 | 0.489 | 19.79 | 4.42 | 217596.2 | 50.1 |
| 11.75 | 1005.8 | 333.73 | 20.4 | 0.492 | 20.98 | 4.16 | 219035.0 | 50.3 |
| 12.00 | 1007.0 | 333.73 | 20.8 | 0.492 | 20.98 | 4.16 | 219035.0 | 50.5 |
| 12.25 | 1003.2 | 333.73 | 21.1 | 0.492 | 20.98 | 4.16 | 219035.0 | 50.5 |
| 12.50 | 994.7 | 333.50 | 21.4 | 0.489 | 19.79 | 4.42 | 217596.2 | 50.6 |
| 12.75 | 981.2 | 333.50 | 21.7 | 0.489 | 19.78 | 4.42 | 217596.2 | 50.5 |
| 13.00 | 963.1 | 333.50 | 21.9 | 0.489 | 19.78 | 4.42 | 217596.2 | 50.3 |
| 13.25 | 940.2 | 333.45 | 22.0 | 0.489 | 19.55 | 4.47 | 217284.4 | 50.0 |
| 13.50 | 912.8 | 333.22 | 22.2 | 0.486 | 18.18 | 4.81 | 215854.3 | 49.7 |
| 13.75 | 881.0 | 333.05 | 22.2 | 0.484 | 17.05 | 5.12 | 214802.0 | 49.2 |
| 14.00 | 845.0 | 333.00 | 22.3 | 0.484 | 16.75 | 5.22 | 214493.2 | 48.5 |
| 14.25 | 804.9 | 332.79 | 22.2 | 0.466 | 15.08 | 5.80 | 213200.1 | 47.7 |
| 14.50 | 761.0 | 332.74 | 22.2 | 0.465 | 14.71 | 5.94 | 212893.0 | 46.6 |
| 14.75 | 713.5 | 332.52 | 22.2 | 0.461 | 12.41 | 7.04 | 211546.2 | 45.4 |
| 15.00 | 662.6 | 332.56 | 22.2 | 0.462 | 13.03 | 6.71 | 211790.6 | 43.8 |
| 15.25 | 608.8 | 332.34 | 22.1 | 0.457 | 10.05 | 8.61 | 210449.0 | 41.9 |
| 15.50 | 552.3 | 332.28 | 22.0 | 0.456 | 9.04 | 9.27 | 210084.3 | 39.4 |
| 15.75 | 493.6 | 332.14 | 22.0 | 0.454 | 4.12 | 19.47 | 209235.1 | 36.3 |
| 16.00 | 433.0 | 332.10 | 21.9 | 0.453 | 3.33 | 22.37 | 208993.0 | 32.1 |
| 16.25 | 371.2 | 332.06 | 21.8 | 0.452 | 3.78 | 17.30 | 208751.0 | 26.3 |
| 16.50 | 308.7 | 331.98 | 21.7 | 0.451 | 0.84 | 57.81 | 208267.8 | 18.2 |
| 16.75 | 246.5 | 332.62 | 21.5 | 0.463 | 0.59 | 5.98 | 212157.6 | 4.7 |
| Average | 726.8 | 332.83 | 19.2 | 0.472 | 12.63 | 9.35 | 213485.4 | 40.0 |
| Maximum | 1007.0 | 333.73 | 22.3 | 0.492 | 20.98 | 57.81 | 219035.0 | 50.6 |

| Time of Day | Insolation W/sq.m | System Temp deg K | Ambient Temp deg C | Increased Water Temp deg K | Flow Rate l/m | Time for Stroke s | System Pressure kPa(abs) | Panel Efficiency % | Heat Input W |
|---|---|---|---|---|---|---|---|---|---|
| 7.25 | 274.7 | 312.17 | 12.8 | 0.277 | 4.06 | 34.38 | 112501.6 | 28.0 | 796.6 |
| 7.50 | 337.8 | 312.28 | 13.1 | 0.277 | 14.27 | 9.78 | 112915.0 | 35.4 | 979.6 |
| 7.75 | 400.5 | 312.51 | 13.4 | 0.279 | 22.98 | 6.07 | 113783.1 | 40.3 | 1161.5 |
| 8.00 | 462.3 | 312.56 | 13.7 | 0.280 | 13.15 | 5.72 | 113972.5 | 44.0 | 1340.7 |
| 8.25 | 522.4 | 312.74 | 14.1 | 0.281 | 15.56 | 4.84 | 114656.4 | 46.7 | 1515.0 |
| 8.50 | 580.4 | 313.01 | 14.5 | 0.283 | 18.77 | 4.01 | 115688.2 | 48.8 | 1683.2 |
| 8.75 | 635.9 | 313.29 | 14.9 | 0.285 | 21.50 | 3.50 | 116765.8 | 50.4 | 1844.1 |
| 9.00 | 688.5 | 313.69 | 15.3 | 0.288 | 24.96 | 3.02 | 118318.9 | 51.6 | 1996.7 |
| 9.25 | 737.8 | 314.01 | 15.8 | 0.290 | 27.36 | 2.75 | 119572.8 | 52.7 | 2139.6 |
| 9.50 | 783.7 | 314.41 | 16.3 | 0.294 | 30.15 | 2.50 | 121154.8 | 53.5 | 2272.7 |
| 9.75 | 825.8 | 314.69 | 16.8 | 0.296 | 31.91 | 2.36 | 122271.8 | 54.3 | 2394.8 |
| 10.00 | 864.0 | 314.90 | 17.3 | 0.298 | 33.19 | 2.27 | 123114.8 | 54.9 | 2505.6 |
| 10.25 | 897.9 | 315.18 | 17.7 | 0.300 | 34.80 | 2.16 | 124245.9 | 55.4 | 2603.9 |
| 10.50 | 927.5 | 315.35 | 18.2 | 0.301 | 35.76 | 2.10 | 124936.5 | 55.9 | 2689.8 |
| 10.75 | 952.6 | 315.62 | 18.7 | 0.304 | 37.25 | 2.02 | 126039.5 | 56.3 | 2762.5 |
| 11.00 | 973.1 | 315.86 | 19.2 | 0.306 | 38.49 | 1.96 | 127026.3 | 56.6 | 2822.0 |
| 11.25 | 988.8 | 316.03 | 19.6 | 0.307 | 39.35 | 1.91 | 127728.9 | 56.8 | 2867.5 |
| 11.50 | 999.7 | 316.03 | 20.0 | 0.307 | 39.36 | 1.91 | 127728.9 | 57.1 | 2899.1 |
| 11.75 | 1005.8 | 316.07 | 20.4 | 0.307 | 39.56 | 1.90 | 127894.6 | 57.3 | 2916.8 |
| 12.00 | 1007.0 | 316.07 | 20.8 | 0.307 | 39.56 | 1.90 | 127894.6 | 57.4 | 2920.3 |
| 12.25 | 1003.2 | 316.07 | 21.1 | 0.307 | 39.56 | 1.90 | 127894.6 | 57.5 | 2909.3 |
| 12.50 | 994.7 | 316.03 | 21.4 | 0.307 | 39.36 | 1.91 | 127728.9 | 57.6 | 2884.6 |
| 12.75 | 981.2 | 316.03 | 21.7 | 0.307 | 39.36 | 1.91 | 127728.9 | 57.6 | 2845.5 |
| 13.00 | 963.1 | 315.79 | 21.9 | 0.305 | 38.15 | 1.97 | 126737.8 | 57.6 | 2793.0 |
| 13.25 | 940.2 | 315.62 | 22.0 | 0.304 | 37.26 | 2.02 | 126039.5 | 57.5 | 2726.6 |
| 13.50 | 912.8 | 315.58 | 22.2 | 0.303 | 37.04 | 2.03 | 125875.6 | 57.4 | 2647.1 |
| 13.75 | 881.0 | 315.18 | 22.2 | 0.300 | 34.81 | 2.16 | 124245.9 | 57.2 | 2554.9 |
| 14.00 | 845.0 | 315.13 | 22.3 | 0.300 | 34.57 | 2.18 | 124043.3 | 56.9 | 2450.5 |
| 14.25 | 804.9 | 314.86 | 22.2 | 0.297 | 32.95 | 2.28 | 122953.9 | 56.5 | 2334.2 |
| 14.50 | 761.0 | 314.45 | | | | | | | |

# Appendix 5
# Engineering Drawings

## Key to Drawing Numbers

## 1/ Prototype Pump / Prime Mover Body

STWP 2001 - Body Assembly

STWP 2002 - Water and Vapour Chamber Housings

STWP 2003 - Centre Dividing Plate

STWP 2004 - Water Chamber Cover Plates

STWP 2005 - Displacer Plates

STWP 2006 - Displacer Core

STWP 2007 - Feed Pump Housing and Water Ports

## 2/ Spool Valve

STWP 1001 - Spool Valve Assembly

STWP 1002 - Spool Housing

STWP 1003 - Spool Housing End Caps

STWP 1004 - Spool Housing Components

STWP 1005 - Spool Valve and Sleeve

STWP 1006 - Detent and Components

For the purposes of presentation, the following drawings are not to scale.

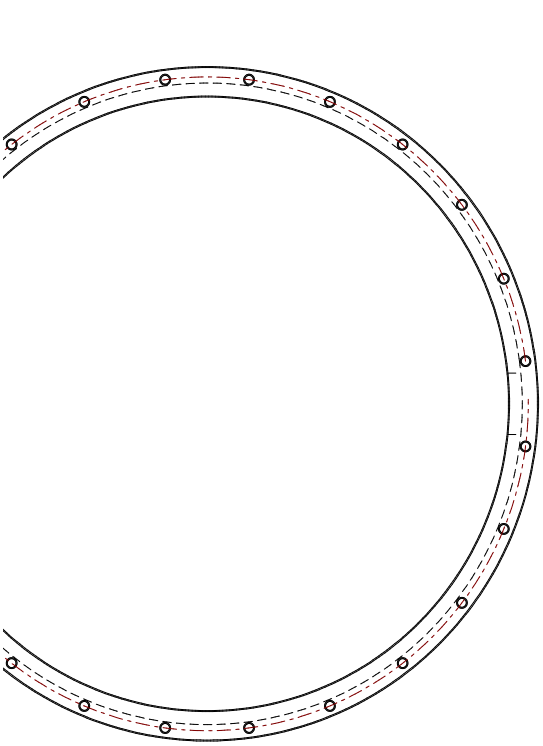

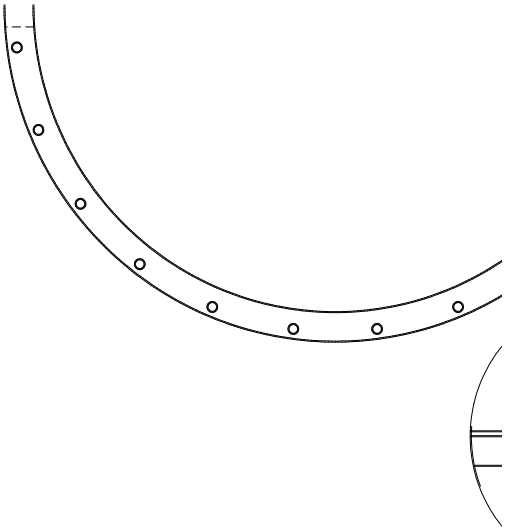

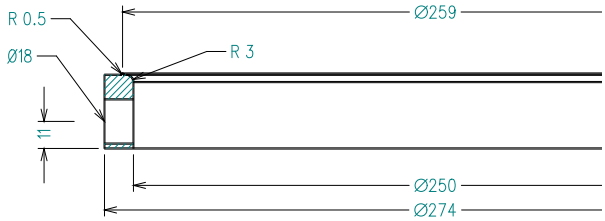


ITEM 15

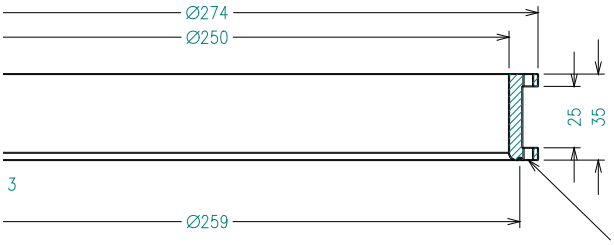


ITEM 11

| ITEM | DESCRIPTION |
|---|---|
| 15 | VAPOUR CHAMBER H |
| 11 | WATER CHAMBER HO |

SOLAR THERMAL WATER PUMP

PUMP CHAMBER HOUSINGS

SCHOOL
MECHANICAL E

SCALES : 1:2 ALL DIMENSIONS IN mm

CHKD : DRI

DATE :

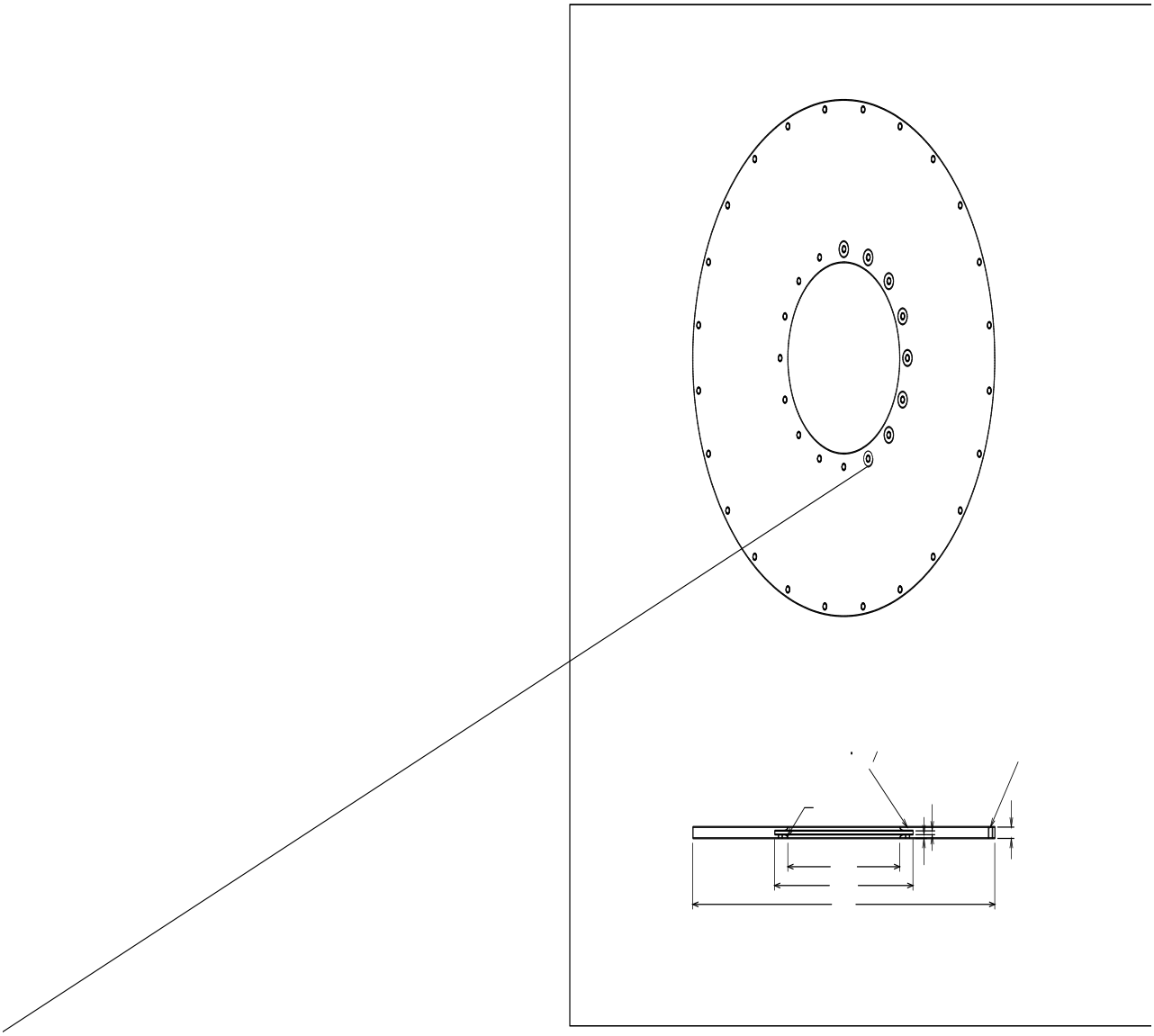

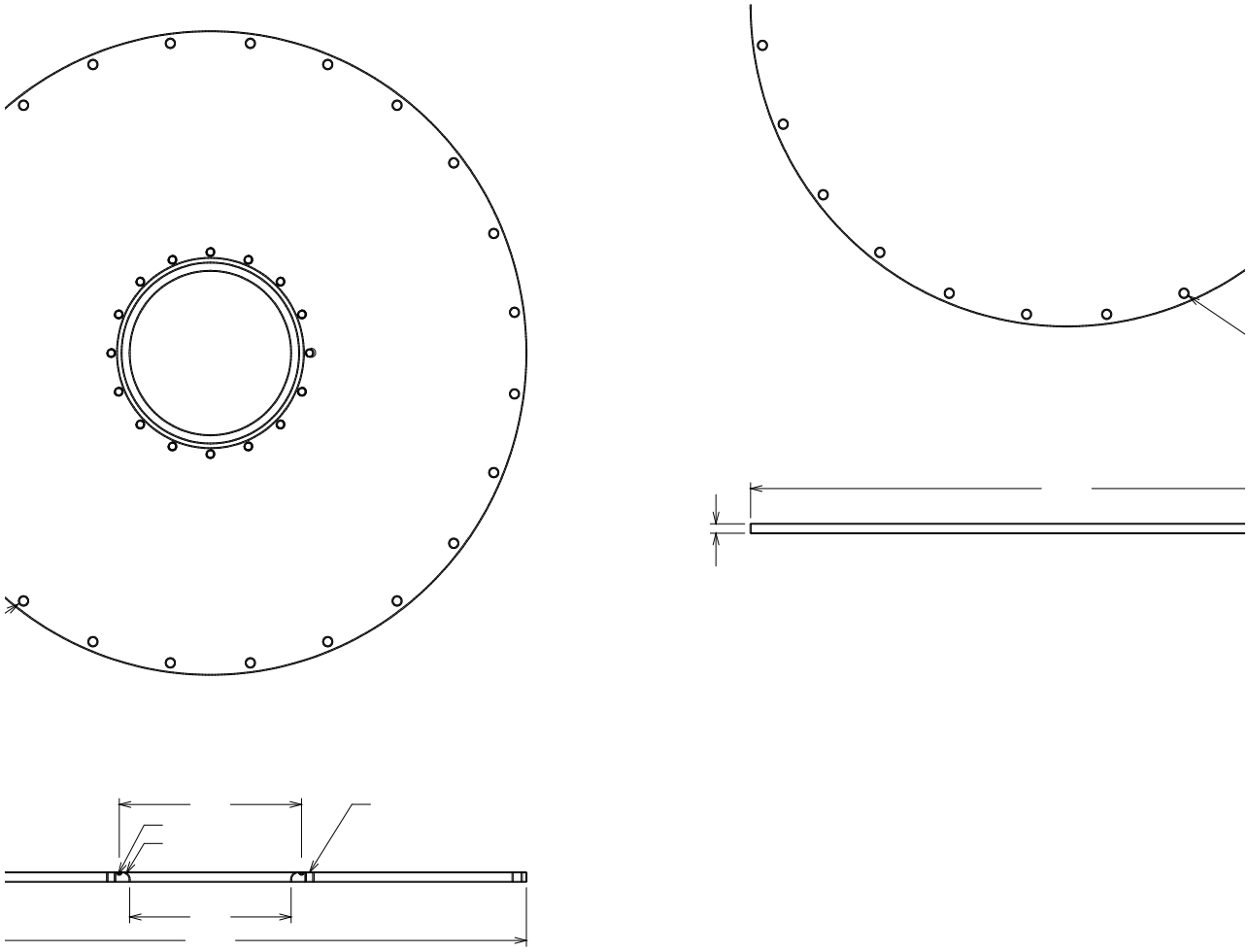

| ITEM | DESCRIPTION |
|---|---|
| SOLAR THERMAL WATER PUMP | SCHOOL MECHANICAL E. |
| | CHKD : DRN |
| SCALES : 1:2 ALL DIMENSIONS IN mm | DATE : |

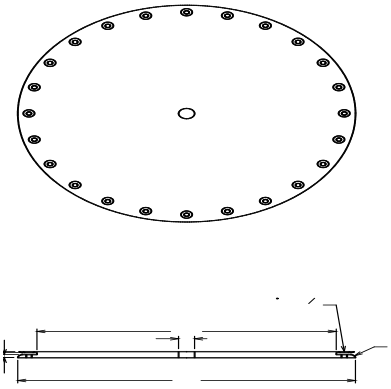

ITEM 7

| ITEM | DESCRIPTION | MATL | REQD |
|---|---|---|---|
| 7 | MAIN DISPLACER PLATE | | 2 |

SOLAR THERMAL WATER PUMP
MAIN DISPLACER PLATES

SCHOOL OF ENGINEERING
MECHANICAL ENGINEERING DEPARTMENT

SCALES : 1:2 ALL DIMENSIONS IN mm

CHKD : DRN : DRF DRG No : STWP 2005

DATE :

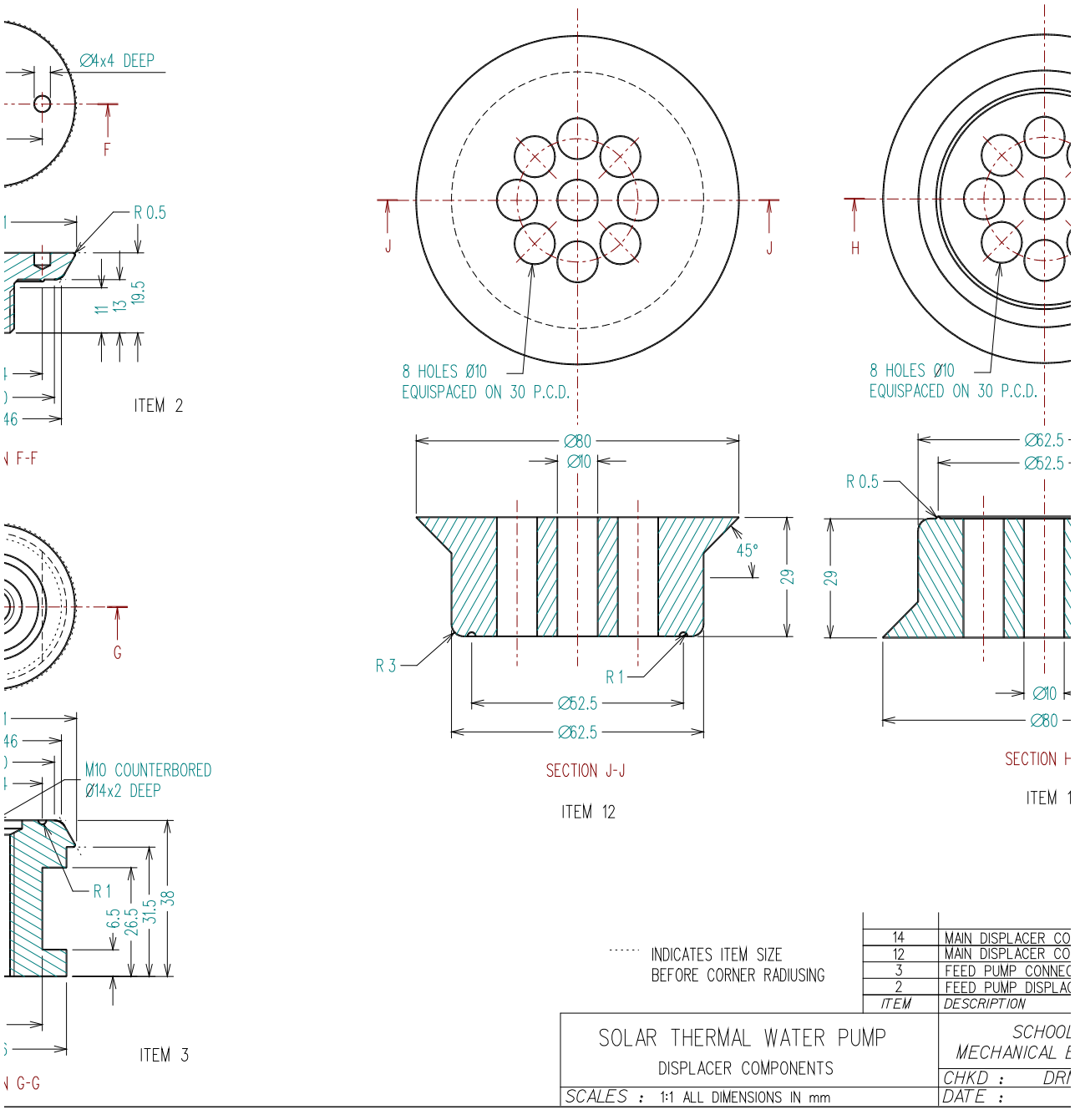
Ø4x4 DEEP
F
R 0.5
11
13
19.5
46
ITEM 2
F-F
G
M10 COUNTERBORED
Ø14x2 DEEP
R 1
6.5
26.5
31.5
38
ITEM 3
G-G
J
J
8 HOLES Ø10
EQUISPACED ON 30 P.C.D.
Ø80
Ø10
45°
29
R 3
R 1
Ø52.5
Ø62.5
SECTION J-J
ITEM 12
H
8 HOLES Ø10
EQUISPACED ON 30 P.C.D.
Ø62.5
Ø62.5
R 0.5
29
Ø10
Ø80
SECTION H
ITEM 1
INDICATES ITEM SIZE
BEFORE CORNER RADIUSING
14 MAIN DISPLACER CO
12 MAIN DISPLACER CO
3 FEED PUMP CONNEC
2 FEED PUMP DISPLAC
ITEM DESCRIPTION
SOLAR THERMAL WATER PUMP
DISPLACER COMPONENTS
SCALES : 1:1 ALL DIMENSIONS IN mm
SCHOOL
MECHANICAL E
CHKD : DRI
DATE :

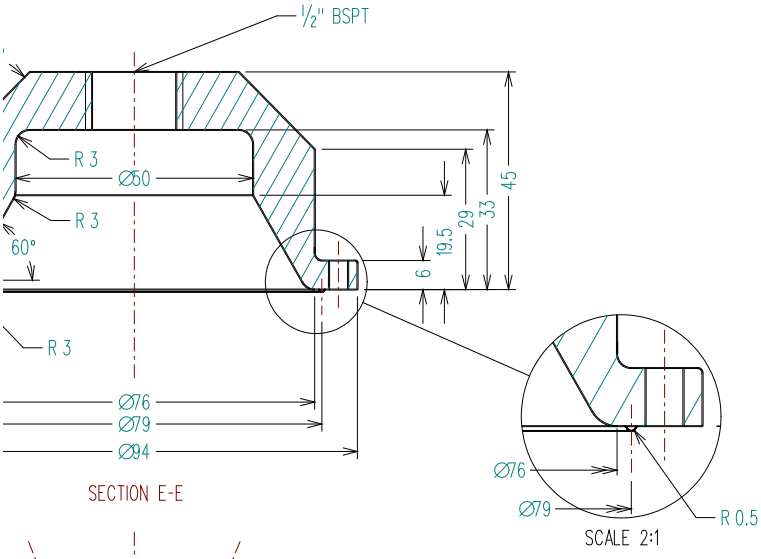


SECTION E-E

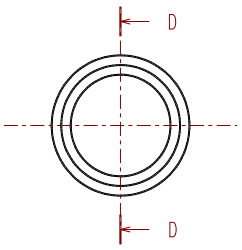


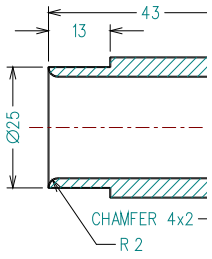


SECTION I

ITEM 19

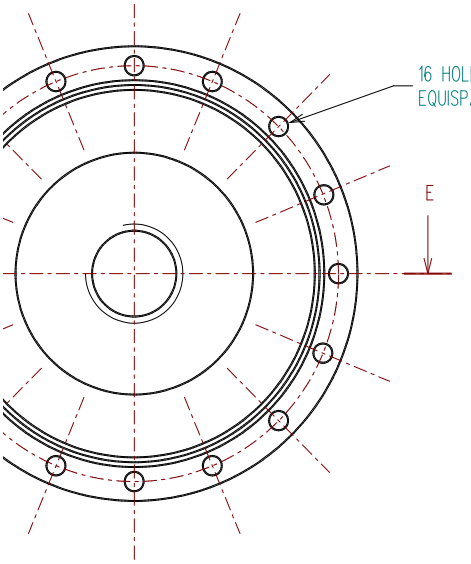


ITEM 1

| ITEM | DESCRIPTION |
|---|---|
| 19 | WATER INLET / DISC |
| 1 | FEED PUMP HOUSING |

SOLAR THERMAL WATER PUMP

WATER CHAMBER COVER PLATES

SCALES : 1:1 ALL DIMENSIONS IN mm

SCHOOL MECHANICAL E.

CHKD : DRN

DATE :

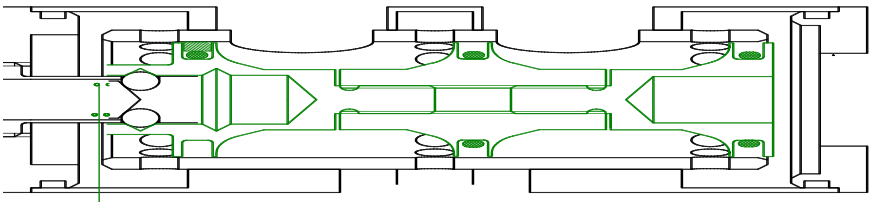

| ITEM | DESCRIPTION |
|---|---|
| 24 | END CAP SCREWS (M4x 10 CAP SCREWS) |
| 23 | VAPOUR CHAMBER PORT SEAL (O-RING 15x1.5 |
| 22 | VALVE ACTUATING LEVERS |
| 21 | END CAP SEAL (O-RING 34x2 N70) |
| 13A | DETENT |
| 12 | SPOOL SEAL (OMNIRING 65544-X0250 CARBOI |
| 9A | SPOOL |
| 8 | SPOOL VALVE SLEEVE |
| 6A | END CAP AND EXHAUST PORT |
| 5 | END CAP (DETENT END) |
| 3 | INLET MANIFOLD |
| 2 | VAPOUR CHAMBER PORTS |
| 1A | SPOOL VALVE HOUSING |

ALL COMPONENTS TO BE 304L STAINLESS STEEL UNLESS SPECIFIED

SOLAR THERMAL WATER PUMP ASSEMBLY

SCALES : 2:1 ALL DIMENSIONS IN mm

SCHOOL MECHANICAL E.

CHKD : DRN

DATE :

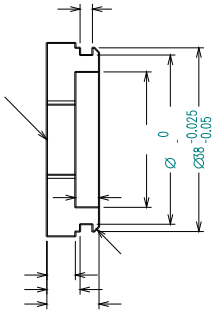


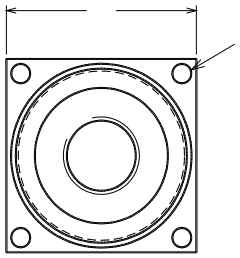

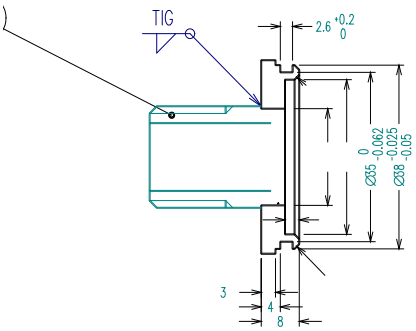


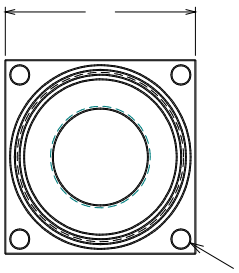

ALL COMPONENTS TO BE
304L STAINLESS STEEL

| ITEM | DESCRIPTION |
|---|---|
| 7 | EXHAUST MANIFOLD ( |
| 6 | SPOOL VALVE END C |
| 5 | SPOOL VALVE END C |

3.2 OR BETTER UNLESS OTHERWISE SPECIFIED

SOLAR THERMAL WATER PUMP
SPOOL VALVE HOUSING END CAPS

SCALES : 1:1 ALL DIMENSIONS IN mm

SCHOOL
MECHANICAL E.
CHKD : DRN
DATE :

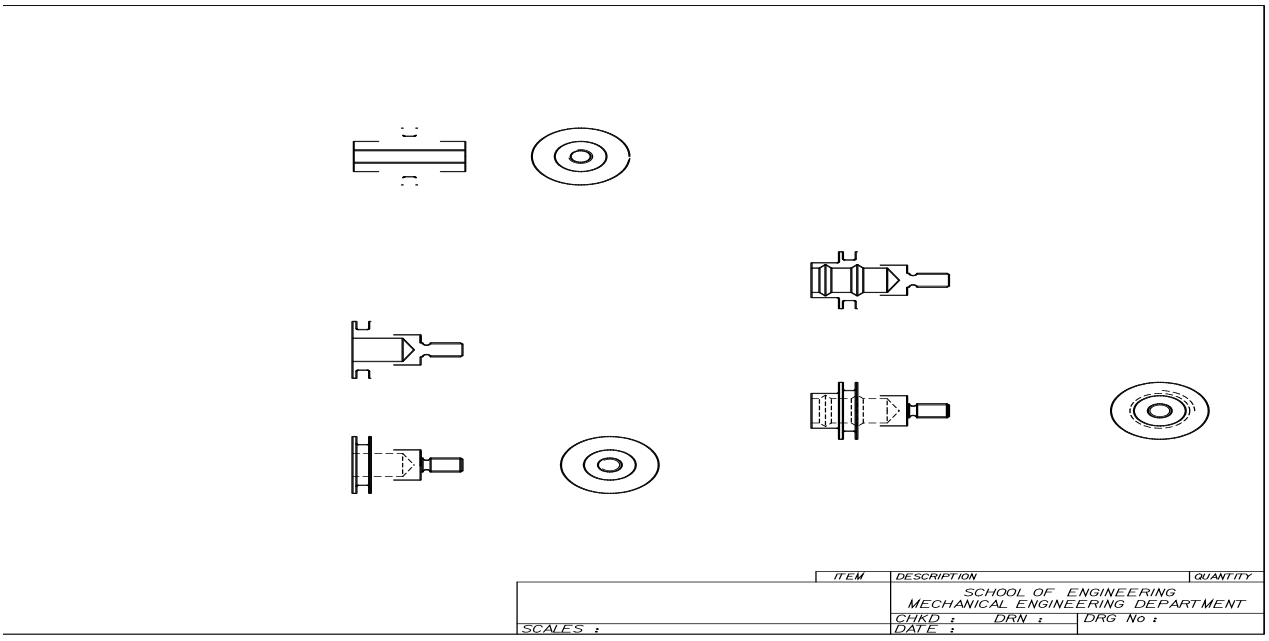
ITEM
DESCRIPTION
QUANTITY
SCHOOL OF ENGINEERING
MECHANICAL ENGINEERING DEPARTMENT
CHKD :
DRN :
DRG No :
SCALES :
DATE :

# Appendix 6

# Pump Assembly/Disassembly Procedure

## To Dismantle the Pump Body:

1- Remove pipework from the water manifolds (intake side and discharge side).

2- Remove the water manifolds from the one way valves. The valves may be removed from the water chamber if required.

3- Remove the vapour feed pipe from the spool valve.

4- Remove the vapour exhaust pipe from the spool valve.

5- Remove the spool valve mounting brackets connecting the spool valve to the pump body (6xM4 cap screws, 4xM4 domed nuts).

6- Pull the spool valve out from the pump body.

7 - Remove the feed pump housing from the top water chamber to expose the feed pump diaphragm (16xM4 cap screws).

8- Remove the feed pump diaphragm (optional).

9- Remove the upper water chamber (24xM4 domed nuts). Slide off threaded studs.

10- Remove the lower water chamber (24xM4 domed nuts). Slide off threaded studs.

11- Remove central displacer bolt (M10 feed pump piston serves as nut).

12- Remove upper displacer and diaphragm subassembly. The diaphragm may be removed from the displacer disc (24xM4 CSK screws) if required.

13- Remove upper central displacer core.

14- Remove lower displacer and diaphragm subassembly.

15- Remove lower central displacer core.

16- Central diaphragm may be removed from the central vapour chamber dividing plate (16xM4 CSK screws).

17- Remove vapour chamber body rings from central dividing plate.

## Assembly:

1- Reverse the above procedure.

2- The vapour chamber body rings are sealed to the central dividing plate using a Loctite™ or similar sealing compound.
3- M4 domed nuts and cap screws are torqued to 3Nm. The central M10 displacer bolt is torqued to 10 Nm.

## To Disassemble the Main Controlling Valve:

1- Remove the lower (exhaust port) endcap (4xM4 cap screws).
2- Remove the detent locking nut (optional).
3- Remove the detent subassembly (optional).
4- Remove the upper endcap (4xM4 cap screws).
5- Using appropriate tool, unscrew the detent (upper) end of spool and remove from the valve body.
6- Remove the upper actuating spring.
7- Using appropriate tool, unscrew the exhaust port (lower) end of spool and remove from the valve body.
8- Remove the lower actuating spring.
9- Remove the central piece of the spool from the valve body. Avoid damaging the spool seals on the internal ports of the valve.

## To Assemble the Main Controlling Valve:

1- The procedure is the reverse of that outlined above.
2- Align the two actuating springs during assembly.
3- Torque M4 cap screws to 3 Nm.
4- Check and/or replace all O-ring seals. (2x 15x1.5 N70 on valve body + 2x 34x2 N70 on end caps).

# Appendix 7
# Condenser Calculation

The calculation of condenser size is based on the worst operating case calculated by the simulation for the range of heads simulated. This would ensure the condenser is capable of operating satisfactorily under all conditions. Oversizing the condenser will have no detrimental effects on pump performance. It will result in reduced condenser pressure, increased condensation rate and therefore increased vapour exhaust flow rate resulting in an increased driving pressure differential between the pumps two vapour chambers.

There are two possible operating conditions where maximum condenser heat transfer is required:

(i) Low static water head and maximum flow rate where the pump is cycling rapidly. There is a high volumetric displacement of vapour but at high specific volume.

(ii) High static water head and maximum flow rate. There is a lower volumetric displacement of vapour but at a higher pressure (lower specific volume and greater mass flow per stroke).

Condition (i) is the worst case as the system is operating at lowest efficiency, therefore a greater amount of heat will be rejected to the condenser. The simulation predicts approximately 1 kW of heat rejection to the condenser for condition (i) and approximately 850 W for condition (ii).

For condition (i) above:

Heat extracted from vapour during condensation: ≈1 kW

Mean vapour flow rate into condenser: ≈1.5 litres/s @0.48 $m^3$/kg

Mean liquid flow rate out of condenser: ≈3 ml/s

Cooling water flow (worst case): ≈250 ml/s

(15 l/min)

Vapour-liquid condensers come in many different physical forms and can be air cooled or liquid cooled, or liquid/vapour cooled (evaporative). The requirement for the STWP is a simple, cheap unit that utilises the flow of the pumped water for cooling. This restricts the type of condenser to a simple double pipe, immersed coiled tube or cheap shell and tube variety.

**Condenser Sizing** - an approximate calculation of condenser geometry for a single or multiple tube condenser.

If the condensation process is assumed to be film condensation on a vertical tube

$$\delta=\left[\frac{4k_f v_f z\left(T_g-T_w\right)}{\rho_f g h_{fg}\left(1-\frac{\rho_v}{\rho_f}\right)}\right]^{\frac{1}{4}}$$

then:

where: $\delta$ = Film Thickness

$k_f$ = Thermal Conductivity (BTU/hr.ft.°R)

$v_f$ = Kinematic Viscosity of liquid ($ft^2/s$)

$z$ = Vertical Displacement from top of tube (ft)

$T_g$ = Vapour Temp (°F)

$T_w$ = Wall Temp of Condenser (°F)

$\rho_f$ = Liquid Density ($lbm/ft^3$)

$\rho_v$ = Vapour Density ($lbm/ft^3$)

$g$ = Gravity ($ft/s^2$)

$h_{fg}$ = Latent heat of Vapourisation (BTU/lb)

The liquid properties are an approximation taken at $(T_g+T_w)/2$ (ie ≈37°C (98.6°F)) giving:

$k_f$ = 0.06528 BTU/hr.ft.°R

$v_f$ = $3.335 \times 10^{-6}$ $ft^2/s$

z = variable (ft)

$T_g$ = 109.4 to 132.8 (average = 121.1°F)

$T_w$ = 77 °F

$\rho_f$ = 40.3 $lbm/ft^3$

$\rho_v$ = 0.229 to 0.333 (average = 0.28 $lbm/ft^3$)

g = 32.2 $ft/s^2$

$h_{fg}$ = average = 149.2 BTU/lb

$$h_z = \frac{k_f}{\delta}$$

now:

where: $h_z$ = Local Convection Coefficient

$$\overline{h_L} = \frac{4}{3} h_z \Big]_{z=L}$$

and:

where: $h_L$ = Average Convection Heat Transfer Coefficient

combining 7.1, 7.2, 7.3 at z=L:

$$\overline{h_L} = \frac{4 k_f}{3\left[\dfrac{4 k_f v_f L \left(T_g - T_w\right)}{\rho_f g h_{fg}\left(1 - \dfrac{\rho_v}{\rho_f}\right)}\right]^{\frac{1}{4}}}$$

now the heat transferred:

$$q = A_s \overline{h_L} \left( T_g - T_w \right)$$

where: q = Heat Transfer (BTU/hr)

$A_s$ = Surface Area of Tube ($ft^2$)

If there is a number (n) of identical vertical tubes of outside diameter (OD) and length (L) (as in a shell and tube condenser) heat transfer is given by:

$$q = n.\pi.OD.L.\overline{h_L} \left( T_g - T_w \right)$$

Using equations 7.4 and 7.5 an equation can be derived giving condenser length (L) for a number of tubes (n) of specified diameter (OD) with the following assumptions:

- negligible interaction on condensation rate with number of tubes
- tube radius >> film thickness
- filmwise condensation is occurring
- flow is approximately steady
- fluid properties are approximately constant
- flow in film is laminar

$$\overline{h_L} = 179.34 L^{-\circ} \qquad (BTU/hr.ft\grave{A}\_\_\_\_$$

Substituting in fluid properties to 7.4 gives:

Substituting into 7.5 using $T_g$ = 109.4 to give a conservative estimate of condenser

$$q = 5810.62 \times n.\pi.OD.L^{¾} \quad (BTU/hr)$$

*or in S.I. units*

$$q = 13610.64 \times n.\pi.OD.L^{¾} \quad (W)$$

heat capability:

If the condenser is to dissipate 2kW (allowing a safety factor of 2 from the capability calculated and to ensure the condenser has sufficient capability to be set up safely

with the simulated boiler) using 31 x ¼" (6.35mm) tubes then the corresponding condenser length using equation 7.7 would be 147mm or 5.79".

A heat exchanger from Savage Heat Transfer Ltd was chosen, being of a suitable design. These came in standard lengths of 5", 9", or 12" with a shell diameter of 2" and 31 internal tubes of outside diameter ¼". A 9" long heat exchanger was chosen as oversizing condenser capability will have system performance. This gave:

Heat dissipation:

2.8 kW

Internal volume (vapour):

0.24 litres

Water flow area (31 tubes at 5mm ID): $6.1 \times 10^{-4}$ $m^2$

compared with 32mm waste pipe: $8 \times 10^{-4}$ $m^2$

The internal volume of this condenser is small allowing for minimal expansion of the exhausting vapour. To ensure the drop in pressure in the exhausting vapour chamber is rapid, the initial rate of condensation must be high allowing the exhausted vapour to be condensed as soon as it reaches the condenser. If the rate of condensation does not give a rapid drop in pressure in the exhausting chamber it may be necessary to provide an additional expansion volume (essentially increasing the internal volume of the condenser) that the exhausting vapour may expand into before entering the condenser. For experimental purposes this may be added after testing and verification of the condensation process.

This calculation is conservatively based on using one vertical pipe. A shell and tube condenser with multiple internal tubes would be expected to give better performance than predicted by equation 7.7 as there is a greater surface area available at the vapour entry to the condenser for which the liquid film thickness ($\delta$) around the condensing tubes is minimal.

# Appendix 8
# Abstracts from Published Papers

From Raine et al. (Feb. 1994)

## DEVELOPMENT OF SINGLE AND DOUBLE-ACTING SOLAR-THERMAL WATER PUMPS

J.K. Raine*, D.R. Foster** and M.R. Amor***[1]

**Abstract**

This paper describes the design of a single-acting double-diaphragm solar-powered water pump which delivers 177 litres per hour of water at suction and delivery heads of 6.4 and 1.5 m respectively. A later double-acting design offering a more compact layout and potentially greater output and reliability is also described. The design of the prototype pumps has been based on low cost manufacture, simplicity, and reliability. The working fluid is n-pentane in both cases. The second pump is designed to be ideally suited for water circulation in solar-powered heating systems for swimming pools.

In these diaphragm pumps useful work is done during the evaporation and condensation stages of the Rankine cycle, but there is a large exergy loss during an unresisted expansion which precedes condensation. Pump efficiency is therefore low, but this is typical of low cost non-steady flow devices where there is no flow work done on a turbine. Laboratory test results for the first pump are presented, together with results of a computer simulation of the second pump, which is now under construction.

[1] *Senior Lecturer, **M.E. student, ***M.E. graduate.
Department of Mechanical Engineering, University of Canterbury

From Raine et al. (Nov. 1994)

# COMPUTER SIMULATION AND TEST BED PERFORMANCE OF SINGLE AND DOUBLE-ACTING SOLAR-THERMAL WATER PUMPS

J.K. Raine,* BE(Hons) PhD CEng, FIMechE, MSAE-A (Fellow)
D.R. Foster,** BE(Hons)
M.R. Amor,*** BE(Hons), ME[2]

## Abstract

This paper describes the design, computer simulation and performance of a single-acting double-diaphragm solar-powered water pump, and a later double-acting design offering a more compact layout, higher output and potentially greater reliability. The design of the prototype pumps has been based on low cost manufacture, simplicity, and reliability. The working fluid is n-pentane in both cases. The second pump is designed to be ideally suited for water circulation in solar-powered heating systems for swimming pools.

In these diaphragm pumps useful work is done during the evaporation and condensation stages of the Rankine cycle, but there is a large exergy loss during an unresisted expansion which precedes condensation. Pump efficiency is therefore low, but this is typical of low cost non-steady flow devices where there is no expansion work done on a piston or turbine. Laboratory test results are presented for the first pump on n-pentane. Results of a computer simulation of the second pump are described, together with initial performance tests done with compressed air. These results indicate that the double-acting pump is likely to meet its computer-predicted performance.

[2]* Senior Lecturer, ** M.E. Student, *** M.E. graduate in Mechanical Engineering, University of Canterbury

# Appendix 9
# Data Sheets for Omniring Piston Seals

The piston seals are relatively simple to assemble, however unless the Type “Z” seal is used, once assembled into position they cannot be removed without being destroyed. Method of assembly for standard Omniring piston seals:

1/ Place the backing O-ring into the seal groove in the spool.
2/ Heat the Carbon filled PTFE seal in hot water (80 to 100°C) to soften the seal.
3/ Expand the seal over a mandrel and slide into the groove in the spool.
4/ Reheat the assembly to shrink the seal to its original size in the groove.

The following pages contains the manufacturers data for these seals.

FLUOROCARBON MECHANICAL SEAL DIVISION

# OMNIRING™ PISTON SEAL METRIC SERIES

*Style No. 65544 (and Derivatives)*

OMNIRING is a double-acting seal which has been designed and developed to provide superior performance while maintaining reliability and simplicity of hardware and installation.

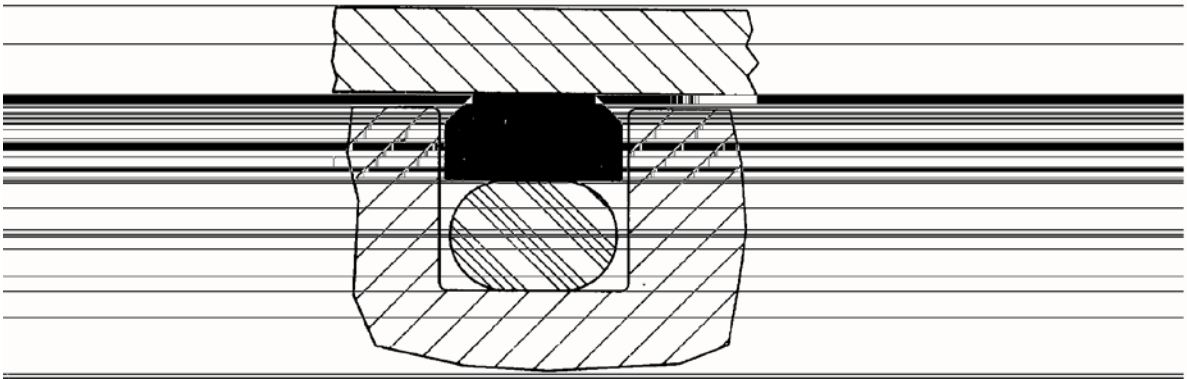

OMNIRING is a double-acting seal which has been designed and developed to provide superior performance while maintaining reliability and simplicity of hardware and installation.

An important feature of OMNIRING is the small chamfers on style 65544, which maintains a hydrodynamic bearing effect at moderately fast speeds, while the remainder of the geometry of the seal maintains a [illegible] velocities.

## OMNIRING™ ADVANTAGES

- OMNIRINGS are machined from virgin PTFE stock Teflon® and can be supplied to any diameter up to 2.5 metres (See note 1.)
- Low friction resulting in low energy absorption, lower heat generation and longer seal life
- Static and dynamic friction are virtually identical, resulting in stick-free operation
- Can be reversed
- Utilizes minimum spaces
- Simple groove profile
- Stable design
- Excellent wear resistance
- Compatible with most fluids
- Wide temperature range
- High resistance to extrusion, even at moving clearances
- Non-rotation within groove to maximize mating surface
- Simple installation

# OMNIRING PISTON SEAL METRIC SERIES

*Style No. 65544 (and Derivatives) Installation and Hardware Dimensions*

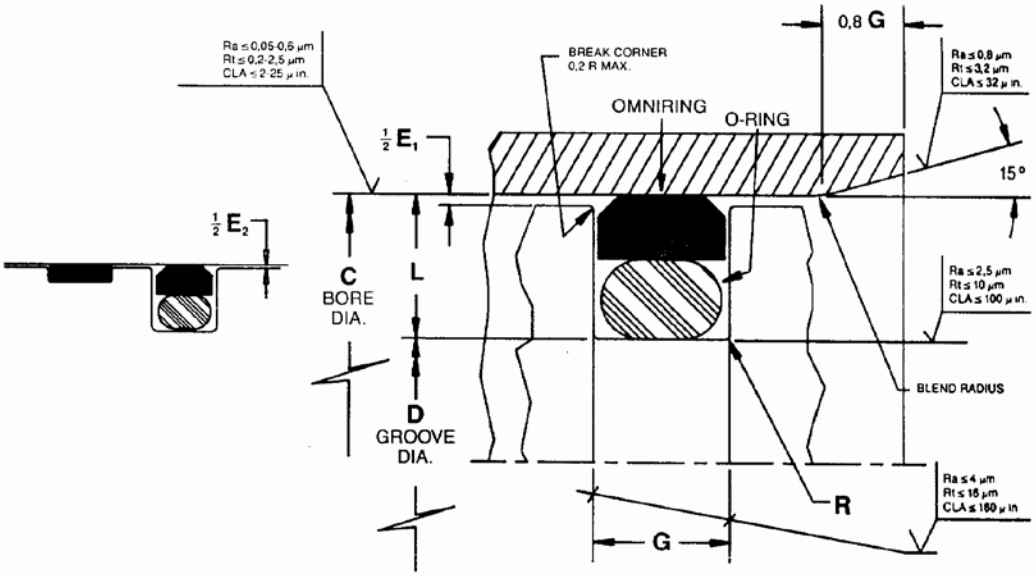


| ØC BORE DIA. H9 | | | ØD | L | G | R | DIAMETRAL CLEARANCE | | | | | | O-RING | |
|---|---|---|---|---|---|---|---|---|---|---|---|---|---|---|
| LIGHT DUTY 65522 65532 65542 | STD. DUTY 65524 65534 65544 | HEAVY DUTY 65526 65536 65546 | GROOVE DIA. | GROOVE DEPTH | GROOVE WIDTH | RADIUS | E1 PRESSURE, BAR | | | E2 PRESSURE, BAR | | | | |
| | | | h9 | | +0,2 −0 | MAX | 0 | 200 | 400 | 0 | 200 | 400 | SERIES | SECTION |
| 15,0 to 39,9 | 8,0 to 14,9 | | C − 4,9 | 2,45 | 2,2 | 0,3 | 0,4 | 0,2 | 0,05 | 0,9 | 0,5 | 0,15 | 0 | 1,78 |
| 40,0 to 79,9 | 15,0 to 39,9 | | C − 7,5 | 3,75 | 3,2 | 0,5 | 0,6 | 0,3 | 0,1 | 1,65 | 0,8 | 0,3 | 100 | 2,62 |
| 80,0 to | 40,0 to | 15,0 to | C − 11,0 | 5,50 | 4,2 | 0,7 | 0,6 | 0,3 | 0,1 | 1,75 | 0,9 | 0,4 | 200 | 3,53 |
| 7,75 | 6,3 | 1,2 | 0,8 | 0,4 | 0,2 | 2,0 | 1,0 | 0,4 | 300 | 5,33 | | | | |
| 10,5 | 8,1 | 1,5 | 1,0 | 0,6 | 0,4 | 2,25 | 1,1 | 0,5 | 400 | 7,00 | | | | |
| 12,25 | 8,1 | 1,5 | 1,0 | 0,6 | 0,4 | 2,25 | 1,1 | 0,5 | 400 | 7,00 | | | | |
| 14,0 | 9,5 | 2,0 | 1,2 | 0,8 | 0,5 | 2,4 | 1,2 | 0,8 | 500 | 8,40 | | | | |
| | | | | | | | | | | | | | 133,0 to 329,9 | 80,0 to 132,9 | 40,0 to 79,9 | C − 15,5 |
| | | | | | | | | | | | | | 330,0 to 669,9 | 133,0 to 329,9 | 80,0 to 132,9 | C − 21,0 |
| | | | | | | | | | | | | | 670,0 to 999,9 | 330,0 to 669,9 | 133,0 to 329,9 | C − 24,5 |
| | | | | | | | | | | | | | | 670,0 to 999,9 | 330,0 to 669,9 | C − 28,0 |

# OMNIRING PISTON SEAL METRIC SERIES

*Style No. 65544 (and Derivatives)*

## WORKING PARAMETERS

### PRESSURE

Tabulations show pressures up to 400 Bar. Experience has shown Fluorocarbons materials capable of working at pressures up to 4,000 Bar. For pressures above 400 Bar, contact Fluorocarbon Co.

### TEMPERATURE

The limitations of our Teflon based materials are −250 °C to +260 °C. However, the working temperature is limited by that of the energizing elastomer.

### VELOCITY

Reciprocating; up to 15 m/sec. Oscillatory; up to 5 m/sec. (All modes; for frequencies in excess of 5 Hz please contact Fluorocarbon Co. and refer to the section of our catalog for oscillatory seals).

### LOW TEMPERATURE RESPONSE

At low temperatures (−20 °C and below) it may be advantageous to order with a 'Z' cut as shown. The 'Z' cut allows faster response when thermal contraction can exert extra load on the O-ring. Leakage control under these conditions is, however, reduced.

**TYPE Z STEP-CUT**

## ALTERNATIVE DESIGNS

**65522 65524 65526**

**65532 65534 65536**

**65542 65544 65546**

**65522 65524 65526** Lower friction seal, also with longer service life in high velocity applications, due to the hydrodynamic bearing effect generated by the slow chamfers. However, dynamic leakage control is reduced and the seal may suffer some damage in contaminated systems. Static leakage control and friction are improved.

**65532 65534 65536** More suited to low speed reciprocating applications, this style has the greatest stability and is useful in contaminated systems.

**65542 65544 65546** Multi-purpose profile used in the majority of applications. Stability of the 65533 is retained while providing some hydrodynamic effect on high velocity, and maintaining good resistance to contamination.

## ORDERING EXAMPLE:

| | |
|---|---|
| CYLINDER BORE | 80mm |
| CYLINDER MATERIAL | Steel |
| FLUID | Hydraulic Oil |
| TEMPERATURE RANGE | −40 °C to +120 °C |
| APPLICATION | Raise/Lower Cylinder on Snowplough |

**65534 - X0800 - 56 31 Z**

- 65534 — OMNIRING STYLE NO.
- X0800 — BORE DIA. INDICATOR
- 56 — OMNIRING MATERIAL CODE See Section 10
- 31 — ELASTOMER MATERIAL CODE See Section 10
- Z — Z-CUT

**Note 1.** Example shown is for Z-Cut Seal. This type is not supplied with Notches.

**Note 2.** It is recommended that Notches are used as a standard feature on sizes 20mm and above, and require the 'N' suffix to the Part No. Where notches are not required, omit suffix 'N'. Notches are not supplied on 'Z' cut seals.

**Note 3.** For installation information refer to the Installation Data Section 11 of this catalog.

FLUOROCARBON MECHANICAL SEAL DIVISION

# PISTON SEAL ASSEMBLY DETAILS

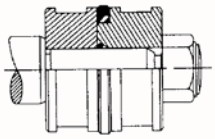

Industrial piston seals can be assembled on to a two-piece piston without the aid of any assembly tools. Lubricate all associated components.

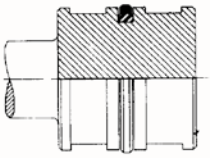

Assembly of piston seals on to one piece pistons can be performed by hand on small quantities. By carefully stretching the Teflon® component, introducing it to the groove, and then squeezing down by hand, it is possible to introduce the seal into the cylinder. However, on larger production quantities, it is advantageous to use assembly tools. Fluorocarbon Co. can supply assembly tools on request, and alternatively give design advice.

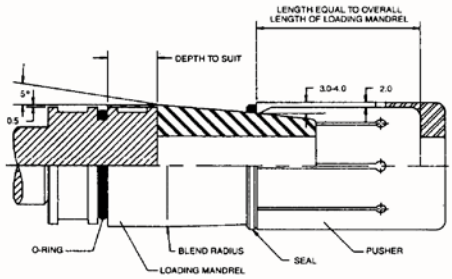


## STAGE 1

The tapered Mandrel is introduced on to the piston. (Note the length in relation to the groove, depending on the type of seal). Firstly, push the O-ring up the Mandrel and into the seal groove. Then place the piston seal on the Mandrel. Lubricate all parts to assist assembly.

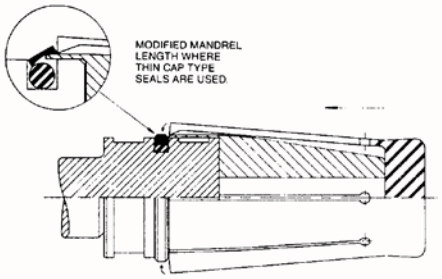


## STAGE 2

Using the Pusher, quickly push the seal along the Mandrel and into the groove. Remove the assembly tools, and add the GUIDERINGS to their appropriate grooves, staggering the gaps.

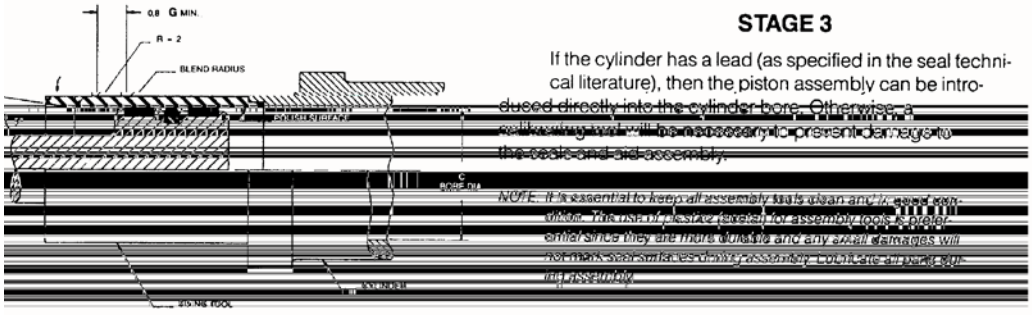


## STAGE 3

If the cylinder has a lead (as specified in the seal technical literature), then the piston assembly can be introduced directly into the cylinder bore. Otherwise a [illegible] will be necessary to prevent damage to the seals and seal assembly.

NOTE: It is essential to keep all assembly tools clean and free from abrasion. The use of a [illegible] for assembly tools is preferential since they are more durable and any small damages will not mark seal surfaces during assembly. Lubricate all parts during assembly.